BMR JOURNAL
OF AUSTRALIAN GEOLOGY & GEOPHYSICS

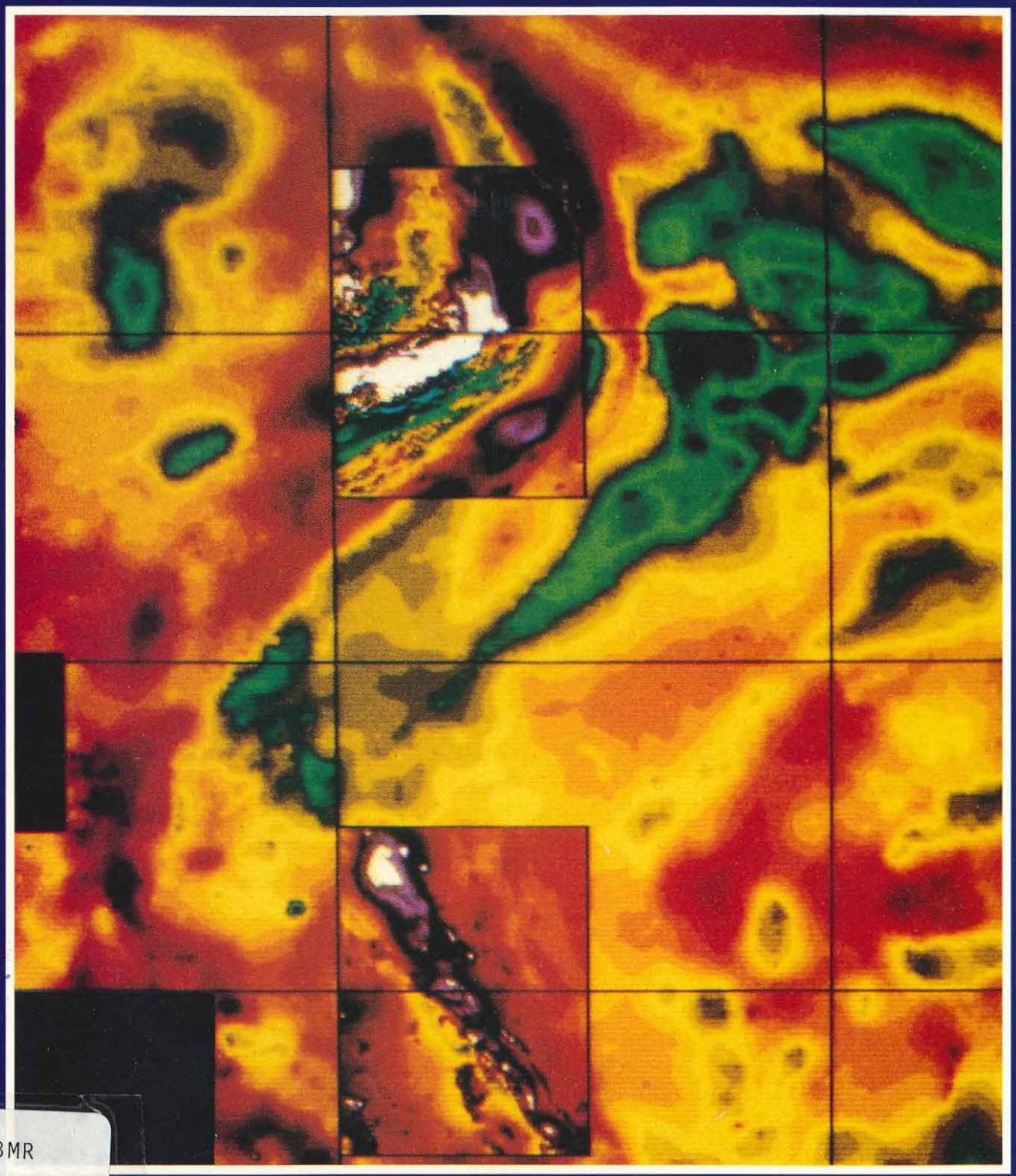

VOLUME 9 NUMBER 4 DECEMBER 1984

BMR JOURNAL

OF AUSTRALIAN GEOLOGY & GEOPHYSICS

VOLUME 9 NUMBER 4 DECEMBER 1984

CONTENTS

Front cover: Combined Bouguer anomaly and total magnetic intensity (inserts) pixel maps for the Murray Basin and its fringe areas, southern Australia. The colour scales range from dark green for lows to red for highs in the Bouguer anomaly data, and from blue (lowest) through green, yellow, red, purple, and white (highest) for the total magnetic intensity. This composite presentation of the data is able to highlight those areas where one or the other data set better demonstrates trends and patterns. The data are *not* combined mathematically. In this example, a subtle northwest linear gravity trend is emphasised by the very prominent trend visible in the lower magnetic insert. The upper insert highlights two intense circular magnetic anomalies (purple). These are known to coincide with the axes of two linear gravity lows over the Menindee Trough and Bancannia Trough, and probably represent magnetic granitoids at considerable depth. The two small black areas in the lower left quadrant are areas of no data.

Department of Resources and Energy

Minister: Senator the Hon. Gareth Evans, Q.C.

Secretary: A. J. Woods, A.O.

Bureau of Mineral Resources, Geology and Geophysics

Director: R. W. R. Rutland

Editor, BMR Journal: I. M. Hodgson

The BMR Journal of Australian Geology & Geophysics is a quarterly journal of research. It contains papers and shorter notes by scientists of the BMR or others who are collaborating with BMR. Discussion of papers is invited from anyone.

Subscriptions to the BMR Journal are managed by the Australian Government Publishing Service (Mail Order Sales, GPO Box 84, Canberra, ACT 2601; telephone (062) 95 4485), to which enquiries should be directed.

Other matters concerning the Journal should be sent to the Director, marked for the attention of the Editor, BMR Journal.

Month of issue: August, 1985

ISSN 0312-9608

Printed by Graphic Services Pty. Ltd. 516-518 Grand Junction Road, Northfield, S.A. 5085

BMR Journal of Australian Geology & Geophysics, 9, 267-295

Palynology of the Oligocene–Miocene sequence in the Oakvale-1 corehole, western Murray Basin, South Australia

E.M. Truswell[1], I.R. Sluiter[2] & W.K. Harris[3]

Palynological analysis of the marine Oligocene—Miocene Geera Clay and Renmark Group in the Oakvale-1 corehole in the western Murray Basin has shown diverse and well-preserved assemblages of spores, pollen, and dinoflagellates throughout the sequence. Pollen of *Nothofagus* is present throughout, with *Nothofagidites emarcidus* the most common form. Myrtaceous pollen is abundant: most types are referable to closed forest genera such as *Syzygium*, *Acmena* and *Tristania*, although a significant component of *Eucalyptus* type pollen is present. Podocarpaceae are common, and include types comparable to the extant *Podocarpus*, *Dacrycarpus*, *Phyllocladus*, *Microcachrys* and *Dacrydium*. Araucariaceae, probably as *Araucaria*, locally reaches high frequencies. Casuarinaceae is consistently present, and Cyperaceae and Poaceae at some levels reach frequencies in excess of 10 per cent. A group of pollen and spores that were first recorded from Tertiary strata in the modern tropics is present, although in low numbers; these include *Polypodiisporites usmensis, Margocolporites vanwijhei*, and a form similar to *Perfotricolpites digitatus*. The site provides good fossil records for a number of extant Australian taxa — *Acacia* pollen (as *Acaciapollenites myriosporites*) is present from the late Oligocene, and Gyrostemonaceae pollen was recorded from the same interval — and also the first fossil record in Australia for pollen of *Utricularia* (as *Polycolpites* sp.) and *Gardenia* (as *Triporotetradites* sp.). There is clear evidence too of diversity within the Cyperaceae by the late Oligocene. Recycled Permian and early Cretaceous spores and pollen are most common in the upper part of the Geera Clay.Dinoflagellate cysts occur throughout the section. The assemblages are dominated by the *Spiniferites ramosus* complex, with *Hystrichokolpoma rigaudae, Lingulodinium machaerophorum, Operculodinium centrocarpum*, and *Systematophora placacantha* the most common of the other components. There is a general similarity to coeval assemblages from Europe and elsewhere, but one major difference is the absence of peridinioid forms such as *Deflandrea*, *Wetzeliella* sensu lato, and *Palaeocystodinium*. These apparently did not persist into the late Oligocene in this region. The base of the *Triporopollenites bellus* Zone of the Gippsland Basin has been tentatively identified at 80 m. A quantitative zonation for this corehole sequence, based on the frequencies of the major pollen taxa, has been statistically calculated, enabling a division into two major zones; the younger of these has been further divided into four sub-zones. The basal Zone II, incorporating the Olney Formation and lower Geera Clay, is characterised by high Myrtaceae and high *Nothofagus brassi* type values. *N. brassi*, however, is lower here than at coeval sites in southeastern Australia. These assemblages are considered to indicate the presence of evergreen rainforest with abundant myrtaceous trees, in association with the *N. brassi* producers. A climatic regime of high, year-round precipitation may have supported this forest type. In the late Oligocene, the vegetation changed; *N. brassi* became reduced in importance, and *Araucaria* became more prominent. This has been interpreted as reflecting a drier type of rainforest growing under a mildly seasonal moisture regime.

Introduction

This study provides a palynostratigraphic analysis of the Oligocene— Miocene Geera Clay in the Oakvale-1 corehole. The hole was drilled by the South Australian Department of Mines and Energy in May—June, 1981, and is located at 32°59.3′S, 140°54.9′E, in the Olary 1:250 000 Sheet area, in the northwestern part of the Murray Basin (Fig. 1).

The purpose of the palynological analysis was, firstly, to provide a reference section for palynological studies currently being undertaken on sequences of comparable age in the Lake Eyre Basin, and, secondly, to establish the nature of vegetation communities in the area for comparison with other sites of similar age, and thereby form a basis for inferences about palaeoclimates. The sequence in Oakvale-1 is ideal as a reference section, as it is fully cored and contains foraminiferal faunas; analysis of these by Lindsay (1983) has allowed correlation with intercontinental time scales. The palynological study enables spore, pollen, and dinoflagellate assemblages to be directly related to the foraminiferal faunas, and hence to the standard time scale.

The area in which Oakvale-1 is situated is sufficiently close to Lake Eyre for it to be anticipated that the mid-Tertiary vegetation in the two regions would have been similar, making palynological comparisons between the Murray and Lake Eyre Basins relatively easy, in contrast to difficulties experienced in comparing these present inland sites and sequences in the Otway and Gippsland Basins. The palynofloras of coastal and inland basins are sufficiently different to make zonal schemes developed in the former very difficult to apply to the latter.

[1] Division of Continental Geology, BMR, Canberra.
[2] Geography Dept, Monash University, Clayton, Victoria.
[3] Western Mining Corporation (Exploration Division — Petroleum), Adelaide.

Lithology and foraminiferal stratigraphy

In Oakvale-1, the interval between 32.17 m and 125.58 m was assigned to the Geera Clay (Lindsay, 1983). This unit is overlain by 32 m of predominantly quartz sand, which is yellow and white, highly oxidised, and unlikely to yield

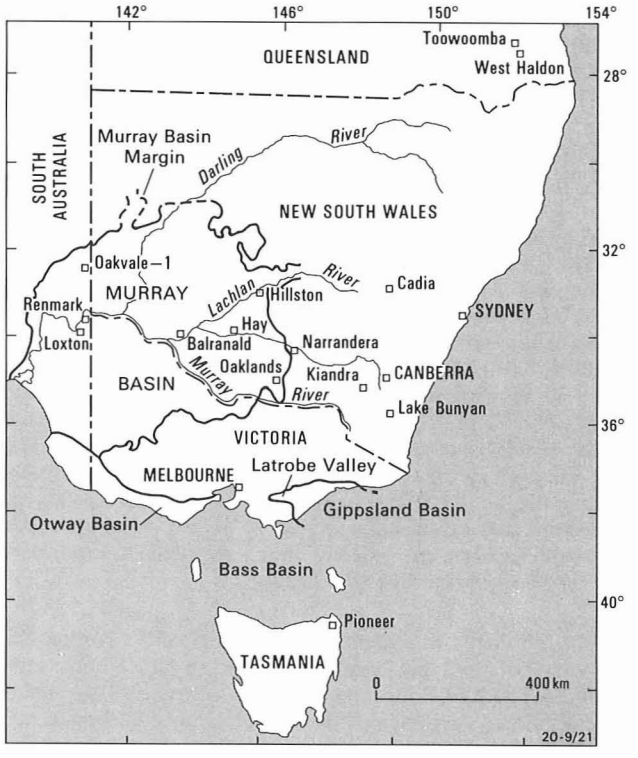

Figure 1. Locality map of southeastern Australia showing position of Oakvale-1 corehole in the western Murray Basin.
Other sites mentioned in the text are also marked.

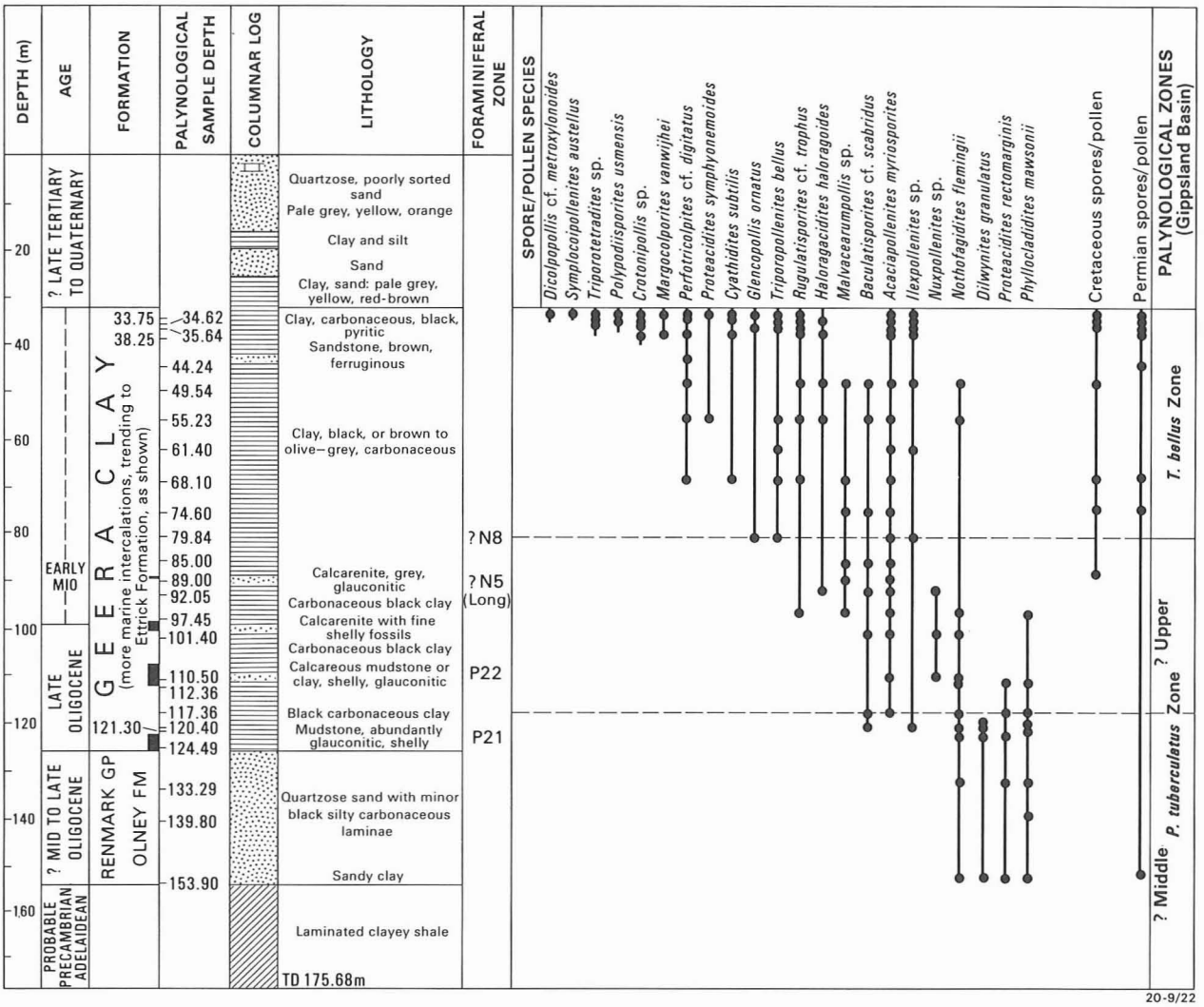

Figure 2. Ranges of selected spore and pollen species in Oakvale-1 matched against the lithological sequence.
Black bars in 'Formation' column are intervals of most intense marine influence as identified by Lindsay (1983). Distribution of recycled Cretaceous and Permian spores and pollen shown on right. Possible boundaries of Gippsland Basin spore-pollen zones shown in extreme right-hand column.

palynomorphs. According to Lindsay (1983), this unit, below 3 m, could be identified as Parilla Sand.

The Geera Clay in Oakvale-1 is predominantly dark brown, olive-grey to black clay with sparse shelly fossils and thin intervals of glauconitic sand (Fig. 2). It is pyritic and carbonaceous, particularly in the top 5 or 6 m. A number of glauconitic and shelly calcarenites and calcareous mudstone intervals were described by Lindsay as tongues or lenses showing stronger than average marine influence and comparable to the Ettrick Formation of South Australia and its younger diachronous equivalent, the Winnambool Formation in Victoria, with which the Geera Clay intergrades laterally in its type area in northern Victoria. In the Oakvale section, marine influence appears to decline in the upper part of the Geera Clay, where a much restricted foraminiferal fauna suggests a lagoonal facies.

The lithology of the Geera Clay in Oakvale-1 is comparable to that of the type section in the Geera No. 1 bore, some 30 km south of Robinvale, Victoria (Lawrence, 1966, 1975), except that the Oakvale sequence is more carbonaceous. Lawrence (1966) concluded that the unit was deposited in a shallow marine and lagoonal environment that was subject to influx of terrigenous muds. Brown (1984) has suggested that deposition occurred in interdistributary bays of a delta system draining broad marshlands, with perhaps a tidal flat component (Fig. 3). The palynological data presented here are in accord with this suggested environment of deposition: dinoflagellates of marine origin are present throughout the sampled sequence; spores and pollen representing terrestrial vegetation are abundant, and there is too a substantial component of algae that may have thrived in freshwater swamps and lakes in the marshlands.

Using foraminifera, Lindsay (1983) was able to date four intervals of intensified marine influence within the Geera Clay. The interval 88.50–88.66 m he dated firmly as representing the Longfordian Stage (early Miocene), noting that planktonic forms close to *Globigerinoides primordius* suggest an age no younger than early Zone N5, and suggesting a correlation with the earliest Miocene sea-level peak TMI.1 of Vail & others (1977). The microfauna from the interval 99.97–100.08 m contains planktonic forms indicative of a late Oligocene age, and possibly represents a transgressive episode equivalent to the late Oligocene TO2.2 peak of the global sea-level curve. The marine interval represented by faunas between 107 and 112 m is also late Oligocene, and at least as young as Zone P22. The oldest identifiable marine interlude, at the very base of the Geera Clay, between 121 and 125 m, may represent late Zone P21, and is thus still within the late Oligocene; correlation with eustatic cycle TO2.1 is suggested.

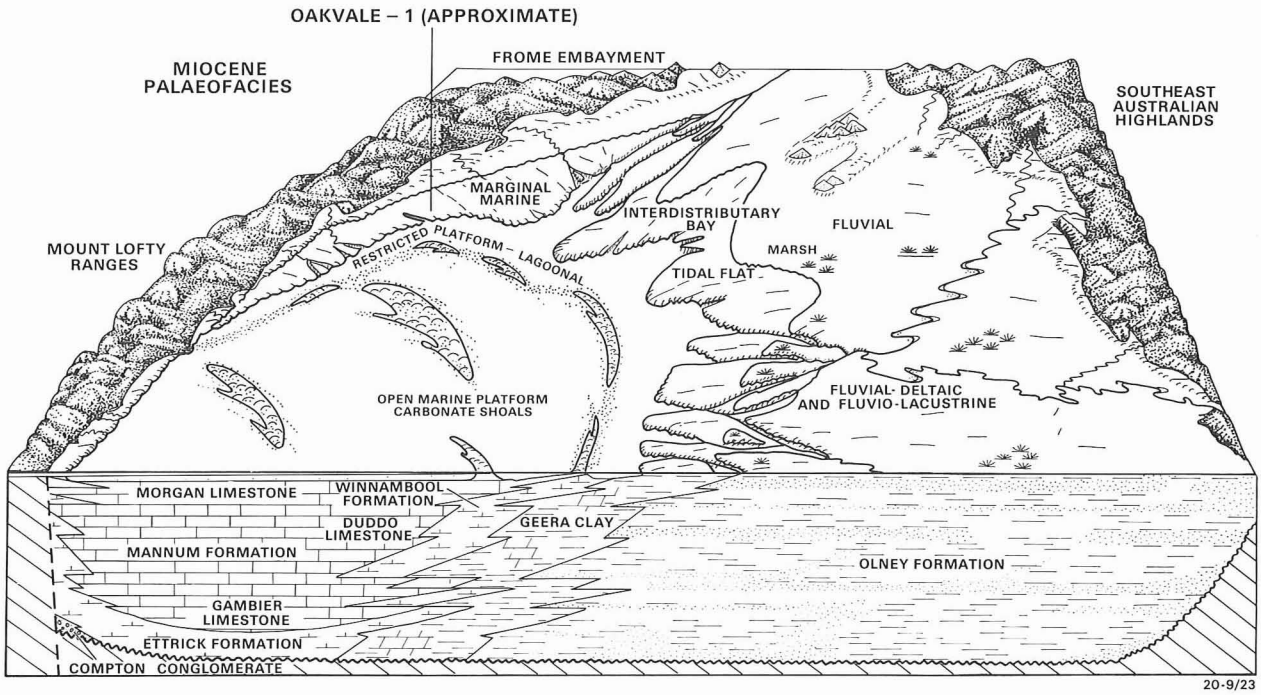

Figure 3. Diagrammatic representation of Miocene palaeofacies in the Murray Basin (from Brown, 1984)

Between 125.64 m and 153.97 m, a unit of greyish-brown and greenish quartz sands with some clayey and carbonaceous intervals was assigned by Lindsay (1983) to the Warina Sand of the Renmark Group. Lindsay could find no calcareous marine fossils in the interval, and listed a possible age of Palaeocene to Oligocene, basing the older age limits on the known age limits of the Renmark Group in deeper sections of the Murray Basin. The present palynological study has shown dinoflagellates, spores, and pollen to be present in this lithological unit, indicating deposition in shallow marine conditions, and suggesting an age probably not significantly older than late Oligocene. Correlation with the Olney Formation of the Renmark Group thus seems more appropriate. The Olney Formation overlies the Warina Sand in the type section of the Renmark Group formations in the Olney No. 1 bore in northwest Victoria (Lawrence, 1975), and, according to Brown (1983) interfingers with the Geera Clay (Fig. 3). Preservation of the Warina Sand appears to be confined to deeper parts of the Murray Basin.

Oakvale-1 bottomed in green chloritic claystone and laminated green shale, which R.A. Callen (personal communication 1984) considers to be Tapleys Hill Formation or possibly Amberoona Shale, of Adelaidean age.

Sampling and composition of palynological assemblages

Twenty-six core samples were selected from Oakvale-1 for palynological preparation. Twenty-three of these were from the Geera Clay, and three from the most carbonaceous lithologies in the Olney Formation beneath. All but one of the samples yielded diverse and well-preserved assemblages of spores, pollen, and dinoflagellates (Fig. 2) Counts of relative frequencies of pollen and spores were undertaken on all samples (Fig. 4, Table 1). A number of palynomorph taxa encountered in the study are of particular biostratigraphic, phytogeographic or botanical interest, and these are illustrated in Figures 6–11. The specimens figured are held in collections of the Bureau of Mineral Resources (CPC numbers) and Western Mining Corporation, Adelaide (WM numbers).

Spores and pollen

The spore and pollen assemblages from Oakvale-1 are diverse. The taxa listed in Table 1 include 5 possible bryophytes, 23 pteridophytes, 10 gymnosperms, and over 80 angiosperms. These are minimum figures, especially for the angiosperms, which contain undescribed pollen types, especially tricolporates, not included in the table.

Broadly, the assemblages from the Geera Clay and Olney Formation contain a mixture of taxa indicative of rainforest and herbaceous vegetation formations. Possible explanations for this combination, in terms of habitats and plant communities, are presented in a separate section below.

Pollen of the southern beech, *Nothofagus* (as *Nothofagidites*) is present in every sample, with *N. 'brassi'* type predominating, particularly as *Nothofagidites emarcidus*; *N. 'fusca'* and *N. 'menziesii'* types occur in small amounts. Podocarpaceae are also significant, and include pollen morphologically close to that of the extant genera *Dacrycarpus*, *Podocarpus*, *Phyllocladus*, *Microcachrys* and *Dacrydium*. Araucariaceae, probably as *Araucaria*, are consistently present, and locally reach frequencies as high as 35 per cent. Frequencies of myrtaceous pollen are very high at most levels; most pollen types are probably derived from genera with closed forest affinities, such as *Syzygium*, *Acmena*, and *Tristania*, although a significant component of *Eucalyptus*-type pollen was recorded. Casuarinaceae pollen is always present in Oakvale-1, in frequencies up to 27 per cent. Grass pollen (Poaceae) occurs in most samples, locally reaching a maximum of 10 per cent, and pollen of the herb families, Cyperaceae and Sparganiaceae, is also consistently present and locally abundant. No pollen of Compositae was seen.

It is among the minor taxa that much of the phytogeographic and palaeobotanical interest of these Murray Basin suites lies. There is present in Oakvale-1 a group of pollen and spore types that have hitherto been recorded mainly from Tertiary sequences in the modern tropics. A number of these taxa provided useful marker species in a system of pan-tropical zones erected by Germeraad & others (1968) to subdivide thick

Table 1. Percentages of spore and pollen species in samples from Oakvale-1.
Percentages are based on counts of 200 grains. Dot indicates observed in sample, but not in count.

MFP No.	8173	8172	8171	8170	8169	8168	8167	8166	8164	8163	8162	8161	8160	8159	8158	8157	8155	8154	8153	8151	8152	8150	8149	8148	8147
Depth (m)	33.75	34.62	35.64	38.25	44.24	49.54	55.23	61.40	68.10	74.60	79.84	85.00	89.00	92.05	97.45	101.40	110.50	112.36	117.36	120.40	121.30	124.49	133.29	139.80	153.90
Bryophyta: Lycophyta																									
cf. *Crassoretitriletes* sp.									●	●															
Herkosporites elliotti Stover									●	●			●	●		●	●		●	●		●	●		●
Lycopodiumsporites sp.		●							●	●															
Rouseisporites sp.	0.5	0.5	●	●		●	●	0.5	2.0	0.5	●	1.5	●	1.0	1.0	●		●	●				●	●	●
Stereisporites antiquasporites (Wilson & Webster)		●	1.5	0.5	●					●	●		1.0		0.5	●						●			
Pteridophyta																									
Azolla sp.			●																						
Baculatisporites comaumensis (Cookson)		●				●							●							●					
B. sp. cf. *B. scabridus* Playford						●	●			●		●		●		●			●	●					
Camarozonosporites sp.			●	●							●		●		●							●			
Concavissimisporites sp.			●																						
Cyatheacidites annulatus Cookson							●			●												●			
Cyathidites subtilis Partridge	●	●		●					●																
C. minor/australis	2.5	3.5	5.5	1.0	0.5	4.5	3.0	9.0	5.0	9.0	8.0	6.0	3.5	3.0	6.5	6.0	4.0	1.5	5.0	6.5	4.0	2.0	0.5	5.0	3.5
Deltoidospora sp.	●	●	●	●		●	1.0	●	●	1.5	●	1.0		3.0	2.5	4.0	●				●				●
Distaverrusporites cf. *D. simplex* Muller									●																
Foveotriletes lacunosus Partridge														●											
Gleicheniidites sp.	●	2.0	0.5	2.5	●	●	2.5	2.5	2.0	1.5	●	6.5	0.5	3.0	1.5	3.5	0.5	3.5	0.5	13.5	2.0	1.5	3.0	0.5	1.5
Klukisporites sp.									●																
Laevigatosporites major (Cookson)	●													●											
L. ovatus Wilson & Webster	2.5	3.5	0.5	0.5	●	3.5	4.0	2.5	0.5	●	3.0	1.0	1.5		1.5	1.0	●	1.0	1.5	0.5	0.5	0.5	●	2.5	1.0
Matonisporites ornamentalis (Cookson)							●		●	1.5	●					●						●		●	
Peromonolites sp. (cf. *Paesia* aff. *scaberula)*	●	●	●	●			●		●	●	●			●								0.5			
Polypodiaceoisporites cf. *retirugatus* Muller	●	●	●			●			●	●				●									●		
Polypodiisporites usmensis (Van der Hammen)	●	●																							
P. sp.	●		●	●			●	●	●		●					●					●				
Rugulatisporites sp. cf. *trophus* Partridge	1.5	4.0	1.0	●		●	0.5		●	1.5					●										
Reticuloidosporites sp.		●																							
Trilites tuberculiformis Cookson		●					●	●		●		●		●					●		●	●			
Gymnosperms																									
Araucariacites australis Cookson	5.0	13.0	6.5	6.0	11.0	5.0	6.5	10.0	4.5	8.0	12.5	16.5	35.0	8.0	3.0	12.5	2.5	0.5	2.0	4.0	1.5	4.0	3.5	2.0	1.5
Cupressaceae	●	●	●			●			●		●	●	●	●	●	●		●		●	●	●	●	●	●
Dacrycarpites australiensis Cookson & Pike	2.0	4.0	1.5	0.5	1.5	1.5	6.0	1.5	4.0	1.0	2.5	2.0	4.5	1.0	1.0	2.0	2.5	0.5	1.5	0.5	1.0	1.0	1.0	3.0	0.5
Dacrydiumites florinii Cookson & Pike	3.0	1.5	1.0	2.0	3.5	1.5	4.5	1.5	3.5	5.0	5.0	3.0	6.5	5.0	1.5	1.5	1.5	2.0	1.5	1.0	0.5	0.5	1.5	2.5	0.5
Ephedripites sp.																					●				
Microcachryidites antarcticus Cookson			●						0.5	1.0		1.0			1.0							0.5	0.5		1.0
Phyllocladidites mawsonii Cookson															●			●	1.0	●	●		●	●	0.5
P. palaeogenicus (Cookson & Pike)	●	0.5	●	●				0.5	1.0		1.0	0.5		●	1.0	●	0.5	0.5	0.5	0.5	0.5	0.5			0.5
Podocarpidites ellipticus Cookson	6.5	5.0	4.0	5.5	5.0	2.0	6.0	5.5	5.0	2.5	3.5	5.0	11.5	10.0	11.5	13.5	3.5	6.0	2.0	9.0	8.5	3.0	5.0	2.0	5.5
P. sp.																									
Angiosperms																									
Acaciapollenites myriosporites (Cookson)	0.5	0.5	1.0	●		●	●	●	●	●	●	●	●	●	0.5	●	●		●						
A. sp.													●												
Arecipites waitakiensis (McIntyre)		●	●		0.5		1.0	●	●	●	●			●		0.5		1.0	●	0.5	0.5		0.5	0.5	0.5
Banksieidites arcuatus Stover	●							●									●		●		●	●			
B. minimus Cookson	●		●															●							
Chenopodipollis chenopodiaceoides (Martin)	●	●		●	●	●		●	●	●		●	●		●		●	●	●		●	●	●		
Crotonipollis sp.	●	●	●	●																					
Cunoniaceae	1.0	0.5	1.0	1.0		0.5	1.5	1.0	1.0	1.0	●	●		0.5	0.5		4.5	1.0	1.0	1.5	2.5	4.0	0.5	●	1.5
Cupanieidites orthoteichus Cookson & Pike	●	●	●	●		●			0.5	1.0	●			0.5				●				●		●	0.5
C. reticularis Cookson & Pike																					●		●	●	●
Cyperaceaepollis spp.	2.0	2.0	2.0	2.5	24.5	27.5	3.5	5.5	5.5	2.0	7.5	4.0	0.5	●	2.5	2.0	1.0	●	●	1.0	●	●	0.5	2.0	1.5
Dicolpopollis cf. *metroxylonoides* Khan	●																								
Dilwynites granulatus Harris																				●	●	●			●
Echiperiporites sp.	●	●																				●	●		
cf. Elaeocarpaceae	1.0	0.5	1.0	0.5		1.0	0.5	1.0	●	0.5				0.5		1.0	1.0			0.5		4.0	1.0	1.0	●
Ericipites crassiexinous Harris	●	●	●	0.5			●	●	●													●			
E. scabratus Harris	●		●							●			●	●							●				
Glencopollis ornatus Pocknall & Mildenhall	●		●								●														
Gothanipollis sp.							●											●		●					●
Graminiidites spp.	0.5	0.5	2.0	2.0	10.5	5.0	1.0	1.0	0.5		2.0	1.0	●	●	●	0.5	1.5	1.0	●		0.5	0.5	●		0.5
cf. Gyrostemonaceae									●									●				●	●		
Haloragacidites haloragoides Cookson & Pike		●		●		●	●							●											
H. harrisii (Couper)	9.0	10.0	19.5	14.0	27.5	14.0	20.5	23.0	14.5	11.0	9.0	21.0	11.0	10.5	6.5	5.0	5.0	12.0	7.0	9.0	9.5	8.0	10.5	13.0	9.0

	MFP No.	8173	8172	8171	8170	8169	8168	8167	8166	8164	8163	8162	8161	8160	8159	8158	8157	8155	8154	8153	8151	8150	8152	8149	8148	8147
	Depth (m)	33.75	34.62	35.64	38.25	44.24	49.54	55.23	61.40	68.10	74.60	79.84	85.00	89.00	92.05	97.45	101.40	110.50	112.36	117.36	120.40	121.30	124.49	133.29	139.80	153.90
Haloragacidites sp.					●							●														
Ilexpollenites sp.		●	●	1.5	●		●		●			●										●				
Liliacidites spp.		0.5	1.0		●		0.5	0.5	0.5	0.5				●				●	2.0			0.5		0.5	1.5	
Malvacearumpollis sp.							●			●	●		●	●		●										
Malvacipollis subtilis Stover		0.5	1.5	●	●	2.5	●	●	0.5	●	1.0		●	0.5	1.0	0.5	0.5									
M. sp.		0.5	0.5		0.5		●		0.5		1.0	0.5	0.5	1.0	●	●			●			●	●	1.0	1.0	0.5
Margocolporites vanwijhei Germeraad,Hopping & Muller		●			●																					
Milfordia homeopunctata McIntyre		●			1.0			0.5		0.5		●	0.5	0.5	●	●	●		●	●	●		0.5		1.0	1.0
M. sp. cf. *M. hypolaenoides* Erdtman		●	●		1.0	●	0.5	0.5	●	0.5		●	1.0		●			1.0					0.5		1.5	2.0
Myrtaceidites eucalyptoides Cookson & Pike		9.5	4.0	4.5	3.5		4.5	1.5		0.5	1.0	1.5	1.5	0.5	5.5	12.5	8.5	7.0	1.0	0.5	2.0	2.0	2.5	0.5	1.5	
M. eugeniioides Cookson & Pike		2.5	●	0.5	0.5		●				0.5	●			2.5	1.5		●		●						
M. mesonesus Cookson & Pike		7.5	3.5	6.0	3.5		0.5	3.0		2.5	1.5	4.0	1.0	2.5	8.5	6.5	2.5	4.0	9.0	1.0	2.5	4.5	3.5	1.5	4.0	
M. parvus Cookson & Pike		14.5	10.0	14.5	20.5	1.0	5.0	14.0	1.0	16.5	17.5	16.0	6.5	9.0	18.5	8.0	7.5	32.5	21.5	9.5	8.5	10.5	17.0	23.0	12.5	5.0
M. rhodamnoides Martin				●		●	●	●	0.5						●	1.5	1.5	4.0	0.5		1.0	2.0	3.0	0.5		
M. verrucosus Partridge		●	●	0.5	●		●			1.0	●	●			●		●		●			●				
Nothofagidites asperus (Cookson)		0.5	2.0	●		0.5	1.5	2.5	0.5	1.0	1.0	1.0	2.0		●	0.5	0.5	●	●	0.5		0.5	0.5	1.0		0.5
N. brachyspinulosus (Cookson)				●		0.5	0.5				0.5				1.0		0.5			1.0	0.5	0.5	1.5	0.5	0.5	
N deminutus (Cookson)		0.5	0.5	1.5	1.0			2.0	1.0	●		●	0.5			●		●	2.0	8.0	1.0	4.0	1.0		2.0	0.5
N. emarcidus (Cookson)		14.5	10.5	8.5	18.5	3.0	5.5	4.5	14.0	10.5	14.5	6.5	4.5	4.5	10.0	10.5	13.5	6.0	20.5	28.0	17.5	24.0	17.0	24.5	16.5	25.5
N. falcatus (Cookson)		2.0	3.0	5.5	2.5		●	0.5	2.0	0.5	1.5	2.0	2.0	●	3.5		0.5	0.5	1.5	13.5	2.0	1.5	5.0	6.0	6.0	3.0
N. flemingii (Couper)							●	●								0.5	0.5	1.0	5.0	2.5	2.0	4.0	2.5	1.5		0.5
N. goniatus (Cookson)		0.5	1.0				0.5			●			●									●				
N. heterus (Cookson)		●	0.5	●		●		●		1.5	0.5	●	0.5	●	●	●	0.5		4.5	1.0	1.5	2.5	2.5	4.0	1.0	9.0
cf. *Nuxpollenites* sp.															●		●	●								
Perfotricolpites sp. cf. *P. digitatus* Gonzalez Guzman		●	●		●	●	●	●		●																
Periporopollenites sp.										●																
Polycolpites esobalteus McIntyre		●			●																	●				
P. reticulatus Couper		●										●			●											
P sp. *Utricularia*												●														
Polyorifices oblatus Martin		0.5	0.5		●		2.5		1.0	●		1.0			●	●	1.0	●	●		1.0	1.0	●	1.0	0.5	1.0
Propylipollis sp. cf. *P. annularis* (Cookson)					●									●	●								●	●		●
P. sp.			●				●																			
Proteacidites pachypolus Cookson & Pike		0.5	●			●		●		●		●								●						
P. rectomarginis Cookson																			●	●			●	●		●
P. symphyonemoides Cookson								●							●											
P. sp. cf. *P.symphyonemoides* Cookson		●																								
P. sp. cf. *P. simplex* Dudgeon		●	●	●						●																
P. sp. cf. *P. sinulatus* Dudgeon			●				●			●												●				
Psilodiporites sp. cf. *P. redundantis* Gonzalez Guzman		●	●				●			●	●		●					●	●		●					
Pseudowinterapollis calathus (Stover)							0.5	●																		
Quintinia psilatispora Martin		●	0.5	●	●					●	●							●					●			
Rhoipites alveolatus (Couper)		1.5	●		●																	●				
R. sphaerica (Cookson)		●		●																			●			
R. sp. C of Foster, 1982		0.5	●	●	●		0.5	●		0.5			●		●										0.5	
Sapotaceoidaepollenites rotundus Harris				●																●			●			
Sparganiaceaepollenites barungensis Harris		2.0	0.5	0.5	0.5	2.5	1.0	2.5	3.5	3.0	0.5	●	2.0	0.5	1.5	2.0	1.5	●	●	1.5	0.5	1.0		0.5	1.0	1.0
S. sp.		0.5	1.5	1.0	3.5	1.0	2.0	1.0	1.5	1.5	2.0	2.0	2.5	1.0		0.5					1.0	●	0.5	1.5	4.5	12.5
cf. *Sphenostemon*		●	●																							
Stephanocolpites oblatus Martin					●							●			●											
Symplocoipollenites austellus Partridge		●																								
Tricolporopollenites endobalteus McIntyre			1.5		0.5		1.0	●	0.5		0.5	1.0			0.5										0.5	
T. sp. cf. *T. endobalteus* McIntyre			●				●																			
T. spp.		3.0	5.5	6.5	2.5	3.5	5.5	5.0	6.0	8.0	11.0	9.5	3.5	4.0	3.5	12.0	6.0	12.0	3.0	8.5	9.5	9.5	9.0	4.0	8.5	7.5
Triporopollenites ambiguus Stover																						●				
T. bellus Partridge		0.5	●	●	●	●		●	●	●	●	●														
T. chnosus Partridge							●																			
Triporotetradites sp.		●	●	●																						
cf. *Weinmannia* sp.																		●				●				

20-9/26

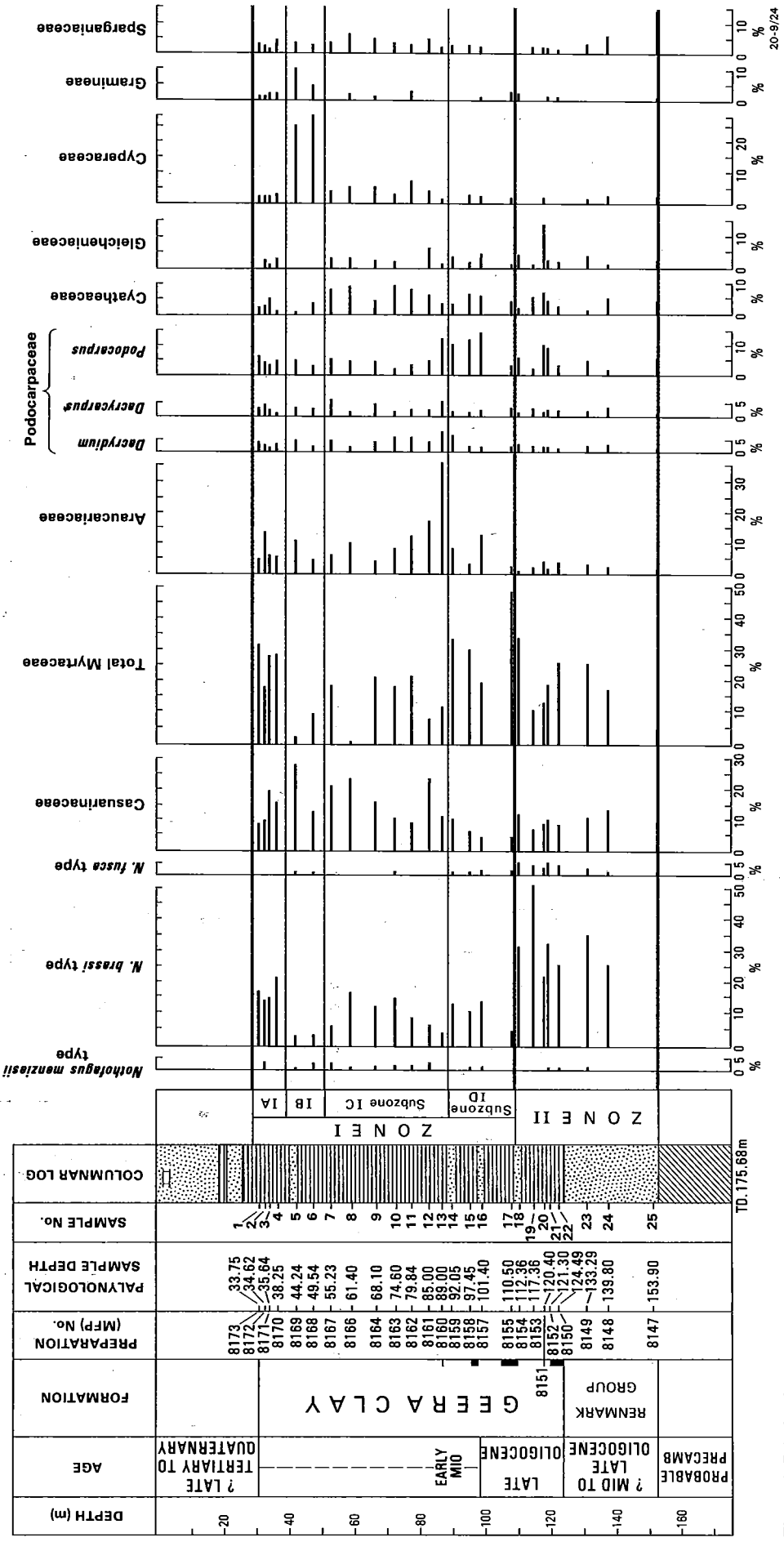

Figure 4. Relative frequencies of major pollen and spore taxa in Oakvale-1.
Based on counts of 200 grains per sample. Sample numbers shown include preparation numbers (MFP) and sample numbers used in PERCINF program (numbers 1–25). Zones I and II, with sub-zones IA to ID are those based on statistical identification of frequency changes.

continental sequences in the tropical regions of Africa, central America, and southeast Asia. Such species include the monolete fern spore *Polypodiisporites usmensis* van der Hammen, the tricolporate *Margocolporites vanwijhei* Germeraad, Hopping & Muller, and a tricolpate form very close to *Perfotricolpites digitatus* Gonzalez Guzman. Other forms close to taxa previously reported from tropical Tertiary sequences include spores with a morphological resemblance to *Baculatisporites scabridus* Playford, described from the New Guinea Neogene (Playford, 1982), and others similar to *Distaverrusporites simplex* Muller and *Polypodiaceoisporites retirugatus* Muller, both originally from the Tertiary of Borneo (Muller, 1968), and to *Dicolpopollis metroxylonoides* Khan, a palmoid pollen from the New Guinea Neogene (Khan, 1976). Pollen grains assigned to *Malvacearumpollis* and to *Psilodiporites* cf *P. redundantis* Gonzales Guzman, and those compared to the extant genus *Sphenostemon* are others with tropical fossil records or extant tropical distributions.

The Oakvale site has also provided good fossil records of some extant Australian taxa. *Acacia* pollen, for instance, is present from 117 m upwards: this is the first evidence to be published that *Acacia* was present in the late Oligocene in Australia — most previous accounts suggest that it appeared in the early Miocene (Stover & Partridge, 1973; Martin, 1978). The Oakvale core also contains a record of the wheel-fruit family Gyrostemonaceae in the Oligocene, and the second record of the tricolporate pollen that Kemp (1976) compared to *Diplopeltis* (but which is very close to the living *Dodonaea triquetra*). It has also provided the first fossil record in Australia of pollen of *Utricularia* and *Gardenia*.

Dinoflagellates

Marine dinoflagellate cysts were recorded consistently throughout Oakvale- 1, but reach their greatest diversity and abundance in lithologies such as the glauconitic sands, which indicate nearshore neritic environments. Within the finer-grained lithologies of the Geera Clay, dinoflagellate cysts are less abundant, and the distribution of individual long-ranging species is sporadic. For this reason a distribution or range chart is not presented here. Rather, it is more appropriate to consider the assemblage as a whole, with the samples from near the base of the Geera Clay being considered representative.

Species identified include: *Achomosphaera ramulifera* (Deflandre) Evitt 1963, *A. crassipellis* (Deflandre & Cookson) Stover & Evitt 1978, *A. sagena* Davey & Williams *in* Davey & others 1966, *Adnatosphaeridium* sp., *Apteodinium australiense* (Deflandre & Cookson) Williams 1978, *Areosphaeridium arcuatum* Eaton 1971, *Chiropteridium dispersum* Gocht 1960, *Cyclopsiella* cf. *C. elliptica* Drugg & Loeblich 1967, *Dapsilidinium pseudocolligerum* (Stover) Bujak & others 1980, *Glaphyrocysta* cf. *G.intricata* (Eaton) Stover & Evitt 1978, *Hystrichokolpoma rigaudae* Deflandre & Cookson 1955, *H.stellata* (Maier) Harris comb. nov., *Impletosphaeridium* sp., *Lingulodinium machaerophorum* (Deflandre & Cookson) Wall 1967, *Melitasphaeridium choanophorum* (Deflandre & Cookson) Harland & Hill 1979, *?Paucisphaeridium* sp., *Operculodinium centrocarpum* (Deflandre & Cookson) Wall 1967, *Pentadinium laticinctum* Gerlach 1961, *Polysphaeridium zoharyi* (Rossignol) Bujak & others 1980, *Pterodinium cingulatum* (O. Wetzel) Below 1981, *Saeptodinium* sp., *Spiniferites ramosus* (Ehrenberg) Loeblich & Loeblich 1966 complex, *S. trabeculiferum* (Deflandre & Cookson) Lentin & Williams 1973, *Systematophora placacantha* (Deflandre & Cookson) Davey & others 1969, *Tectatodinium pelitum* Wall 1967, and *Thalassiphora spinifera* (Cookson & Eisenack) Stover & Evitt 1978. The assemblages are generally dominated by the *S. ramosus* complex with *H. rigaudae*, *L. machaerophorum*, *O. centrocarpum* and *S. placacantha* as common components.

Australian dinoflagellate cyst assemblages of mid-Tertiary age have received little attention in the literature since Deflandre & Cookson (1955) described several new species and illustrated others from Balcombe Bay, Victoria. These included: *Apteodinium australiense*, *Lingulodinium machaerophorum*, *Operculodinium centrocarpum*, *Pterodinium cingulatum*, *Rottnestia borussica* (Eisenack) Cookson & Eisenack 1961, *Spiniferites bulloideus* (Deflandre & Cookson) Sarjeant 1970, *S. hyperacanthus* (Deflandre & Cookson) Cookson & Eisenack 1974, *S. ramosus*, *S. trabeculiferum*, and *Systematophora placacantha.*

Nematosphaeropsis balcombiana Cookson & Eisenack 1955 was described from sediments of similar age from the Gellibrand Clay, Western Victoria. Whilst the assemblage described here has many similarities to the list of Balcombe Bay species, a detailed comparison would require a re-study of the Balcombe Bay assemblages. There is, however, some suggestion that the presence of *P. laticinctum*, *C. dispersum* and *G.* cf. *G. intricata* in the Oakvale assemblages indicates an older age.

Comparison of the Oakvale assemblages with suites from outside Australia shows that, apart from well-documented assemblages from Europe (Brosius, 1963; Benedek, 1972; Chateauneuf, 1980; Eisenack, 1954; Gerlach, 1961; Gocht, 1969; Maier, 1959), there is little else with which they may be compared. Drugg & Loeblich (1967) described four new species of dinoflagellates from the Eocene and Oligocene of the Gulf Coast, U.S.A., and Stover (1977) documented a well-dated Oligocene to Miocene sequence from the Blake Plateau, in which *Deflandrea* spp. and *Wetzeliella* spp. range throughout the Oligocene, and *Tuberculodinium vancampoae* begins its range in the early Miocene.

A Miocene assemblage described by Shimakura & others (1971) from Japan has several species in common with both the Balcombe Bay assemblage and that described here from Oakvale. Their assemblage, however, lacks *P. laticinctum*, *C. dispersum* and *G.* cf. *G. intricata*. *T. vancampoae* was recorded, suggesting that the assemblage described from the Sea of Japan is younger.

Oligocene–Miocene dinoflagellate assemblages from Norwegian–Greenland Sea sediments (Manum, 1976) are essentially similar, but are clearly more diverse; however, *C. dispersum* does not appear above the middle Oligocene. Nor are *Deflandrea* or *Wetzeliella* species recorded above the late Eocene.

As previously noted, European Oligocene and Miocene assemblages have been discussed by a number of authors. The early Oligocene (Eisenack, 1954; Gocht, 1969; Chateauneuf; 1980) is distinctly different from the Oakvale material. In particular, *Deflandrea* spp. and *Wetzeliella* spp. (sensu lato) are absent from Oakvale, but prominent components of the European assemblages. Gerlach (1961, p. 218) recorded both genera from the middle and late Oligocene of Germany, but not from the Miocene. In other aspects the assemblages are similar, except for the greater diversity of the German assemblages. Similar conclusions can be drawn also from Brosius (1963). Benedek's (1972) monograph on assemblages from the Tonisberg Shaft, Krefeld, lists 140 species from the middle and late Oligocene sequence, with both *Deflandrea* spp. and *Wetzeliella* spp. ranging throughout.

Gamerro & Archangelsky (1981) list sixteen species from the Miocene–Pliocene of Colorado Basin of Argentina, and the species appear comparable with those at Oakvale. *T. vancompoae*, however, appears to range from the Oligocene.

In conclusion, the assemblages from Oakvale are broadly comparable with assemblages of similar age elsewhere. However, it appears that certain groups of species, particularly those with peridinoid characteristics (e.g. *Deflandrea*, *Wetzeliella* sensu lato and *Palaeocystodinium*) did not persist in the region. These groups in southern Australia were prominent in late Eocene and early Oligocene assemblages. The absence of *T. vancompoae* possibly indicates an age no younger than early Miocene.

Non-marine algae

In addition to dinoflagellate cysts of marine origin, freshwater algae are present throughout the Oakvale-1 section, probably reflecting drainage to the site through lakes and swamps. *Botryococcus*, *Pediastrum*, and some spores of Zygnemataceae occur throughout, with *Pediastrum* the most common form. An abundance of *Pediastrum* in Quaternary sediments at Lake George, New South Wales, has been interpreted by Singh & others (1981) as reflecting prolonged open-water conditions; high frequencies at the Oakvale site may thus mean that drainage to the depositional area was through long-lived lakes. *Pediastrum* is most abundant at 44.24 m; residue from this sample is dominated by large, intact colonies of the alga. The abundances of grass and sedge pollen also peak at this depth, confirming the proximity of swamp and lake-margin vegetation. Also notable in the sequence are cysts of a probable freshwater dinoflagellate, *Saeptodinium* sp. (Fig. 11B,C), and a probable algal aplanospore (Fig. 9W,X,Y) of unknown affinity.

Palynological biostratigraphy

As noted above, reference sections for Australian Tertiary palynology, utilising pollen and spores, have been developed in the Gippsland and Otway Basins in southeastern Australia (Stover & Evans, 1973; Stover & Partridge, 1973; Harris, 1971). The Gippsland Basin contains the most complete sedimentary record for the Tertiary, and has been most intensely studied from a palynological viewpoint. Palynological zones erected in that basin have been correlated with planktonic foraminiferal zones (Abele, 1976, table 8.1) and thus integrated into a global Tertiary time scale.

In practice, recognition of the palynological zones in the Gippsland Basin depends on the first appearance in time of a limited number of taxa, which unfortunately makes their recognition difficult away from the basin in which they were originally defined. Martin's (1977) study of sediments in the Hay—Balranald—Wakool area of the eastern Murray Basin emphasised this difficulty; in particular, she found it hard to identify subdivisions within the Oligocene–Miocene *Proteacidites tuberculatus* Zone. Pollen types regarded as time markers in the Gippsland Basin are rare in the Murray Basin, and the zone could thus be divided only on broad characteristics of the assemblages. Because the aim of the present study is to provide a biostratigraphic standard that can be used in inland regions, well away from the coastal basins that have up till now provided the stratigraphic reference sections, we are hesitant to place too much emphasis on identifying the Gippsland Basin zones; nonetheless we have tentatively identified some zone boundaries. These are noted in Figure 2, together with plots of the distribution of all those taxa with restricted ranges in the sequence, and with the quantitative data presented in Figure 4, should provide a basis for future comparisons for inland sequences that lack faunas for dating.

Quantitative zonation

To aid description and quantify changes occurring through the Oakvale-1 pollen diagram (Fig. 4), zone boundaries have been drawn between samples where major pollen changes occur. These zones have been statistically calculated with the aid of the computer program PERCINF (Kershaw & Sluiter, 1982), which measures the similarity of adjacent pairs of pollen spectra by an extension of the information statistic devised by Dale & others (1971) and expresses it as a hierarchical grouping structure (Fig. 5). PERCINF is based on the pollen zonation computer program CONSLINK of Gordon & Birks (1972), and both programs are designed to handle quantitative data in percentage form.

The results of the analysis are shown in Figure 5. A major break in the hierarchical grouping structure (Fig. 5) occurs between samples 17 and 18, i.e. between 110.50 m and 112.36 m (Fig. 4). At this point the pollen diagram is divided into Zone I (samples 1–17) and Zone II (samples 18–25). There are minor breaks between samples 4 and 5, 6 and 7, and 13 and 14 in Zone I (Fig. 5), which is thus divided into four sub-zones.

Zone II (samples 25–18) has the highest *Nothofagus brassi* group values, although they vary from 22 per cent (sample 20) to 51 per cent (sample 19). Myrtaceae are also very well represented, and generally increase from the base of the zone to the top. Casuarinaceae are moderately well represented throughout, with *Podocarpus/Dacrydium* the best represented of the remaining taxa. Zone II also contains the only significant record of *Nothofagus fusca* group pollen, although it is less than 5 per cent of total pollen. Sparganiaceae and Gleicheniaceae are sporadically abundant.

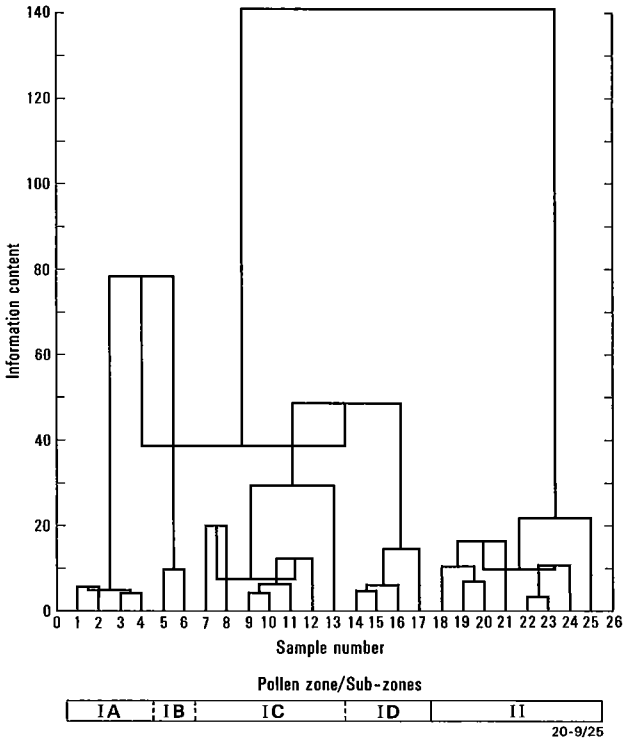

Figure 5. PERCINF — Stratigraphically constrained hierarchical classification of Oakvale-1 samples.

Sub-zone ID (samples 14–17) shows a marked reduction in *N. brassi* group values, to less than 15 per cent; Myrtaceae generally increase, as do Araucariaceae and *Podocarpus/Dacrydium*. Most other taxa are poorly represented, with the exception of Casuarinaceae, which is consistently represented. Two of Lindsay's (1983) four recognisable phases of intensified marine influence occur within this sub-zone.

Sub-zone IC (samples (7–13) is characterised by falling Myrtaceae values (generally less than 20%) with a concomitant increase in Casuarinaceae, Araucariaceae, Cyatheaceae, and, to a lesser extent, Cyperaceae, *Dacrycarpus* and *Dacrydium*; the last two reach their highest values, although these remain less than 5 per cent. Araucariaceae values are highest at the base of the subzone, while *N. brassi* group values remain at less than 15 per cent.

Sub-zone IB (samples 5 and 6) is dominated by high Cyperaceae values. Myrtaceae, *N. brassi* group and Cyatheaceae drop to their lowest levels, while Araucariaceae and Casuarinaceae remain moderately well represented. Poaceae (Gramineae) are significant only in this sub-zone.

Sub-zone IA (samples 1–4) is clearly dominated by high Myrtaceae and moderately high *N. brassi* group. Cyperaceae and Poaceae have decreased to very low levels. The representation of other taxa is very similar to that in sub-zone IC.

Comparison with Gippsland Basin spore-pollen zones

In terms of previously established zones, the main conclusions we have drawn are as follows.

1. It is possible to tentatively identify the base of the *Triporopollenites bellus* Zone of Stover & Partridge (1973) at 80 m in Oakvale-1. The nominate species is consistently present from 80 m upwards. The identification of this level with the base of the *T. bellus* Zone is tentative, because few of the index species of the zone were recorded. Of the six species described by Stover & Partridge as defining the zone base, only *T. bellus* appears at that level. Two other species, *Symplocoipollenites austellus* Partridge and *Proteacidites symphyonemoides* Cookson, appear in the Oakvale sequence *above* the appearance of *T. bellus*, the former at 55 m, the latter at 33 m. Another stratigraphically useful species, *Haloragacidites haloragoides* Cookson & Pike, which in the Gippsland Basin appears above the base of the *T. bellus* zone, first appears in Oakvale-1 below the level at which *T. bellus* appears consistently. Because of these apparent discrepancies in the ranges of key taxa, we cautiously place the base of the *T. bellus* Zone at 80 m in Oakvale. We have sampled much closer in the Oakvale section than Stover & Partridge (1973) did in their initial setting up of the Gippsland Basin zones, and this finer resolution, combined with local factors of vegetation distribution, may account for the discrepancies in the time of appearance of species between the Gippsland and Murray Basins.

The *T. bellus* Zone, according to Stover & Partridge (1973), is essentially late Miocene. Its base, however, according to the correlation charts presented in Abele (1976), lies in the latest early Miocene, probably in the planktonic foraminiferal zone N8. This, on present intercontinental correlations, as summarised by Harland & others (1982), would be 15–16 Ma old.

2. All the Geera Clay above 80 m is tentatively assigned to the *T. bellus* Zone, with the top of the unit in Oakvale-1 being no younger than approximately mid-Miocene. Evidence for such an age limit is poor, however. It is based on the observation that the floras in the Geera Clay are essentially uniform throughout, without major changes suggestive of time breaks. The only observable change occurs near the top of the Geera Clay section, where samples from 36.25 m to 33.75 m contain a higher diversity of species than those below and include the first appearances of *Margocolporites vanwijhei*, *Crotonipollis* sp., and *Triporotetradites* sp. As the first-named of these has not previously been recorded in Australia, and the other forms are undescribed, their stratigraphic significance cannot be assessed. For the present, we prefer to consider this uppermost interval of the Geera Clay as reflecting a minor, probably local, environmentally determined vegetation change of no time-stratigraphic significance.

3. The interval between 153.97 m and 80 m, encompassing the lower part of the Geera Clay and what Lindsay (1983) referred to as the Warina Sand of the Renmark Group, can, in terms of its overall composition, be equated with the *Proteacidites tuberculatus* Zone. In the Gippsland Basin, this zone was divided into three sub-zones by Stover & Partridge (1973); however, as reported by Martin (1977a), it has proved extremely difficult to identify these sub-zones away from their basin of deposition.

The uppermost subdivision of the *Proteacidites tuberculatus* Zone is defined, in the Gippsland Basin, by the first appearance of *Acaciapollenites myriosporites* (Cookson) and *Psilastephanocolporites micus* Partridge. In Oakvale-1, *Acaciapollenites myriosporites* is consistently present in samples from 117.36 m upwards but *P. micus* has not been recorded. The presence of *Acaciapollenites* might support the interval 117–80 m in the Geera Clay being equated with the upper *P. tuberculatus* Zone of the Gippsland Basin. There is a discrepancy, however, in correlating this interval with foraminiferal zones as these have been identified in the Murray and Gippsland Basins. The base of the upper part of the *P. tuberculatus* Zone in the Gippsland Basin, according to Stover & Partridge (1973), lies approximately at the Oligocene–Miocene boundary. In Oakvale-1, however, the foraminiferally determined Oligocene–Miocene boundary lies above 99 m, well above the appearance of the palynological marker species. This apparent discrepancy highlights the problems associated with the recognition of biostratigraphic units based on small numbers of marker species. It may reflect different pollen ranges in the two basins — in particular it seems possible that *Acacia* pollen appears earlier in the Murray Basin than it does in the Gippsland.

The unit below the Geera Clay, which we have referred to the Olney Formation, shows very little difference, either in terms of quantitative or qualitative palynology, from the clays above. Thus, it seems unlikely that there is any significant age difference between the two units. We therefore assign the interval to the middle of the *Proteacidites tuberculatus* Zone and consider a mid to late Oligocene age likely.

Recycled palynomorphs

The palynological assemblages from Oakvale-1 contain a number of species that are clearly recycled from older sediments. Spores and pollen of Early Cretaceous age occur in the upper part of the Geera Clay, and forms of Permian age have been noted throughout the sequence, but are found most consistently in the upper Geera Clay. The stratigraphic levels at which the redeposited taxa occur are shown in Figure 2; the taxa identified and their distribution are shown in Table 2.

RECYCLED FORMS	Depth (m)	MFP No.	8173	8172	8171	8170	8169	8168	8167	8166	8164	8163	8162	8161	8160	8159	8158	8157	8155	8154	8153	8151	8152	8150	8149	8148	8147
			33.75	34.62	35.64	38.25	44.24	49.54	55.23	61.40	68.10	74.60	79.84	85.00	89.00	92.05	97.45	101.40	110.50	112.36	117.36	120.40	121.30	124.49	133.29	139.80	153.90
CRETACEOUS																											
Aequitriradites spinulosus (Cookson & Dettmann)					●																						
Callialasporites dampieri (Balme)											●																
C. trilobatus (Balme)			●				●																				
Cicatricosisporites australiensis Cookson			●																								
Classopollis sp.				●																							
Ischyosporites punctatus Cookson & Dettmann					●																						
Leptolepidites verrucatus Couper												●			●												
Lycopodiumsporites austroclavatidites (Cookson)				●								●															
Neoraistrickia truncatus (Cookson)				●																							
PERMIAN																											
Didecitriletes uncinatus (Balme & Hennelly)				●																							
D. sp. cf. *D. ericianus* (Balme & Hennelly)			●																								
Dulhuntyispora parvithola (Balme & Hennelly)											●																
Granulatisporites micronodosus Balme & Hennelly				●																							
Marsupipollenites striatus Balme & Hennelly						●	●																				
M. sp.					●																						
Praecolpatites sinuosus (Balme & Hennelly)											●																
Protohaploxypinus spp.					●	●	●					●															●

20-9/27

Permian spores and pollen are mostly well preserved. The list in Table 2 includes some types, such as the taeniate disaccate pollen *Protohaploxypinus*, and species of *Marsupipollenites*, which are relatively long-ranging through the Permian; and others, such as *Didecitriletes uncinatus* (Balme & Hennelly), *Dulhuntyispora parvithola* Balme & Hennelly, and a species tentatively referred to *Didecitriletes ericianus* (Balme & Hennelly), which are restricted to Late Permian sequences. *Dulhuntyispora parvithola*, in particular, is diagnostic of Upper Stage 5 of the palynostratigraphic sequence in common usage in eastern Australia (Kemp & others, 1977; Price, 1983).

There is no ready explanation for the presence of Late Permian palynomorphs in the Geera Clay at Oakvale-1, as there are no sequences of that age known to be present now in the general region of the western Murray Basin. The graben-like structures of the Renmark, Tararra and Menindee Troughs in the western part of the basin contain Cape Jervis beds equivalents, which yield Stage 2 microfloras of probable Late Carboniferous age (O'Brien, 1981). The only known sequences of Late Permian age in the Murray Basin are the Coorabin Coal Measures, which underlie Mesozoic and Cainozoic units in the Oaklands–Coorabin area of the eastern Murray Basin. The Coorabin Coal Measures do contain Stage 5 microfloras (Morgan, 1977), including *Dulhuntyispora parvithola* and other species indicative of upper Stage 5. In the Ovens Graben the Coorabin Coal Measures extend as far north as the Murrumbidgee River, so it seems possible that this area could have provided a source for recycled material within Oligocene–Miocene sediments of the western basin. Alternatively, and perhaps more likely, Late Permian sediments, equivalent to those now preserved in the Oaklands area, were formerly much more widespread, and the recycled material at Oakvale derives from beds further west, which are now eroded.

It is of interest to note that Permian palynomorphs are commonly recycled into Tertiary sediments in other areas of southeastern Australia. Harris (1965) described them from the Otway Basin sequences in western Victoria, and they are known, from unpublished data, to occur in Tertiary rocks in the offshore Bass Basin. Source areas for these occurrences remain unknown.

The Cretaceous element in the Geera Clay consists entirely of spores and pollen; no marine dinoflagellate cysts were recorded. Given the known diversity of Early Cretaceous spore and pollen assemblages in southeastern Australia, the recycled suite from Oakvale-1 is rather impoverished; the combined stratigraphic ranges of the taxa identified suggest their derivation from beds of latest Jurassic through Neocomian age. Sources could lie either within or beyond the present geographic limits of the Murray Basin. Within or, more accurately, below the present basin, Early Cretaceous sequences are known from the Loxton area (Ludbrook, 1961), from northwestern Victoria (Douglas & others, 1976), and from the Ivanhoe area in the eastern part of the basin (Evans & Hawkins, 1967; McMinn, 1981a). The sequence at Ivanhoe, where non-marine beds of Neocomian age are present, appears to contain the oldest Cretaceous rocks known within the basin; in the Loxton area the predominantly marine sequence spans the Aptian/Albian.

Given the rather limited assemblage of recycled Cretaceous microfossils in Oakvale-1, it is hazardous to predict a precise source. They may have come from sequences such as those mentioned above, which might formerly have been widespread, or they could have come from further afield, perhaps from southern parts of the Great Artesian Basin via an ancestral Darling River drainage.

Comparison with other Oligocene–Miocene palynofloras

A comparison of the spore and pollen assemblages from this western Murray Basin site with others in southeastern Australia and in New Zealand shows that it is, within southeastern Australia at least, a distinctive suite of palynomorphs. This distinctiveness from previously described assemblages lies principally in (a) the relatively high frequencies of taxa of open vegetation types; (b) the importance of the Myrtaceae and Araucariaceae; and (c) the occurrence of the 'tropical Tertiary' pollen taxa. The

differences between pollen assemblages from these sites and those from Oakvale-1 are elaborated below.

Eastern margin of the Murray Basin

Palynological assemblages from the eastern margins of the Murray Basin, in the Hillston, Hay, and Narrandera areas of western New South Wales, have been described by Martin (1977a, 1984). Relative frequencies of pollen types in these were also presented by Martin (1978). The deposits from which these were described are mostly lignites and carbonaceous clays of the Olney Formation, deposited in fluvio-lacustrine and swamp environments. The *Proteacidites tuberculatus* Zone is thick (up to 170 m) in this region, and most lignites and carbonaceous sediments fall within this zone. The younger *Triporopollenites bellus* Zone is also present, though less widely recognised, and the sequences are characterised by an upwards decrease in the carbonaceous content of sediments.

Assemblages from these biostratigraphic units in the eastern Murray Basin show a broad basic similarity with those from Oakvale, being characterised by *Nothofagidites*, especially *N. brassi* types, and by Myrtaceae and Casuarinaceae as dominants. There are differences, however, between the sites on the eastern and western margins of the Murray Basin: the Oakvale site, for instance, has a higher frequency of Araucariaceae and a greater abundance of the pollen of open vegetation taxa — the grasses and sedges. The diverse 'tropical Tertiary' suite of spores and pollen grains described above from Oakvale has not been reported from the eastern Murray Basin.

As noted, Martin (1977a), in her initial study, found great difficulty in subdividing the *P. tuberculatus* Zone, because of the rarity of marker species. In order to effect sub-divisions with at least local value in bore to bore correlation, Martin (1984) has used peak abundances of selected pollen types. These pollen types include *Phyllocladidites mawsonii* Cookson, akin to pollen of Tasmania's extant Huon Pine, *Lagarostrobus franklinii* (Hook f.); *Nothofagidites flemingii* Couper, a grain of the *Nothofagus fusca* type; and high Myrtaceae to *Nothofagus* ratios. Of these, *Phyllocladidites mawsonii* is only very sporadically represented in the Oakvale sequence, whereas in the eastern Murray Basin it occasionally occurs in frequencies as high as 10–12 per cent of the pollen count. The reasons for the differences between the two areas are both stratigraphic and, probably, geographic. They are stratigraphic in that the peak frequencies of *P. mawsonii* occur in what has been tentatively identified as the lower unit of the *P. tuberculatus* Zone in the eastern Murray Basin; this interval may not have been penetrated in Oakvale-1, although there is a clear indication there that *P. mawsonii* becomes consistently present, in low frequencies, towards the base of the penetrated sequence. Restrictions in the geographic distribution of *P. mawsonii* have been described by Martin (1984), who noted that high ratios of the species are most common in the southern part of the Murray Basin, a distribution that may to be linked with climatic and hydrological factors that together would provide the wetter conditions more conducive to its expansion.

High frequencies of *Nothofagidites flemingii* were identified by Martin (1984) at two levels in the eastern Murray Basin; these she considered to lie near the base and in the upper part of the *P.tuberculatus* Zone. In Oakvale-1, *N. flemingii* is rare, except for an interval between 112 and 124 m, where it is present in frequencies of 3–5 per cent of the total pollen count. This 'peak' is associated with rare *Proteacidites rectomarginis* Cookson and rare *Phyllocladidites mawsonii*, an association that Martin used to identify the lower of her two high-frequency levels. However, foraminiferal data from Oakvale indicate a late Oligocene age for this peak, which is in contrast to the early Oligocene age generally accepted for the lower *P. tuberculatus* Zone. This discrepancy may reflect poor age control in the eastern Murray Basin or, alternatively, it may simply mean that the interval of high *N. flemingii* in Oakvale-1 represents a local, rather than a basin-wide increase in the frequency of this pollen type.

The other marker used by Martin (1984) is a high ratio of Myrtaceae to *Nothofagus* — usually 0.8 and above. Figures in the high ratio range occur in Oakvale throughout most of the sequence — at least from 133 m upwards. This means that, in general, myrtaceous pollen is much more abundant in the *P.tuberculatus* Zone interval there than it is in the eastern Murray Basin. In Oakvale-1, the frequency of *Nothofagus* type pollen declines markedly in the basal part of the Geera Clay (Fig. 4). This late Oligocene age for the decline in *Nothofagus* differs from that in the eastern Murray Basin, where Martin (1977a, 1978) drew attention to a decline in *Nothofagus* frequencies in the early Miocene, pointing out that this in turn was earlier than the frequency drop in coastal Victoria suggested by Stover & Partridge (1973).

Latrobe Valley, Victoria

In the Latrobe Valley, the interval coeval with the Geera Clay, spanning the *P. tuberculatus* and *T. bellus* Zones, includes the Morwell and Yallourn coal seams and interseam sediments. The palynology of the younger Yallourn Seam was described in detail and interpreted in terms of plant communities by Luly & others (1980). The Morwell seams were similarly treated by Kershaw & Sluiter (1982), and the two seams were compared in Sluiter & Kershaw (1982). Stover & Partridge's (1973) study was largely concerned with correlating these onshore sediments with those of the offshore Gippsland Basin, and hence was less concerned with quantitative palynology. In the Latrobe Valley studies, the palynological assemblages were shown to vary systematically with variations in lithotype. In the Oakvale well, no such correlations were attempted. This difference in the level of detail examined between the two studied areas means that comparisons between pollen spectra from the sequences can be made in broad terms only, as this variable is not allowed for.

Similarities between the pollen spectra from the two regions are the high frequencies of *Nothofagus* pollen, especially that of the *N. brassi* type, and high frequencies of Myrtaceae and Casuarinaceae. *N. brassi* figures for Oakvale are, however, lower than they are in the Latrobe Valley. In both regions, the frequency of *Nothofagus* declines with decreasing age. As mentioned above, at the Oakvale site the marked frequency drop occurs in the late Oligocene *P. tuberculatus* Zone; Stover & Partridge (1973) suggested that this decline was gradual throughout the late Miocene in the Gippsland Basin. However, Kershaw & Sluiter (1982) and Kershaw & others (in press) have demonstrated that in the Latrobe Valley coal measures, major increases in the importance of Myrtaceae, usually accompanied by increases in Elaeocarpaceae, occur significantly from the early Miocene to the mid-Miocene. Minor reversions to *Nothofagus brassi* dominance occur throughout this period, and again throughout at least part of the mid to late Miocene (Dawson, 1983). It remains unclear as to whether any significant decline in the importance of the genus occurs before the Pliocene. Points of significant difference between the western Murray Basin sequence and those of the Latrobe Valley are: the much higher frequency of araucarian pollen and other conifers, especially *Dacrycarpus* (as *Dacrycarpites australiensis* Cookson), but also *Dacrydium* in the former; the lower frequency in Oakvale

of the rainforest angiosperms Elaeocarpaceae and Cunoniaceae; a much higher frequency at Oakvale of grass pollen, and the presence there of Cyperaceae, frequently in significant amounts, which contrasts with its virtual absence in the Latrobe Valley; and the consistent presence of *Acacia* at Oakvale, and its absence from the Latrobe Valley. The assemblages from Oakvale are unique among described floras in Australia in their component of 'tropical Tertiary' spores and pollen — none of the forms in this category have been reported from the Latrobe Valley.

Southeastern highlands of Australia

Assemblages correlative with the *P. tuberculatus* and *T. bellus* Zones have been described from a number of sites in the southeastern highlands of Australia. These include pollen suites from sediments interbedded with or overlain by basalts at Cadia and Kiandra in New South Wales (Owen, 1975), and from lake deposits extensively developed near Cooma, also in New South Wales (Tulip & others 1982).

Kiandra. At Kiandra, fluvio-lacustrine sedments, including carbonaceous clays, underlie basalts radiometrically dated at 18–22 Ma. Owen (1975) extracted diverse microfloral assemblages from the sediments, which she considered to represent the middle *P. tuberculatus* Zone. They are thus equivalent to or slightly older than the oldest assemblages recovered from Oakvale-1. The assemblages described by Owen are in general dominated by *Nothofagus*, especially of the *N. brassi* type, with minor *N. menziesii* and very limited *N. fusca* forms. A variety of podocarps is present, in frequencies up to 16 per cent, and fern spores are common locally. The percentages of Araucariaceae, Casuarinaceae, and Myrtaceae are, in general, considerably lower than the frequencies of these taxa at the Oakvale site.

Cadia. At Cadia, near Orange, sediments interbedded with basalts 10–12 Ma old contain microfloral assemblages that accord with a middle to early-late Miocene age (Owen, 1975). They may thus be younger than the uppermost sections represented in Oakvale-1, although not significantly so. At Cadia, *Nothofagus* types, chiefly *N. brassi*, occur in frequencies of 14–60 per cent, which is higher than the usual frequencies at Oakvale, where the decline in *Nothofagus* occurred earlier. Counts for Casuarinaceae are comparable between the two sites, but Araucariaceae, Gramineae, and Myrtaceae are much more prominent at Oakvale than at Cadia. Cyperaceae, which is locally abundant at Oakvale, and the 'tropical Tertiary' component were not reported from Cadia.

Lake Bunyan. Pollen and spore assemblages from coals and carbonaceous clays in lacustrine sediments at Lake Bunyan, near Cooma, were attributed tentatively to the lower *T. bellus* Zone by Tulip & others (1982). If this age assessment is correct, they should be coeval with assemblages from the upper part of the Geera Clay at Oakvale-1. However, the assemblages from the two sites differ significantly. In Lake Bunyan, diversity is low, perhaps as a consequence of the cooler highland environment. *Nothofagus brassi* group forms are abundant and *N. menziesii* and *N. fusca* types are locally common, reaching frequencies of 15 and 17 per cent, respectively. These groups together with the Podocarpacae are more frequent at Lake Bunyan than at Oakvale. The composition of the conifer element differs also — at Lake Bunyan, *Podosporites microsaccatus* (Couper) Dettmann is a major component in the pollen spectrum: at Oakvale-1, it is rare. Araucariaceae are abundant at Oakvale, but rare at Lake Bunyan. The impoverished Lake Bunyan assemblage lacks the rainforest angiosperm component, such as Elaeocarpaceae, Cunoniaceae, and *Quintinia*, which are consistently present, although in low frequencies, at Oakvale. Taxa representative of open (e.g. Casuarinaceae) and herbaceous vegetation, and some bryophytes are also much more abundant in the western Murray Basin than they are at this montane site.

Home Rule, Gulgong. Assemblages from sub-basaltic sediments at the Home Rule kaolin deposit, near Gulgong, were briefly described by McMinn (1981b). Details provided are too sparse for detailed comparisons to be made with these mid to late Miocene assemblages, but, from the available data, it appears that they too lack the diversity apparent in the Murray Basin floras — they lack the grasses and sedges, the abundant Araucariaceae, Myrtaceae, and *Acacia*.

Pioneer, northeastern Tasmania. At Pioneer, in the Ringarooma Valley of northeastern Tasmania, Hill & Macphail (1983) used both macrofossil — chiefly leaf — and pollen data to reconstruct Oligocene vegetation. They considered the pollen assemblages to be correlative with the lower *P. tuberculatus* Zone and, hence, probably somewhat older than the sequence in Oakvale-1. Nevertheless, a comparison with assemblages from the older part of the sequence at Oakvale may highlight broad regional differences in the vegetation. Both assemblages are dominated by pollen of the *Nothofagus brassi* type, but it is more abundant at Pioneer. There too, pollen of the *N. menziesii* type (as *Nothofagidites asperus* (Cookson) is more common. Both sites have a significant conifer component, but compositional differences exist between them; for example, both *Phyllocladidites mawsonii* and *P. palaeogenicus* are much more abundant at Pioneer than at Oakvale, and *Podosporites erugatus* Mildenhall, which has affinity with *Microstrobus*, is unrecorded at Oakvale. The angiosperm component shows both similarities and differences between the two sites. In the presence of the rainforest Elaeocarpacaeae, Cunoniaceae, and *Quintinia*, and the rainforest associate Gyrostemonaceae, the sites show similarities in minor but ecologically significant elements. The Murray Basin assemblage, however, lacks large periporate forms such as *Periporopollenites demarcatus* Stover, which is common at Pioneer. This and the presence of *Acacia* at Oakvale but not at Pioneer may be related to age differences between the assemblages, with the Oakvale assemblage being slightly younger. The very high abundance of Myrtaceae at Oakvale, however, which contrasts with its poor representation at Pioneer, is due probably to ecological rather than age differences.

Comparisons with New Zealand

Sediments, including lignites, from Southland, New Zealand, contain rich spore and pollen assemblages of late Oligocene through Miocene age. These have been described by Pocknall (1982) and Pocknall & Mildenhall (1984).

The assemblages from the Australian and New Zealand sites show considerable similarity in over-all composition, and also in some of the rarer angiosperm elements. Such similarities may reflect similar coastal/estuarine habitats, with pollen from both local marsh and more remote rainforests being deposited together. In terms of the dominant taxa in the pollen assemblages, both areas are distinguished by abundant *N. brassi* group pollen and by common Podocarpaceae, Araucariaceae, and Casuarinaceae. In the Murray Basin, Myrtacaeae are among the dominants: in the New Zealand assemblage they are less abundant.

The group of taxa that in Oakvale-1 are referred to broadly as the 'tropical Tertiary' group have representatives in the New Zealand suite. Common to both assemblages are *Malvacearumpollis*, *Margocolporites vanwijhei*, and

Perfotricolpites sp. cf. *P. digitatus*. Other shared taxa include Elaeocarpaceae, *Quintinia*, and *Weinmannia* (Cunoniaceae). Differences among the minor taxa include the diversity of Liliaceae in New Zealand, compared to its relative scarcity in the Murray Basin, and the presence only in New Zealand of a number of pollen types assigned to the Onagraceae — types such as *Epilobium* and *Corsinipollenites*.

Vegetation communities and palaeoclimatic considerations

The Oakvale site, on the basis of sedimentological models that have been developed for the Murray Basin (Brown, 1984), was probably situated in a position where it received pollen from a variety of different habitats (Fig. 3). As has been shown, the pollen assemblages differ from sites of similar age in southeastern Australia, in that they contain an unusual combination of taxa from rainforest and herbaceous vegetation formations. In this section, we describe in more detail the nature of the vegetation in existence at Oakvale throughout the depositional period, and offer some interpretations about possible palaeoclimates. The likely vegetation existing during the times represented by Zone II and Zone I samples is treated separately below. The discussion has been structured in this way to emphasise the major vegetation change occurring at the Zone II/Zone I boundary.

The late Oligocene evergreen rainforest period (Zone II)

The co-dominance of *Nothofagus brassi* group pollen and Myrtaceae (Fig. 4) in the late Oligocene in southeastern Australia is unique to this site. Similar assemblages have been reported, however, for the early Miocene in both the eastern Murray Basin and the Latrobe Valley, Victoria. In the late Oligocene at all other sites in southeastern Australia, *N. brassi* dominates pollen assemblages, a situation which prompted previous workers to invoke the existence of extensive *N. brassi* beech-dominated forests (see Kemp, 1978 for a summary). In these earlier accounts, little attention was paid to numerically subordinate taxa, and even less to detailed pollen production and dispersal studies carried out in New Guinea (Powell, 1970; Hope, 1973, Martin, 1978) and Australia (Kershaw, 1973) in rainforest vegetation communities that probably provide the closest living analogues to the Tertiary communities.

The New Guinea situation is particularly relevant, because of the existence there of large tracts of evergreen beech and mixed beech rainforests. Modern pollen transport studies at Mount Hagen (Powell, 1970) and Mount Wilhelm (Hope, 1973), where *Nothofagus* commonly occurs at mid-montane elevations (2000–2770 m; see Johns, 1982, for an explanation of New Guinea vegetation zonation), clearly point to the over-representation of *N. brassi* types in the pollen rain. Values are highest within pure beech forests (up to 90% of total pollen) and also in open vegetation communities in upland areas, where production and deposition of pollen from local sources is relatively low. *Nothofagus brassi* types are generally less than 20 per cent in mixed rainforest at mid and lower montane elevations (1000–2000 m), where filtration and local pollen producers dilute their representation.

Myrtaceous genera in New Guinea occur commonly in all mixed forests from the lower montane (1000–2000 m) to the upper montane zones (2700 –3200 m). Their pollen is generally well represented locally, but variably represented regionally, a fact which led Powell (1970) to suggest that they are not good indicators of forest type. In Australia, the rainforest Myrtaceae *Syzygium* and *Acmena* are generally equally well represented, and extra-locally to regionally dispersed (Kershaw, 1973); others, such as *Tristania*, are known to be under-represented (Ladd, 1978).

Most pollen types recorded at Oakvale can probably be related to closed forest taxa such as *Syzygium*, *Acmena* and *Tristania*, with minor amounts of verrucate pollen referable to genera such as *Decaspermum*, *Austromyrtus*, and *Rhodamnia*. *Syzygium* is a known associate of *N. brassi* species in mixed rainforests in both New Guinea and New Caledonia, together with taxa such as *Weinmannia* (Cunoniaceae), *Quintinia* (Escalloniaceae), and *Tasmannia* (Winteraceae). These families are present at Oakvale, although poorly represented. The pollen-rain information presented above suggests that the *N. brassi* group values are low enough to indicate that *N. brassi* pollen producers were not dominant elements in the regional vegetation, but were instead part of a mixed rainforest with a high component of myrtaceous species.

The occurrence near the depositional site of swamp vegetation characterised by *Sparganium* or *Typha*, as opposed to the local presence of forest, would enhance the *Nothofagus* representation if such swamp lands included stretches of open water, although there must have been forest relatively close by, as judged by the high Myrtaceae values. Alternatively, the high Myrtaceae counts could be due to an influx of water-borne pollen from streams draining into the swamp flats. Floyd (1979) listed many species of New South Wales rainforest Myrtaceae that prefer streamside, gully, and riparian habitats, a factor that would greatly enhance their representation in a water-borne assemblage.

The climatic significance of the high frequency of Myrtaceae relative to *N. brassi* has been discussed by Kershaw & Sluiter (1982) and Martin (1984) for the Gippsland and eastern Murray Basins, respectively; their interpretations differ. Kershaw & Sluiter suggested that the increase in Myrtaceae, which is usually accompanied by increases in Elaeocarpaceae, could indicate the expansion of a complex 'sub-tropical' vegetation community in response to a warmer and wetter climate. Alternatively, Martin believes that a progressively drier climate led to an increase in Myrtaceae relative to *N. brassi*.

A further possibility, based on the hypothesis of Nix (1982), is that fluctuations in the areal extent of Tertiary vegetation types may result from shifts in the light regime as governed by the amount of cloud cover. The characteristic occurrence of cloud cover over *Nothofagus* forest in New Guinea has been pointed out by Ash (1982). At Mount Wilhelm, the local persistence of dense cloud cover has led to the development of a 'cloud forest' vegetation type that is characterised by species of *Dacrycarpus*, Myrtaceae, Elaeocarpaceae and Cunoniaceae (Hope, 1973). While cloud forest is today characteristic of high elevations in the tropics, the higher surface temperature of the Tertiary sea may have induced more frequent and lower cloud cover. The idea of frequent cloud is also consistent with a suggestion made by Bowler (1982) that moist foggy winters and warm wet summers would have prevailed at times of higher sea-surface temperature in the Tertiary in Australia.

The regional vegetation that existed during much of the late Oligocene at Oakvale appears then to have been dominated by evergreen rainforests. Myrtaceous genera must have been extremely important components of these rainforests, which seem likely to have thrived under a climatic regime characterised by high annual effective precipitation. Year-round rainfall would have been necessary to sustain the *N. brassi* producers, although pollen-rain data suggest that these

were less important here than at other contemporary sites in southeastern Australia.

Latest Oligocene to mid-Miocene araucarian rainforest period (Zone I)

The characteristic features of this interval are the dominance of Myrtaceae, the reduction in the importance of *N. brassi* types, and concomitant increases in Araucariaceae and the podocarp genera *Dacrydium* and *Dacrycarpus*. The change from the pattern of Zone II appears to have been quite sudden — over the 2-m interval between samples 17 and 18 — although the possibility of some hiatus here cannot be entirely excluded.

Apart from a brief phase near the top of the zone, when a swamp vegetation of sedges and grasses appears to have encroached close to the sample site, pollen would have been derived, as in the older zone, mainly from regional sources. The importance of water transport in this period is highlighted by the increased representation of two families, Cyatheaceae and Araucariaceae. For Cyatheaceae, representatives such as *Cyathea* are particularly important streamside colonisers, although they are also important understorey components of mature forest. Their spores are usually over-represented locally (Hope 1973; Dodson, 1983) in terrestrial deposits, although their significance would be reduced at sites receiving a predominantly regional pollen rain. Nonetheless, *Cyathea* spores are easily transported by water, and their consistent presence at more than 5 per cent of the pollen sum, especially in sub-zone IC, points to their riparian existence in the Oakvale regional environment.

The two extant genera in the Araucariaceae, viz., *Araucaria* and *Agathis*, are thought to be wind pollinated and both are relatively large pollen producers Kershaw (1973, 1976). However, their aerial dispersal is limited, and *Araucaria*, at least, is only well recorded from within *Araucaria*-dominated forests. Transport of the pollen grains at Oakvale must have been almost entirely by water. The Araucariaceae pollen recorded at Oakvale is considered to most closely resemble *Araucaria*. Grains are generally quite large (50 μm) and characterised by a surface sculpturing of fine granulae. In addition, the grains have a tendency to fold rather than to crack, as occurs in *Agathis*.

The ecology of *Araucaria* in Australia has been well documented by Webb & Tracy (1967), and in New Guinea by Enright (1982a,b,c,d). In Australia, *Araucaria* is found only north of the southern limit of summer rainfall (Sluiter & Kershaw, 1982), in various types of vine forest with 800–1900 mm annual rainfall, although it is most extensive on relatively high-nutrient soils in southern Queensland, where annual rainfall is 800–1400 mm. Throughout most of *Araucaria*'s range, rainfall shows a slight to moderate seasonal bias (Nix, 1982). *Araucaria* is generally excluded from the more complex and 'wetter' rainforest types. In New Guinea, *Araucaria* occurs mainly in the lower montane zone, primarily in vine forests where the canopy is relatively open, although it occasionally occurs in complex rainforests. Here the annual rainfall is 800–4000 mm, but it is generally less than 2000 mm. Thus, *Araucaria* in New Guinea appears to grow in wetter situations; Kershaw (1976) has suggested that this difference may be offset by more efficient drainage compensating for the higher rainfall in New Guinea.

The incidence of high values of Myrtaceae along with *Araucaria*, *Dacrydium*, *Dacrycarpus*, and, to a lesser extent, *Podocarpus/Dacrydium* (Fig. 4) would appear to reflect a forest type with no known extant analogue. It is interesting to note, however, that at Lynch's Crater in northeast Queensland, Kershaw (1976, 1984) proposed the existence of a gymnosperm-dominated 'drier rainforest' for long periods within the last 200 000 years. These periods approximately coincide with the last two global glacial cycles, and pollen assemblages are characterised by the consistent presence of *Araucaria*, *Dacrydium*, and *Podocarpus*. Although the Myrtaceae are relatively unimportant and *Dacrycarpus* is not recorded at Lynch's Crater, some broad similarities can be seen, at least at the structural level, between these and the past Oakvale forests. The recent demise of these forests in northeast Queensland probably resulted from their sensitivity to fire, an environmental factor that was accentuated by aboriginal man (Kershaw 1976).

The Myrtaceae must have been very important representatives of the regional vegetation communities throughout this period. If the structure of the araucarian forests resembled that of present-day forests, *Araucaria* would have been growing as an emergent above a canopy stratum of smaller rainforest trees. At present, it is unusual to record significant quantities of any pollen type other than *Araucaria* in a rainforest containing significant *Araucaria*, although *Eucalyptus* and/or *Casuarina*, which occur in sclerophyll vegetation outside the rainforest, can be important. The highest *Eucalyptus* values for the core (up to 12%) — recorded as *Myrtaceidites eucalyptoides* Cookson & Pike) — also coincide with the highest *Araucaria* values, at the base and top of Zone I. The *Eucalyptus* could have come from communities just outside the rainforest at Oakvale; the occurrence there certainly provides the oldest pollen evidence for the genus being present in some abundance.

If comparisons with the present are appropriate, as Nix (1982) has proposed, then some seasonality of rainfall seems probable for Zone I time at Oakvale, with periods of lower precipitation perhaps in winter and spring. Interestingly, recent data collected by Nix (personal communication, 1984) indicate that the two Australian species of *Araucaria* now grow within a narrowly defined climatic envelope. Mean annual air temperatures and mean annual precipitation calculated from sites covering the geographic range of *A. cunninghamii* and *A. bidwilli* gave values of 19.1 $\pm$ 2.9°C and 18.0 $\pm$ 1.6°C, and 1364 $\pm$ 420 mm and 1283 $\pm$ 505 mm for the respective species.

Broadly comparable climatic parameters may have existed in the western Murray Basin in the early Miocene, but such an interpretation must remain tentative. While it is clear that the major change from Zone II to Zone I was the increased importance of conifers, (especially *Araucaria*) at the expense of the *Nothofagus brassi* pollen producers, there remained a small but none-the-less consistent presence of beech within the region, perhaps in limited areas of constant wetness. It is also noteworthy that the lower precipitation limit for *N. brassi* species in New Guinea is about 1500–800 mm, which overlaps with the upper range of *Araucaria* as indicated by Nix.

Why was the climate from the latest Oligocene seasonally drier at Oakvale than at other sites in southeastern Australia? The Oakvale site is far to the west of other study sites discussed (Fig. 1): it is some 5° north of the most intensively studied locality to date, that of the Latrobe Valley, which exists today and would have existed in the Tertiary, in a relatively humid part of the Australian continent. If the southern margin of Australia was situated north of the sub-tropical high-pressure belt and the continent was under the influence of a predominantly summer rainfall regime, as

Bowler (1982) suggested, any intensification of anticyclonic circulation to the south of the continent could be expected to be felt initially in terrestrial areas to the west and centre of the continent. Whilst Oakvale could scarcely be called a terrestrial site in the Oligocene—Miocene, it did exist on the northwestern edge of the Murray Basin, backed by extensive land areas to the west. Bowler (1982) suggested that the Nullarbor region would have been most profoundly affected by the onset of severely arid conditions in the late Miocene: such conditions would have resulted from the northward movement and intensification of the southern belt of sub-tropical high-pressure cells. It could be that the Oakvale vegetation, in the latest Oligocene and early Miocene, reflected the early, perhaps erratic, beginnings of this trend.

Conditions appear to have become drier later in the eastern Murray Basin, judging by the reduction in *Nothofagus* frequencies there in the early Miocene (Martin, 1977a, 1984). *Araucaria* pollen is nowhere as abundant as it is in Oakvale-1; however, high frequencies have been reported from sediments tentatively dated as late Miocene to Pleistocene on the eastern margin of the Great Artesian Basin (Martin, 1980, 1981). Data from these inland sites, along with the disjunct distribution of *Araucaria* forests in Australia today, were considered by Sluiter & Kershaw (1982) to provide strong evidence for a broader distribution of araucarian vegetation in the late Tertiary. The information from the Oakvale corehole strongly supports this contention and demonstrates that the replacement of the older, *Nothofagus*-rich rainforests by those dominated by *Araucaria* was a complex process that occurred earlier in the more westerly sites than it did closer to the eastern seaboard.

Taxonomic, biostratigraphic and botanical notes on selected taxa

The sequence in Oakvale-1, with its firm faunal age control and its diverse and well-preserved palynomorph assemblages, has provided a wealth of data on the stratigraphic distribution of a large number of species. In some cases the occurrence of particular forms in the Oakvale sequence represents an extension of previously documented time ranges. For other forms, the Oakvale sequence has provided the first record of a particular taxon in Australia, and in yet other cases, the record is the first fossil record in Australia for certain elements among the living vegetation. This section contains brief and informal descriptive notes on those taxa for which the Oakvale record extends existing knowledge. In the organisation of these notes, we have used no morphologic suprageneric classification, but have simply arranged the taxa in alphabetical order within the broad phyletic groupings, as in Table 1.

Bryophyte spores

Rouseisporites sp.
Figure 6A–U

This is a highly variable spore, especially in the degree of definition of the laesurae, and the preservation, or otherwise, of the membranous equatorial zona. It has a finer reticulum than the species described by Hekel (1972, Pl. 2, fig. 13) from the Queensland Tertiary, but may be conspecific with that referred to *Rouseisporites* by Martin (1973, p. 4, fig. 4). Affinities are probably with *Riccia* or *Fossombronia*, which in Australia are represented by species of generally open habitats, and are not usually halophytes.

The spores recorded have a size range of 45–56 μm. They were recorded throughout the sampled sequence.

Pteridophyte spores

Baculatisporites sp. cf. ***B. scabridus*** Playford 1982
Figure 6K,L

Trilete spores bearing spinose or conate processes are here compared to *B. scabridus*, which Playford (1982, p. 32, Pl. 1, figs 1—4) described from the Neogene of Papua New Guinea. The Australian form differs in having a less dense distribution of spines distally, in having straight rather than sinuous laesurae, and in having more densely ornamented contact faces. Points of similarity are the presence of proximal curvaturae, and the fused nature of the spines to give processes with multiple terminations. Recorded size range: 43–49μm (5 specimens measured). The form is present as a rare element through much of the Geera Clay (Fig. 2), except for the uppermost few metres. This type may have been produced by either a fern or a bryophyte.

Camarozonosporites sp.
Figure 6E,F

This distinctive form has simple laesurae, pronounced interradial crassitudes, and a distal sculpture of coarse, sharply angled rugulae. It does not resemble any forms described previously from the Australian Tertiary; *C. bullatus* Harris (1965, p. 82, Pl. 26, figs 2,3) has less prominent and sharply defined distal sculpture. Spore diameter: 38–46 μm (4 specimens measured); it occurs as a rare form throughout the sampled sequence. Affinities are possibly lycopodiaceous.

Distaverrusporites sp. cf. ***D. simplex*** Muller 1968
Figure 6M,N

The single specimen observed, from 68.10 m in the Geera Clay, has a thicker wall and less regular verrucae than *D. simplex*, which Muller (1968, p. 5, Pl. 1, fig. 2) reported from the early Tertiary of Sarawak. Affinity unknown.

Peromonolites sp.
Figure 6A,B

This form is given an informal designation only, as it does not strictly conform with any previously described Australian species. The perispore is more mat-like than that of *P. densus* Harris 1965, but less dense than in *P. vellosus* Partridge 1973. It is similar to a spore that Couper (1960) compared to the extant *Paesia scaberula* (A. Rich) Kuhn of the Pteridaceae. Its known range in New Zealand is mid-Oligocene to Recent (Mildenhall, 1980; Pocknall, 1982).
Grain dimensions: 38–44μm long, 27–32μm wide. (5 specimens measured). It occurs as a rare form throughout the sequence in Oakvale-1.

Polypodiaceoisporites sp. cf. ***P. retirugatus*** Muller 1968
Figure 6G–J

This species is smaller than *P. retirugatus*, described from the early Tertiary of Sarawak (Muller, 1968, p. 7, Pl. 1, fig. 8), and the distal elements are coarser and notably steeper-sided. This distinction is confirmed by Playford's (1982) description of *P. retirugatus* from the Neogene of Papua New Guinea. *Cingulatisporites papuanus* Khan (1976, p. 757, fig. 6), also from Papua New Guinea, differs in being verrucate both proximally and distally. The form illustrated by Hekel (1972, p. 5, Pl. 2, figs 2,3) has a more dense, generally lower distal ornament. This species is rare, but consistently present throughout the Geera Clay. Size range: 32–39μm; affinity lies probably with Pteridaceae.

Polypodiisporites usmensis (van der Hammen) Khan & Martin 1971
Figure 6C,D

Synonymy
1956 *Verrumonolites usmensis* van der Hammen, p. 116, fig. 7

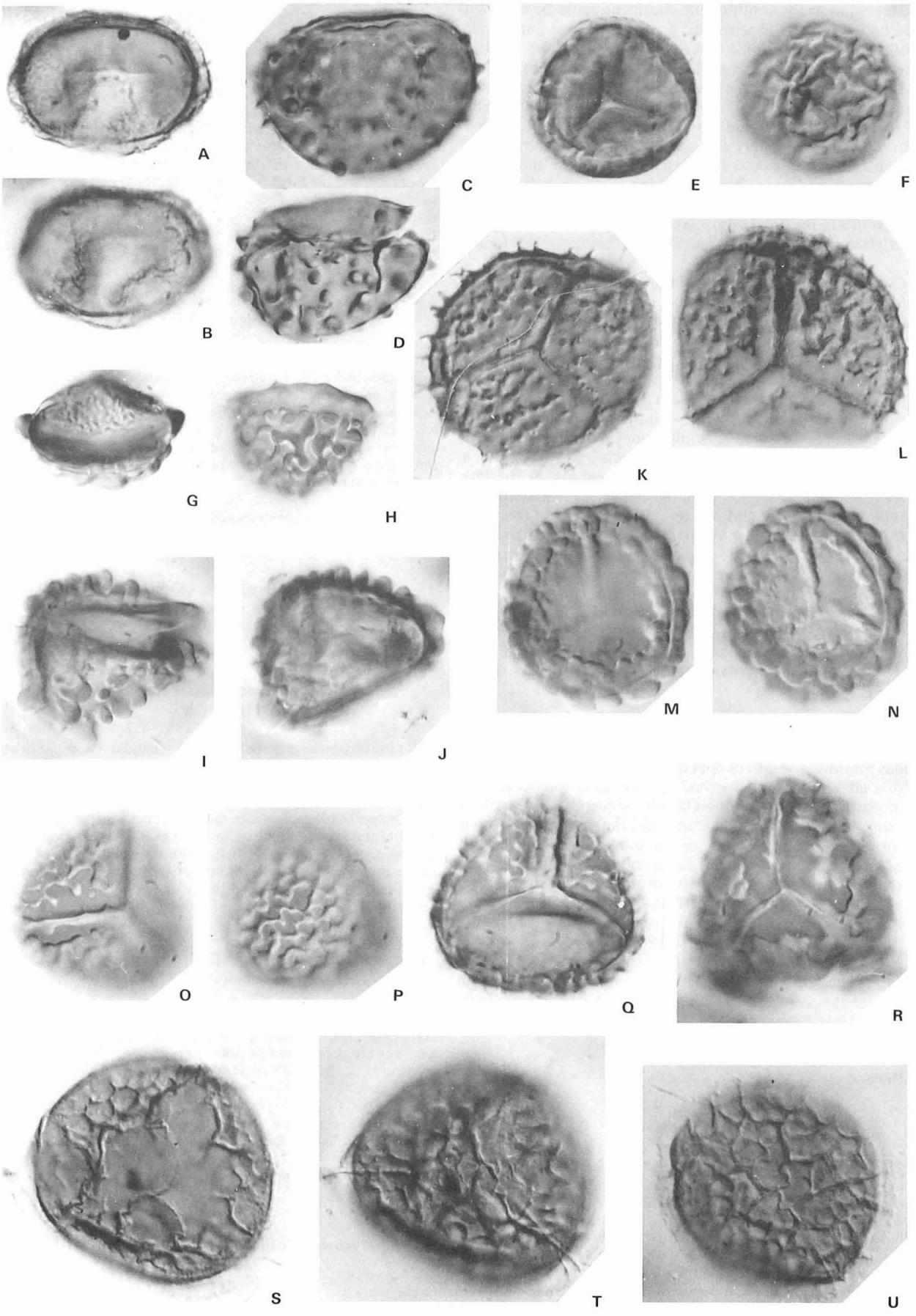
A
C
E
F
B
D
K
L
G
H
M
N
I
J
O
P
Q
R
S
T
U

1968 *Verrucatosporites usmensis* (van der Hammen) Germeraad, Hopping & Muller, p. 290, Pl. 2, fig. 3.
1971 *Polypodiisporites (Verrucatosporites) usmensis* (van der Hammen) in Khan & Martin, p. 478.
1972 *Polypodiidites usmensis* (van der Hammen) Hekel, p.6, Pl.1, figs. 8,9.

Specimens referable to *P. usmensis* occur as rare elements in the top two samples of the Geera Clay. This is the first record of the species in southern Australia. It has previously been reported as having a pan-tropical distribution, with an Eocene to Holocene range (Germeraad & others, 1968). Cookson (1956) and Playford (1982) reported it from the late Tertiary of Papua New Guinea, and Hekel (1972) recorded forms very similar to those in Oakvale-1 from his units 4 and 5 (late early Miocene) of the Capricorn and Aquarius wells in Queensland. Dimensions: 36–40μm long, 25–31μm wide (3 specimens measured). Suggested affinities, according to Germeraad & others (1968), may be to the climbing swamp fern *Stenochlaena palustris* (Burm. f.) Bedd. of the Blechnaceae.

Rugulatisporites sp. cf. ***R. trophus*** Partridge 1973
Figure 6O–R

This species shows a very large range in morphology, especially in exine sculpture. The rugulae of the proximal and distal faces are densely spaced and flat-topped. They are only rarely mushroom-shaped in profile, and so are excluded from *Rugulatisporites mallatus* Stover; the sculpture is too coarse for their inclusion in *R. micraulaxus* Partridge. The most coarsely ornamented end members of the morphological range are close to R. *trophus*, but most specimens have a denser pattern of rugulae than shown by that species, and are also considerably smaller. They are therefore placed in comparison only. The range in size is 37–46μm (10 specimens measured). It was not observed below 97.45 m, so may be of some stratigraphic significance.

Angiosperm pollen

Acaciapollenites myriosporites (Cookson) Mildenhall 1972
Figure 7DD,EE

The specimens in Oakvale-1 conform well with *A. myriosporites*. In all observed polyads, individual cells show distinct, depressed pseudofurrows, and have a smooth to very faintly scabrate exine. Diameter of polyads: 32–45μm (10 specimens measured).

The species occurs as a rare (less than 1%) component in all samples down to a depth of 117 m, which puts its first appearance clearly in the late Oligocene, according to Lindsay's (1983) foraminiferal data; this provides an earlier datum than the earliest Miocene age cited previously by Stover & Partridge (1973) and Martin (1978). A similar late Oligocene report of *Acaciapollenites* was made by Pocknall (1982) from the Pomahaka Estuarine Bed, but the species reported from the New Zealand locality differs from *A. myriosporites*, in lacking pseudofurrows and in being more strongly sculptured.

Acaciapollenites sp.
Figure 7HH

Rare specimens of *Acaciapollenites* differ from *A. myriosporites* in having a distinctly scabrate to finely granulate surface, and less well defined pseudofurrows. Such specimens were only observed at 89.0 m; diameter of polyads: 39–43μm.

Chenopodipollis chenopodiaceoides (Martin) Truswell comb. nov.
Figure 7A–D

1973 *Polyporina chenopodiaceoides* Martin, p. 28, figs 118–120.

Krutzsch (1966) observed that the type of species of *Polyporina* may be a freshwater planktonic organism, therefore casting doubt on the morphological basis of the genus. *Chenopodipollis* Krutzsch 1966 is described as being 'minutely columellate' (Krutzsch, 1966, p.35), and thus provides a more appropriate taxon within which to place the species that Martin (1973) described as having a baculate sexine.

The specimens observed in Oakvale-1 conform closely to *C. chenopodiaceoides*. The pores, 50–60 in number, are circular, depressed, with remains of granulate pore membranes sometimes visible. The exine stratification is faintly discernible, and the surface smooth to very finely granulate. Diameter: 13–19μm (8 specimens measured). The species ranges throughout the Geera Clay, always as a rare element. Affinity with Chenopodiaceae/Amaranthaceae.

Crotonipollis sp.
Figure 7FF,GG

This rare form bears a dense, probably supratectal, cover of baculate elements that are arranged in a definite crotonoid pattern. Individual elements are 1.5–1.7μm high, 1.0–1.2μm in basal diameter, and trapezoidal in surface view. No apertures could be discerned; the exine of most specimens showed irregular patches where it had broken down, but these could be preservational artifacts. No similar forms appear to have been recorded previously from Australian Tertiary sediments. *Crotonipollis negvelii* Baksi, Deb & Siddhanta 1979, from the South Arcot district of India, has coarser sexinal elements, as have forms recorded from the early Tertiary of southern Africa (Scholtz, 1985). Diamter: 34–39 μm (5 specimens measured). *Crotonipollis* sp. occurs as a rare form in the uppermost 4 samples in Oakvale-1. More detailed morphological information, including details of any apertures, is necessary before the affinities can be determined, but they may lie with Euphorbiaceae or Thymeleaceae.

Cyperaceaepollis spp.
Figure 7W–Z

Bell-shaped pollen grains morphologically identical with those produced by living sedges are here referred to *Cyperaceaepollis* Krutzsch 1977. The Oakvale sequence provides an excellent record of these pollen types, and indicates that, by the late Oligocene, the sedges were well established, diverse, and an important part of some plant communities. The only specimens previously figured from the Australian Tertiary were those from supposed Eocene sediments at Napperby in central Australia (Kemp, 1976); confirmation of the occurrence of cyperaceous pollen in the Eocene in Australia was subsequently provided by Harris (in Martin, 1978), who recorded the type from the middle Eocene Maslin Sands. Cyperaceous pollen has also been reported from the late Oligocene of Tasmania by Hill & Macphail (1983), from the early Miocene at Lake Bunyan by Tulip & others (1981), from the Pliocene Lachlan Formation of western New South Wales (Martin, 1973) and, in New Zealand, from the late Oligocene by Pocknall (1982). Its virtual absence from many contemporaneous sequences in southeastern Australia, including the coal basins of the Latrobe Valley in the Gippsland Basin (Stover & Partridge, 1973; Luly & others, 1980) is therefore difficult to explain, although it could be related to substrate nutrient status.

Figure 6. Selected spores from Oakvale-1.
All magnifications x1000. A,B, *Peromonolites* sp., 33.75 m, CPC25476, proximal and distal foci. C,D, *Polypodiisporites usmensis* (van der Hammen): C, 34.62 m, CPC25477; D, 33.75 m, CPC25478. E,F, *Camarozonosporites* sp., 38.25 m, CPC25479, proximal and distal foci. G–J, *Polypodiaceoisporites* sp. cf. *P. retirugatus* Muller: G, 33.75 m, CPC25480, equatorial view; H, 33.75 m, CPC25481, distal equatorial view; I,J, 55.23 m, CPC25482, distal and proximal foci. K,L, *Baculatisporites* sp. cf. *B. scabridus* Playford: K, 120.4 m, CPC25483; L, 92.05 m, CPC25484, both proximal foci. M,N, *Distaverrusporites* sp. cf. *D. simplex* Muller, 68.10 m, CPC25485, median and proximal foci. O–R, *Rugulatisporites* sp. cf. *R. trophus* Partridge: O,P, 33.75 m, CPC25486, proximal and distal foci; Q, 33.75 m, CPC25487, proximal focus; R, 33.75 m, CPC25488, proximal focus, form with large sculptural elements. S–U, *Rouseisporites* sp.: S, 97.45 m, CPC25489, distal focus; T,U, 49.54 m, CPC25490, proximal and distal foci.

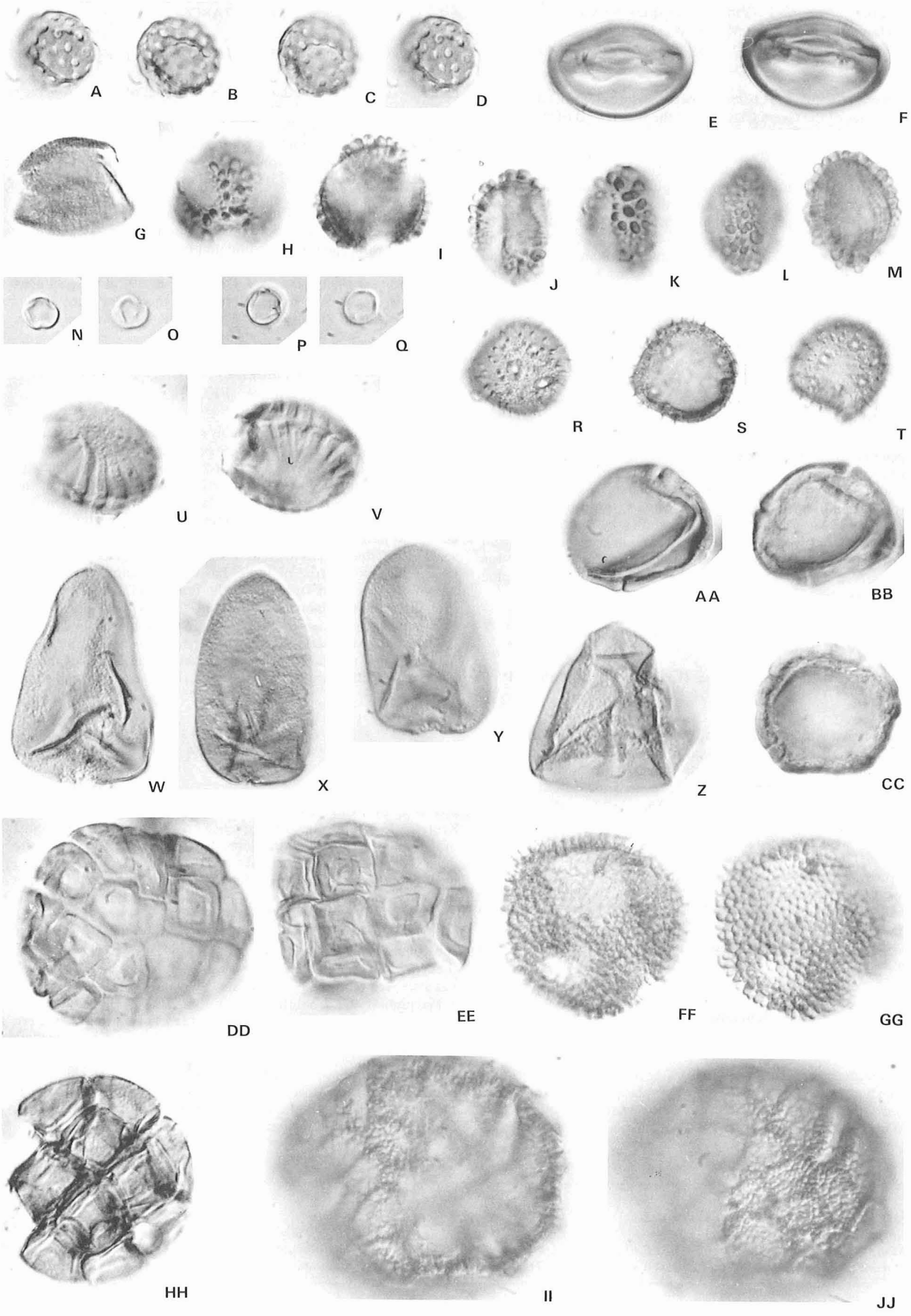
A
B
C
D
E
F
G
H
I
J
K
L
M
N
O
P
Q
R
S
T
U
V
AA
BB
W
X
Y
Z
CC
DD
EE
FF
GG
HH
II
JJ

Several broad morphological categories are evident. They include bullet-shaped grains with a sharply defined apical aperture (Fig. 7X,Y), pear-shaped forms with diffuse apical and elongate, rather vague lateral apertures (Fig. 7W), and triangular forms with a wide base and a thin, much-folded exine (Fig. 7Z).

Dicolpopollis sp. cf. *D. metroxylonoides* Khan 1976
Figure 7G

Dicolpate pollen grains with ragged colpus margins, and a scabrate or finely granulate sexine are compared here to *D. metroxylonoides*, which Khan (1976, fig. 13) described from the Neogene of Papua New Guinea. The two specimens from Oakvale are significantly smaller than the New Guinea form, having grain lengths of 27 and 29 μm. Khan compared the fossil species to pollen of *Metroxylon americanum* Wendl. (Palmae), a sago palm of the Papuan swamps. There is a resemblance also to pollen of the lawyer vine or rattan cane, *Calamus*. Larger dicolpate forms, with a fine sexine reticulum also occur in the Eocene at Bungonia, New South Wales (Truswell & Owen, unpublished data).

Echiperiporites sp.
Figure 7R–T

Small periporate pollen grains with clearly rimmed pores of uncertain number, but probably not more than 24, are grouped in this category. The wall is clearly stratified, columellate, and the sexine bears acutely pointed spines up to 1.5 μm long. Closely similar forms were assigned to *Echiperiporites* sp. by Partridge (1971) from the *Triporopollenites bellus* Zone of the Gippsland Basin. They differ from the pollen species *Micrantheum spinyspora* of Martin (1973, p. 32, figs 141–143) in having fewer pores, and spines that bear little relation to the distribution of pores; in *M. spinyspora* the spines are grouped around the pores in rosette fashion. In Oakvale-1 the form is rare, occurring in samples near the base and the top of the Geera Clay. Diameter: 14–23 μm (5 specimens measured). Affinity may rest with Euphorbiaceae.

cf. **Elaeocarpaceae**
Figure 7N–Q

Tiny, smooth-walled tricolporate pollen grains, of diameter 6–10 μm, are here compared informally to Elaeocarpaceae. They are very similar to *Elaeocarpus* comp., figured by Luly & others (1980, Pl. 5, fig. 10), and occur throughout the sampled sequence at Oakvale, in frequencies of up to 4 per cent of the total pollen count.

Glencopollis ornatus Pocknall & Mildenhall 1984
Figure 7II,JJ

These distinctive pollen grains are similar to forms described from the early Miocene through Pliocene of Southland, New Zealand, by Pocknall & Mildenhall (1984). The grains are spherical, polyrugate, with colpae 9–10 μm long developed between the muri of a prominent sexine reticulum. The colpi are often difficult to discern unless they are gaping, so the number of colpi is uncertain, but 10–12 seems likely from the interpreted geometry of their distribution. The muri of the reticulum are formed of wide prominent columellae; the floors of the intervening lumina are covered with densely spaced columellae which are shorter than those of the muri. The columellae flooring the lumina are more prominent in the Australian forms than they are in the New Zealand species, but this is not sufficient to separate them as a distinct species. Diameter: 34–50 μm (3 specimens measured); the species was recorded only from the upper part of the Geera Clay. Pocknall & Mildenhall (1984), suggest an affinity with the Polygonaceae.

cf. **Gyrostemonaceae**
Figure 7E,F

Tricolporate pollen grains with a pronounced equatorial constriction of the colpi, and a thick (about 2 μm), apparently homogenous psilate exine, are comparable with pollen of the wheel-fruit family Gyrostemonaceae. Previous fossil records in Australia are from the Gippsland Basin, where Luly & others (1980) reported the form from the Miocene Yallourn Seam; and from the Pioneer deposit in Tasmania (Hill & Macphail 1983), a record which is possibly early Oligocene. At Oakvale the species is sparsely distributed through the Geera Clay and uppermost Olney Formation. Dimensions: diameter, 19–27 μm; equatorial diameter, 15–19 μm (4 specimens measured).

Haloragacidites haloragoides Cookson & Pike 1954
Figure 7CC

Specimens observed at Oakvale conform closely with those described originally by Cookson & Pike (1954; p. 202, Pl. 1, figs 7–9). The species was reported by Stover & Partridge (1973) as first appearing in the upper part of the *Triporopollenites bellus* Zone in the Gippsland Basin; the record at Oakvale predates this first appearance as the species is present at 92.05 m, where foraminifera of earliest Miocene age are found (Lindsay 1983). Diameter: 25–29 μm (4 specimens measured). Affinity is probably with Haloragaceae.

Haloragacidites sp.
Figure 7AA,BB

This form is distinguishable from *Haloragacidites haloragoides* in having a thinner exine between the apertures, and from *Haloragacidites amolosus* Partridge 1973 in lacking prominent, dome-like apertures. It was observed only in two samples from the upper part of the Geera Clay. Diameter: 19, 24 μm (2 specimens). Affinity probably with Haloragaceae.

Ilexpollenites sp.
Figure 7H–M

This small form of *Ilexpollenites* bears club-shaped clavae, which are circular or slightly elongate in surface view. The clavae are widely spaced, and the intervening exine bear small grana. This morphotype is very similar to one described by Partridge (1971) as *I.* cf. *clifdenensis* McIntyre; the species differs from *I. clifdenensis* in having relatively larger and more widely spaced clavae, and in being smaller. Partridge (1971) described the Gippsland Basin form, which may be conspecific with this Murray Basin type, as occurring in the *T. bellus* Zone, and, more frequently, in younger sediments. In the Oakvale sequence, the species occurs sparsely throughout the Geera Clay, but is more consistently present in samples near the top of the sequence. Dimensions are 21–25 μm polar diameter, 13–20 μm equatorial diameter (15 specimens measured). Affinity is probably with *Ilex* (Martin, 1976).

Figure 7. Selected pollen taxa from Oakvale-1.
All magnifications x1000. A–D, *Chenopodipollis chenopodiaceoides* (Martin), 38.25 m, CPC25491. E,F, cf. Gyrostemonaceae, 68.10 m, CPC25492, median and high foci. G, *Dicolpopollis* sp. cf. *D. metroxylonoides* Khan, 33.75 m, CPC25493. H–M, *Ilexpollenites* sp.: H,I, 33.75 m, CPC25494, polar view, high and median foci; J,K, 33.75 m, CPC25495, equatorial view, median and high foci; L,M, 121.30 m, CPC25496, high and median foci; N–Q, cf. Elaeocarpaceae: N,O, 124.49 m, CPC25497: P,Q, 124.49 m, CPC25498. R–T, *Echiperiporites* sp., 33.75 m, CPC25499, high, median and low foci. U,V, *Polycolpites* sp., 79.84 m, CPC25500, high and low foci. W–Z, *Cyperaceaepollis* spp.: W, 33.75 m, CPC25501, bell-shaped form; X, 61.40 m., CPC25502; Y, 44.24 m, CPC 25503, bullet-shaped forms; Z, 33.75., CPC25504, wide-based form. AA,BB, *Haloragacidites* sp., 38.25 m, CPC25505. CC, *Haloragacidites haloragoides* Cookson & Pike, 34.62 m, CPC25506. DD,EE, *Acaciapollenites myriosporites* (Cookson): DD, distorted specimen, 33.75 m, CPC25507; EE, 35.64 m, CPC25508. FF,GG, *Crotonipollis* sp., 33.75 m, CPC25509. HH, *Acaciapollenites* sp., 89.00 m, CPC25510. II,JJ, *Glencopollis ornatus* Pocknall & Mildenhall, 35.64 m, CPC25511, median and high foci on colpi.

Malvacearumpollis sp.
Figure 8P–R

The presence of sturdy spines set atop a cushion formed by elongate columellae in the sexine characterises *Malvacearumpollis* Nagy 1962, and provides a point of difference between that genus and *Malvacipollis* Harris. In the Oakvale specimens figured here, the spines are clearly set on such cushions, so reference to *Malvacearumpollis* is appropriate. The spines are constricted at the base, up to 5 μm high, and 2–3 μm diameter at their widest point, which occurs a little above the base. There are 4–6 pores, although they are often difficult to see because of the thickness of the exine; they are surrounded by a thickening of the nexine, and are outwardly expressed as narrow slits in the sexine. Diameter: 50–76 μm (8 specimens measured).

The species observed at Oakvale appears to have a much thicker wall than the form referred to *Malvacearumpollis estelae* Germeraad, Hopping & Muller by Hekel (1972) from Queensland Tertiary sequences. Foster (1982) drew attention to the inappropriateness of this assignment, pointing out that *M. estelae* has many more pores than the Queensland species; he reassigned the species as *Malvacipollis* sp. C (Foster, 1982, Pl. 11, fig. 8). Affinity possibly with Malvaceae.

Margocolporites vanwijhei Germeraad, Hopping & Muller 1968
Figure 8A,B

Two specimens of this distinctive pollen type were recorded from the uppermost Geera Clay. They conform closely to the original descriptions given by Germeraad & others (1968, p. 342, Pl. 18, fig. 3) from the Tertiary of Venezuela. The reticulum of the intercolpia is, however, somewhat finer than in the type material, but falls well within the range of variation described. In the observed specimens, the sexine is 0.9 μm thick, and the muri of the reticulum in the intercolpia are clearly underlain by a single row of columellae. Diameter: 31 and 32 μm.

The species has not previously been reported from Australia. *Margocolporites* sp., figured by Foster (1982, Pl. 10, fig. 6) from the Queensland Tertiary, is more coarsely reticulate and differs in the form of the costae adjacent to the colpi. In tropical regions, *M. vanwijhei* was reported by Germeraad & others (1968) as having an Eocene–Recent range in the Carribean, an Oligocene–Recent range in Borneo, and an Eocene–Oligocene range in West Africa. Extra-tropical records of the species are those from the late Oligocene in Southland New Zealand (Pocknall, 1982), and the Neogene of southern Africa (Partridge, 1978). Affinity probably with the Caesalpinioidae of the Fabaceae; Germeraad & others (1968) noted a close similarity with two species of *Caesalpinia*.

cf. *Nuxpollenites* sp.
Figure 8E,F

Fossil forms previously referred by Kemp (1976) to aff. *Diplopeltis* are here placed in an informal category comparing them to the form genus *Nuxpollenites* Elsik 1974. Comparison is tentative, as *Nuxpollenites* has a columellate layer, a feature that can only rarely be discerned in the Australian fossil form. The Australian form also has prominent thickened ora, not common in *Nuxpollenites*, and has the major sexinal thickening in subpolar, not polar regions. Clearly, the Australian forms should be placed in a distinct, probably new form genus; however, there is at present insufficient material to permit this.

Dimensions: 27–31 μm polar diameter, 14–18 μm equatorial diameter (4 specimens measured). Affinity with *Diplopeltis* (Sapindaceae) was suggested by Kemp (1976) for supposed Eocene specimens from central Australia. However, A.P. Kershaw (personal communication) has pointed out close similarities between the fossil form and pollen of the extant *Dodonaea triquetra*, Wendl., also in Sapindaceae. *Nuxpollenites* sp. is rare in the lower part of the Geera Clay.

Perfotricolpites sp. cf. *P. digitatus* Gonzalez Guzman 1967
Figure 8S–W

These distinctive tricolpate pollen grains have colpi extending nearly to the poles, and a clearly stratified exine in which the columellae of the sexine digitate. In the Oakvale specimens, the columellate sexine is 2.0–2.7 μm thick, and the columellae branch close to the tectal surface. The colpus margins are ragged. Dimensions: polar diameter 55 and 66 μm (2 specimens measured); equatorial diameter, 38–54 μm (5 specimens measured). This taxon occurs only in the upper part of the Geera Clay.

The specimens from Oakvale-1 are similar to but smaller than *P. digitatus*. They are also smaller and thinner-walled than *P. maculosus* Playford 1982, described from the New Guinea Neogene. This is the first record of *P. digitatus* from Australia; it has, however, been reported from the late Oligocene of New Zealand (Pocknall, 1982).

Germeraad & others (1968) suggested that *P. digitatus* might have affinities with the genus *Merremia* of the Convulvulaceae. From the survey of pollen types within this family made by Sengupta (1972), it is apparent that affinities might also lie within *Convulvulus* or *Cuscuta*.

Polycolpites sp.
Figure 7U,V

Oblate pollen grains with 19–20 colpi are included in this category. Where the colpi are expanded at the equator, they are separated by a smooth colpus membrane. There may be small pores at the equator, but these are obscure. No exine stratification was seen. The exine surface of the apocolpia and intercolpia is scabrate. Equatorial diameter: 25 and 27 μm (2 specimens measured).

Although this form is extremely rare, it is reported here because of its similarity to pollen of the extant bladderwort *Utricularia* (Lentibulariaceae), and, as such, constitutes the first fossil record of this genus from Australia. Muller (1981) listed other records of the genus, including that of Medus (1975) from the Miocene of Senegal; specimens figured from this area are sturdier, thicker-walled and smoother externally than the Australian ones. Both types fall within pollen group I of Thanikaimoni's (1966) study of the genus. In the Oakvale sequence the form was observed only at 79.84 m, which is earliest Miocene.

Proteacidites pachypolus Cookson & Pike 1954
Figure 8J,K

The specimens of *P. pachypolus* recovered in Oakvale-1 are of a consistent morphotype. They are always deeply concave-sided, with a relatively thin (about 1 μm) exine and a fine surface reticulum in which the diameter of the lumina rarely exceeds 1 μm. Diameters: 28–31 μm (4 specimens measured). *P. pachypolus* occurs as a rare form throughout the Oakvale sequence. This Murray Basin record provides a clear indication that *P. pachypolus* does extend into the

Figure 8. Selected pollen taxa from Oakvale-1.
All magnifications x1000. A,B, *Margocolporites vanwijhei* Germeraad, Hopping & Muller, 33.75 m, CPC25512. C,D, *Psilodiporites* sp. cf. *P. reduntantis* Gonzalez Guzman: C, 33.75 m, CPC25513; D, 34.62 m, CPC25514. E,F, cf. *Nuxpollenites* sp., 110.50 m, WM2133, median and high foci. G–I, *Rhoipites alveolatus* (Couper): G,H, 34.62 m, CPC25515, high and median foci, polar view; I, 34.62 m, CPC25516. J,K, *Proteacidites pachypolus* Cookson & Pike, 33.75 m, CPC25517, median focus, and high focus on polar boss. L,M, *Proteacidites rectomarginis* Cookson, 153.9 m: L, CPC25518; M, CPC25519, composite focus showing surface and wall in section. N,O, *Proteacidites* sp. cf. *P. sinulatus* Dudgeon, 49.54 m, CPC25520, focus on wall in section and on grain surface. P–R: *Malvacearumpollis* sp., Q,R, 74.60 m, CPC25521, focus on spinae, and on wall in section showing rimmed pore; P, 49.54 m, CPC25522, showing spinae and bases in profile. S–W *Perfotricolpites* sp. cf. *P. digitatus* Guzman: S,T, 49.0 m, WM2128, median and high foci, polar view; U,V, 33.7 m,CPC25523, equatorial view; W, 68.10 m, CPC25524, broken specimen, showing wall in section.

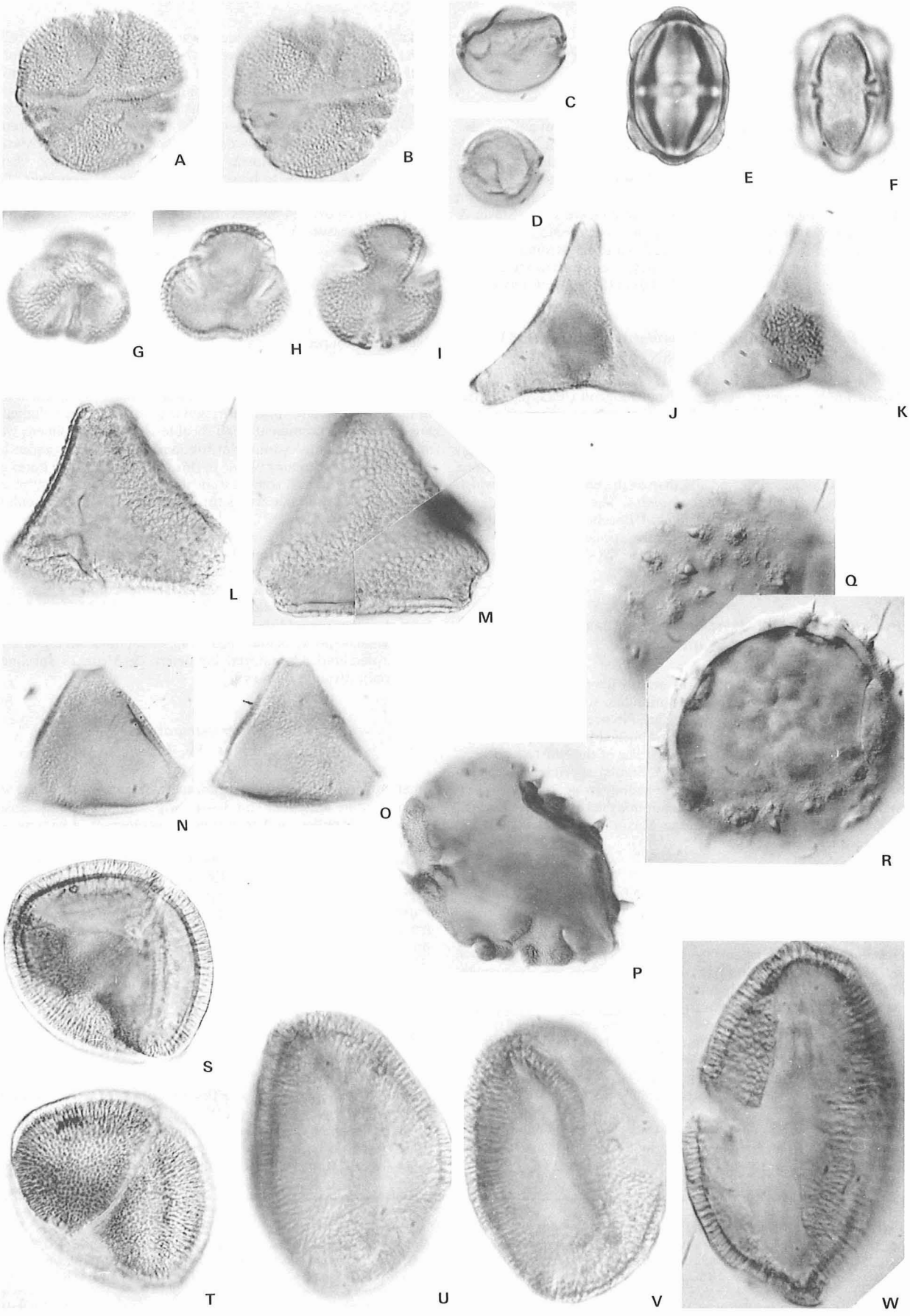
A
B
C
D
E
F
G
H
I
J
K
L
M
N
O
P
Q
R
S
T
U
V
W

Miocene, a range noted previously by Owen (1975) in an unpublished thesis, and by Dudgeon (1982).

Proteacidites rectomarginis Cookson 1950
Figure 8L,M

The sexine in this species is composed of a distinctive arrangement of verrucae and rugulae, the interstices of which form an irregular negative reticulum. The wall consists of nexine about 2.5 μm thick and sexine 1.5 μm thick; both layers show a slight thinning towards the pores. These forms are identical to those that Harris (1972) named *Proteacidites clintonensis*, separating them from *P. rectomarginis* on the basis of their larger pores and more concave sides. Stover & Partridge (1973) recombined the two species. The species has a clearly limited range in Oakvale-1, being confined to the Renmark Group and the very basal part of the Geera Clay; it was thus observed only in Oligocene sediments. Diameter: 48–60 μm (5 specimens measured).

Proteacidites sp cf. *P. sinulatus* Dudgeon 1983
Figure 8N,O

Proteacidites sinulatus was erected by Dudgeon (1983, p. 355, fig. 18) to incorporate triporate pollen grains with a semi-tectate exine in which the nexine thickens both interradially and at the poles to give a Y-shaped zone of thickening in polar view. The specimens observed in Oakvale-1 have a similar exine pattern, but the thickening is more pronounced interradially than at the poles, a feature which may differentiate them from *P. sinulatus*. The record of Dudgeon (1983) was from sediments of alleged Eocene age at Yaamba in Queensland; in Oakvale the comparative species was observed as a rare form in the Geera Clay. Diameter: 28–31 μm (5 specimens measured).

Psilodiporites sp. cf. *P. redundantis* Gonzalez Guzman 1967
Figure 8C,D

Small diporate pollen grains with variably developed annuli about the pores, and a scabrate to finely granulate surface, occur in low frequencies throughout the Geera Clay. No account of such forms in the Australian Tertiary has been published previously, although they have been recorded from the Oligocene of the Ninetyeast Ridge, Indian Ocean (Kemp & Harris 1977). Similar specimens have also been observed in sub-basaltic Eocene sediments at Bungonia, New South Wales (Truswell & Owen, unpublished data). Affinity is probably with Moraceae/Urticaceae. Maximum diameter: 14–18 μm (10 specimens measured).

Quintinia psilatispora Martin 1973
Figure 9G

Specimens indistinguishable from *Quintinia psilatispora*, described by Martin (1973, p. 20, figs. 80, 81) occur in low frequencies throughout the Geera Clay and in the Renmark Group formations below. This record provides a firmly dated occurrence of the form in a late Oligocene through early Miocene interval. Previous records are those of Martin (1973) from vaguely dated Eocene–Miocene sequences, of Luly & others (1980) from the early Miocene Yallourn Seam, and of Hill & Macphail (1983) from probable lower *P. tuberculatus* Zone (?early Oligocene) sediments at Pioneer, Tasmania.

In some of the grains observed at Oakvale, both pores and the semi-circular end of the colpus described by Martin (1973) were visible. Equatorial diameter: 9–13 μm (10 specimens measured).

Rhoipites alveolatus (Couper) Pocknall & Crosbie 1982
Figure 8G–I

A detailed synonymy of this species was given by Pocknall & Crosbie (1982, p. 8). The forms observed in the Oakvale sequence conform to the emended description, in that they have prominent, smooth margos bordering the colpi, and a sexinal reticulum with muri about 1 μm in diameter. The grains are significantly smaller than Couper's (1953) type material. In size range and general morphological features, the specimens are close to *Tricolporopollenites transversalis* Martin 1973, from the eastern Murray Basin; this species was considered by Pocknall & Crosbie to be synonymous with *R. alveolatus*. The species occurs in four samples in the Geera Clay, but is most common in the uppermost few metres. Equatorial diameter: 21–25 μm (5 specimens measured).

Rhoipites sp. *C.* of Foster, 1982
Figure 9M–O,R,S.

Specimens grouped here may include more than one taxon. All are tricolporate pollen grains with a sexine two or three times as thick as the nexine, formed of rather sparse columellae, 2.0–2.5 μm high. The columellae are linked to form simplibaculate muri, which are, in turn, organised to form an irregular reticulum. The columellae are distinct and prominent at all focal levels. Most specimens were seen in polar compressions, but the marked thickening about the equatorial pores remains visible in this orientation — the pores are surrounded by annuli some 2.0 μm thick. The colpus margins are sharply defined and cut across the lumina of the sexine reticulum.

The species is morphologically very close to that figured by Foster (1982, Pl. 3, figs. 6, 7) from the Yaamba Basin of Queensland and believed to be Eocene. The Oakvale specimens appear to be much smaller, however, and to have relatively shorter colpi. There is some resemblance to *Canthiumidites oblatus* Pocknall & Mildenhall 1984 from the Oligocene–Miocene of Southland, New Zealand, but the New Zealand species is more nearly spherical, and has a granulate colpus membrane. Equatorial diameter: 29–33 μm (8 specimens measured); affinity unknown.

cf. *Sphenostemon* sp.
Figure 9K–L

Small pollen grains of about 10 μm diameter, with a stratified wall bearing a fine reticulum and 3–4 poorly delineated pores, closely resemble the pollen of *Sphenostemon papuanum*, a canopy and secondary canopy tree in New Guinea rainforests. In the Oakvale sequence, they were observed as a very rare component in the uppermost two samples of the Geera Clay. *Sphenostemon* has also been recorded from the late Oligocene to the mid-Miocene of the Latrobe Valley, Victoria, although the specimens are generally larger (10–13 μm) and usually lack the fine reticulum (Sluiter, work in preparation). The only Australian species, *Sphenostemon lobosporus* (F. Muell.), is a common shrub of moist gullies in high-altitude rainforest in northeast Queensland. Its pollen has not been examined.

Triporopollenites ambiguus Stover 1973
Figure 9P–Q

Triporopollenites ambiguus was first described from the Gippsland Basin, where Stover & Partridge (1973, p. 269, Pl. 21, fig. 7) reported its range as being early to late Eocene. The same authors (Stover & Partridge, 1982) subsequently reported it from the Eocene of southwestern Australia. In the Oakvale sequence, sturdy specimens

Figure 9. Selected palynomorph taxa from Oakvale-1.

Magnifications x1000, unless stated otherwise. A–F, *Triporotetradites* sp.: A,B, 33.75 m, CPC25525, median focus on pores, high focus on surface; C,D, 34.62 m, CPC25526, median and high foci; E,F, 33.75 m, CPC25527, median and high foci. G, *Quintinia psilatispora* Martin, 74.60 m, CPC25528. H–J, Cunoniaceae cf. *Weinmannia* sp., 124.49 m, CPC25529, equatorial view, high, median and low foci. K,L, cf. *Sphenostemon* sp., 33.75 m, CPC25530. M–O,R,S, *Rhoipites* sp. *C.* of Foster, 1982: M, 34.60 m, CPC25531, polar view; N,O, 33.75 m, CPC25532, median and high foci, polar view; R,S, 34.62 m, CPC25533, high and median foci, showing annulate pore. P,Q, *Triporopollenites ambiguus* Stover, 120.40 m CPC25534. T, *Lingulodinium machaerophorum* (Deflandre & Cookson), 110.50 m, WM2133, x600, less common form with very short processes and Type 1P archaeopyle. See also Fig. 11P. U,V, *?Paucisphaeridium* sp., 110.50 m, WM2133, x600. W–Y, Incertae cedis: W, 34.93 m, WM2126; X, 33.75 m, CPC25535; Y, 55.23 m, CPC25536.

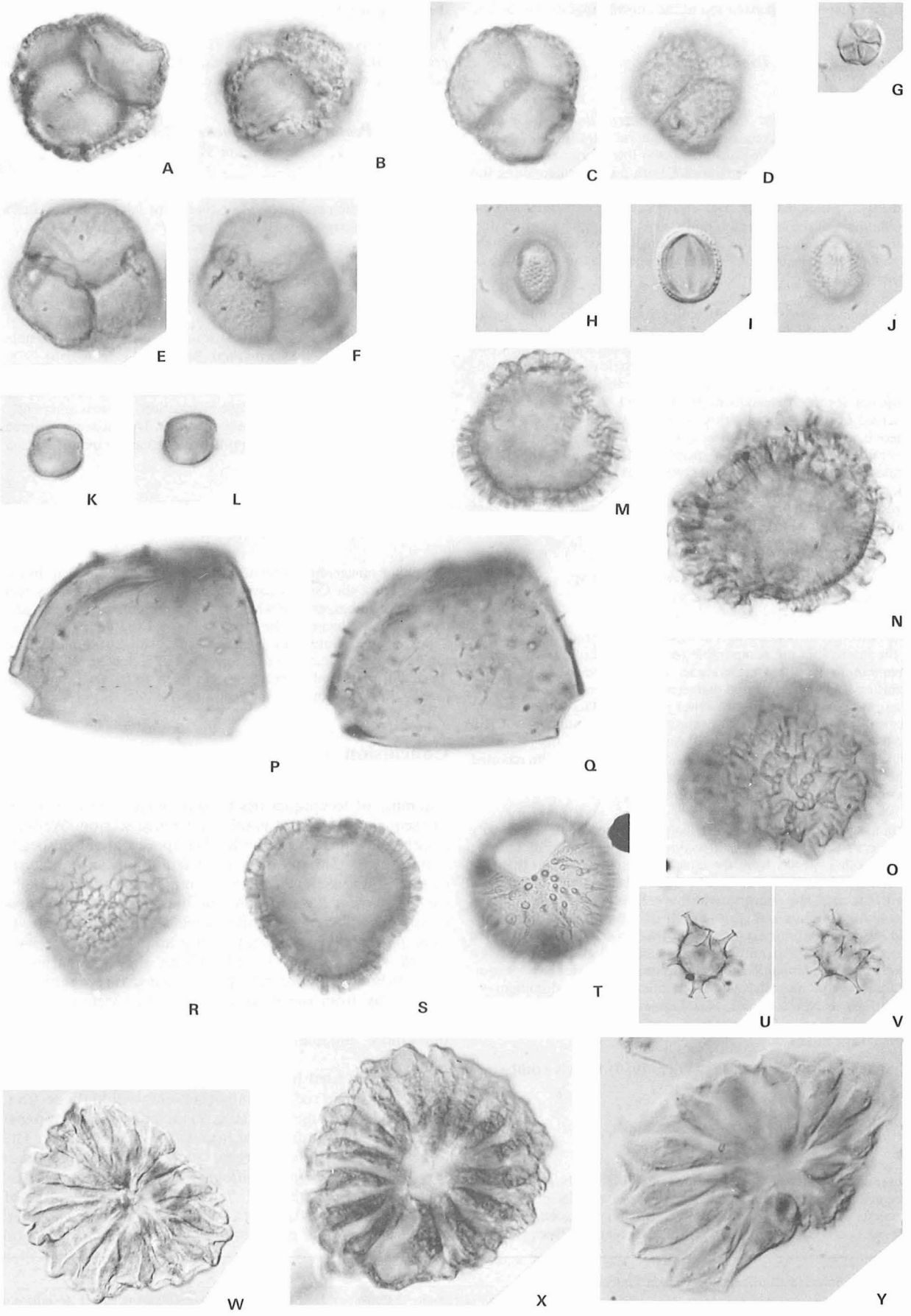
A
B
C
D
G
E
F
H
I
J
K
L
M
N
P
Q
O
R
S
T
U
V
W
X
Y

considered to be conformable with *T. ambiguus* were found at 121.30 m, near the base of the Geera Clay. This late Oligocene record appears to represent an extension of the known range of the species.

Triporotetradites sp.
Figure 9A–F

Pollen grains assigned here to *Triporotetradites* van Hoeken-Klinkenberg 1964 are retained in tetrahedral tetrads. They bear a surface ornament of irregular grana and low verrucae. Individual grains within the tetrad are triporate, with pores located along the centre of a line joining two adjacent grains. The pores are annulate and 2.0–2.5μm in diameter. Wall stratification is indistinct, and the development of the surface sculpture varies from grana to irregularly shaped verrucae up to 3.0μm in maximum diameter and 1.0μm high. Overall tetrad diameter: 26–31μm (5 specimens measured); individual grains 20–24μm.

The Oakvale species shows considerable similarity to *Triporotetradites letouzeyi* Salard-Cheboldaeff 1978, from the early Miocene of Cameroun. It is however, slightly smaller, and the sculptural elements are less regularly disposed than in the African species. Salard-Cheboldaeff (1978) suggested an affinity with Rubiaceae, possibly *Gardenia*, for the African form. In Oakvale-1, *Triporotetradites* was observed in the uppermost three samples of the Geera Clay only, where it was a rare form. An examination of the pollen of several Australian and New Guinean species of *Gardenia* shows a basic similarity in form and sculpture between these and the fossil species. The New Guinean species *Gardenia hansemanni-papuana* is particularly close to the fossil form, showing markedly annulate pores and a pronounced verrucate sculpture.

Cunoniaceae cf. ***Weinmannia*** sp.
Figure 9H–J

Small tricolporate pollen grains in which the sexine reticulum coarsens in the intercolpia are comparable to those produced by the genus *Weinmannia* of the Cunoniaceae. Dimensions: 10–13μm polar diameter, 10–12μm equatorial diameter (4 specimens measured). They occur in two samples from the lower part of the Geera Clay. Recent records of this taxon in the Australasian region include those of Hill & Macphail (1983) who compared some of the forms they identified with Cunoniaceae to *Weinmannia*, and Pocknall (1982) who reported *Weinmannia* from the late Oligocene in New Zealand. Neither of these records is supported by illustrations.

Cunoniaceae of dicolporate and tricolporate types are figured in Luly & others (1980). Both types are common constituents of Latrobe Valley pollen spectra from the late Oligocene through to the mid-Miocene, although the tricolporate type is also recorded consistently from the mid-late Eocene (Kershaw & others, in press). The tricolporate grains are slightly smaller than the Oakvale specimens, and are referred to the extant genera *Ackama* and *Pullea*, which are canopy dominants of rainforest in Queensland and northern New South Wales. *Weimmannia* does not occur within Australia at present, although it is an extremely widespread canopy dominant of rainforests in New Zealand, New Guinea, and New Caledonia.

Dinoflagellates

Hystrichokolpoma stellata (Maier, 1959) Harris comb. nov
Figure 10H

1959 *Hystrichosphaeridium stellatum* Maier, p. 320–321. pl. 33, fig. 3–4.

Stover & Evitt (1978, p. 56) considered this species to be provisionally accepted as a species of *Hystrichosphaeridium*, but noted that it had processes of two distinctly different widths and suggested that it was a species of *Hystrichokolpoma*. Studies of material from Oakvale, Oligocene assemblages from the Gippsland Basin, and late Eocene to early Oligocene assemblages from the St Vincent Basin confirm the reassignment.

The species most closely resembles *H. rigaudae*, but differs in having processes that are mostly flared distally, and in having only one process for each para-cingular plate.

Pentadinium laticinctum Gerlach 1961
Figure 11A

This species demonstrates a range of variability with respect to the definition of the paraplates. Most specimens fall within Benedek's (1972) circumscription of his sub-species *P. imaginatum*.

Adnatosphaeridium sp.
Figure 11I–L

This is a small species, which appears at first to resemble *?Areosphaeridium actinocoronatum* (Benedek) Stover & Evitt 1978. Benedek (1972, Pl. 12, fig. 13) figured only one specimen, in which it is difficult to see the true nature of the process tips. However, his text-figure 13 clearly shows a single bifurcation. There is apparently no distal connection between the process tips. The specimens figured here have complexly bifurcating process tips that are interconnected with very fine trabeculae.

Incertae cedis
Figure 9W–Y

Discoid or saucer-shaped bodies with serrated margins occur in the upper part of the Geera Clay. The discs are supported by a system of radiating tubes, each of which flares from a constricted base, and then constricts again at the distal margin of the body. The tubes appear to be enclosed in a hyaline sheath, which is crumpled and folded at the centre of the structure. Overall diameter: 47–60μm (8 specimens measured). Affinities seem likely to be algal, but more precise identification has not been possible.

Conclusion

In this study of the Oakvale-1 corehole we have employed a number of techniques designed to maximise the value of the sequence as a stratigraphic reference section. We have documented the ranges of individual spore and pollen species within the section, and have provided quantitative analyses of the variations in abundance of major taxa. Additionally, we have provided descriptions and illustrations of those taxa — spores, pollen, and dinoflagellates — that we consider to have potentially significant stratigraphic value. We have placed less emphasis on identifying the boundaries of previously described spore—pollen zones, as recognition of these away from the basin in which they were originally defined is often difficult, and their use may obscure potentially valuable biostratigraphic data.

The methods used have enabled us to recognise a number of biological and sedimentological events within the section. The qualitative range data (Fig. 2) include the first and last appearances of a number of taxa within the local area. The appearance data for species such as *Acaciapollenites myriosporites*, *Triporopollenites bellus*, *Proteacidites rectomarginis*, and the 'tropical Tertiary' suite of *Polypodiisporites usmensis*, *Margocolporites vanwijhei*, *Perfotricolpites* sp. cf. *P. digitatus*, *Crotonipollis* sp., and

Figure 10. Selected dinoflagellates from Oakvale-1.
All magnifications approximately x600. A–C, *Hystrichokolpoma rigaudae* (Deflandre & Cookson), 110.5 m, WM2133. D–F, *Glaphyrocysta* cf. *G. intricata* (Eaton), 110.5 m, WM2133. G, *Spiniferites trabeculiferum* (Deflandre & Cookson), 110.5 m, WM2133. H, *Hystrichokolpoma stellatum* (Maier), 110.5 m, WM2133. I,J, *Chiropteridium dispersum* Gocht, 110.5 m, WM2133. K,L, *Glaphyrocysta* sp., 110.5 m, WM2133. M,N, *Glaphyrocysta* sp., 110.5 m, WM2133.

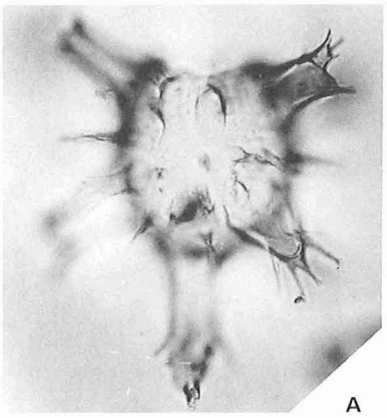
A

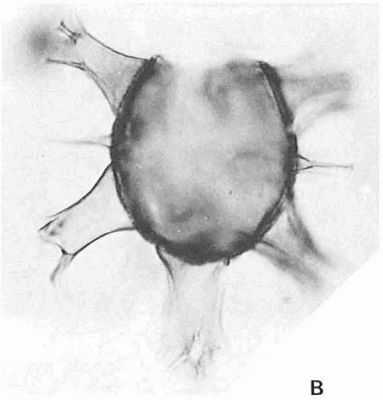
B

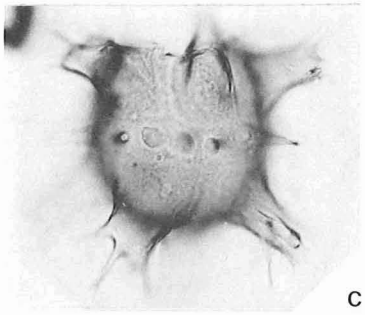
C

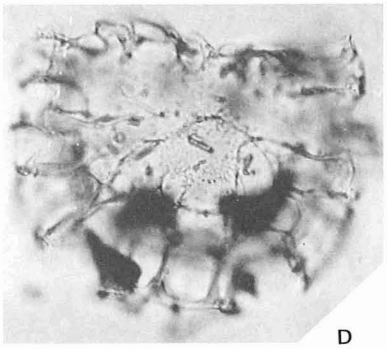
D

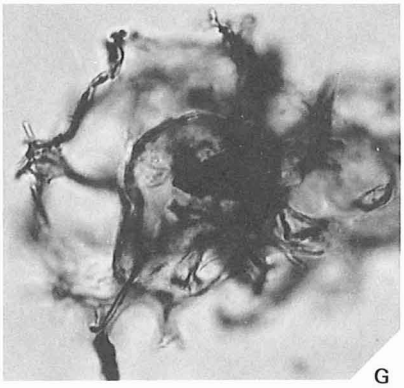
G

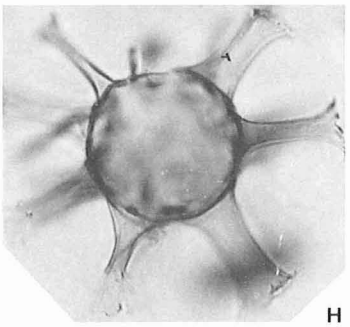
H

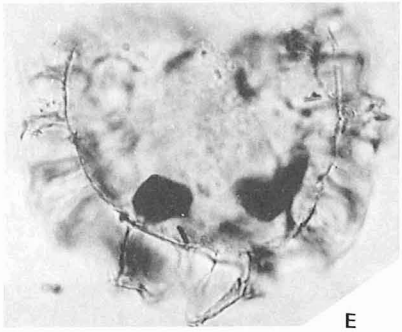
E

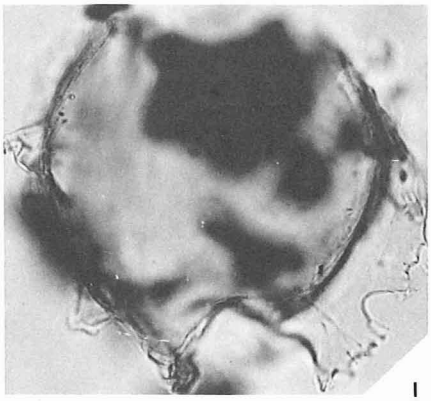
I

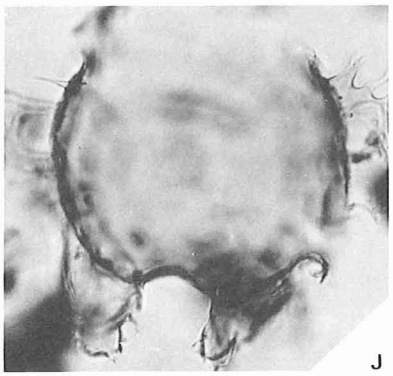
J

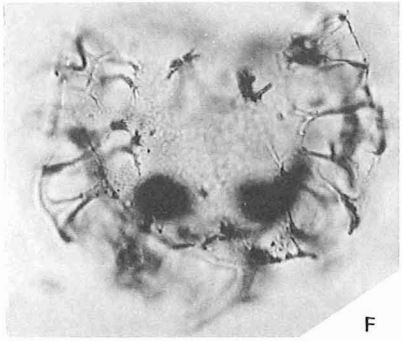
F

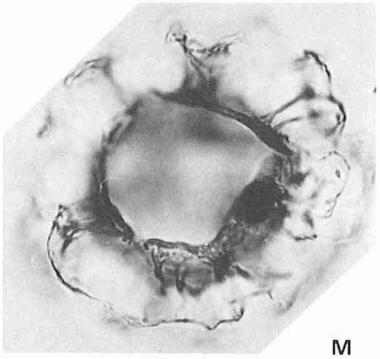
M

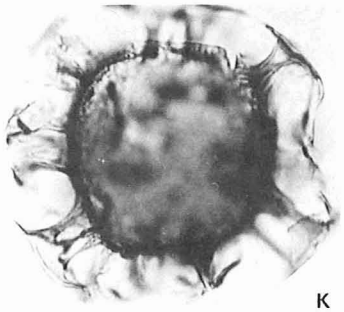
K

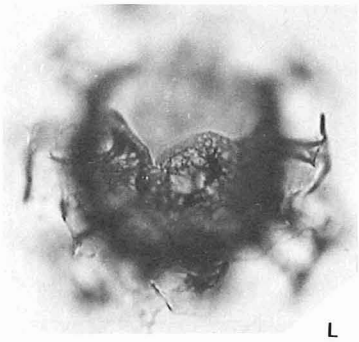
L

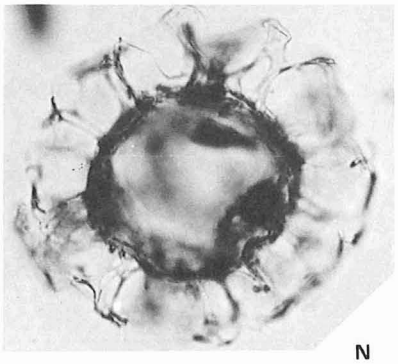
N

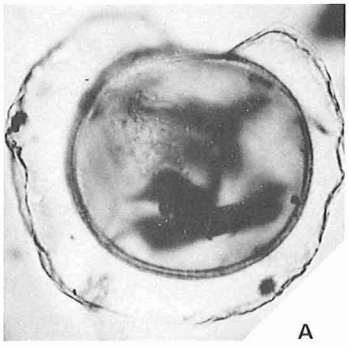
A

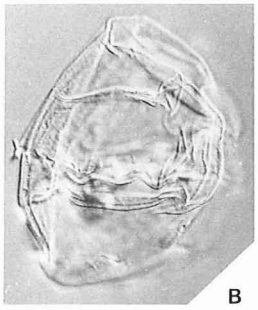
B

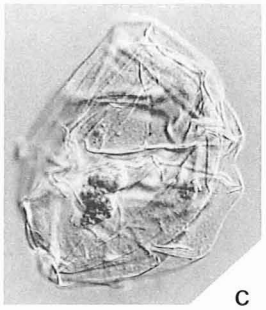
C


D

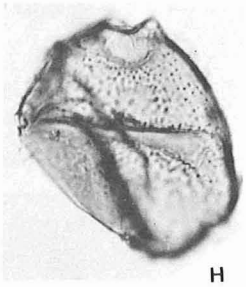
H

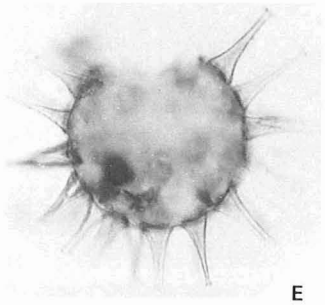
E

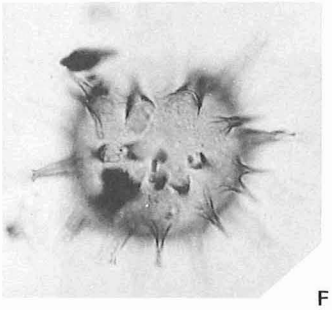
F

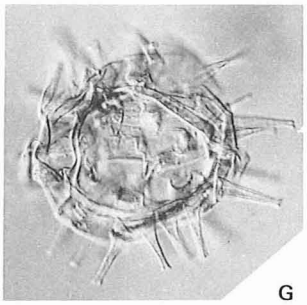
G

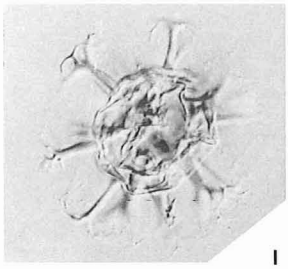
I

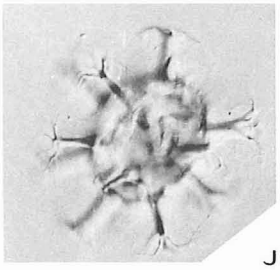
J

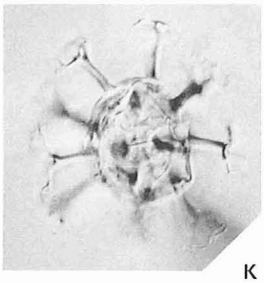
K

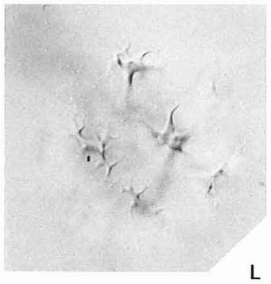
L

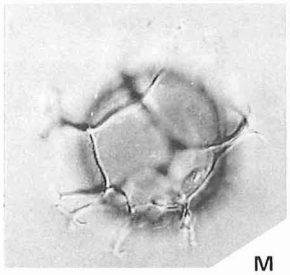
M

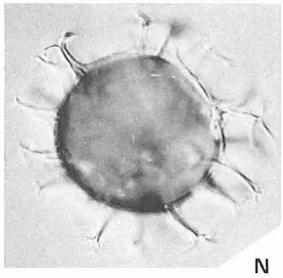
N

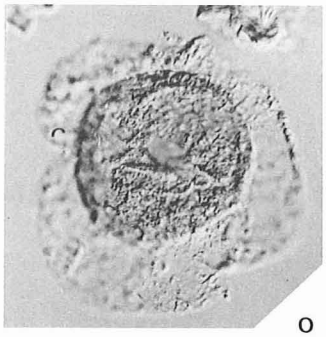
O

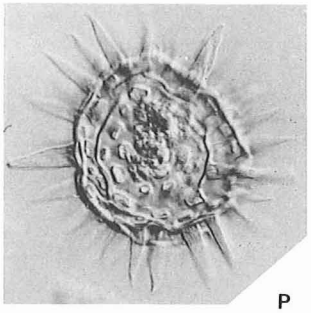
P

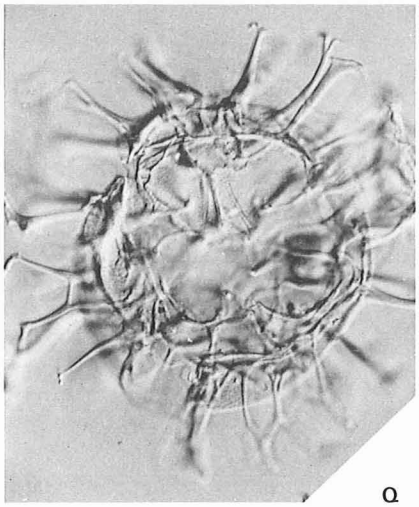
Q

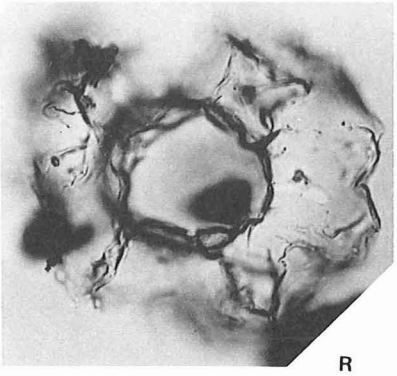
R

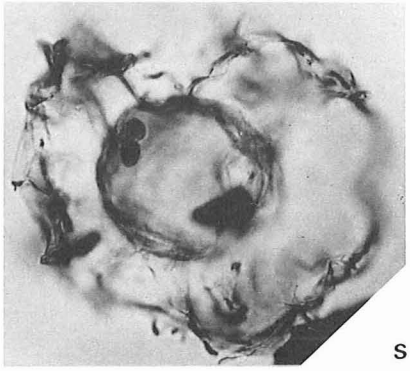
S

Triporotetradites sp., may be of local, and perhaps regional, correlative value. The distribution of recycled palynomorphs within the sequence, with a distinct increase in these in the upper part of the Geera Clay, must reflect sedimentary events; the extent of these remains unknown.

The quantitative data (Fig. 4) show a major change in vegetation composition to have occurred within the late Oligocene, marking the top of our Zone II. This we have interpreted as a climate-controlled change reflecting a transition from an essentially non-seasonal to a mildly seasonal precipitation regime. This is an event that we expect to be discernible through a reasonably wide region of inland Australia. We have suggested that it is a time-transgressive change, and that the same events occurred later in the eastern Murray Basin. The four subzones we have identified within Zone I at Oakvale may reflect local changes in the vegetation. Finally, we must stress that the Oakvale section has provided what must be regarded at this stage as no more than a preliminary evaluation of the biological, climatic, and sedimentological events affecting the western part of the Murray Basin; further sequences must be examined to assess over how wide an area these events can be recognised.

Acknowledgements

We are grateful to Roger Callen and Campbell Brown for the provision of valuable stratigraphic information; Campbell Brown also kindly gave us permission to use his diagram as our Figure 3. We thank Helene Martin and David Pocknall for thorough reviews of the manuscript and, with, Dallas Mildenhall, for access to unpublished palynological data. Henry Nix provided data on the present environments of *Araucaria*; and Peter Kershaw commented on parts of an early draft of the manuscript. The figures were drafted by M. Steele.

References

Abele, C., 1976 — Tertiary: Introduction. *In* Douglas, J.G., & Ferguson, J.A., (editors), Geology of Victoria. *Geological Society of Australia, Special Publication* 5, 177–191.

Ash, J., 1982 — The *Nothofagus* Blume (Fagaceae) of New Guinea. *In* Gressitt, J.L., (editor), Biogeography and ecology of New Guinea, *W. Junk, The Hague.*

Baksi, S.K., Deb., V., & Siddhanta, B.K., 1979 — On *Crotonipollis* — a new genus from the Paleocene-Eocene of India. *Indian Journal of Earth Science*, 6, 2.

Benedek, P.N., 1972 — Phytoplanktonen aus dem Mittel-und Oberoligozan von Tonisberg (Niederrheingebeit). *Palaeontographica B*, 137, 1–71.

Bowler, J.M., 1982 — Aridity in the late Tertiary and Quaternary of Australia. *In* Barker, W.R., & Greenslade, P.J.M., (editors), Evolution of the flora and fauna of arid Australia. *Peacock Publications, Adelaide.* 35–45.

Brosius, M., 1963 — Plankton aus dem Nordhessischen Kasseler Meeseessand (Obeoligozan). *Zeitschrift der Deutschen Geologischen Gesellschaft*, 114, 32–56.

Brown, C.M., 1983 — Discussion: a Cainozoic history of Australia's southeast highlands. *Journal of the Geological Society of Australia*, 30, 483–486.

Brown, C.M., 1984 — Murray Basin. *BMR 84, Yearbook of the Bureau of Mineral Resources, Geology & Geophysics.*

Chateauneuf, J.J., 1980 — Palynostratigraphie et paleoclimatologie de l'Eocene superieur et de l'Oligocene du Bassin de Paris. *Bureau des Recherches Geologiques et Minieres, Memoir* 116, 1–360.

Cookson, I.C., 1956 — On some Australian Tertiary spores and pollen grains that extend the geological and geographical distribution of living genera. *Proceedings Royal Society of Victoria*, 69, 41–53.

Cookson, I.C., & Pike, K.M., 1954 — Some dicotyledonous pollen types from Cainozoic deposits in the Australian region. *Australian Journal of Botany*, 2, 197–219.

Couper, R.A., 1953 — Upper Mesozoic and Cainozoic spores and pollen grains from New Zealand. *New Zealand Geological Survey, Paleontological Bulletin*, 22.

Couper, R.A., 1960 — New Zealand Mesozoic and Cainozoic plant microfossils. *New Zealand Geological Survey, Palaeontological Bulletin*, 32.

Dale, M.B., Lance, G.N., & Albrecht, L., 1971 — Extensions of information analysis. *Australian Computer Journal*, 3, 29–34.

Dawson, J.R., 1983 — Late Neogene vegetation communities and climatic implications ascertained from a study of eight cores from the Latrobe Valley depression, southeastern Australia. *B.Sc. (Hons.) Thesis, Monash University.*

Deflandre, G., & Cookson, I.C., 1955 — Fossil microplankton from Australian Late Mesozoic and Tertiary sediments. *Australian Journal of Marine and Freshwater Research*, 6, 292–313.

Dodson, J.R., 1983 — Modern pollen rain in southeastern New South Wales, Australia. *Review of Palaeobotany and Palynology*, 38, 249–268.

Douglas, J.G., Abele, C., Benedek, S., Dettmann, M.E., Kenley, P.R., & Lawrence, C.R., 1976 — Mesozoic. *In* Douglas, J.G., & Ferguson, J.A., (editors), Geology of Victoria. *Geological Society of Australia, Special Publication* 5, 143–176.

Drugg, W.S., & Loeblich, A.R. Jr., 1967 — Some Eocene and Oligocene phytoplankton from the Gulf Coast, U.S.A. *Tulane Studies in Geology*, 5, 181–194.

Dudgeon, M.J., 1983 — Eocene pollen of probable proteaceous affinity from the Yaamba Basin, central Queensland. *In* Roberts, J., & Jell, P.A., (editors), Dorothy Hill Jubilee Memoir. *Association of Australasian Palaeontologists, Memoir* 1, 339–362.

Enright, N.J., 1982a — The ecology of *Araucaria* species in New Guinea. I — Ordination studies of forest types and environments. *Australian Journal of Ecology*, 7, 23–38.

Enright, N.J., 1982b — The ecology of *Araucaria* species in New Guinea. II — Pattern in the distribution of young and mature individuals and light requirements of seedlings. *Australian Journal of Ecology*, 7, 39–48.

Enright, N.J., 1982c — The ecology of *Araucaria* species in New Guinea. III — Population dynamics of sample stands. *Australian Journal of Ecology*, 7, 227–237.

Enright, N.J., 1982d - The *Araucaria* forests of New Guinea. *In* Gressitt, J.L., (editor), Biogeography and ecology of New Guinea. *W.Junk, The Hague.*

Eisenack, A., 1954 — Microfossilien aus Phosphoriten des Samlandischen Unteroligozans and uber die Einheitlichkeit der Hystrichosphaerideen. *Palaeontographica A*, 105, 49–95.

Evans, P.R., & Hawkins, P.J., 1967 — The Cretaceous below the Murray Basin. *Bureau of Mineral Resources, Australia, Record* 1967/137.

Floyd, A.G., 1979 — N.S.W. Rainforest Trees. Part III. Family Myrtaceae. *Forestry Commission of New South Wales, Research Note* 28, Second Edition.

Foster, C.B., 1982 — Illustrations of Early Tertiary (Eocene) plant microfossils from the Yaamba Basin, Queensland. *Geological Survey of Queensland Publication* 381.

Gadek, P., & Martin, H.A., 1981 — Pollen morphology in the subtribe Metrosiderinae of the Leptospermoideae (Myrtaceae) and its taxonomic significance. *Australian Journal of Botany*, 29, 159–184.

Gamerro, J.C. & Archangelsky, S., 1981 — Palinozonas Neocretacicas y Tertiarias de la plataforma continental Argentina en la Cuenca del Colorado. *Revista Espanola de Micropaleontologia*, 13, 119–140.

Figure 11. Selected dinoflagellates from Oakvale-1.

All magnifications approximately x600. A, *Pentadinium laticinctum* Gerlach, 110.5 m, WM2133. B,C, *Saeptodinium* sp., 49.0 m, WM2128. D, *Tectatodinium pellitum* Wall, 110.5 m, WM2133. E,F, *Dapsilodinium pseudocolligerum* (Stover), 110.5 m, WM2133. G, *Polysphaeridium zoharyi* (Rossignol), 49.0 m, WM2128. H, *Cyclopsiella* cf. *C. elliptica* Drugg & Leoblich, 110.5 m, WM2133. I–L, *Adnatosphaeridium* sp., 49.0 m, WM2128. M,N, *Spiniferites ramosus* (Ehrenberg) 49.0 m, WM2128. O, Species indeterminate, 49.0 m, WM2128. P, *Lingulodinium machaerophorum* (Deflandre & Cookson), 49.0 m, WM 2128. Q, *Areosphaeridium* sp., 34.93 m, WM2126. R,S, ?*Membranilarnacia* sp., 110.5 m, WM2133.

Gerlach, E., 1961 — Mikrofossilien aus dem Oligozan and Miozan nordwestdeutschlands, unter besonderer Berucksichtigung der Hystrichosphaeren und Dinoflagellaten. *Neues Jahrbuch fur Geologie und Palaontologie, Abhandlungen.*

Germeraad, J.H., Hopping, C.A., & Muller, J., 1968 — Palynology of Tertiary sediments from tropical areas. *Review of Palaeobotany and Palynology* 6, 189–348.

Gocht, H., 1969 — Formengemeinschaften Alttertiaren Mikroplanktons aus Bohrproben des Erdolfeldes Meckelfeld bei Hamburg. *Palaeontographica B*, 126, 1–100.

Gordon, A.D. & Birks, H.J.B., 1972 — Numerical methods in Quaternary palaeocology. I. Zonation of pollen diagrams. *New Phytologist*, 71, 961–979.

Harland, W.B., Cox, A.V., Llewellyn, P.G., Pickton, C.A.G., Smith, A.G. & Walters R., 1982 — A geologic time scale. *Cambridge University Press, Cambridge.*

Harris, W.K., 1965 — Basal Tertiary microfloras from the Princetown area, Victoria, Australia. *Palaeontographica B*, 115, 75–106.

Harris, W.K., 1971 — Tertiary stratigraphic palynology, Otway Basin. *In* The Otway Basin of southeastern Australia. *Special Bulletin of the Geological Surveys of South Australia and Victoria*, 67–87.

Harris, W.K., 1972 — New form species of pollen from southern Australian early Tertiary sediments. *Transactions of the Royal Society of South Australia*, 96, 53–65.

Hekel, H., 1972 — Pollen and spore assemblages from Queensland Tertiary sediments. *Geological Survey of Queensland Publication* 335. *Palaeontological Paper* 30.

Hill, R.S., & MacPhail, M.K., 1983 — Reconstruction of the Oligocene vegetation at Pioneer, northeast Tasmania. *Alcheringa* 7, 281–299.

Hope, G.S., 1973 — The vegetation history of Mt. Wilhelm. *Ph.D. Thesis, Australian National University.*

Johns, R.T., 1982 — Plant zonation. *In* Gressitt, J.L., (editor), Biogeography and ecology of New Guinea. *W. Junk, The Hague.*

Kemp, E.M., 1976 — Early Tertiary pollen from Napperby, central Australia. *BMR Journal of Australian Geology & Geophysics*, 1, 109–114.

Kemp, E.M., Balme, B.E., Helby, R.J., Kyle, R.A., Playford, G., & Price, P.L., 1977 — Carboniferous and Permian palynostratigraphy in Australia and Antarctica: a review. *BMR Journal of Australian Geology & Geophysics*, 2, 177–208.

Kemp, E.M., & Harris, W.K., 1977 — The palynology of Early Tertiary sediments, Ninetyeast Ridge, Indian Ocean. *Palaeontological Association, Special Papers in Palaeontology*, 19, 1–70.

Kershaw, A.P., 1973 — Late Quaternary vegetation of the Atherton Tableland, northeast Queensland, Australia. *Ph.D. Thesis, Australian National University.*

Kershaw, A.P., 1976 — A Late Pleistocene and Holocene pollen diagram from Lynch's Crater, northeastern Queensland, Australia. *New Phytologist*, 77, 469–498.

Kershaw, A.P., 1984 — An extended late Quaternary vegetation record from north-eastern Queensland and its implications for the seasonal tropics of Australia. *Proceedings Ecological Society of Australia*, 13.

Kershaw, A.P., & Sluiter, I.R., 1982 — The application of pollen analysis to the elucidation of Latrobe Valley Brown coal depositional environments and stratigraphy. *Australian Coal Geology* 4, 169–186.

Kershaw, A.P., Sluiter, I.R., Dawson, J.R., Wagstaff, B.E., & Whitelaw, M., in press — The history of rainforest vegetation in Australia — evidence from pollen. *In* Australian national rainforest. *Study report to World Wildlife Fund Australia*, Vol. 1.

Khan, A.M., 1976 — Palynology of Tertiary sediments from Papua New Guinea. 1 — New form genera and species from Upper Tertiary sediments. *Australian Journal of Botany* 24, 753–781.

Khan, A.M., & Martin, A.R.H., 1971 — A note on genus *Polypodiisporites* R. Potonie. *Pollen et Spores*, 13 (3), 475–480.

Krutzsch, W., 1966 — Zur Kenntnis praquartarer periporater Pollenformen. *Geologie*, 15(55) 16–72.

Ladd, P.G., 1978 — Vegetation history of Lake Curlip in lowland eastern Victoria, from 5000 B.P. to present. *Australian Journal of Botany*, 26, 393–414.

Lawrence, C.R., 1966 — Cainozoic stratigraphy and structure of the Mallee Region, Victoria. *Proceedings of the Royal Society of Victoria*, 79, 517–553.

Lawrence, C.R., 1975 — Geology, hydrodynamics and hydrochemistry of the southern Murray Basin. *Memoirs of the Geological Survey of Victoria*, 30.

Lindsay, J.M., 1983 — Oligo-Miocene transgressive events in Geera Clay, Oakvale 1, northern Murray Basin. *Geological Survey of South Australia, Quarterly Geological Notes*, 85, 5–12.

Luly, J., Sluiter, I.R., & Kershaw, A.P., 1980 — Pollen studies of Tertiary brown coals: preliminary analyses of lithotypes within the Latrobe Valley, Victoria. *Monash University, Publications in Geography*, 23.

Ludbrook, N.H., 1961 — Stratigraphy of the Murray Basin in South Australia. *Geological Survey of South Australia, Bulletin* 36.

Maier, D., 1959 — Planktonuntersuchungen in tertiaren und quartaren marinen Sedimenten. *Neues Jahrbuch fur Geologie und Palaontologie, Abhandlungen* 107, 278–340.

Manum, S., 1976 - Dinocysts in Tertiary Norwegian-Greenland sea sediments (Deep Sea Drilling Project Leg 38), with observations on palynomorphs and palynodebris in relation to environment. *In* Talwani, M., Udintsev, G., & others, *Initial Reports of the Deep Sea Drilling Project*, 38, 897–919.

Martin, H.A., 1973 — Upper Tertiary palynology in southern New South Wales. *Geological Society of Australia, Special Publication* 4, 35–54.

Martin, H.A., 1977a — The Tertiary stratigraphic palynology of the Murray Basin in New South Wales. 1. The Hay—Balranald—Wakool districts. *Royal Society of New South Wales, Journal and Proceedings*, 110, 41–47.

Martin, H.A., 1977b — The history of *Ilex* (Aquifoliaceae) with special reference to Australia: evidence from pollen. *Australian Journal of Botany* 25, 655–73.

Martin, H.A., 1978 — Evolution of the Australian flora and vegetation through the Tertiary: evidence from pollen. *Alcheringa* 2, 181–202.

Martin, H.A., 1979 — Stratigraphic palynology of the Mooki Valley, New South Wales. *Royal Society of New South Wales, Journal and Proceedings*, 112, 71–78.

Martin, H.A., 1980 — Stratigraphic palynology from shallow bores in the Namoi River and Gwydir River Valleys, North-Central New South Wales. *Royal Society of New South Wales, Journal and Proceedings*, 113, 81–87.

Martin, H.A., 1981 — Stratigraphic palynology of the Castlereagh River Valley, New South wales. *Royal Society of New South Wales, Journal and Proceedings*, 114, 77–84.

Martin, H.A., 1982 — Changing Cenozoic barriers and the Australian palaeobotanical record. *Annals of the Missouri Botanical Garden*, 69, 625–667,

Martin, H.A., 1984 — The use of quantitative relationships and palaeoecology in stratigraphic palynology of the Murray Basin in New South Wales. *Alcheringa*, 8, 253–272.

McMinn, A., 1981a — Palynological results from the Murray Valley Drilling Project. *Geological Survey of New South Wales, unpublished palynological report*, 81/6.

McMinn, A., 1981b — A Miocene microflora from the Home Rule Kaolin deposit. *Geological Survey of New South Wales, Quarterly Notes*, 43, 1–4.

Medus, J., 1975 — Palynologie de sediments Tertiares du Senegal meridional. *Pollen et Spores*, 17, 545–608.

Mildenhall, D.C., 1980 — New Zealand Late Cretaceous and Cenozoic plant biogeography: a contribution. *Palaeogeography, Palaeoclimatology, Palaeoecology*, 31, 197–233.

Morgan, R., 1977 — Stratigraphy and palynology of the Oaklands Basin, New South Wales. *Geological Survey of New South Wales, Quarterly Notes*, 29, 1–16.

Muller, J., 1968 — Palynology of the Pedawan and Plateau Sandstone Formations (Cretaceous-Eocene) in Sarawak, Malaysia. *Micropaleontology* 14(1), 1–37.

Muller, J., 1981 — Fossil pollen records of extant angiosperms. *Botanical Review*, 47, 1–142.

Nix, H., 1982 — Environmental determinants of biogeography and evolution in Terra Australis. *In* Barker, W.R., & Greenslade, P.J.M., (editors), Evolution of the flora and fauna of arid Australia. *Peacock Publications, Adelaide*, 47–66.

O'Brien, P.E., 1981 — Permian sediments beneath the Murray basin. *Bureau of Mineral Resources, Australia, Record* 1981/60.

Owen, J.A., 1975 — Palynology of some Tertiary deposits from New South Wales. *Ph.D. Thesis, Australian National University.*

Partridge, A.D., 1971 — Stratigraphic palynology of the onshore Tertiary sediments of the Gippsland Basin, Victoria. *M.Sc. Thesis, University of New South Wales.*

Partridge, A.D., 1978 — Palynology of the Late Tertiary sequence at Site 365, Leg 40, Deep Sea Drilling Project. *In* Bolli, H.M., Ryan, W.B.F., & others, *Initial Reports of the Deep Sea Drilling Project* 40, 953–961.

Playford, G., 1982 — Neogene palynomorphs from the Huon Peninsula, Papua New Guinea. *Palynology* 6, 29–54.

Pocknall, D.T., 1982 — Palynology of late Oligocene Pomahaka Estuarine Bed sediments, Waikoikoi, Southland, New Zealand. *New Zealand Journal of Botany*, 20, 263–287.

Pocknall, D.T., & Crosbie, Y.M., 1982 — Taxonomic revision of some Tertiary tricolporate and tricolpate pollen grains from New Zealand. *New Zealand Journal of Botany*, 20, 7–15.

Pocknall, D.T. & Mildenhall, D.C., 1984 — Late Oligocene - Early Miocene spores and pollen from Southland, New Zealand. *New Zealand Geological Survey Paleontological Bulletin*, 51.

Powell, J.M., 1970 — The impact of man on the vegetation of the Mt. Hagen region, New Guinea. *Ph.D. Thesis, Australian National University.*

Price, P.L., 1983 — A Permian palynostratigraphy for Queensland. Proceedings of the symposium on the Permian geology of Queensland. *Geological Society of Australia (Queensland Division), Brisbane*, 155–211.

Salard-Cheboldaeff, M., 1978 — Sur la palynoflore Maestrichtienne et Tertiare du bassin sedimentaire littoral du Cameroun. *Pollen et Spores* 20, 215–60.

Scholtz, A., 1985 — The palynology of the Upper lacustrine sediments of the Arnot Pipe, Banke, Namaqualand. *Annals of the South African Museum*, 95, 1–109.

Sengupta, S., 1972 — On the pollen morphology of Convulvulaceae, with special reference to taxonomy. *Review of Palaeobotany and Palynology*, 13, 5–143.

Shackleton, N.J. & Kennett, J.P., 1975 - Palaeotemperature history of the Cenozoic and the initiation of Antarctic glaciation: oxgyen and carbon isotope analyses in DSDP sites 277, 279, 281. *In* Kennett, J.P., Houtz, R.E., & others, *Initial Reports of the Deep Sea Drilling Project* 29, 743–55.

Shimakura, M., Nishida, S., & Matsuoka, K., 1971 - Some plant microfossils from the Yamato-tai, Sea of Japan. *Bulletin Nara University of Education, (Nat.)*, 20, 63–70.

Singh, G., Opdyke, H.D., & Bowler, J.M., 1981 — Late Cainozoic stratigraphy, palaeomagnetic chronology and vegetational history from Lake George, N.S.W. *Journal of the Geological Society of Australia*, 28, 435–452.

Sluiter, I.R., & Kershaw, A.P., 1982 — The nature of Late Tertiary vegetation in Australia. *Alcheringa* 6, 211–222.

Stover, L.E., 1977 — Oligocene and Early Miocene dinoflagellates from Atlantic Corehole 5/5B, Blake Plateau. *American Association of Stratigraphic Palynologists, Contributions*, 5A, 66–90.

Stover, L.E., & Evans, P.R., 1973 — Upper Cretaceous—Eocene spore-pollen zonation, offshore Gippsland Basin, Australia. *Geological Society of Australia, Special Publication* 4, 55–72.

Stover, L.E. & Evitt, W.R., 1978 — Analyses of pre-Pleistocene organic-walled dinoflagellates. *Stanford University Publications in Geological Science*, 25.

Stover, L.E., & Partridge, A.D., 1973 — Tertiary and Late Cretaceous spores and pollen from the Gippsland Basin, southeastern Australia. *Royal Society of Victoria, Proceedings*, 85(2), 237–86.

Stover, L.E. & Partridge, A.D., 1982 — Eocene spore-pollen from the Werillup Formation, Western Australia. *Palynology*, 6, 69–95.

Thanikaimoni, C., 1966 — Pollen morphology of the genus *Utricularia. Pollen et Spores*, 8, 265–84.

Tulip, J.R., Taylor, G., & Truswell, E.M., 1982 — Palynology of Tertiary Lake Bunyan, Cooma, New South Wales. *BMR Journal of Australian Geology & Geophysics*, 7, 255–268.

Vail, P.R., Mitchum, R.M. Jnr., & Thompson, S., 1977 — Seismic stratigraphy and global changes of sea level. Part 4: Global cycles of relative changes of sea-level. *In* Payton, C.E., (editor), Seismic stratigraphy — application to hydrocarbon exploration. *American Association of Petroleum Geologists, Memoirs*, 26, 83–97.

Van Der Hammen, T., 1956 — Description of some genera and species of fossil pollen and spores. *Boletin Geologica* (Bogota), 4, (2/3), 111–117.

Webb, L.J. & Tracey, J.G., 1967 — An ecological guide to new planting areas and site potential for Hoop Pine (*Araucaria cunninghamii* Ait) *Australian Forestry*, 31, 224–39.

BMR Journal of Australian Geology & Geophysics, 9, 297-302

Australian long-wavelength magnetic anomalies

Peter Wellman[1], A.S. Murray[1], & M.W. McMullan[2]

A long-wavelength magnetic anomaly map is derived from near-surface observations. The data can be continued upward for comparison with maps derived from satellite data. Compared with a map from 400-km altitude observations of the MAGSAT satellite, the highs and lows are in a similar geographic position, but the MAGSAT map is smoothed, possibly by uncorrected variations in satellite altitude. The long-wavelength magnetic anomalies have no significant correlation with heat flow or seismically measured crustal thickness, and have an amplitude higher than that expected for a non-magnetic sediment. In central and western Australia, magnetic highs are spatially associated with crustal block boundaries defined by elongate, high-amplitude, associated gravity highs and lows. Consequently, the long-wavelength magnetic anomalies are thought to be caused by rocks of high magnetisation in the upper or lower crust.

Introduction

The long-wavelength magnetic field is important because of its potential to give significant new information on long-wavelength crustal properties that is independent of other methods. Magnetic measurements on POGO and MAGSAT satellites have recently been used to determine long-wavelength magnetic anomalies over Australia (Mayhew & others, 1980; Langel & others, 1982).

In this study the long-wavelength anomalies calculated from near-surface magnetic measurements are compared with the satellite long-wavelength anomalies, and are used to investigate the lithospheric source of the anomalies. Long-wavelength magnetic observations have previously been described by Dooley (1979), Dooley & McGregor (1982) and Mayhew & others (1980).

MAGSAT satellite magnetic anomaly map

Figure 1 gives the MAGSAT satellite magnetic anomaly field at 400 km altitude with a 2° grid (Langel & others, 1982). The profiles are at a 7° angle from north to south, with average altitude varying from 349 km to 467 km. The regional field used is MGST 4/81, a 13th degree and order spherical harmonic model derived from world MAGSAT measurements (Langel & others, 1981).

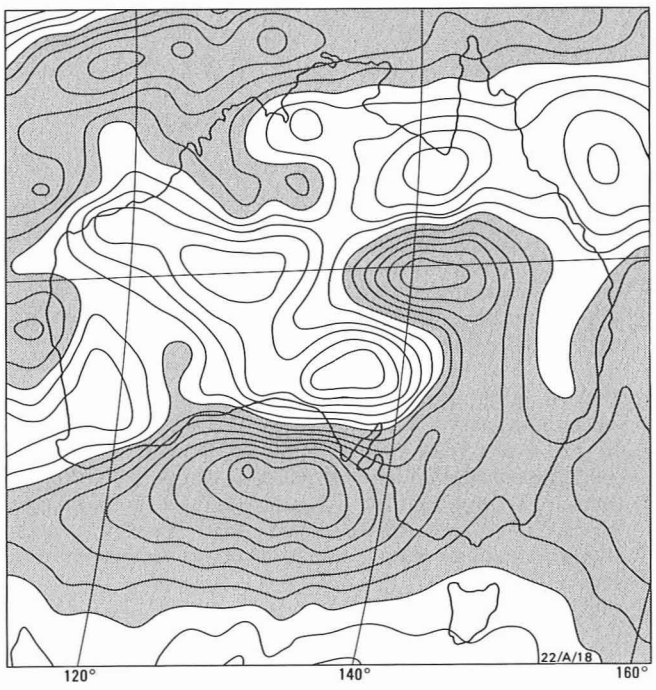

Figure 1. MAGSAT anomaly map, 200 km grid, 400 km (349–467 km) altitude, 2 nT contour interval.
Negative anomalies are stippled (after Langel & others, 1982).

Aeromagnetic long profiles

Numerous profiles across Australia of the total magnetic field were flown between 8 November 1975 and 8 March 1976, using a Bureau of Mineral Resources aeromagnetic aircraft (Dooley & McGregor, 1982) (Fig. 2). Flights were at 3 km altitude with one exception, and mainly between 2100 and 0600 hours UT. The magnetic field was measured with a proton precession magnetometer and paper chart recorder. The charts were subsequently digitised at 1 minute intervals, which is equivalent to an average horizontal ground distance of 5 km. Navigation was by normal aircraft navigation aids and maps. Anomalies were corrected for the secular variation between flight date and 1980.0 with the model of McEwin & others (1981). This secular variation model is a polynomial derived mainly from repeat readings at 62 first-order magnetic stations within Australia. The regional field model MGST 4/81 was used for the 1980.0 field, so that the anomalies would have the same regional as those of Langel & others (1982).

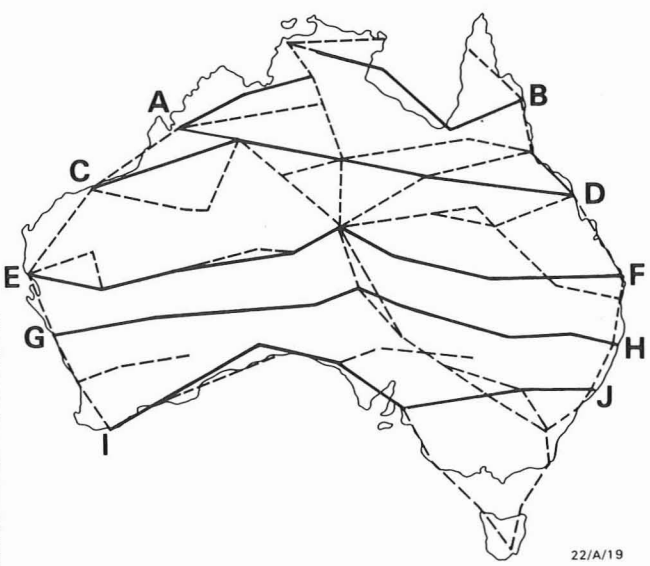

Figure 2. Flight lines of 1975–1976 long-profile survey.
Profiles in Figure 3 are those shown as solid lines.

During most flights a temporary ground station recorded diurnal variation. However, almost all ground recording stations were near the coast, so the recorded diurnal variation over-emphasised the coastal effect and was often over 1000

[1]Division of Geophysics, BMR
[2] Present address: Learmonth Solar Observatory, Exmouth, Western Australia 6707

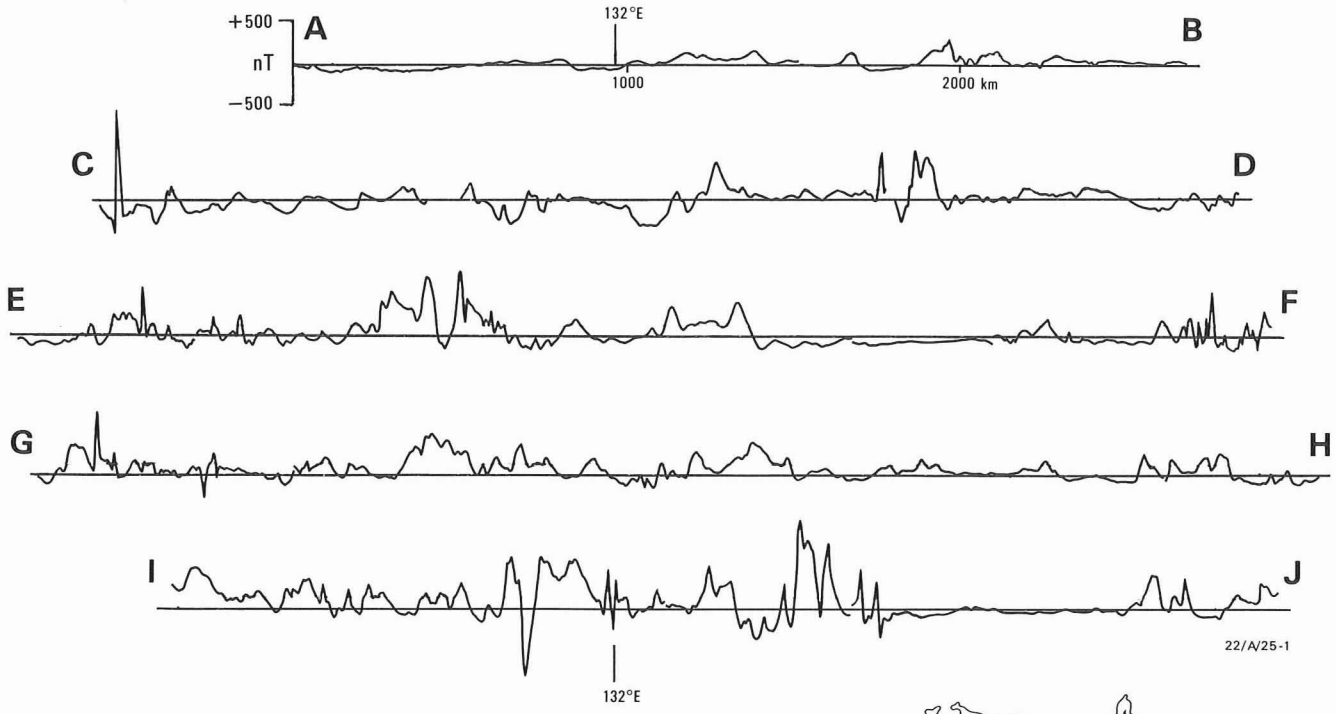

Figure 3. Magnetic anomaly profiles across Australia at 3 km altitude.
Location of profiles is shown in Figure 2.

km from the flight recording. Diurnal corrections were found to decrease rather than increase the consistency of measurements at flight-crossing points, so the diurnal corrections were not used. The 10 368 anomaly values had a mean of −91 nT, which was subtracted from the anomalies to give a zero mean. Figure 3 shows a selection of east-west profiles.

Third-order ground spot readings

From 1967 to 1975 the observatory section of BMR made surface spot readings of three magnetic components over most of Australia (Dooley & McGregor, 1982) (Fig. 4). In the desert area of central and western Australia readings were taken on a grid of 15 minutes (25 km) spacing, using helicopter transport. Over most of Australia they are at approximately 15-km intervals along roads, the roads being spaced approximately 100 km apart. The 7800 readings of total magnetic intensity were made with proton precession magnetometers.

Observations were made during daylight hours. No diurnal corrections have been made. Secular variation corrections from the observation date to 1975.0 have been made by linearly interpolating between three magnetic observatories in the Australian region and approximating the observatory mean-annual-values by a linear change. The changes used between 1967.0 and 1975.0 are for the three observatories: PMG −26 nT, GNA −108 nT, TOO −144 nT.

Secular variation from 1975 to 1980 is from McEwin & others (1981), and the regional magnetic field used for 1980.0 is MGST 4/81. To get a zero mean, 41 nT has been added to the anomalies.

Comparison of zero-level of data sets

Contour maps of third-order anomalies are generally similar in level and form to maps of long-profile anomalies. The exception is the northwestern corner of Australia, where the

Figure 4. Station distribution of third-order survey of 1967—1975.

third-order anomalies seem to be about 30 nT more negative. The discrepancy may be due to incorrect secular variation correction in that area.

Diurnal variation during daylight hours is up to 50 nT in Australia (McEwin & others, 1981). The mean long-profile field of −91 nT and the mean third-order field of −41 nT are therefore much more negative than can be explained by diurnal variation and the difference in local time between the satellite and near-surface observations. These differences in mean anomaly may be due to errors in the secular and regional fields.

Comparison of near-surface and satellite anomalies

Near-surface composite maps were prepared, the third-order and long-profile data being used together to obtain the maximum number of observations. The data were gridded, continued upward, and contoured on the CSIRONET Cyber 7600 computer (Murray, 1977). Figure 5 shows the anomalies

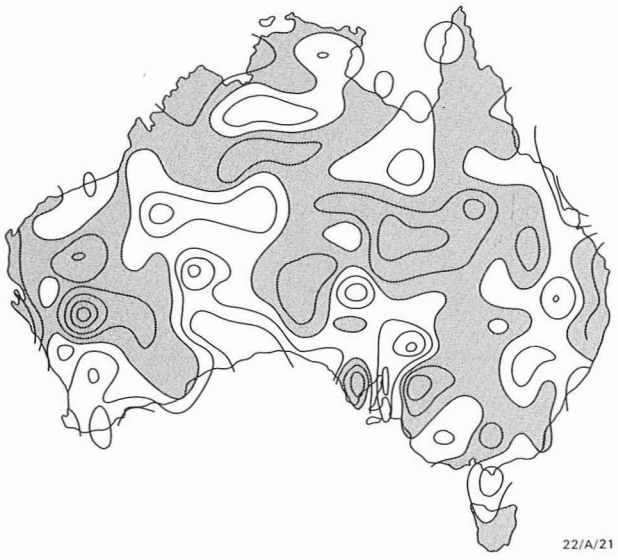

Figure 5. Anomalies from third-order plus long-profile surveys, 200 km grid, 1.5 km altitude, 50 nT contour interval.

with the same size grid as the MAGSAT map of Figure 1 (200 km), but with a 1.5 km rather than 400 km mean altitude. The position and relative amplitude of the anomalies on these two maps are so similar that both sets are likely to be mainly due to a real geographic variation in magnetic anomaly.

Figure 6 has been prepared from a 100 km grid (Fig. 7) continued upward to 400 km by applying the upward-continuation coefficients for a plane (Henderson, 1960) to the 100-km grid points and taking the mean of four adjacent grid points to give 200 x 200 km mean values, like those of the MAGSAT map of Figure 1. Upward continuation of a 100 km grid gives edge effects of smaller geographic extent than those resulting from a 200 km grid. The use of plane rather than spherical upward continuation is thought to lead to errors of no more than 5 per cent in amplitude at 400 km altitude (Vints & others, 1970; J.C. Dooley, personal communication). High-amplitude short-wavelength components in the third-order and long-profile data are suppressed by both the coarse grid averaging and the upward continuation, so they should have a negligible effect on the values of the 200 km grid at 400 km altitude. Long-wavelength anomalies should be preserved by the gridding and upward continuation.

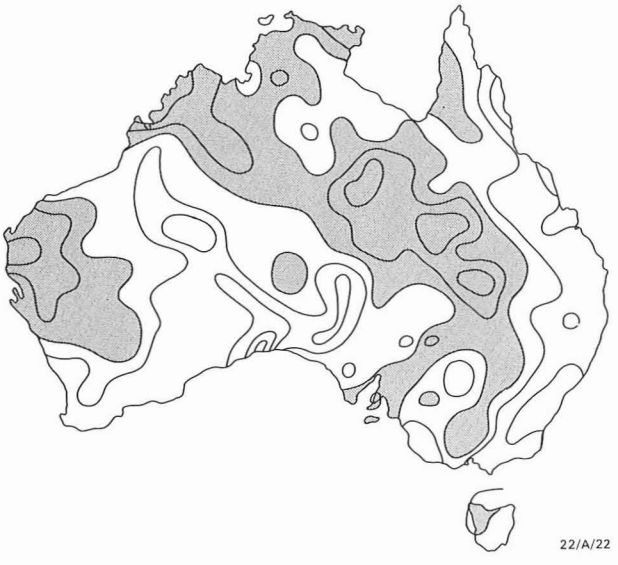

Figure 6. Anomalies from third-order plus long-profile surveys, 200 km grid, 400 km altitude, 10 nT contour interval.

Near the centre of Australia the anomalies calculated for 400 km from near- surface data have a wavelength of about half and an amplitude about twice those shown on the MAGSAT map. This amplitude and wavelength difference between near-surface and satellite data is also found if near-surface data are first gridded at 200 km and then continued upward to 400 km altitude. The difference in amplitude and wavelength is attributed to smoothing of the MAGSAT map caused by both the considerable difference in altitude of the satellite passes and adjacent profiles having different zero level because the fitted and subtracted quadratic functions do not precisely remove the effects of external fields. An amplitude discrepancy that is smaller but in the same direction is found between near-surface and MAGSAT anomalies over Canada (fig. 2a, b of Langel & others, 1980) and the USA (von Frese & others, 1982; Won & Son, 1982).

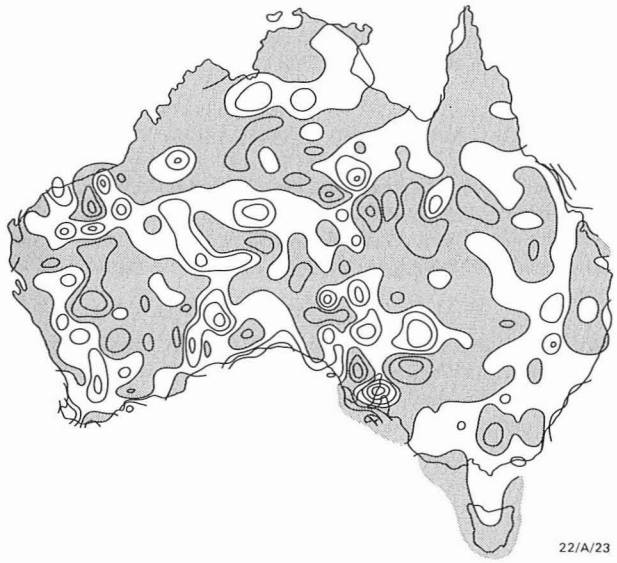

Figure 7. Anomalies from third-order plus long-profile surveys, 100 km grid, 1.5 km altitude, 100 nT contour interval.

Cause of long-wavelength magnetic anomalies

Long-wavelength magnetic anomalies could be caused by either long-wavelength magnetic sources or many adjacent short-wavelength sources. The magnetic sources could be abnormally high or abnormaly low magnetisation in either the upper or lower part of the crust.

Possible variation in thickness of the magnetised lower crust

If the lower crust has uniform magnetisation, then regional variation in heat flow should show a negative correlation with long-wavelength magnetic anomalies, the hotter crust having a shallower Curie point and so being less magnetic. A composite heat-flow map (Fig. 8) does not show the expected correlation with Figure 5: in particular, eastern South Australia has high heat flow and high magnetic anomaly, and the central part of Western Australia has low heat flow and low magnetic anomaly. Figure 9 shows that there is no significant correlation between mean heat flow at the better (>333) heat-flow sites of Cull (1982) and the 2° grid magnetic anomaly (Fig. 5).

Figure 8. Heat flow in Australia, 3° grid, 10 mW.m^{-2} contour interval (after Cull & Conley, 1983).

If the crust has uniform magnetisation, but varies in thickness, then the thicker crust will be more magnetic. Seismic refraction determinations of crustal thickness, using amplitudes and synthetic seismograms (Wellman, 1982; Finlayson & others, 1984), do not show the expected positive correlation with long-wavelength magnetic anomalies (Fig. 10).

Both the above comparisons are with the observed magnetic anomaly, not the intensity of magnetisation of the magnetic source model. Mayhew & others (1980) showed that most of the long-wavelength anomalies are not significantly offset from their source body.

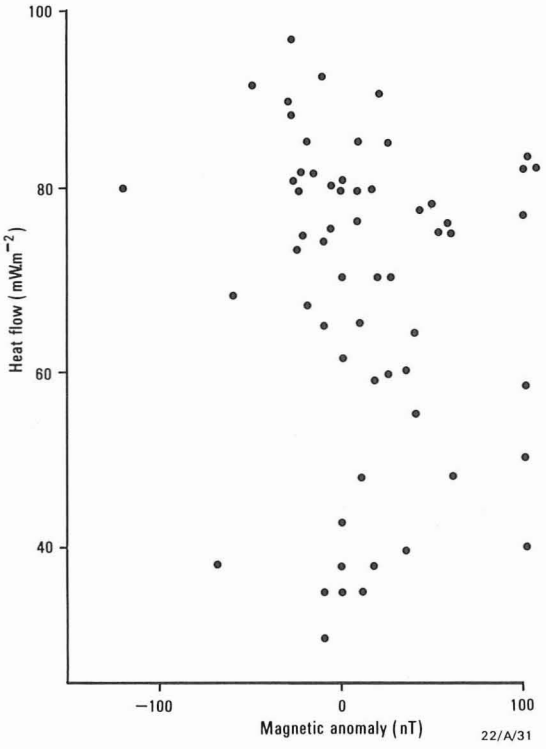

Figure 9. Correlation between heat flow and magnetic anomaly (2° grid).

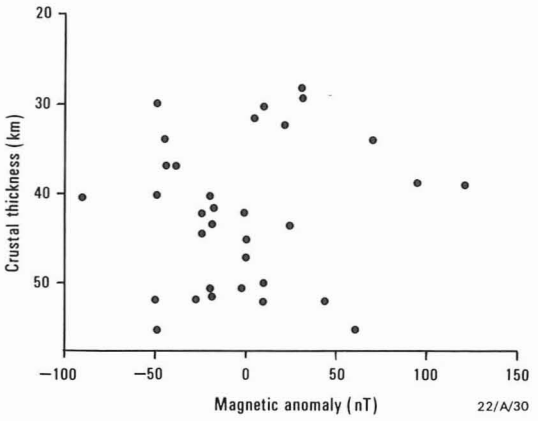

Figure 10. Correlation between seismic crustal thickness and magnetic anomaly (2° grid).

As heat flow and crustal thickness do not have a significant correlation with long-wavelength magnetic anomalies, the long-wavelength magnetic anomalies are unlikely to be caused by variation in the thickness of the magnetic layer in the lower crust.

A cause of low magnetic anomalies in sediments within the upper crust

The major low magnetic anomalies of Figures 1 and 5 are extensive areas of low-amplitude anomaly with a slightly negative mean (Figs. 3, 7, 11) The major areas of low magnetic anomalies in eastern Australia (Figs. 1, 5) correspond in position with the major post-cratonisation sedimentary basins of Phanerozoic age — the Carpentaria, Eromanga, and Murray Basins (Dooley, 1979; Mayhew & others, 1980). The major areas of low magnetic anomaly in western Australia do not overlie single tectonic units, but large parts of them correspond with the major post-cratonisation sedimentary basins of Proterozoic age.

The magnetic anomaly due to the two sedimentary basins has been modelled two-dimensionally, by assuming that the sediments are non-magnetic and that the non-sedimentary rocks underlying the basin have an apparent susceptibility

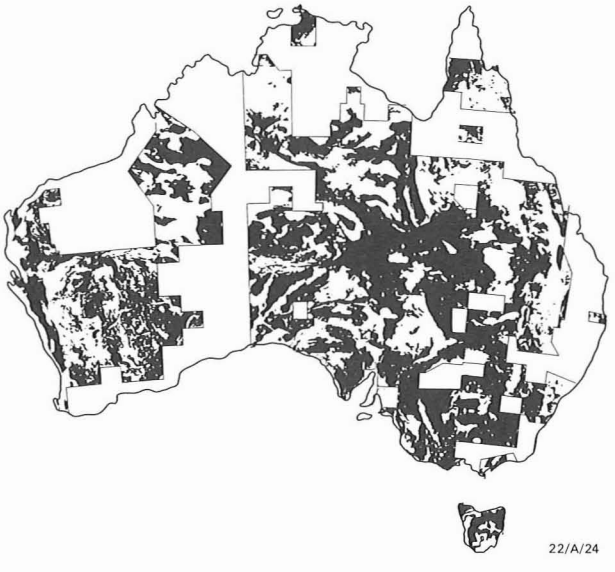

Figure 11. Aeromagnetic anomalies, black negative (from BMR, 1976).

of 0.0016 emu in the c.g.s. system (0.02 in SI system). There are few accurate measurements of mean apparent susceptibility of the uppermost crust. The value used here is that determined for Enderby Land in Antarctica (Wellman, 1983a); this value is likely to be too high, because Enderby Land is deeply eroded (Wellman, 1983b) and within a MAGSAT anomaly high (Ritzwoller & Bently, 1982). At the Earth's surface the calculated peak-to-peak amplitudes of the long-wavelength anomalies that coincide with the basins are 5 nT for the Eromanga Basin, of 3 km depth and 750 km width, and 1 nT for the Canning Basin, which is deeper but more irregular in depth. These anomalies are small compared with those at 1.5 km (Fig. 5) and 400 km (Figs. 1, 6). This suggests that the low magnetic anomalies are not caused principally by lower magnetisation of the sediments relative to the average crust.

Changes in magnitude of crustal magnetisation as a cause of high magnetic anomalies

Amplitudes of long-wavelength anomalies are lower in the Phanerozoic eastern third of Australia than in the Precambrian western two-thirds (Fig. 7). In the eastern third of Australia the long-wavelength magnetic anomalies correlate roughly with areas of exposed basement. In the western two-thirds of Australia the positive magnetic anomalies correlate well with outcropping and subcropping crustal block boundaries (Fig. 12) inferred from analysis of gravity anomaly trends (Wellman, 1976) and from large, adjacent positive and negative gravity anomalies (Wellman, 1978). The ground location of the high magnetic anomalies is shown on the aeromagnetic maps of Australia; data to 1976 are given in Figure 11. The high magnetic anomalies are associated with the high gravity anomalies at one side of the junction of crustal blocks. Both gravity and magnetic anomalies are thought to be due to lower crustal material that has been obducted to near the Earth's surface (Karner & Watts, 1983).

Frey & others (1983) have shown that on a reassembled Gondwanaland the MAGSAT anomalies reduced to poles are continuous across Gondwanaland fragments. This is consistent with a cause of the anomalies in crustal block boundaries as these boundaries predate the break up of Gondwanaland.

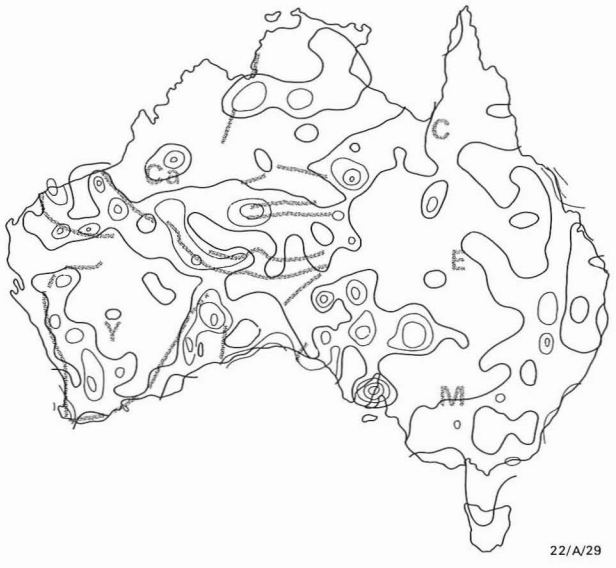

Figure 12. Positive magnetic anomalies (1° grid) and crustal block boundaries from gravity anomalies (from Wellman, 1978).

Conclusions

Magnetic anomalies at satellite altitudes can be determined using near-surface observations, provided that the near-surface observations have an accurate datum and the secular variation is known.

These near-surface observations are more useful than MAGSAT anomalies for studies of the lithosphere, because they contain the shorter-wavelength information that is necessary to reliably correlate anomalies with crustal features.

The long-wavelength anomalies in Australia are interpreted here as mainly due to high apparent-susceptibility rock in the upper or lower crust. The rock occurs in areas of basement uplift in eastern Australia and at one side of block boundaries in central and western Australia.

Acknowledgements

I thank J.C. Dooley, A.J. McEwin, P.M. McGregor, G.R. Small, and anonymous reviewers for comments on data reduction and the text, and R.W. Bates and P. Corbett for the drafting.

References

BMR, 1976 — Magnetic map of Australia, residuals of total intensity, scale 1:2 500 000. *Bureau of Mineral Resources, Australia.*

Cull, J.P., 1982 — An appraisal of Australian heat-flow data. *BMR Journal of Australian Geology & Geophysics*, 7, 11–21.

Cull, J.P., & Conley, D., 1983 — Estimates of temperature and heat flow in the sedimentary basins of Australia, *BMR Journal of Australian Geology & Geophysics*, 8, 329–337.

Dooley, J.C., 1979 — A geophysical profile across Australia at 29⅛S, *BMR Journal of Australian Geology & Geophysics*, 4, 353–359.

Dooley, J.C., & McGregor, P.M., 1982 — Correlative geophysical data in the Australian region for use in the MAGSAT project, *Bulletin of the Australian Society of Exploration Geophysicists*, 13, 63–67.

Frey, H., Langel, R.A., Mead, G., & Brown, K., 1983 — Pogo and Pangea. *Tectonophysics*, 95, 181–189.

Finlayson, D.M., Collins, C.D.N., & Lock, J., 1984 — P-wave velocity features of lithosphere under the Eromanga Basin, eastern Australia, including a prominent mid-crustal (Conrad?) disconformity. *Tectonophysics*, 101, 267–291.

Henderson, R.G., 1960 — A comprehensive system of automatic computation in magnetic and gravity interpretation. *Geophysics*, 25, 569–585.

Karner, G.D., & Watts, A.B., 1983 — Gravity anomalies and the flexure of the lithosphere at mountain ranges. *Journal of Geophysical Research*, 88, 10449–10477.

Langel, R.A., Berbert, J., Jennings, T., & Horner, R., 1981 — MAGSAT data processing: an interim report for investigators. *NASA TM 82160, Nov 1981.*

Langel, R.A., Coles, R.L., & Mayhew, M.A., 1980 — Comparisons of magnetic anomlies of lithospheric origin measured by satellite and airborne magnetometers over western Canada. *Canadian Journal of Earth Sciences*, 17, 876–887.

Langel, R.A., Phillips, J.D., & Horner, R.J., 1982 — Initial scalar magnetic anomaly map from Magsat. *Geophysical Research Letters*, 9, 269–272.

Mayhew, M.A., Johnston, B.D., & Langel, R.A., 1980 — An equivalent source model of the satellite altitude magnetic anomaly field over Australia. *Earth & Planetary Science Letters*, 51, 189–198.

McEwin, A.J., McGregor, P.M., & Small, G.R., 1981 — Total magnetic intensity, Australia, epoch 1980.0, scale 1:10 000 000. *Bureau of Mineral Resources, Australia.*

Murray, A.S., 1977 — A guide to the use and operation of program CONTOR. *Bureau of Mineral Resources, Australia, Record* 1977/17.

Ritzwoller, M.H., & Bentley, C.R., 1982 — MAGSAT magnetic anomalies over Antarctica and the surrounding oceans. *Geophysical Research Letters*, 9, 285–288.

Vints, B.D., Pochtarev, V.I., & Rakhmatulin, R.Sh., 1970 — Method of computing the geomagnetic field upwards in nearrth space. *Geomagnetism & Aeronomy*, 10, 90–98.

von Frese, R.R.B., Hinze, W.J., Sexton, J.L., & Braile, L.W., 1982 — Verification of the crustal component in satellite magnetic data. *Geophysical Research Letters*, 9, 293–295.

Wellman, P., 1976 — Gravity trends and the growth of Australia: a tentative correlation. *Journal of the Geological Society of Australia*, 23, 11–14.

Wellman, P., 1978 — Gravity evidence for abrupt changes in mean crustal density at the junctions of Australian crustal blocks. *BMR Journal of Australian Geology & Geophysics*, 3, 153–162.

Wellman, P., 1982 — Australian seismic refraction results, isostasy and altitude anomalies. *Nature*, 298, 838–841.

Wellman, P., 1983a — Interpretation of geophysical surveys — longitude 45° to 65°E, Antarctica. *In* Oliver, R.L., James, P.R., & Jago, J.B., (editors) Antarctic Earth Science. *Australian Academy of Sciences, Canberra,* 522–526.

Wellman, P., 1983b — Origin and subglacial erosion of part of the coastal highland of east Antarctica. *Journal of Geology*, 91, 471–480.

Won, I.J., & Son, K.H., 1982 — A preliminary comparison of the Magsat data in the continental U.S. *Geophysical Research Letters*, 9, 296–298.

BMR Journal of Australian Geology & Geophysics, 9, 303-312

Granitoids of northeastern Tasmania

M.P. McClenaghan[1]

The granitoids of northeastern Tasmania comprise the composite Scottsdale, Blue Tier, and Eddystone batholiths, and intrude the folded Ordovician to Lower Devonian Mathinna beds, which consist of interbedded quartzwacke, siltstone, and slate, regionally metamorphosed to low grade. The granitoids were intruded in the Devonian, having K-Ar ages ranging between 395 and 368 Ma. They post-date the regional folding of the country rocks, which is correlated with the Tabberabberan deformation of eastern Australia. Emplacement was at a high level, with narrow metamorphic aureoles, and the granitoids are associated with a small amount of volcanics.

The granitoids fall into four types: granodiorite, biotite adamellite, biotite-garnet adamellite, and alkali-feldspar granite. The last type is strongly metasomatised and associated with tin mineralisation. Field relations indicate that, generally, the granodiorite plutons are the oldest and the alkali-feldspar granite plutons the youngest. The granitoids have been derived from partial melting of both igneous and sedimentary source rocks. Unequivocal S-type granites are restricted to the Eddystone batholith. Minor crystal fractionation or restite unmixing occurred within plutons. The alkali-feldspar granites were derived from adamellite magma by crystal fractionation.

Introduction

The granitoids of northeastern Tasmania cover an area of 2500 km² and include the Scottsdale, Blue Tier, and Eddystone batholiths (Turner & others, 1983) (Figure 1). These batholiths are composite, having plutons ranging in composition from granodiorite to alkali-feldspar granite (Figure 2). The Eddystone batholith, most of the Blue Tier batholith, and the northern and western parts of the Scottsdale batholith have been mapped in detail by the Geological Survey of Tasmania, and maps at a scale of either 1:50 000 or 1 inch to a mile are available. The remaining areas of the Scottsdale and Blue Tier batholiths have been mapped only at larger scales and are poorly known. The geology of the Blue Tier and Eddystone batholiths has been described by Groves & others (1977), who defined and named individual plutons, and a petrogenetic model was presented by McCarthy & Groves (1979). The petrogenesis of the granitoids has also been discussed by Cocker (1977, 1982) and Higgins & others (in press). Other recent work includes Calcraft (1980), McClenaghan & Williams (1982), Kitto (1982), Robinson (1982), and Turner & others (in press).

The aim of this paper is to describe the geology of the granitoids and to discuss their geochemistry.

Geology

The granitoids intrude the folded Ordovician to Lower Devonian (Banks & Smith, 1968; Rickards & Banks, 1979) Mathinna beds, which consist of interbedded quartzwacke, siltstone, and slate, regionally metamorphosed to low grade. The granitoid intrusion produced narrow contact metamorphic aureoles, and took place shortly after the regional folding of the country rocks, which is correlated with the Tabberabberan deformation of eastern Australia. Individual plutons are generally steep sided and elongated north–south in the general fold-trend. In the southern part of the Blue Tier batholith the St Marys porphyrite has been shown to include a pyroclastic sheet and sub-volcanic feeder dyke (Turner & others, in press).

Elsewhere in the Blue Tier batholith chilled margins to some bodies, such as the 3-km thick Scamander Tier granodiorite dyke (Cocker, 1977), miarolitic cavities in the Lottah pluton (McCarthy & Groves, 1979), and, possibly, the narrowness of the metamorphic aureoles indicate a high level of intrusion. Intrusion appears to have been passive, mainly by upward displacement (Gee & Groves, 1971).

[1] Tasmanian Department of Mines, PO Box 56, Rosny Park, Tasmania 7018.

The granitoids can be divided into four main types: granodiorite, biotite adamellite, alkali-feldspar granite, and biotite-garnet adamellite. The Scottsdale and Blue Tier batholiths include plutons of the first three, while the Eddystone batholith includes all types.

The Scottsdale batholith is divided by a narrow north–south-trending screen of country rock. West of the screen is exclusively granodiorite, while on the east side, biotite adamellite and alkali-feldspar granite occur together with granodiorite. Mapping of the Scottsdale batholith is not yet sufficiently advanced for the individual plutons to be defined, but it is now clear that there are a minimum of two granodiorite plutons and two alkali-feldspar granite plutons in the eastern part of the batholith, together with a large mass of biotite adamellite, which may be composite.

In the Blue Tier batholith the main granodiorite bodies are the Pyengana, Gardens, George River, Scamander Tier and Piccaninny Creek plutons. Other minor granodiorite bodies occur between St Helens and Pyengana. The main biotite adamellite pluton in the Blue Tier batholith is the Poimena. This is a medium-to coarse-grained rock with abundant K-feldspar megacrysts. It is probable that this is a composite body, and recent mapping suggests that the biotite adamellite southst of Pyengana is a separate pluton. Recent detailed mapping in the central Blue Tier area near Lottah (McClenaghan & Williams, 1982) has shown the presence of several small sheet and dome-shaped intrusions of similar composition, but different texture, which were previously included within the Poimena pluton. The other notable biotite adamellite pluton is the Mount Pearson mass. This body is compositionally similar to the Poimena pluton, but is very coarse grained with very abundant K-feldspar megacrysts. Recent mapping has also shown that this body is composite, and part of the adamellite of this type to the west of St Helens is thought to have been intruded later than the mass centred on Mount Pearson. Important alkali-feldspar granite plutons are the Mount Paris and Lottah bodies.

Other smaller bodies occur at Little Mount Horror and Mount Cameron. A sheet-like form has been ascribed to these last three bodies (Gee & Groves, 1971); however, in the case of the Lottah pluton, detailed mapping (McClenaghan & Williams, 1982) has shown that a steep-sided domal body is more likely. The evidence for a sheet-like form for the body at Little Mount Horror is unclear (McClenaghan & others, 1982).

The Eddystone batholith is composed of three main plutons: the Boobyalla, Ansons Bay, and Mount William. The first two are biotite-garnet adamellite and the last is alkali-feldspar granite. Smaller biotite adamellite bodies occur, and there is also a small body of granodiorite. A sheet-like form has

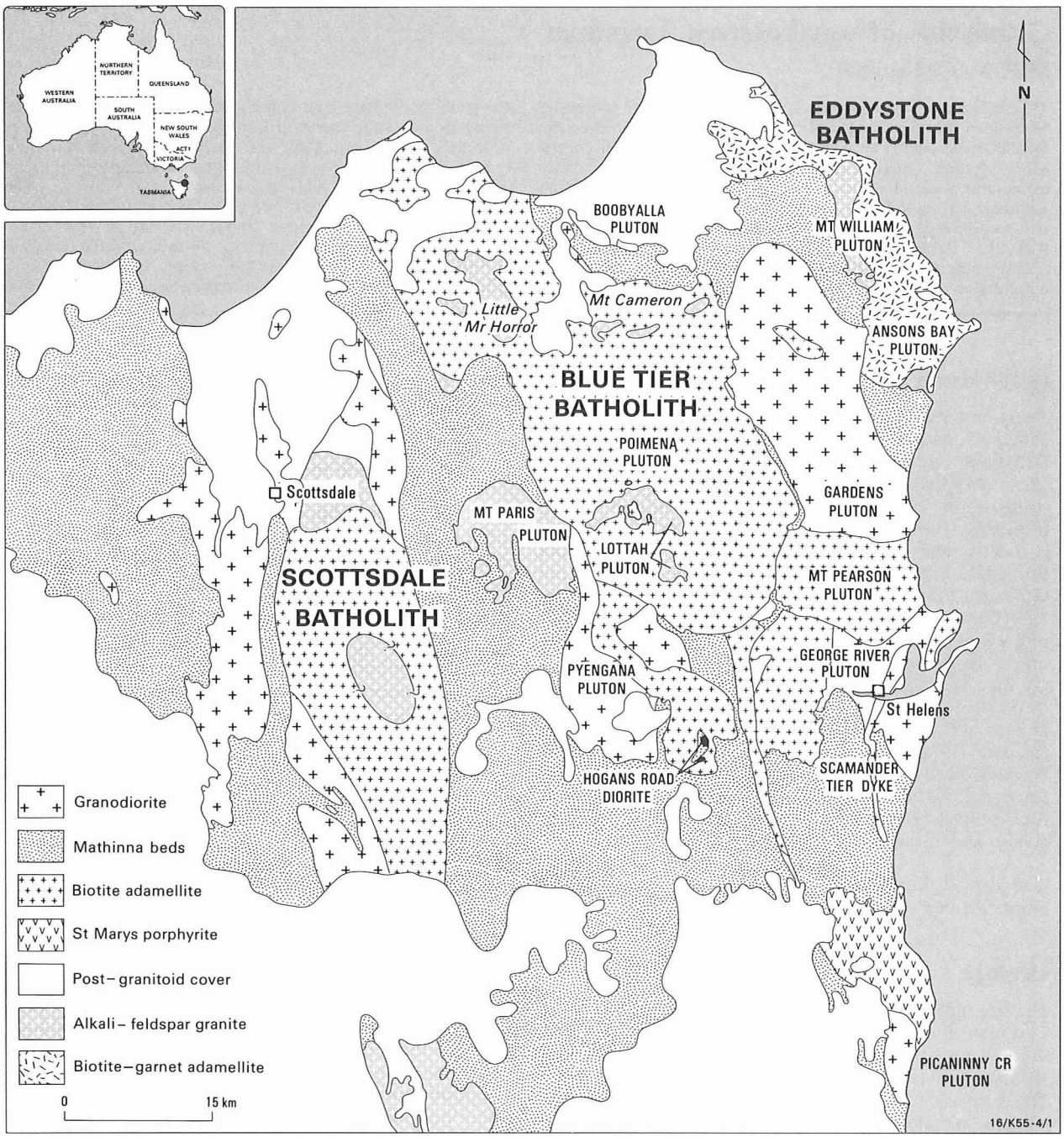

Figure 1. Simplified bedrock geological map of northeastern Tasmania.
Largely from Geological Survey 1 mile to 1 inch, 1:50 000 and 1:250 000 maps.

been ascribed to the Mount William pluton (Gee & Groves, 1971); however, poor exposure makes confirmation of this difficult.

Minor intrusive bodies include quartz-feldspar porphyry and aplite dykes. Some of the quartz-feldspar porphyry dykes are up to 0.25 km wide and can be traced for 5 km (McClenaghan & Williams, 1983). In addition, a suite of dolerite dykes occurs widely in granitoid areas of eastern Tasmania, as far north as the Furneaux Group north of northeastern Tasmania and as far south as Coles Bay on the east coast of Tasmania. The dykes intrude all granite types; however, near Lady Barron, on Flinders Island in the Furneaux Group, a dolerite dyke is intruded by a quartz-feldspar porphyry dyke (pers. comm. P.W. Baillie & N.J. Turner). Since the quartz-feldspar porphyry dykes are thought to have a similar age to the other granitoids, this suggests the dolerites are also of a similar age. Several small (<1 km) bodies of diorite (Hogans Road diorite), included in or associated with strongly hornfelsed Mathinna beds, occur as rafts in a biotite adamellite pluton west of St Helens. These bodies are the most basic rocks associated with the granitoids (McClenaghan, 1984).

The granodiorite plutons contain areas of steep, approximately north—south-trending cataclastic foliation (Gee & Groves, 1971; McClenaghan & others, 1982), usually best developed near the north—south-trending margins, and ascribed to flattening. A foliation, defined by the alignment of K-feldspar megacrysts, is also widely developed in the adamellites. In the northern part of the Poimena pluton two steep foliations of aligned K-feldspar megacrysts are developed — northwesterly (330°–340°) and northeasterly

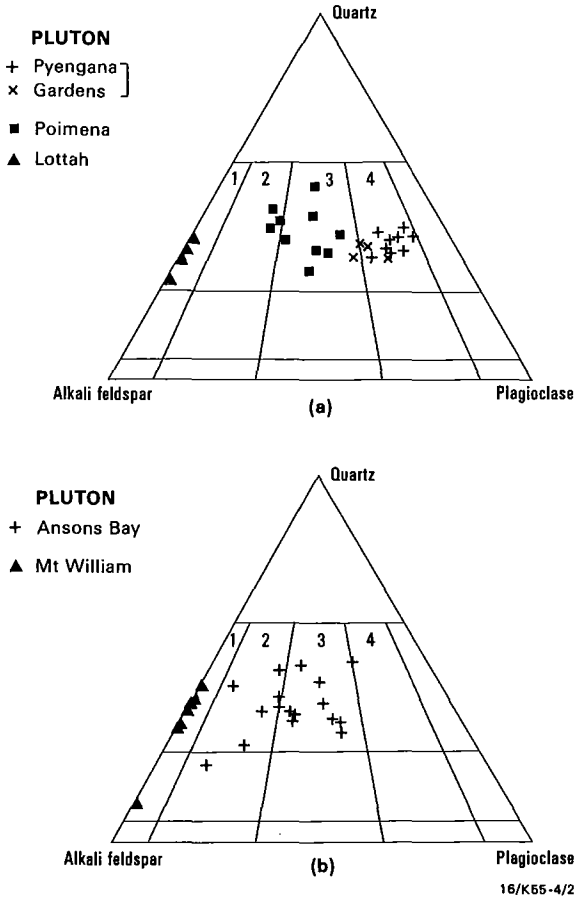

Figure 2. Modal compositions (quartz, alkali-feldspar, plagioclase) of samples from the Blue Tier (a) and Eddystone (b) batholiths. Modal data from Calcraft (1980), McClenaghan & Williams (1982), Kitto (1982) and McClenaghan (unpublished). The classification used is modified from that recommended by the IUGS Subcommission on the Systematics of Igneous Rocks (Streckeisen, 1973). Field 1, alkali-feldspar granite; field 2, granite; field 3, adamellite; field 4, granodiorite.

(30°–60°) (McClenaghan & others, 1982) — both of which may be stress induced.

Similar foliations of different directions are developed in domains in the Mount Pearson pluton (McClenaghan & Williams, 1983). The Ansons Bay pluton shows a well-developed, steeply dipping, curving foliation, defined by K-feldspar megacrysts, which is parallel to the southern boundary (McClenaghan & Williams, 1983) and may be related to flow or flattening against the margins.

Gee & Groves (1971), on the basis of field evidence, postulated the intrusive sequence granodiorite, adamellite, alkali-feldspar granite. Evidence for this consists of the cross-cutting relation of the Poimena adamellite pluton to the foliation in the Pyengana granodiorite, and the similar relation of the Mount Pearson adamellite to the foliation in the Gardens granodiorite. The Lottah alkali-feldspar granite has clear intrusive relations to the Poimena adamellite, and the Mount William alkali-feldspar granite cross-cuts the Ansons Bay adamellite/Mathinna beds contact. The southern margin of the Poimena pluton not only cuts across the Mathinna beds/Mount Pearson pluton boundary but also the foliation in the Mount Pearson pluton, indicating that the Poimena is the younger of these two plutons. A similar intrusive sequence appears to hold for the Scottsdale batholith, as boundary features, such as chilled contacts, show that the adamellites are younger than the granodiorites. An exception to this generalisation occurs north of St Helens, where there is clear evidence of chilling of granodiorite, believed to be part of the Scamander Tier granodiorite, against the Mount Pearson adamellite (Cocker *in* Groves & others, 1977).

K-Ar age data indicate a range of 368–382 Ma for the Scottsdale batholith and 370–395 Ma for the Blue Tier batholith (McDougall & Leggo; 1965: Turner & others, in press). These data, together with Rb-Sr biotite age data from the Blue Tier batholith and Eddystone batholith (Cocker, 1982), are in agreement with the geological relations, except for that between the Scamander Tier granodiorite and the Mount Pearson adamellite. The Scamander Tier granodiorite has Rb-Sr biotite dates of 386.6 Ma (Cocker, 1982) and 386 ± 5 Ma (Turner & others, in press), while the Mount Pearson adamellite is dated as 382.6 Ma (Cocker, 1982). This anomaly has yet to be resolved.

Petrography

Granodiorites and extrusive equivalents

The granodiorites show little variation, being massive, medium to coarse- grained, dark grey rocks, commonly with abundant fine-grained dioritic enclaves.

They consist of euhedral to anhedral amphibole and biotite, plagioclase and intergranular K-feldspar and quartz. Amphibole ranges in composition from actinolite in the core regions of some crystals to hornblende in the rims and in euhedral crystals. Amphibole and biotite are frequently present in intermingled clusters of crystals. Trace amounts of clinopyroxene are present in some plutons in association with actinolite (e.g. Gardens pluton, Piccaninny Creek pluton, and in the western granodiorite of the Scottsdale batholith). Plagioclase frequently contains sericitised, calcium-rich core regions (An_{80-70}), which have sharp boundaries with the clear rim zones (An_{60-35}). Accessory minerals include apatite, zircon, sphene, allanite, and ilmenite. Magnetite is present instead of ilmenite in the Pyengana pluton. Prehnite is commonly developed along the biotite cleavages and chloritic alteration of the biotite is also common.

The St Marys porphyrite is considered to be the extrusive equivalent of the Scamander Tier granodiorite and the Cato Creek microgranodiorite (Turner & others, in press), and consists of plagioclase, quartz, biotite, clinopyroxene, orthopyroxene, and alkali feldspar. The pyroxene is replaced by amphibole at higher levels in the body and in the hypabyssal equivalent microgranodiorite body (Cato Creek microgranodiorite); both orthopyroxene and clinopyroxene remnants are found in amphibole cores. Orthopyroxene is mantled by hornblende, and clinopyroxene by actinolite. Plagioclase contains corroded calcic cores (An_{80-70}) surrounded by zoned rims (An_{65-55}). In the lower part of the sheet the alkali feldspar is sanidine.

Biotite adamellites

The biotite adamellites show textural variations, but all consist of plagioclase, biotite, quartz, and K-feldspar with accessory zircon, ilmenite, and apatite. Plagioclase is generally zoned (An_{45-15}), commonly has thin ($< 1.5\ \mu m$) rims of albite, and K-feldspar is coarsely perthitic. Minor development of secondary muscovite occurs together with chloritic alteration of the biotite.

The adamellites in the northeastern part of the Scottsdale batholith are coarse-grained equigranular to sparsely porphyritic with megacrysts of K-feldspar. Adjacent to the alkali-feldspar granite in that area the adamellite has a distinctive pink colour, but elsewhere is grey.

In the Blue Tier batholith, coarse-grained and very coarse-grained adamellites with very abundant K-feldspar megacrysts are widespread (e.g. Poimena and Mount Pearson plutons). The megacrysts contain up to five concentric zones of plagioclase inclusions (McClenaghan & Williams, 1982). In the central part of the batholith near Lottah small bodies of medium and fine-grained adamellite intrude the Poimena pluton (McClenaghan & Williams, 1982).

Biotite garnet adamellites

The Ansons Bay pluton in the Eddystone batholith resembles the Mount Pearson pluton in composition and texture apart from the additional presence of garnet and cordierite. Garnet is generally an accessory phase associated with biotite, but is more abundant in mafic schlieren. Cordierite is commonly replaced by sericite and secondary biotite. Garnet and cordierite are commonly associated with biotite reaction rims to xenoliths of both granite and Mathinna Beds (Kitto, 1982). Higgins & others (in press) have suggested that schlieren of biotite, garnet, and cordierite trailing away from xenolith reaction zones indicate that much of the mafic layering in the Ansons Bay pluton may be derived from reaction with xenolithic material.

The Boobyalla pluton in the Eddystone batholith is compositionally and texturally similar to the Ansons Bay pluton, but does not contain cordierite.

Alkali-feldspar granites

The classification of these rocks as alkali-feldspar granites rather than granites or adamellites is dependent on the plagioclase being almost pure albite (An <5), since this requires it to be counted as an alkali-feldspar (Streckeisen, 1973). In the case of the Lottah and Mount Paris plutons this is generally the case, though Higgins & others (in press) have reported plagioclase phenocrysts with cores of An_{20} The plagioclase composition for the other alkali-feldspar granite plutons is less well known and may have albite An >5. In spite of this, it seems useful to refer to them as alkali-feldspar granite, emphasising their marked compositional difference from the adamellites.

The Lottah pluton (McClenaghan & Williams, 1982) includes equigranular and quartz and K-feldspar porphyritic varieties, which grade into each other. The granites consist dominantly of K-feldspar, albite, and quartz with the mica content being less than 7 per cent. K-feldspar is present in perthitic and non- perthitic form, the latter commonly overgrowing euhedral K-feldspar cores. Perthitic K-feldspar is invariably more sodic than the non-perthitic K-feldspar (McClenaghan & Williams, 1982, table 1). In the porphyritic granites the dark mica is annite or siderophyllite containing inclusions of zircon and apatite. This mica is replaced to varying degrees by zinnwaldite in the equigranular granites. Muscovite is minor and occurs as an alteration of K-feldspar or derived from the breakdown of annite. Accessory minerals are fluorite, cassiterite, topaz, and tourmaline.

In this granite the temperature calculated from the composition of perthitic K-feldspar, as phenocrysts and in the matrix and assumed to be in equilibrium with plagioclase inclusions, is a constant value of ~ 665°C at 0 MPa (McClenaghan & Williams, 1982). This temperature is lower than would be expected for magmatic crystallisation, as is suggested by the texture. However, it is possible that the high fluorine content of the rocks (4900–2800 ppm, McClenaghan & Williams, 1982, table 7) may have depressed the solidus temperature (Manning, 1981). The temperature calculated from the late-stage non-perthitic K-feldspar (350°C at 0 MPa) (McClenaghan & Williams, 1982) is so low it must be due to sub-solidus recrystallisation and points to sub-solidus mineral–fluid reactions. Zones of greisenisation in the Lottah area (Groves & Taylor, 1973) also indicate local metasomatic alteration of the granite.

Other alkali-feldspar granite bodies have a similar character to the Lottah pluton, but show less metasomatic alteration.

Dolerite dykes

The dolerite dykes consist of a framework of plagioclase (An_{65-26}) laths with intergranular and sub-ophitic clinopyroxene and abundant grains of ilmenite. Accessory minerals are apatite, sphene, and pyrite. In some specimens there is minor alteration of the clinopyroxene to amphibole together with chlorite, while in other specimens the clinopyroxene is completely replaced by green hornblende and a small quantity of biotite is also present. Orthopyroxene is rare.

Diorite rafts (Hogans Road diorite)

The diorite rafts show a considerable range in composition (McClenaghan, 1984). The most mafic extreme is composed of large anhedral amphiboles enclosing olivine, orthopyroxene, clinopyroxene, and biotite. The amphibole is variable in composition and clearly secondary. Accessory minerals are apatite, pyrite, ilmenite, and spinel. In the less mafic parts of the bodies the texture is similar, but plagioclase is also present as inclusions in the amphibole, while orthopyroxene and olivine are absent. Intergranular quartz is also present.

Geochemistry and petrogenetic models

Considerable major and trace element data are available for the Blue Tier and Eddystone batholiths and a lesser amount for the Scottsdale batholith (Groves & others, 1977; Cocker, 1977; McClenaghan & Williams, 1982; Calcraft, 1980; Kitto, 1982; Robinson, 1982; Higgins & others, in press; Turner & others, in press). The data in the case of Scottsdale batholith are from the northern part and for the Blue Tier and Eddystone batholiths are concentrated in a few plutons. Some data obtained by the author have not yet been published. The plots that follow use only part of the available data to avoid congestion and the sources for this are listed in the appendix. Representative analyses are listed in Table 1.

Elsewhere in the Lachlan fold belt the granitoids have been grouped into suites of distinctive chemical character (White & Chappell, 1983), which are thought to reflect their source-rock composition. It is useful to consider whether the northeastern Tasmanian granitoids can be divided into suites on a similar basis.

Harker plots of data from twenty-two samples collected throughout the Scottsdale batholith, and thought to cover all rock types, apparently show a single, moderately well-defined, straight-line trend for most elements. In the case of Ba and Zr, and also, to a lesser extent, CaO and Mgo, it is clear that, in fact, two trends are present (Figure 3). One of the trends, with flatter slopes for Ba and Zr, consists of data from the granodiorites, while the other trend consists of data from adamellites and alkali-feldspar granites. The granodiorite trend contains data from both sides of the Mathinna beds screen that divides the batholith. From this it is clear that the Scottsdale batholith is composed of two

Table 1. Representative analyses from the Scottsdale, Blue Tier, and Eddystone batholiths.

SB21 and SB1 from the granodiorite suite, and SB17, SB19, and SB6 from the adamellite/alkali-feldspar granite suite of the Scottsdale batholith. MAL1 Pyengana pluton. MBT258 Gardens pluton. NM116 St Marys porphyrite. MBT242 Mount Pearson pluton. 40565 Poimena pluton. BT3/42 and TDC Lottah pluton. 43134 Ansons Bay pluton. 702708 Mount William pluton. BT30 and 146 dolerite dyke suite. MSH22 and MSH20 Hogans Road diorite (diorite raft).

	SB21	*SB1*	*SB17*	*SB19*	*SB6*	*MAL1*	*MBT258*	*NM116*	*MBT242*	*40565*	*BT3/42*	*TDC*	*43134*	*702708*	*BT30*	*146*	*MSH22*	*MSH20*
SiO_2	61.94	70.97	67.21	74.37	75.95	64.52	64.37	66.74	74.53	71.96	76.10	73.51	73.14	76.07	47.9	48.4	47.20	48.80
TiO_2	0.79	0.35	0.69	0.17	0.01	0.50	0.55	0.66	0.15	0.41	0.02	0.01	0.49	0.02	3.1	1.2	0.31	0.96
Al_2O_3	15.23	14.04	15.01	12.93	12.70	14.92	15.20	15.25	13.26	13.69	12.79	15.14	13.15	13.30	12.9	16.9	6.88	17.63
Fe_2O_3	1.25	0.70	1.01	0.44	0.43	1.51	1.25	1.13	0.49	2.68	0.25	0.02	3.22	1.12	2.2	2.0	1.57	1.26
FeO	4.30	1.78	3.31	1.18	0.57	3.15	3.53	3.15	1.33	—	1.10	0.72	—	—	11.9	7.3	7.29	8.80
MnO	0.12	0.06	0.07	0.03	0.05	0.07	0.07	0.08	0.03	0.06	0.03	0.02	0.04	0.02	0.26	0.16	0.15	0.20
MgO	3.32	1.20	1.50	0.44	0.08	2.58	2.95	1.61	0.33	0.61	0.07	0.02	0.58	0.07	6.1	8.1	22.58	6.73
CaO	4.83	2.37	3.04	1.19	0.49	4.38	4.85	3.67	1.50	1.75	0.43	0.26	1.48	0.42	8.4	10.7	8.52	9.97
Na_2O	2.73	3.68	3.69	3.64	4.37	2.38	2.43	2.83	3.14	2.74	3.44	5.36	1.87	4.31	2.7	2.5	0.55	1.31
K_2O	2.65	3.54	2.92	4.49	4.44	3.59	2.91	3.55	4.42	4.39	4.96	3.64	4.37	4.39	0.47	0.29	0.92	1.53
P_2O_5	0.24	0.10	0.19	0.04	0.01	0.21	0.14	0.16	0.04	0.12	0.04	0.23	0.15	0	0.70	0.15	0.21	0.20
CO_2	0.26	0.06	0.22	0.04	0.06	0.15	0.10	0.13	0.06		0.12	0.05			—	—	0.15	0.05
H_2O+	1.52	0.93	1.18	1.07	0.38	1.15	1.21	0.95	0.91	1.05*	0.86	1.01	0.81*	0.60*	3.2	2.0	2.03	2.12
H_2O^-	0.05	0.20	0.04	0.02	0.12	0.40	0.15	0.05	0.01		0.10	0.10			0.28	0	0.09	0.10
Total	99.23	99.98	100.08	99.99	99.66	99.51	99.71	99.96	100.20	99.47	100.31	100.08	99.30	100.32	100.11	99.70	98.45	99.66
Trace elements (ppm)																		
Sn	7	7	8	7	19	8	7	175	11	19	35	59	<4	15	<5	—	<3	5
Th	16	20	20	49	37	23	17	18	31	—	19	14	—	—	—	—	9	10
Sr	330	175	200	87	5	360	310	250	98	112	15		103	7	282	160	370	420
U	5	9	6	11	23	7	5	6	8	—	20	8	—	—	—	—	2	2
Rb	135	165	115	185	370	185	130	160	250	280	480	1400	228	366	23	27	30	61
Y	28	27	22	20	47	23	18	35	46	32	45	2	34	65	50	59	11	18
Zr	185	105	260	150	77	140	130	220	130	153	71	21	269	68	363	26	53	78
Nb	9	9	12	7	18	7	6	11	10	13	13	40	12	17	16	—	<3	<3
Ni	25	9	11	3	3	18	17	6	3	—	3	3	—	—	33	48	280	
Ba	610	370	750	420	16	660	510	670	320	357	55	15	750	31	—	—	430	400
Cr	75	19	20	5	5	46	56	28	5	—	<5	<5	—	—	—	—	2100	64
V	120	38	58	14	4	105	105	68	16	—	5	5	—	—	—	—	145	290
Sc	15	9	11	9	9	14	13	14	9	—	<9	<9	—	—	—	—	34	40
Pb	13	31	16	28	52	21	21	33	36	—	29	9	—	—	—	—	4	4
Ga	16	14	17	13	17	16	15	17	16	18	23	38	19	23	—	—	6	17
Zn	71	49	70	34	40	61	62	67	39	—	47	71	—	—	172	104	73	105
Cu	22	9	19	13	3	17	16	10	10	—	10	12	—	—	—	—	29	15

*Co_2 + total H_2O

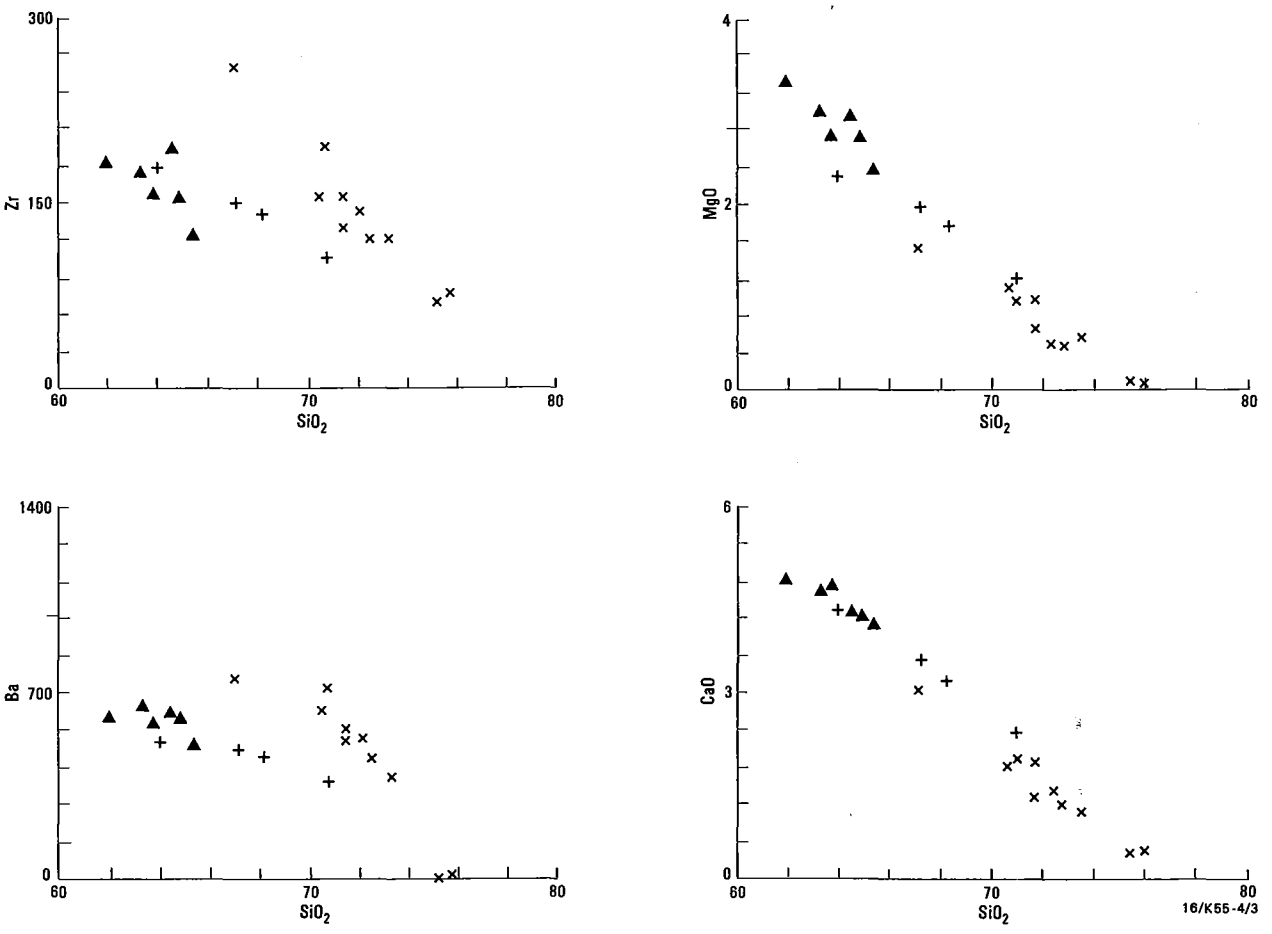

▲ *Granodiorites from west of Mathinna beds screen*

\+ *Granodiorites from east of Mathinna beds screen*

× *Adamellites and alkali-feldspar granites*

Figure 3. Selected Harker diagrams for various elements from the Scottsdale batholith.

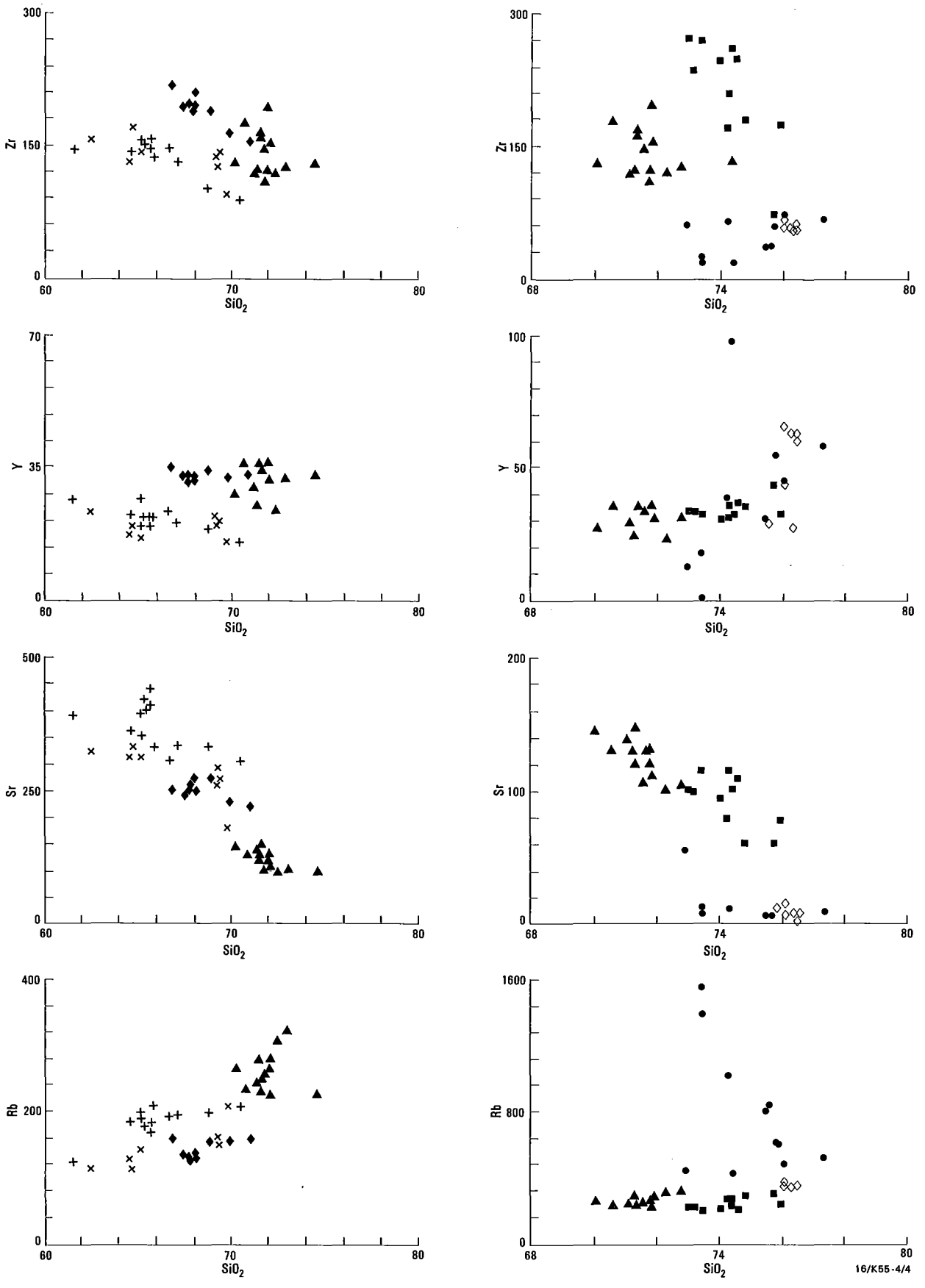

Figure 4. Selected Harker diagrams for various elements from the Blue Tier (left hand column) and Eddystone (right hand column) batholiths. Symbols as for Figure 5. The Poimena pluton (Blue Tier batholith) data have been plotted on both sets of diagrams to facilitate comparison.

suites with the granodiorite suite predominantly in the western part and the adamellite and alkali-feldspar granite suite in the eastern part.

The chemical composition of the Blue Tier and Eddystone batholiths will be discussed using data from some of those bodies for which an adequate amount of data is available, i.e. the Gardens, Pyengana, Poimena, Ansons Bay, Mount William, and Lottah plutons, and the St Marys porphyrite.

Harker plots of the data from these plutons for Y, Sr, Rb, and Zr (Figure 4) show that they cannot be grouped into consistent suites for these elements. Plots for the other elements show an even more confused pattern and indicate that each body has a small range of chemical variation that cannot be combined with other plutons to form unified trends distinctive of different suites. Each body seems to represent a distinct suite.

The restite model (White & Chappell, 1977) has been used widely in the Lachlan fold belt to classify granitoids into those derived from an igneous source rock (I-types) and sedimentary source rock (S-types) (Hine & others, 1978; Chappell, 1978). Cocker (1977) applied the criteria of this model to granitoids of the Blue Tier and Eddystone batholiths, and concluded that the granodiorite bodies were I-types and the other granitoids were S-types. This conclusion is clearly justified for the granodiorite bodies, since they have all the I-type characteristics of hornblende and biotite as the mafic minerals, high Ca, low K_2O/Na_2O (Figure 5), low molecular $Al_2O_3/(Na_2O + K_2O + CaO)$ (Figure 6), and low initial $^{87}Sr/^{86}Sr$ ratios (Figure 7). Also, it is clear that the biotite-garnet adamellites of the Eddystone batholith are S-type on the presence of biotite, garnet, and cordierite, the low Ca, high K_2O/Na_2O (Figure 5), high molecular $Al_2O_3/(Na_2O + K_2O + CaO)$ (Figure 6), and high initial $^{87}Sr/^{86}Sr$ ratio (Figure 7).

Classification for the biotite adamellites of the Blue Tier batholith is less certain. The molecular $Al_2O_3/(Na_2O + K_2O + CaO)$ values for the two major adamellite plutons (Poimena and Mount Pearson) are intermediate between the granodiorite and the biotite-garnet-cordierite adamellite bodies (Figure 6). The K_2O/Na_2O ratio (Figure 5) is also borderline between the two granitoid types. The range of error on the initial $^{87}Sr/^{86}Sr$ ratio (Figure 7) leaves open the possibility that they have similar ratios to the granodiorites, which are concluded to be I-type.

Application of the same criteria to the two suites of the Scottsdale batholith suggests they are both I-type (Figures 8, 9).

The Lottah and Mount Paris plutons of the Blue Tier batholith have some of the characteristics of A-type granite (Collins & others, 1982), which are considered to be derived from the partial melting of felsic granulite residual after the production of a previous granite. These features are annite as the mica, high Nb, Ga, and F, and low Mg and Ca. A-type granites have high K/Rb ratios (Table 2), which are consistent with them being principally a product of partial melting and not having undergone significant feldspar fractionation. This is in marked contrast with the Lottah pluton granites, which have very low K/Rb ratios (Table 2), suggesting that they are highly fractionated rocks. The Lottah and the very similar Mount Paris pluton should not, therefore, be classed as A-type granites.

McCarthy & Groves (1979) proposed a cumulate fractional crystallisation model for the Blue Tier batholith. This model envisaged that the batholith formed by fractional crystallisation of a single magma, of adamellitic composition, which underwent crystallisation in situ by progressive nucleation and solidification from the roof, walls, and floor inwards. Progressive changes in liquids and the cumulate

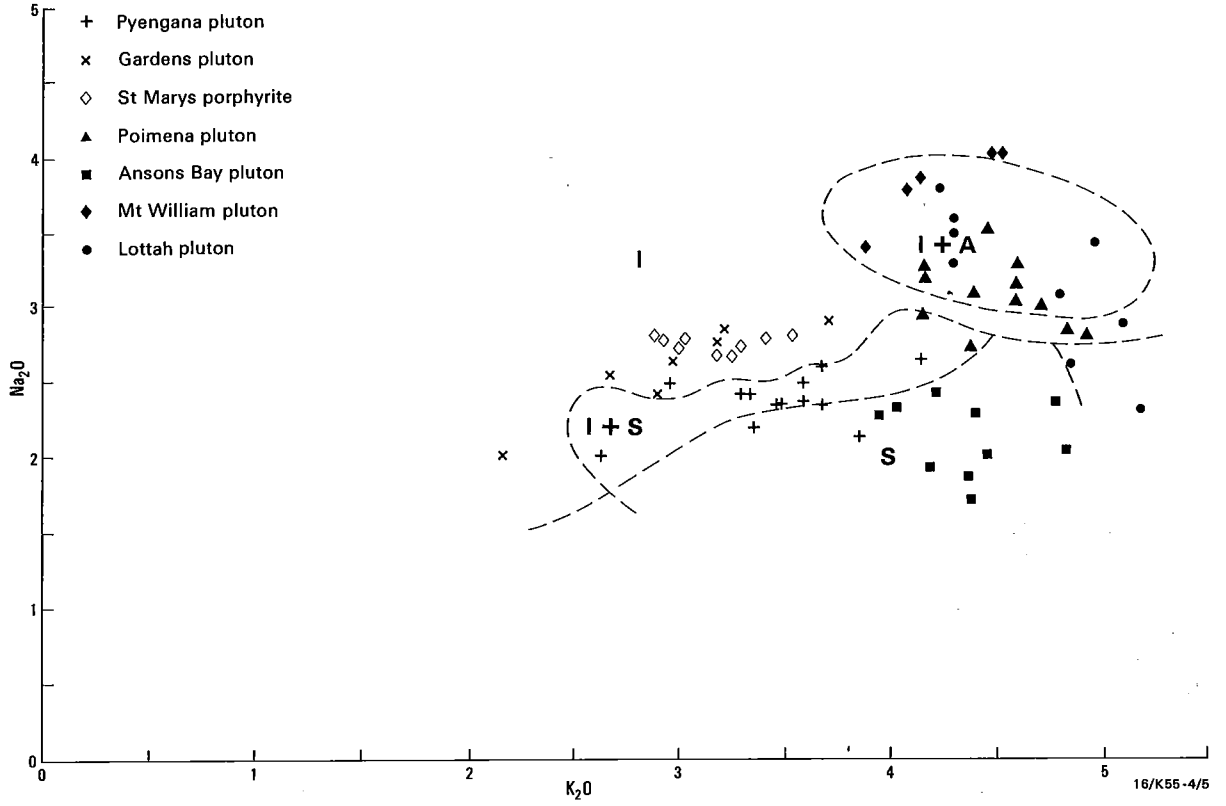

Figure 5. Plot of Na_2O against K_2O for the granitoids of the Blue Tier and Eddystone batholiths.
Fields marked for I-type granitoids (I), S-type granitoids (S) and A-type granitoids (A) from the Lachlan Fold Belt (White & Chappell, 1983, figure 5).

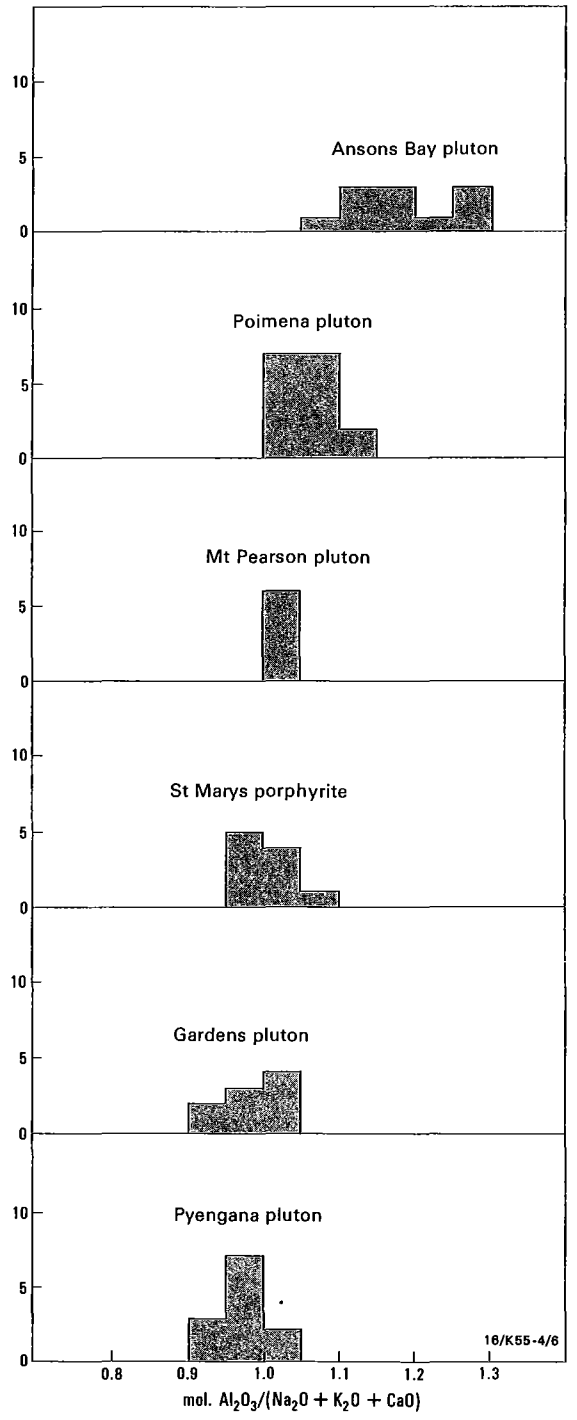

Figure 6. Histogram of molecular $Al_2O_3/(Na_2O + K_2O + CaO)$ in granitoid plutons from the Blue Tier and Eddystone batholiths.

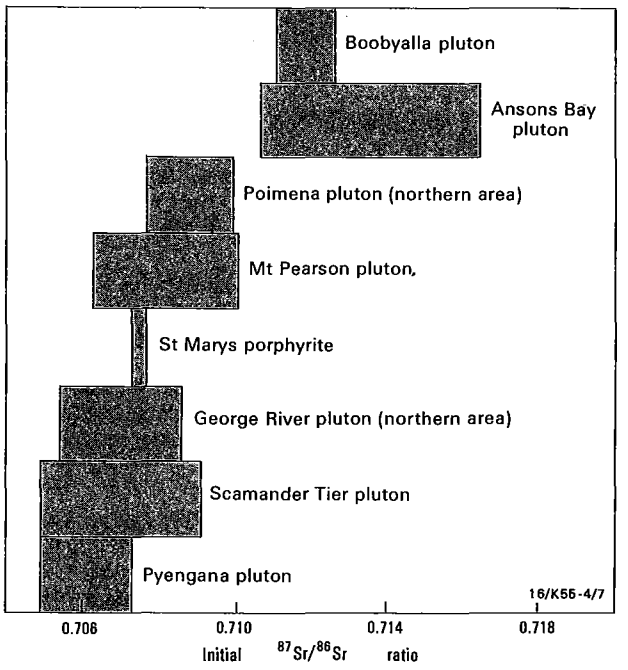

Figure 7. Range of initial $^{87}Sr/^{86}Sr$ ratios in granitoid plutons from the Blue Tier and Eddystone batholiths.

mineralogy during crystallisation led to the observed sequence of early granodiorites followed by biotite adamellites and then alkali-feldspar granites. This model has been criticised by Cocker (1982) on the following grounds: (1) there are no concentrically zoned plutons in the batholith, and no consistent zoned structure to the batholith as a whole; (2) most contacts between rock types can be demonstrated to be intrusive; (3) the sequence of intrusion is not consistently from granodiorite to alkali-feldspar granite; (4) the geochemical trends used to index the progressive differentiation of the batholith include data from metasomatically altered granitoid bodies and do not reflect an entirely magmatic process; (5) the 25 Ma solidification time for the batholith is too large for a single body as suggested by McCarthy & Groves (1979); (6) different initial $^{87}Sr/^{86}Sr$ ratios for the plutons, particularly for the Mount Pearson and Ansons Bay plutons, argue against them having been part of the same body (Figure 7). Cocker (1977) proposed that individual plutons result from crystallisation of melts derived from discrete source rocks of differing chemical composition, without any inter-pluton fractionation. He based this conclusion on the apparently unique mineral, chemical, and isotopic composition of each pluton. Higgins & others (in press) have suggested that the intra-pluton chemical variation of the Pyengana granodiorite may be explained by amphibole, plagioclase, and biotite fractionation. A similar model for the Gardens pluton was proposed by McClenaghan (1984).

Higgins & others (personal communication, 1984) have modelled the variation in composition of the St Marys Porphyrite by fractional crystallisation of quartz, plagioclase, biotite, orthopyroxene, and clinopyroxene. They concluded

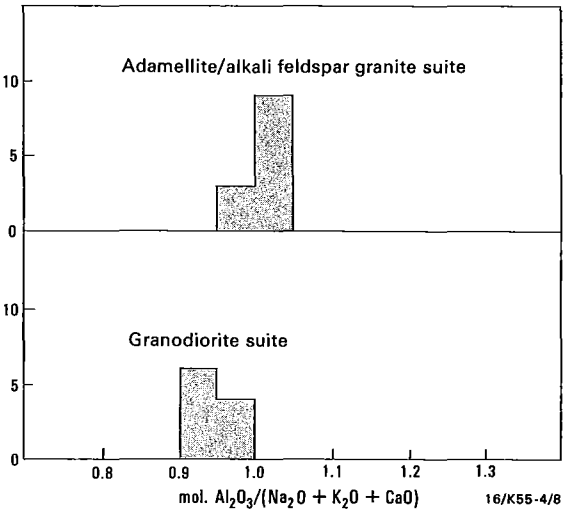

Figure 8. Histogram of molecular $Al_2O_3/(Na_2O + K_2O + CaO)$ in granitoids from the Scottsdale batholith.

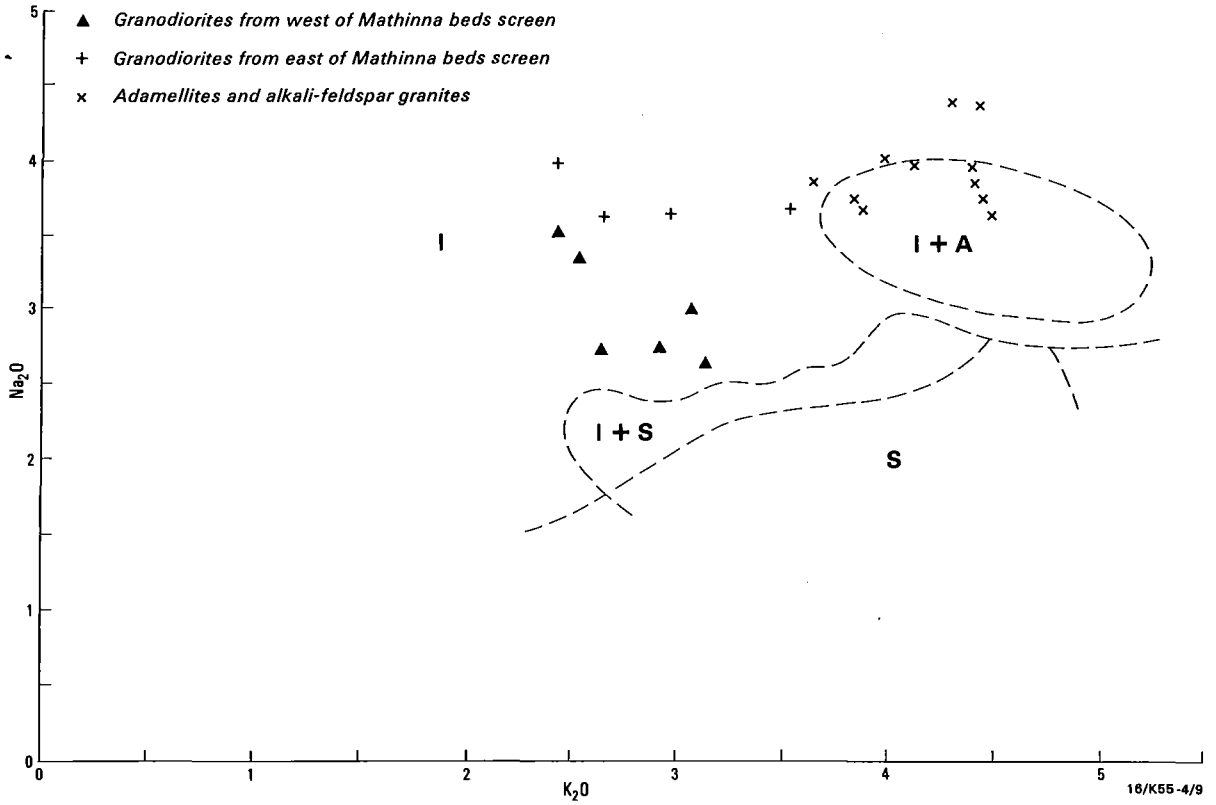

Figure 9. Plot of Na_2O against K_2O for the granitoids of the Scottsdale batholith.
Fields as for Figure 5.

Table 2. Averages of the Mumbulla and Gabo A-type granites (Collins & others, 1982) and the Lottah alkali-feldspar granite.

	A-type granite		
	Mumbulla	*Gabo*	*Lottah*
SiO_2	77.21	73.04	75.04
TiO_2	0.13	0.37	0.04
Al_2O_3	11.79	12.62	13.60
FeO*	1.17	2.98	1.27
MnO	0.03	0.08	0.04
MgO	0.04	0.33	0.06
CaO	0.39	0.96	0.41
Na_2O	3.08	3.70	3.22
K_2O	5.00	4.11	4.51
P_2O_5	0.02	0.08	0.11
Sr	43	148	15
Rb	242	167	758
Y	90	83	35
Zr	170	490	49
Nb	19	25	21
Ga	20	21	27
F	—	—	3660
K/Rb	172	204	49
Number of analyses	8	9	21

* Total iron as FeO

that this body was derived from a high-temperature, anhydrous magma and that a restite component was absent or negligible.

McClenaghan & Williams (1982) suggested that the Lottah alkali-feldspar granite was derived from the Poimena biotite adamellite by crystal fractionation possibly combined with restite unmixing and that the equigranular alkali-feldspar granite was derived from the porphyritic alkali-feldspar granite by crystal fractionation. The compositions of the porphyritic and equigranular alkali-feldspar granites are represented by BT3/42 and TDC, respectively, (Table 1) and are consistent with this model. The decrease in SiO_2 and increase in Al_2O_3, Na_2O, and P_2O_5 with fractionation from the porphyritic granite to the equigranular granite are consistent with a displacement of the ternary minimum towards the albite apex, owing to the build-up of fluorine in the residual liquid (Manning, 1981). Higgins & others (in press) have also advocated crystal fractionation to derive the Lottah alkali-felspar granite from the Poimena adamellite, and suggested that the Mount William alkali-feldspar granite was similarly derived from the contiguous Ansons Bay biotite-garnet adamellite.

It is difficult to assess whether there is a restite unmixing component to the chemical variation shown by the various plutons. Higgins & others (in press) have pointed out that the high temperature of the St Marys Porphyrite magma (1000–700°C, Higgins & others, personal communication, 1984) and of the biotite-garnet adamellite Ansons Bay pluton (900–750°C, Cocker, 1977; Kitto, 1982) reduces the likelihood of a major restite component remaining in the magma. They also suggested that the Pyengana, Piomena, and Ansons Bay plutons are high-temperature, non-minimum melts, on the basis of their position above the cotectic surface in the An–Ab–Or–Qz system. This argument does not seem conclusive, since a minimum melt might contain restite material, which would displace the magma from the Ab–Or–Qz surface, where a pure minimum melt would plot. White & Chappell (1977) pointed out that the unmixing trend lines for minimum melt suites for elements such as Mg and P, which do not enter the minimum melt to an appreciable extent, intersect the axis at about 76 per cent SiO_2. The trend lines for the Pyengana pluton for MgO and P_2O_5 intersect the axis at 73 per cent SiO_2 and 77.8 per cent SiO_2, while, for the Gardens pluton, the corresponding values are 75.9 per cent SiO_2 and 81.3 per cent SiO_2. This suggests that, if the variation in these plutons was due to restite unmixing, they would be close to minimum melts. Petrographic evidence for a restite component in any of the granitoids is uncertain, since plagioclase cores and relict pyroxene may be caused by magma mixing.

If it can be confirmed that the dolerite dyke suite present through the granitoid area is of approximately the same age as the granitoids, then it would indicate that a basic magma was present at depth. This could have been a heat source that caused melting and the production of the granitoids. The Hogans Road diorite, present in a composite raft of Mathinna beds and dolerite in an adamellite body, points to the presence of an extremely basic magma intruding the Mathinna beds at a greater depth than the present exposed level of the granitoids, since it was transported up with its host adamellite. Because granitoid intrusion followed closely after the deposition and deformation of the Mathinna beds (Cocker, 1982), this basic intrusion must have occurred close to the time the granodiorites were produced and thus also points to the presence of a basic magma as a possible heat source.

Cocker (1982), using Sr isotope evolution curves and assuming sedimentary and igneous source rocks for the biotite-garnet adamellites and granodiorites, estimated a range of 800 to 1700 Ma and 1250 to 1400 Ma, respectively, for the age of the source rocks.

The data on the granitoids of northeastern Tasmania support a model in which each body has been formed from separate melts derived by partial melting of various source rocks (Cocker, 1982), both igneous and sedimentary. Variable amounts of crystal fractionation or restite unmixing have occurred within plutons, and the alkali-feldspar granites were derived by extreme crystal fractionation of adamellite magma. Their composition could have also been strongly affected by metasomatism.

Acknowledgement

The figures in this paper were drafted by D. Lawry.

References

Banks, M.R., & Smith, A., 1968 — A graptolite from the Mathinna Beds, north eastern Tasmania. *Australian Journal of Science*, 31, 118–119.

Calcraft, H.J., 1980 — Iron-titanium oxide minerals in some Tasmanian granitoids. *Honours dissertation, University of Tasmania.*

Chappell, B.W., 1978 — Granitoids from the Moonbi district, New England Batholith, eastern Australia. *Journal of the Geological Society of Australia*, 25, 267–83.

Cocker, J.D., 1977 — Petrogenesis of the Tasmanian granitoids. *Ph.D. Thesis, University of Tasmania.*

Cocker, J.D., 1982 — Rb-Sr geochronology and Sr isotopic composition of Devonian granitoids, eastern Tasmania. *Journal of the Geological Society of Australia*, 29, 139–157.

Collins, W.J., Beam, S.D., White, A.J.R., & Chappell, B.W., 1982 — Nature and origin of A-type granites with particular reference to southeastern Australia. *Contributions to Mineralogy and Petrology*, 80, 189–200.

Gee, R.D., & Groves, D.I., 1971 — Structural features and mode of emplacement of part of the Blue Tier Batholith in north eastern Tasmania. *Journal of the Geological Society of Australia*, 18, 41–55.

Groves, D.I., & Taylor, R.G., 1973 — Greisenisation and mineralisation of the Anchor Tin Mine, N.E. Tasmania. *Transactions of the Institution of Mining and Metallurgy*, 82, B135–B146.

Groves, D.I., Cocker, J.D., & Jennings, D.J., 1977 — The Blue Tier Batholith. *Geological Survey of Tasmania, Bulletin* 55.

Higgins, N.C., Solomon, M., & Varne, R., in press — The genesis of the Blue Tier Batholith, N.E. Tasmania, Australia. *Lithos.*

Hine, R., Williams, I.S., Chappell, B.W., & White, A.J.R., 1978 — Contrasts between I- and S-type granitoids of the Kosciusko Batholith. *Journal of the Geological Society of Australia.* 25, 219–234.

Kitto, P., 1982 — The geology and geochemistry of the Ansons Bay pluton, N.E. Tasmania. *Honours dissertation, University of Tasmania.*

Manning, D.A.C., 1981 — The effect of fluorine on liquidus phase relationships in the system Qz–Ab–Or with excess water at 1 Kb. *Contributions to Mineralogy and Petrology*, 76, 206–215.

McCarthy, T.S., & Groves, D.I., 1979 — The Blue Tier Batholith, north eastern Tasmania. *Contributions to Mineralogy and Petrology*, 71, 193–209.

McClenaghan, M.P., Turner, N.J., Baillie, P.W., Brown, A.V., Williams, P.R., & Moore, W.R., 1982 — Geology of the Ringarooma-Boobyalla area. *Geological Survey of Tasmania, Bulletin* 61.

McClenaghan, M.P., & Williams, P.R., 1982 — Distribution and characterisation of granitoid intrusions in the Blue Tier area. *Geological Survey of Tasmania, Paper* 4.

McClenaghan, M.P., & Williams, P.R., 1983 — Geological Atlas, 1:50 000 series sheet 8515N, Blue Tier. *Department of Mines, Tasmania.*

McClenaghan, M.P., 1984 — The petrology, mineralogy and geochemistry of the Pyengana and Gardens granodiorites, the Hogans Road diorite and the dolerite dykes of the Blue Tier Batholith. *Department of Mines, Tasmania, Unpublished Report* 1984/04.

McDougall, I., & Leggo, P.J., 1965 — Isotopic age determinations on granitic rocks from Tasmania. *Journal of the Geological Society of Australia*, 12, 295–333.

Norrish, K., & Hutton, J.T., 1969 — An accurate X-ray spectrographic method for the analysis of a wide range of geological samples. *Geochimica et Cosmochimica Acta*, 33, 431–453.

Rickards, R.B., & Banks, M.R., 1979 — An Early Devonian monograptid from the Mathinna Beds, Tasmania. *Alcheringa*, 3, 307–311.

Robinson, K.P., 1982 — The geology and geochemistry of the Mt Stronach region, Scottsdale. *Honours dissertation, University of Tasmania.*

Streckeisen, A.L., 1973 — Plutonic rocks. Classification and nomenclature recommended by the IUGS Subcommission on the Systematics of Igneous Rocks. *Geotimes* 18 (10), 26–30.

Turner, N.J., Baillie, P.W., & McClenaghan, M.P., 1983 — Definition of the Eddystone Batholith. *Department of Mines, Tasmania, Unpublished Report* 1983/57.

Turner, N.J., Black, L.P., & Higgins, N.C., in press — Composition, structure and age of Devonian dacitic pyroclastics and hornblende-biotite granitoids, St Marys District, Tasmania. *Australian Journal of Earth Sciences.*

White, A.J.R., & Chappell, B.W., 1977 — Ultrametamorphism and granitoid genesis. *Tectonophysics*, 43, 7–22.

White, A.J.R., & Chappell, B.W., 1983 — Granitoid types and their distribution in the Lachlan Fold Belt, southeastern Australia, *Geological Society of America, Memoir*, 159.

Appendix: sources of chemical data used in diagrams.

Scottsdale Batholith, McClenaghan (unpublished data, SB1 – SB22). Blue Tier Batholith: Gardens pluton, McClenaghan (1984, Appendix 1, BT3/58–BT3/61); Pyengana pluton, McClenaghan (1984, Appendix 1, MAL 1–MAL 5), Higgins & others (in press, table 3, 1–6); St Marys Porphyrite, Higgins & others (personal communication, 1984); Poimena pluton, Higgins & others (in press, table 3, 8–21); Mount Pearson, McClenaghan (unpublished data, MBT8, MBT120, MBT123, MBT129, MBT241, MBT242); Ansons Bay pluton, Higgins & others (in press, table 2, 30–40); Lottah pluton, Higgins & others (in press, table 2, 41–44, 49–52), McClenaghan (unpublished data, TDC, BT3/42); Mount William pluton, Higgins & others (in press, 60–65).

Major and trace elements were determined by XRF analysis of glass discs and pressed powder, respectively, using the techniques of Norrish & Hutton (1969), on a Philips X-ray spectrometer. Ferrous iron was determined by $KMnO_4$ titration after HF/H_2SO_4 solution.

Analyses attributable to McClenaghan and Higgins & others (personal communication, 1984) were carried out at the Tasmanian Department of Mines. All other analyses were carried out at the University of Tasmania.

BMR Journal of Australian Geology & Geophysics, 9, 313-316

The response and calibration of seismographs at Riverview College Observatory, New South Wales, 1909–1962

L.A. Drake[1]

Seismograms from Riverview College Observatory for 1909 to 1962 are a valuable record of seismic ground motion in the Sydney region during that time, because the constants of the seismographs at Riverview were carefully and regularly determined. So that the seismograms can be effectively used, this paper sets out where the constants of the seismographs for this period can be found, how the response of the seismographs can be calculated from the values of the constants, and how the constants themselves were determined. The constants from the Wiechert and Mainka seismographs are static magnification, period, damping ratio, and solid friction. The constants for the Galitzin seismographs are galvanometer period, seismometer or pendulum period, damping constant of the seismometer, and synchronous magnification. Simple formulae give the magnification and phase lead of the respective seismographs in terms of the constants.

Introduction

The response characteristics of pre-World-Wide Standard Seismographs are important when studying earthquakes that took place before 1960. Recent work (Kanamori, 1982) indicates that these old seismograms are often of sufficient quality to enable focal mechanisms to be determined and are vital for earthquake risk studies. Thus it is important for the calibration parameters of old seismographs to be readily accessible.

As part of a project to film historical seismograms (Glover & Meyers, 1981), seismograms from Riverview College Observatory (at Lane Cove, NSW) covering the period 17 March 1909 to December 1962 were moved to the Australian Archives in Canberra, where they are now under the care of the Earthquake Seismology Group of the Bureau of Mineral Resources. Anyone wishing to use these needs to know the instrumental constants at the time of recording and how to determine the magnification and phase lead of the seismograph from these constants. This paper sets out: (i) where to find the instrumental constants of the Riverview seismographs; (ii) how to find the magnification and phase lead from these constants; and (iii) how the constants were determined. Because of its importance in the study of earthquake magnitudes, the determination of the static magnification of a Wood-Anderson seismograph is also considered.

A Wiechert seismograph with N–S and E–W components was operated at Riverview from 17 March 1909 until June 1955. A Weichert vertical seismograph was operated from 19 May 1909 until January 1944. Mainka N–S and E–W seismographs were operated from August 1910 until December 1962. Galitzin vertical, N–S, and E–W seismographs were operated from 19 January 1941 until December 1962. The World-Wide Standardized Seismograph Net (WWSSN) Benioff and Sprengnether seismographs have been operated at Riverview since December 1962. The Mainka seismographs were also operational on 9 March 1973, when the Burragorang Valley earthquake of magnitude 5.5 sent the WWSSN seismographs off-scale (Drake, 1974). The Mainka seismograms for this date are still at Riverview.

Seismograph constants

The constants for the Wiechert and Mainka seismographs are static magnification V, period T, damping ratio e, and solid friction r/T^2. Those for the N–S and E–W Wiechert seismograph were published in the *Seismological Bulletin* of Riverview College Observatory each year from 1909 until 1955, except for 1910 and 1931–33. The constants for these years, together with those for 1927 (before the magnification was increased on 2 November 1927) are set out in Table 1. Similarly, the constants of the vertical Wiechert seismograph were published in the Riverview *Seismological Bulletin* from 1909 to 1944, except for 1910 and 1931–33. These constants, together with those for 1927, are also given in Table 1.

Table 1. Wiechert constants

		V	T	e	r/T^2
26 Mar 1910	Z	61	3.6	2.8	0.040
5 Nov 1910	N	203	8.1	10.6	0.020
	E	198	6.6	6.3	0.021
17 Oct 1927	Z	80	5.1	3.3	0.100
	N	158	7.7	4.0	0.030
	E	170	7.6	4.6	0.033
15 Jun 1931	Z	61	5.2	3.7	0.047
	N	199	8.6	3.8	0.019
	E	206	9.5	3.9	0.017
15 Jun 1932	Z	58	5.3	3.2	0.053
	N	202	8.4	3.5	0.020
	E	213	9.2	3.3	0.015
20 Jun 1933	Z	60	5.1	3.0	0.092
	N	209	8.1	3.7	0.021
	E	215	9.2	3.7	0.014

The constants of the N–S and E–W Mainka seismographs were published in the Riverview *Seismological Bulletin* each year from 1911 to 1956, except for 1931 to 1933. For 1910, 1931–33, 1956, 1959, and 1960, they are set out in Table 2.

Table 2. Mainka constants

		V	T	e	r/T^2
18 Nov 1910	N	166	6.3	1.5	0.031
	E	143	6.0	2.2	0.021
15 Jun 1931	N	90	11.9	4.4	0.006
	E	90	6.9	3.3	0.014
15 Jun 1932	N	84	14.3	5.8	0.010
	E	69	10.1	4.8	0.026
20 Jun 1933	N	80	12.2	4.4	0.011
	E	82	13.0	3.8	0.010
11 Dec 1956	N	143	8.5	6.2	0.023
	E	138	9.1	6.8	0.014
8 Aug 1959	N	176	7.8	9.2	0.015
	E	143	8.3	4.2	0.009
15 Jun 1960	N	152	7.1	4.2	0.018
	E	137	8.6	4.3	0.012

The constants for the vertical, N–S and E–W Galitzin seismographs were published in the Riverview *Seismological Bulletin* from 1941 to 1956. They are the period of the galvanometer T_1, the period of the seismometer T, the damping constant of the seismometer μ^2, and the synchronous magnification of the seismograph V. The constants for 1954 (re-calculated with a programmable calculator), 1957, 1959, and 1960 are given in Table 3.

[1] School of Earth Sciences, Macquarie University, North Ryde, NSW 2113

Table 3. Galitzin constants

		T_1	T	$\mu 2$	V
28 Jan 1954	Z	10.9	9.7	0.12	408
	N	11.7	12.3	0.19	582
	E	12.3	12.2	0.03	501
15 May 1957	Z	10.8	10.1	−0.01	510
	N	11.8	12.6	0.19	591
	E	12.5	11.7	−0.02	493
17 Jul 1959	Z	11.1	11.2	0.21	478
	N	11.2	11.0	−0.38	486
	E	12.7	12.5	−0.38	551
7 Jul 1960	Z	11.1	11.2	0.21	478
	N	11.4	11.4	0.95	740
	E	12.7	12.0	−0.74	514

Constants were carefully determined at Riverview, usually every month, from 1909 to 1956, and at longer intervals for the final six years, 1956 to 1962, when the response of the seismographs was fairly stable. Use of the Riverview seismograms in conjunction with the values of the instrumental constants at the time the seismograms were recorded provides a valuable record of seismic ground motion in the Sydney region from 1909 to 1962.

Magnification and phase lead

It can be shown for oscillatory ground motion sin pt, where p is the angular frequency of the motion and t is time, that the displacement of a seismograph is given by:

$$y = \frac{V\sin(pt + \phi)}{[(1 - u^2)^2 + 4\zeta^2 u^2]^{1/2}} \quad \text{with } \tan\phi = \frac{2\zeta u}{1-u^2}$$

where ϕ is phase lead, $u = n/p$, $T = 2\pi/n$, ζ is the fraction of critical damping, $\mu^2 = 1 - \zeta^2$ and $\lg e = \pi\zeta/\mu$ (Sohon, 1932, p.62; Byerly, 1933; Bullen, 1963, p.144; Garland, 1979, p.71). These expressions give the magnification and phase lead of the Riverview Wiechert and Mainka seismographs in terms of their constants, static magnification V, period T, and damping ratio e. The solid (or pen) friction r/T^2 is used to find the damping ratio e, but is not further needed to find the magnification and phase lead. The phase lead is zero at short periods, $\pi/2$ when the ground period is that of the seismograph (T), and π at long periods. At periods longer than T, it is necessary to add π to the principal value of the inverse tangent (that a calculator gives). Causality is not a problem with the phase lead, because we are considering steady oscillatory ground motion and ignoring the transient solutions of the seismograph equation.

For oscillating ground motion sin pt, the displacement of the light spot of a Galitzin seismograph is given by:

$$y = \frac{4uV}{(1 + u^2)^2} \sin(pt + 2\phi - \pi/2),$$

where u and ϕ are as above and V is now the synchronous magnification of the seismograph (Sohon, 1932, p.92). The period of the galvanometer T_1 is assumed to be close to that of the seismometer T. For the routine calculation of ground amplitudes at Riverview, the mean of T_1 and T was used in the value of u. The seismometer and galvanometer of a Galitzin seismograph should be critically damped ($\zeta = 1$); the constant μ^2 ($= 1 - \zeta^2$) indicates to what extent the seismometer was not critically damped, a negative value indicating overdamping. The phase lead of the Galitzin seismograph ($2\phi - \pi/2$) can easily be verified to be a lag up to a ground motion period of 0.414T, and, at a ground motion period of 2T, a lead-in time of 0.91T (i.e. a little less than π radians). The phase lead-in time of the Sprengnether (WWSSN) seismographs is approximately 0.42T for ground motion of twice the period of the seismometer (cf. Drake, 1973). This is consistent with the phase lead of the Galitzin seismographs, because the Sprengnether seismometers are connected to galvanometers of long period (100 s).

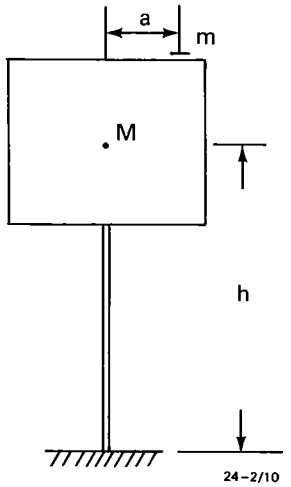

Figure 1. Horizontal Wiechert seismograph with test mass m.

Determination of N—S Wiechert constants

The inverted Wiechert 'astatic' (unstable) pendulum is shown in Figure 1. Its mass is M (1 tonne at Riverview) and its centre of mass is at a height h (940 mm at Riverview) above its point of support. When a small mass m is placed a distance a (346 mm at Riverview) north of the centre of the mass, a torque mga deflects the mass a small angle θ to the north (g is the acceleration of gravity). A torque Mgh sin θ tends to deflect the mass more, but a restoring torque $\beta\theta$ from the spring connections of the seismograph's magnifying levers keeps the mass deflected at angle θ. We have,

$$(\beta - Mgh)\,\theta = mga$$

(Wiechert, 1903a; Sohon, 1932, p. 24). If I is the moment of inertia of the mass about its point of support and T is the period of the seismograph, we also have,

$$(\beta - Mgh)\,\theta = 4\pi^2 I\theta/T^2$$

If l' ($=I/Mh$) is the reduced pendulum length and y is the pen deflection for the mass deflection θ, the static magnification

$$V = \frac{y}{l'\theta} = \frac{4\pi^2 yMh}{mga\,T^2}$$

Basically, in any static magnification determination, the unknown moment of inertia of the seismometer and its restoring force are replaced by its period of oscillation by means of the pendulum equation. In the determination of static magnification of Wiechert seismographs, the unknown small deflection of the mass (θ) is replaced by the known value of the small deflecting mass m. Static magnification is the magnification of the seismograph at very short periods (u is small in the seismograph displacement equation).

It is worth noticing that in the determination of the static magnification of a Wood-Anderson seismograph (Fig. 2), the small angle of deflection, θ, of the seismometer (Fig. 3) is found by tilting the seismometer sideways a known angle ψ; OZ is the direction of the vertical, i is the inclination of the seismometer (mass M), S is its upper point of support, and

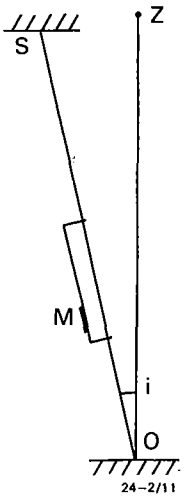

Figure 2. Wood-Anderson seismograph suspension.

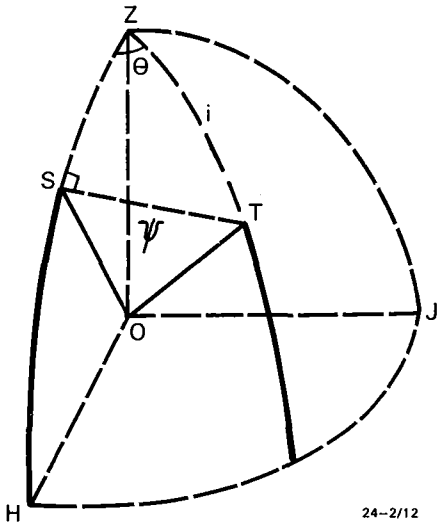

Figure 3. Tilt of Wood-Anderson seismograph $\psi = i\theta$.

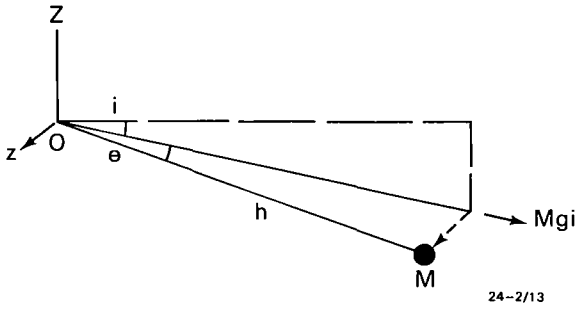

Figure 4. Horizontal seismograph displaced an angle θ.

OHJ is the horizontal plane. By the sine formula for the spherical triangle STZ, sin i = sin ψ /sin θ , or, since the angles are small, $\theta = \psi / i$.

Figure 4 shows the pendulum, mass M, of a horizontal seismograph; OZ is the vertical, and the distance of the centre of mass from the point of support of the pendulum is h; i is the inclination of the pendulum down from the horizontal in its equilibrium position; Mgi is the gravity component in this direction and θ is the angular displacement of the pendulum caused by, say, a ground displacement z. We have, from the pendulum equation,

$$Mgih\,\theta = 4\pi^2 I\,\theta / T^2$$

If l' is the reduced pendulum length of the Wood-Anderson seismometer and y is the light spot displacement for the tilt ψ, we have for the static magnification,

$$V = \frac{y}{l'\theta} = \frac{4\pi^2 y}{g\psi T^2} \qquad \text{since } l' = \frac{I}{Mh}$$

The period T of the N–S Wiechert seismograph is easily observed (with the damping removed). While the damping is removed, an estimate of solid or pen friction is made by measuring successive amplitudes of oscillation y_1 and y_2 (Fig. 5). Without damping, y_1 should be equal to y_2, and the effect of friction has been to increase y_1 by an amount r, where $r = (y_1 - y_2)/2$, and to decrease y_2 by an amount r (Sohon, p. 74). Hence, when the damping is replaced, the estimate of the damping ratio e $(=y_1/y_2)$ is taken to be $(y_1 - r)/(y_2 + r)$.

The determination of the E–W Wiechert seismograph constants is similar to the determination of the N–S constants, and the determinations of the vertical Wiechert and N–S and E–W Mainka seismograph periods and damping ratios are similar to the determinations of the N–S Wiechert period and damping ratio.

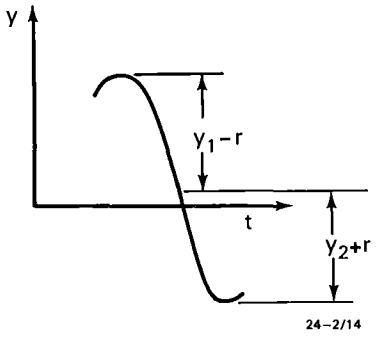

Figure 5. Undamped oscillation decreased by solid (pen) friction.

Determination of the vertical Wiechert static magnification

Figure 6 is a sketch of the pendulum of the Riverview vertical Wiechert seismograph. The pendulum of mass M (80 kg) has a radius of gyration and a reduced pendulum length h about its axis of rotation; it is supported by a spring of stiffness k (insulated from varying temperature). If I is the moment of inertia of the pendulum about its axis of rotation, we have, from the pendulum equation,

$$kh\,\theta/2 = 4\pi^2 I\,\theta/T^2$$

A small mass m (10 g at Riverview) is placed at a distance h/2 from the axis of rotation of the pendulum (Wiechert, 1903b, p.111); the pendulum rotates an angle θ and the pen of the seismograph deflects a distance y. We have $k\theta = mg$ and, since $I = Mh^2$, the static magnification

$$V = \frac{y}{h\theta} = \frac{8\pi^2 My}{mgT^2}$$

Determination of the Mainka static magnification

The N–S and E–W Mainka seismographs can be represented by Figure 4 (M at Riverview is 450 kg). A small mass m (5 g at Riverview) is attached to M by a horizontal thread over a pulley and deflects the pendulum an angle θ and the pen of the seismograph a distance y (Sohon, 1932, p.21). We have

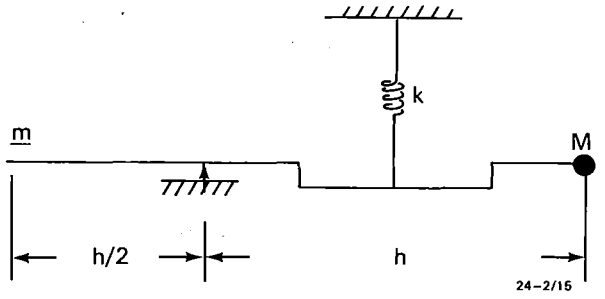

Figure 6. Wiechert vertical seismograph with test mass m.

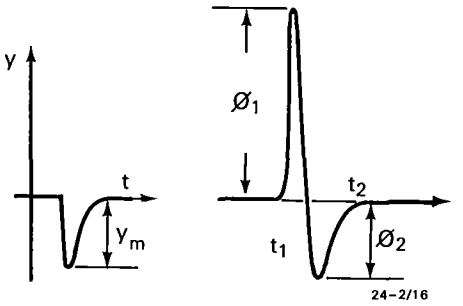

Figure 7. Galitzin pendulum and galvanometer 'tap' deflections.

mg = Mgi θ and, from the pendulum equation for a horizontal seismograph, we have the static magnification

$$V = \frac{y}{\ell\theta} = \frac{4\pi^2 My}{mgT^2} \quad \text{since } \ell = \frac{I}{Mh}$$

Determination of the Galitzin constants

It is interesting that Galitzin was able to find the magnification of an electromagnetic seismograph without using either a shaking table or a low- frequency alternating-current source.

The undamped period of the galvanometer T_1 is found with the galvanometer on open circuit. The damping constant of the pendulum μ^2, the undamped period of the pendulum T, and the synchronous magnification V are found by giving the pendulum a small (electrical) tap (Fig. 7). A mirror is attached near the point of support of the pendulum and the angular movement θ_m of the pendulum after the tap can be found by measuring the displacement y_m of a light spot. If the galvanometer is critically damped, the ratio of the galvanometer angular displacements ϕ_1 and ϕ_2 (at times t_1 and t_2) gives the damping constant of the pendulum μ^2 (Sohon, 1932, p. 118),

$$\mu 2 = 2.886 - 1.258\ \phi 1/\phi 2$$

The time of zero crossing of the galvanometer trace t_o ($t_1 < t_o < t_2$) and the undamped period of the galvanometer T_1 give the undamped period of the pendulum T,

$$T = 4.189t_o + T_1 (0.1\mu^2 - 1)$$

Finally, the synchronous magnification V is estimated from the ratio of ϕ_2 and θ_m

$$V = \frac{(40.6 - 13.8\mu 2)\ A_1 T \phi_2}{4\pi\ell T_1\ \theta_m}$$

where A_1 cm is the distance from the galvanometer mirror to the recording drum and ℓ is the reduced pendulum length (Sohon, 1932, p. 125).

The method of determination of the constants of the vertical, N–S and E–W Galitzin seismographs is as just described.

Acknowledgements

Assistance of Dr David Denham and Mr Ron Smith in transporting the Riverview seismograms to Canberra and in maintaining the collection is most gratefully acknowledged. The figures were drafted by M. Steele.

References

Bullen, K.E., 1963 — An introduction to the theory of seismology, *Cambridge University Press.*

Byerly, P., 1933 — Reduction of trace amplitudes. *Bulletin of the National Research Council*, 90, 198–205.

Drake, L.A., 1973 — Rayleigh and Love waves in the Tasman Basin. *New Zealand Journal of Geology and Geophysics*, 16, 997–1007.

Drake, L.A., 1974 — The seismicity of New South Wales. *Journal and Proceedings of the Royal Society of N.S.W.*, 107, 35–40.

Garland, G.D., 1979 — Introduction to geophysics, *Saunders, Philadelphia.*

Glover, D.P. & Meyers, H., 1981 — Historical seismogram filming project: third progress report. *World Data Center A for Solid Earth Geophysics, Boulder, Colorado.*

Kanamori, H., 1982 — Importance of historical seismograms for geophysical research. *Program and Abstracts of Regional Workshop of the IASPEI/UNESCO Working Group on Historical Seismograms, Earthquake Research Institute, University of Tokyo, Japan.*

Sohon, F.W. 1983 — Seismometry. *Volume 2* of Macelwane, J.B. & Sohon, F.W., Introduction to theoretical seismology. *Wiley, New York.*

Wiechert, E., 1903a — Ein astatisches Pendel hoher Empfindlichkeit zur mechanischen Registrierung von Erdbeben (An unstable pendulum of higher sensitivity for the mechanical recording of earthquakes). *Physikalische Zeitschrift*, 4, 821–829.

Wiechert, E., 1903b — Theorie der automatischen Seismographen (Theory of automatic seismographs). *Abhandlungen der Koeniglichen Gesellschaft der Wissenschaften zu Gottingen. Mathematisch-Physikalische Klasse. Neue Folge* Band 11. Nro. 1.

BMR Journal of Australian Geology & Geophysics, 9, 317–328

Eastern Creek Volcanics: their geochemistry and possible role in copper mineralisation at Mount Isa, Queensland

I.H. Wilson[1], G.M. Derrick[2], & D.J. Perkin[3]

New chemical analyses of relatively low-grade metabasalt from the Eastern Creek Volcanics, 120–150 km north of Mount Isa, Queensland, show them to be continental tholeiites. A 2-stage model of fractional crystallisation is proposed to explain the major and trace element variation in the suite. The uncommonly high Cu content of the metabasalt (about 200 ppm) is attributed to concentration of an immiscible sulphide phase during fractionation. Examination of all available chemical data has led to the recognition of 5 types of alteration. The Cu content is depleted in metabasalts that are anomalously enriched in K_2O, MgO, or CO_2, but is not affected in metabasalt enriched in CaO or Na_2O. This Cu depletion supports earlier models that attribute Cu mineralisation at Mount Isa to leaching of Cu from the Eastern Creek Volcanics and its redeposition in favourable pyritic, dolomitic sediments of the Mount Isa Group. The ore localisation has been associated with brecciation and appears to depend on the juxtaposition of the Mount Isa Group and the Eastern Creek Volcanics largely by faulting.

Introduction

The Cu ore bodies at Mount Isa, which originally contained at least 230 Mt at 3% Cu, occur in brecciated and recrystallised dolomitic shale ('silica dolomite') of the Middle Proterozoic (1680 Ma) Urquhart Shale (Mathias & Clark, 1975; Derrick & others, 1976b; Williams, 1980; Page, 1981). Some workers (Solomon, 1965; Bennett, 1965; Stanton, 1972; Finlow-Bates & Large, 1978; Plimer, 1978; Finlow-Bates & Stumpel, 1979) have considered that the Cu mineralisation occurred at or very near the time of sedimentation of the host rocks. However, other workers (e.g. Fisher, 1960; Cordwell & others, 1963; Smith & Walker, 1971; Perkins, 1981, 1984) favoured an epigenetic origin. Mathias & Clark (1975) and Robertson (1982) suggested the Cu was introduced during sedimentation, but was subsequently partly mobilised during deformation and brecciation. Smith & Walker (1970, 1971) provided geochemical evidence that Cu was derived from the Eastern Creek Volcanics, a thick sequence of tholeiitic lavas that is older than, but locally faulted against, the Urquhart Shale. Scott & Taylor (1982) have shown that the Eastern Creek Volcanics could also be the source of Cu mineralisation at Mammoth Mine, 150 km north of Mount Isa.

This paper examines new petrological and geochemical data on 50 specimens from the Eastern Creek Volcanics, collected in the north of the Mount Isa Inlier, (areas 1, 2 and 3 in Figure 1). Most specimens are from a nearly complete and little metamorphosed section of the formation southeast of Gunpowder (Fig. 2). The least altered rocks are compared geochemically with other suites from the Eastern Creek Volcanics to identify the types of alteration.

Previously unpublished evidence of alteration in drill core of the Eastern Creek Volcanics from near the Crystallena Block, about 11 km south of Mount Isa is interpreted as supporting earlier models that relate Cu mineralisation at Mount Isa to the Eastern Creek Volcanics.

Geological setting

The Eastern Creek Volcanics (Carter & others, 1961; Robinson, 1968; Derrick & others, 1976a) crop out in a north-trending belt covering about 8000 km², centred roughly on Mount Isa and bounded by 19°15'S and 22°05'S and 139°00'E and 139°50'E (Fig. 1). Most of the exposure and the thickest sequences occur within the Leichhardt River Fault Trough (Glikson & others, 1976; Derrick, 1982). The volcanics thin rapidly towards the eastern margin of the fault trough; the western margin is poorly defined geologically, but Derrick (1982) used geophysical data to locate it approximately.

Three members are recognised in the Eastern Creek Volcanics (Derrick & others, 1976a). From the oldest they are: the Cromwell Metabasalt Member (1750–5430 m thick), Lena Quartzite Member (200–1000 m), and Pickwick Metabasalt Member (50–700 m). The stratigraphic relations of these members to other units are summarised in Figure 3. The unconformable relationship of the younger Mount Isa and McNamara Groups (Derrick & others, 1976b) is shown diagrammatically. Faulting has juxtaposed the Eastern Creek Volcanics and the Mount Isa Group in the Mount Isa mine area and also in Crystallena Block.

The structures and sequences of structural events in the Leichhardt River Fault Trough have been described by Derrick (1982). An age of 1710 ± 25 Ma (Gulson & others, 1983) for the Eastern Creek Volcanics is consistent with ages obtained and observed relationships in or near the Leichhardt River Fault Trough (Page, 1980, 1981; Page & others, 1982). A recent structural study (Swager, 1983) concluded that the Cu mineralisation at Mount Isa occurred late in or soon after the major regional metamorphism that was active between 1650 and 1500 Ma.

Lithology

The dominant rock type in the Eastern Creek Volcanics is metabasalt, which occurs in moderately well-defined flows from 20 to 50 m thick. Most flows have a thin basal amygdaloidal zone, and a massive medium to coarse-grained middle section that fines upward into an upper amygdaloidal zone. The amygdales are mostly well rounded, but some are almond shaped, and pipe amygdales are rarely developed. Flow-top breccia is present in some flows. Phenocrysts are not abundant, xenoliths are rare, and fluidal banding, pillow-structures, and hyaloclastites have not been identified. In the lower part of the Eastern Creek Volcanics, tuffs are rare, but mafic tuffs increase in abundance upward and are a significant component of the Pickwick Metabasalt Member. Dolerite dykes, mainly north-trending, are common in the Eastern Creek Volcanics and in the immediately underlying stratigraphic units.

Quartzose and feldspathic sandstones are common as lenticular sedimentary intercalations. Thick, mostly carbonate-rich, conglomerate intercalations occur in the more eastern exposures, especially northeast of Mount Isa. Carbonate-rich siltstone, stromatolitic chert, mud-cracked sandstone, and epidotic sandstone occur in minor amounts. Although the volcanics appear to be subaerial, the sediments

[1] Premier's Department, Box 185, Brisbane North Quay, Queensland 4000
[2] G.M. Derrick & Associates, Box 184, Corinda, Queensland 4075
[3] Resource Assessment Division, BMR

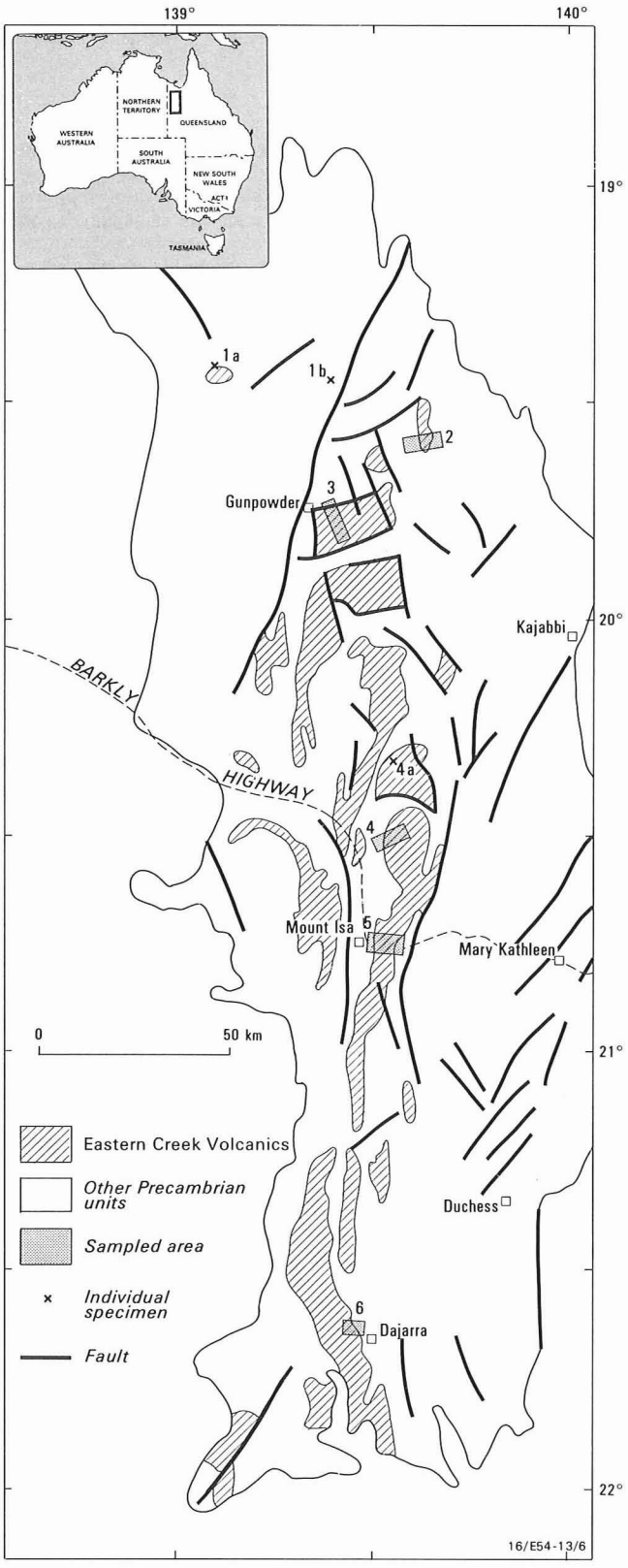

Figure 1. Locality map, showing areas of Eastern Creek Volcanics sampled by the authors (1,2,3), Scott & Taylor (3), Glikson (4,5), Ellis (4a,6), Walker (5), Smith & Walker (5), Solomon (5).

are more typical of lacustrine, lagoonal, or shallow marine environments.

The least deformed metabasalt is typically dark green to black, massive, fine-grained, unfoliated, and locally amygdaloidal. Most amydales consist of quartz, but others contain calcite, epidote, chlorite, or sulphide. The metabasalt retains a primary basaltic texture despite greenschist facies metamorphism. Rare euhedral phenocrysts of plagioclase are set in a mesh of randomly oriented small euhedral plagioclase laths containing epidote grains and rare patches of calcite. The intersertal ferromagnesian minerals have largely been replaced by chlorite, actinolite, and sphene, although relict primary pyroxene, magnetite, and sulphides occur in some specimens, and pseudomorphs after clinopyroxene and olivine? have been recognised in a few specimens.

In more deformed metabasalts, the plagioclase occurs as granoblastic mosaics of albite/oligoclase, which is commonly untwinned. Hornblende is the dominant ferromagnesian mineral, although biotite, epidote, sphene, and opaques are common. The texture ranges from granoblastic to nematoblastic, but the biotite-rich rocks are lepidoblastic. In the highest-grade sequences, in the west and southwest, the dominant rock is a massive unfoliated amphibolite, containing some slightly porphyroblastic hornblende in a granuloblastic mosaic of plagioclase (oligoclase/andesine), biotite, sphene, opaque minerals, quartz, and epidote.

Extreme alteration has produced rocks that contain unusually large amounts of calcite, albite, or epidote in areas where the deformation has been slight. Chlorite is the dominant mineral in highly altered shear zones. Smith & Walker (1971) reported that chloritic schists containing veins of calcite and minor chlorite, quartz, and feldspar are common in the Mount Isa mine area. Similar chloritic rocks have been intersected in drill holes in the Crystallena Block adjacent to the faulted contact with the Native Bee Siltstone. The 'greenstone' beneath the Cu orebodies in the Mount Isa mine contains thin layers of siliceous rocks, which are interpreted as sedimentary interbeds from their petrography and trace element composition (viz. V, Sc, Ti) listed in Smith & Walker (1970). The 'greenstone' cannot be interpreted as a 'chlorite-bearing siliceous sediment' as proposed by Finlow-Bates & Stumpel (1979), but is composed mainly of altered metabasalt, together with abundant dolerite and minor metasediments.

Geochemistry of the Eastern Creek Volcanics

The following discussion is based mainly on new analyses of the suite of 46 specimens of metabasalt, tuff, and dolerite from a section 3–15 km southeast of Gunpowder township, and 4 other specimens collected by the authors in 1978. The analyses were performed at the Australian Mineral Development Laboratories, except for the REE, which were analysed by the senior author at the Research School of Earth Sciences, ANU, Canberra, using spark-source mass spectrometer facilites provided by Dr S.R. Taylor. Reference is also made to about 50 previously published analyses for all major and some trace elements and about 1000 unpublished trace element analyses.

Alteration

Regional metamorphism and hydrothermal activity during the Middle Proterozoic and extensive weathering since the Early Tertiary suggest that even the freshest sequences, such as the Gunpowder section, may in fact be altered to some degree. Alteration has been evaluated using element variance, covariance, and the abundance of components such as carbon dioxide, water, ferric iron, and alkali metals. All available chemical data have been used in assessing alteration.

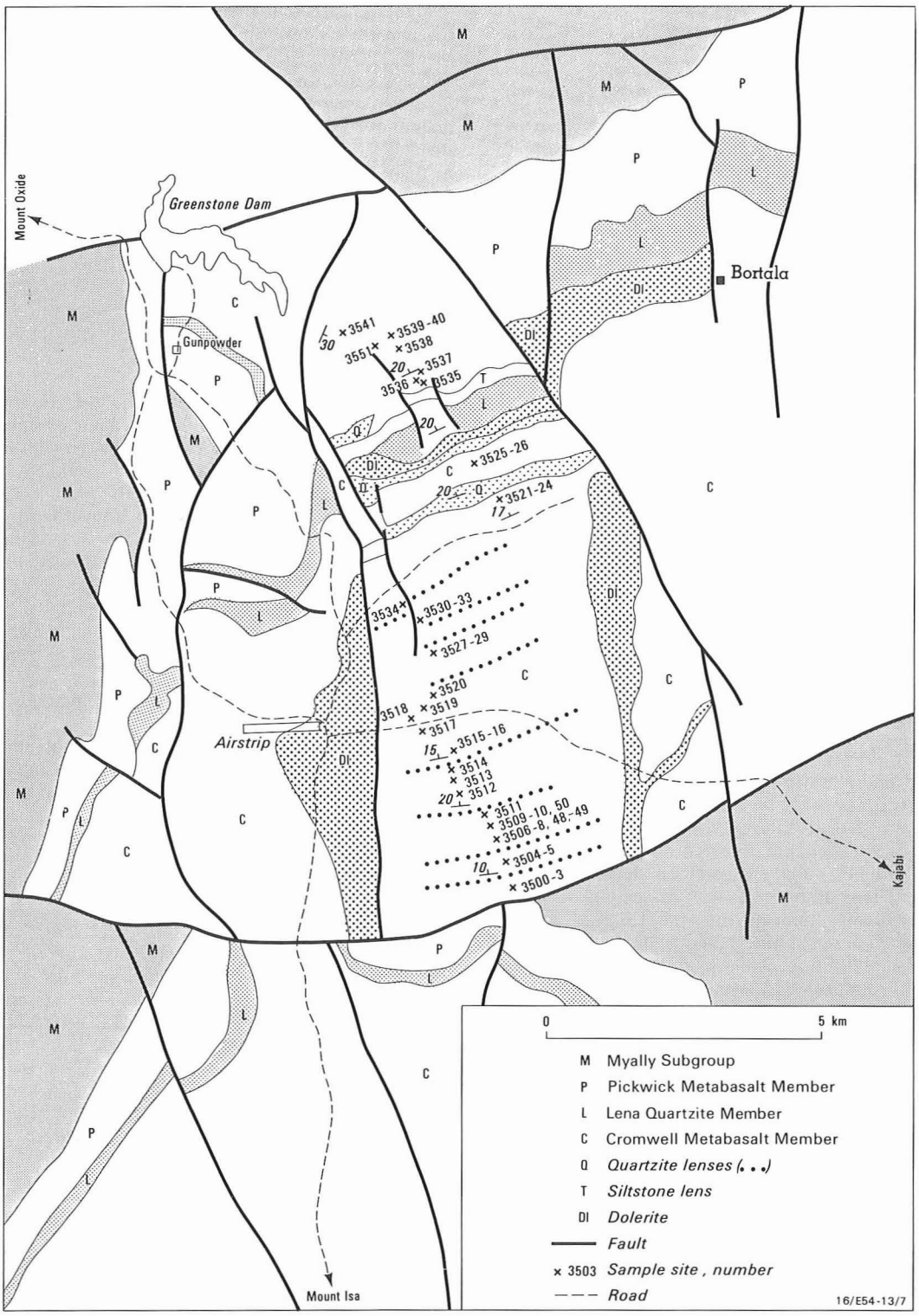

Figure 2. Generalised geology of Mammoth Mines section.

Variance is expected to increase with the intensity of alteration. The extent of this scatter for the Eastern Creek Volcanics can be seen in the plots of analytical values against the stratigraphic position of the specimens (Fig. 4). Several elements (Ti, Fe_{tot}, Co, and Y) show relatively narrow ranges in each of the metabasalt members and these elements have possibly been little affected by alteration in any area. Some other elements (Si, Fe^{3+}, Ca, Na, C as CO_2, Ba, Cu, and Zn) have a narrow range if a small number of 'anomalous' values are ignored. For example, values of CO_2 greater than 0.20 indicate probable alteration. Specimens exhibiting several 'anomalous' elements are considered to be altered.

Covariance, which measures dispersion in two-element variation diagrams, is commonly standardised by dividing by the standard deviation of each element to produce the correlation coefficient. The correlation coefficients in the Pickwick Metabasalt Member and Cromwell Metabasalt Member were calculated separately. In both members strong correlations exist within the following groups of elements:

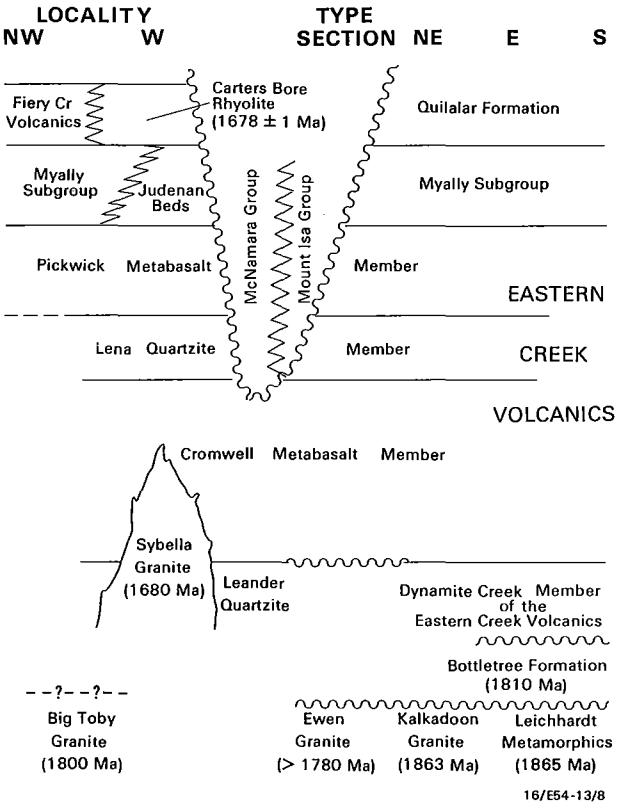

Figure 3. Diagrammatic representation of stratigraphic relations of the Eastern Creek Volcanics.

Zr, Y, P, K, and Nb; Mg, Cr, and Ni; and Na, Ca, Si, and Al. These correlations are typical of igneous differentiation. In the Pickwick Metabasalt Member, Cu and total S as SO_3 are strongly correlated, possibly as a result of the Cu being present as sulphides, but in the Cromwell Metabasalt Member a weak inverse relationship exists between these elements. This reversed trend may indicate that the Cu was originally concentrated in non-sulphide minerals, but, more probably, it indicates mobilisation of Cu from sulphides. The latter explanation is supported by the negative correlations of Cu with Fe^{3+}, H_2O, and CO_2.

Factor analysis further clarifies the inter-element relationships. Each metabasalt member was treated separately, using principal component analysis and varimax rotation (Wilson, 1982). The first factor recognised in each member is dominated by incompatible elements and is inferred to relate to igneous fractionation. Of the other factors identified in the Pickwick Metabasalt Member, only the fourth has any obvious significance. It is dominated by SO_3, Cu, Zn, Th, FeO, and MnO, and is interpreted as the 'mineralisation' factor. The second factor in the Cromwell Metabasalt Member is dominated by Pb, Na_2O, H_2O^+, CO_2, and Fe_2O_3, with a negative input from FeO, K_2O, Rb, CaO, and Cu. Little contribution is made by H_2O^-, SO_3, Co, SiO_2, Al_2O_3, Ce, Cr, La, or Nb. This factor could reasonably be related to alteration. The depletion of Cu in rocks with high H_2O^+, CO_2, and Fe_2O_3 is consistent with Cu leaching from the basalts during alteration.

The distribution of second-factor scores for specimens of the Cromwell Metabasalt Member from the Gunpowder section is bimodal. The larger population ranges from −1.38 to 0.10 with a median of about −0.85, and the smaller more diffuse population ranges from 0.40 to 2.03, and contains 5 specimens, all of which are interpreted as being altered, according to other criteria. Thus a second-factor score greater than 0.1 indicates that alteration is likely to have affected the specimen. It is significant that all specimens of the Cromwell Metabasalt Member from the type section have second-factor scores greater than 0.90, implying that they are altered, Similarly, second-factor scores for 5 specimens from diamond-drill holes in the Mount Isa mine and near Cu mineralisation in the Crystallena Block are probably altered, as their second-factor scores range from 1.41 to 2.73.

The potassic alteration exhibited in the average of 8 analyses of hydrothermally altered metabasalt from near the Mammoth mine (Scott & Taylor, 1982, table 3) has a second-factor score of −0.72, which is strongly influenced by the high potassium content. Although such alteration is rare in the Eastern Creek Volcanics, it obviously will not be detected by examining second-factor scores.

The Beswick & Soucie (1978) test for alteration compares analyses with narrow fields defined by unaltered suites in plots of pairs of log molecular ratios of major elements to K. This test indicates 5 of the more potassic specimens from the Gunpowder section are significantly altered. The high coherence of the remaining analyses is regarded as evidence that any alteration of these specimens has been relatively mild. Another test uses the sensitivity of the **Rittman (1957) serial index** to changes in total alkalies. Most Eastern Creek Volcanics have indices between 1.4 and 4.0, but 7 specimens from the Gunpowder section have significantly higher values, up to a maximum of 19.9, and are suspected of being altered.

The above criteria identify 12 of the 41 metabasalts from the Gunpowder section as significantly altered. Most of these specimens fail 3 or more of the criteria, but none fail all criteria, indicating that there is more than one alteration process. The elements most commonly affected by alteration are K, Na, Si, Ca, C, Ba, Cu, Sr, Zn, and the oxidation state of Fe. The remaining 29 species are regarded as the least altered of the Eastern Creek Volcanics that have been analysed to date. Compared to these, most specimens from other sections appear to be significantly altered: 5 types of alteration are recognised. Scott & Taylor (1982) showed the existence of dichotomous Ca-enriched (epidote) and Na-enriched (albite) assemblages, which are normal alteration types in greenschist metamorphism. Their example of Na-enrichment also exhibits CO_2-enriched (calcite) alteration. A fourth type of alteration involves K_2O enrichment (biotite/potash feldspar), and the fifth type is the MgO-enriched (chlorite) assemblage. Rocks enriched in K_2O, MgO, or CO_2 typically have unusually low Cu contents. This Cu depletion is inferred to have occurred during the alteration.

Chemical characteristics

The new chemical data, and analyses from Glikson & Derrick (1978) are summarised as plots against stratigraphic height in Figure 4. Most data are from the Gunpowder section. This figure gives some indication of variation within flows, temporal trends in each member, differences between the two members, and the lack of spatial variation. The discussion below is based mainly on specimens from the Gunpowder section.

The variation within flows (expressed as average deviation) is 3 to 12 times as large as the analytical error, indicating that compositional variation within the flows is significant (Wilson, 1982). Although much of the variation is due to alteration, some may represent local variations in the primary igneous fractionation during crystallisation of the flow. Systematic variation in these flows was not borne out by the

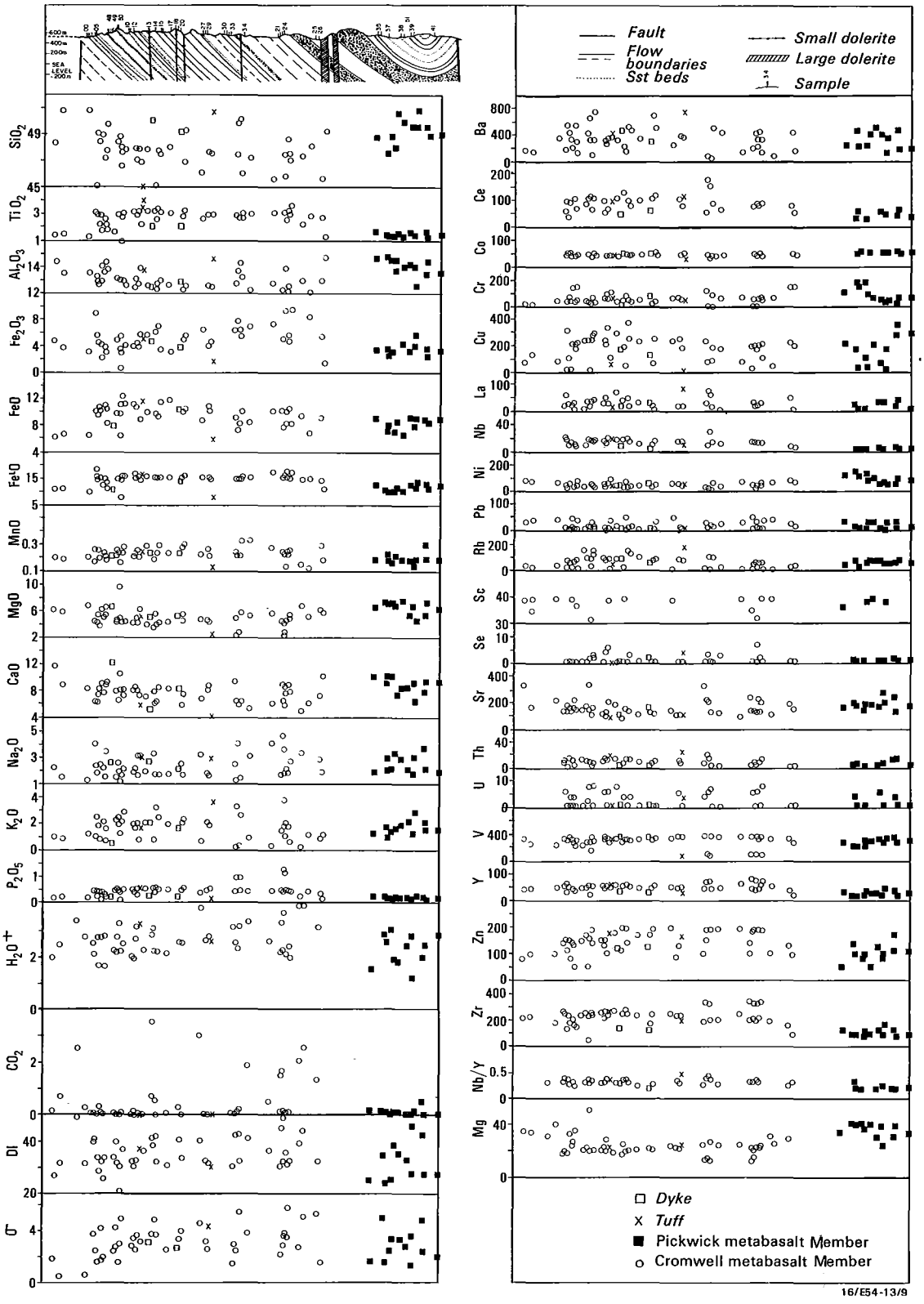

Figure 4. Major and trace element abundances plotted against stratigraphic position.

data available, which is not surprising, as studies of a modern tholeiitic flow from Iceland have shown random variation attributed to short-range segregation during crystallisation (Lindstrom & Haskins, 1981).

Two contrasting temporal sequences occur in the Cromwell Metabasalt Member. The older sequence involves the basal quarter of the member and is marked by increases in TiO_2, total Fe, MnO, K_2O, P_2O_5, Cu, Rb, Th(?), V, Y, and Zn; and decreases in SiO_2, Al_2O_3, MgO, Na_2O, Cr, Ni, and Sr. The younger sequence is notable for its very consistent composition. There is only one temporal sequence in the Pickwick Metabasalt Member and it shows similar variation patterns to the basal part of the Cromwell Metabasalt Member.

The main difference between the two members is the lack of specimens from the Pickwick Metabasalt Member as fractionated as the younger sequence in the Cromwell Metabasalt Member. This sequence of the Cromwell Metabasalt Member contains approximately twice as much TiO_2, Ce, Nb, Th, Y, and Zr, and significantly less MgO, Cr, and Ni compared to the Pickwick Metabasalt Member.

No significant spatial variation has been recognised in the Eastern Creek Volcanics from the limited data available for elements such as Ti, P, Co, Cr, Nb, V, Y, and Zr, which are least likely to be affected by alteration. There is, however, evidence of different alteration types being restricted to specific areas. The Gunpowder section contains few examples of the dichotomous Ca-rich (epidote) and Na-rich (albite) assemblages that occur sporadically throughout the formation. The CO_2-rich assemblages are also widespread, but are particularly common in the type section to the east of Mount Isa. Altered metabasalts, as presented by Scott & Taylor (1982, table 3), which are characterised by abnormally high K_2O contents, are uncommon in the Eastern Creek Volcanics except near the Mammoth mine, but are common in younger volcanics in the region (Wilson, 1982). Alteration involving addition of Mg is evident in the greenstone below the Mount Isa Cu orebodies (Smith & Walker, 1971, table 14, nos. 19–21). The apparently higher Pb values for the type section are probably a result of less accurate analytical techniques being applied during these earlier analyses.

Classification

Chemical classifications are used, because the primary mineralogy of these rocks has been largely obliterated by metamorphism. Chemical classifications based on alkalies, such as plots of total alkalies against silica, the Rittman Serial Index, or plots in the normative olivine–nepheline–quartz triangle are possibly unreliable, because the alkali elements are potentially mobile during metamorphism. Alternative tests, involving relatively immobile trace elements are favoured for classifying metamorphosed volcanics. The Nb/Y ratio exceeds 0.67 in most alkaline rocks (Winchester & Floyd, 1977), but no specimens from the Gunpowder section have ratios greater than 0.5 and the three specimens with ratios greater than 0.4 are a tuff and two highly porphyritic volcanics. Most specimens from the Cromwell Metabasalt Member have ratios of about 0.35 and specimens from the Pickwick Metabasalt Member have ratios of about 0.20. This test indicates that the Eastern Creek Volcanics are subalkaline, confirming the earlier tests based on alkalies (Glikson & others, 1976; Glikson & Derrick, 1978; Wilson, 1982) for all except a few of the most highly altered specimens.

The rocks have low Zr/TiO_2 values consistent with basalts or andesites (Winchester & Floyd, 1977). Iron enrichment typical of tholeiitic basalt is displayed in the AFM diagram (Fig. 5). Most of the specimens are quartz- normative, even when the Fe_2O_3/FeO ratio is recalculated to 0.15. Some specimens are hypersthene-normative, but normative olivine is uncommon. The high K_2O values (about 2 per cent) in the least altered specimens of the Eastern Creek Volcanics are typical of continental (Kristnamurthy & Cox, 1980) or island arc (Pearce, 1976) environments. The relatively high content of TiO_2 (about 3 per cent in at least half the formation) is typical of anorogenic (within plate) basalts (Chayes, 1964; Pearce & Cann, 1973). The lower values of TiO_2 in the Pickwick Metabasalt Member (about 1.40 per cent) are unusual in an anorogenic setting.

In summary, the chemistry of the Eastern Creek Volcanics indicates that they are continental tholeiites. This is consistent with their geological setting in a rift valley (Glikson & others, 1976; Derrick, 1982).

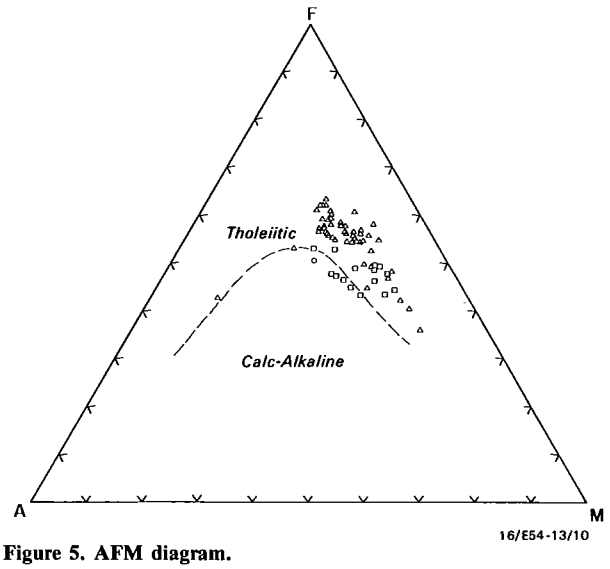

Figure 5. AFM diagram.

Petrogenesis

This section examines evidence for the source of the magma, and evaluates the major and trace element variation patterns for evidence of fractionation. A model is proposed to account for the chemical variation in the Eastern Creek Volcanics.

The ratios of the more incompatible elements are likely to reflect those of the source area. The Zr/Nb ratios (7–28) and the Zr/Hf ratios (32–42) of the Eastern Creek Volcanics are comparable to the chondritic values of 12.6 and 33.5, respectively (Taylor, 1979). Similarly, the K/Rb ratios, which mostly range from 200 to 300 in these rocks, are closely comparable to the chondritic value of 257 (Taylor, 1979), despite the metamorphism. The upper mantle is considered to have ratios of these elements very close to chondritic values and it provides the most likely source area for these volcanics.

The greenschist facies regional metamorphism is a major problem in investigating the igneous variation in the suite, because it has obliterated most of the primary minerals and possibly changed the bulk composition of the rocks. The only minerals that have retained their primary composition are relict clinopyroxene and labradorite in the Pickwick Metabasalt Member and, possibly, some opaque minerals. Least-squares (Bryan & others, 1969) testing of petrogenetic models such as fractional crystallisation is not warranted, because of the lack of reliable primary mineral composition data.

A simple graphical technique, involving projection of bulk composition trends onto the normative olivine–plagioclase–clinopyroxene plane (the simplified basalt system, Cox & others, 1979, p. 156–160) ideally identifies the proportions of these minerals that could produce the observed trends by fractionation. The trends observed in the Pickwick Metabasalt Member (Fig. 6) could result from fractionating olivine, plagioclase, and clinopyroxene in the proportions of 25:50:25, respectively. For the Cromwell Metabasalt Member, the relative proportions are poorly defined, but encompass the same range as the Pickwick Metabasalt Member, as well as proportions with much higher plagioclase contents. Evidence of variable plagioclase extraction is provided by the occurrence of relict plagioclase phenocrysts in a few specimens of this formation.

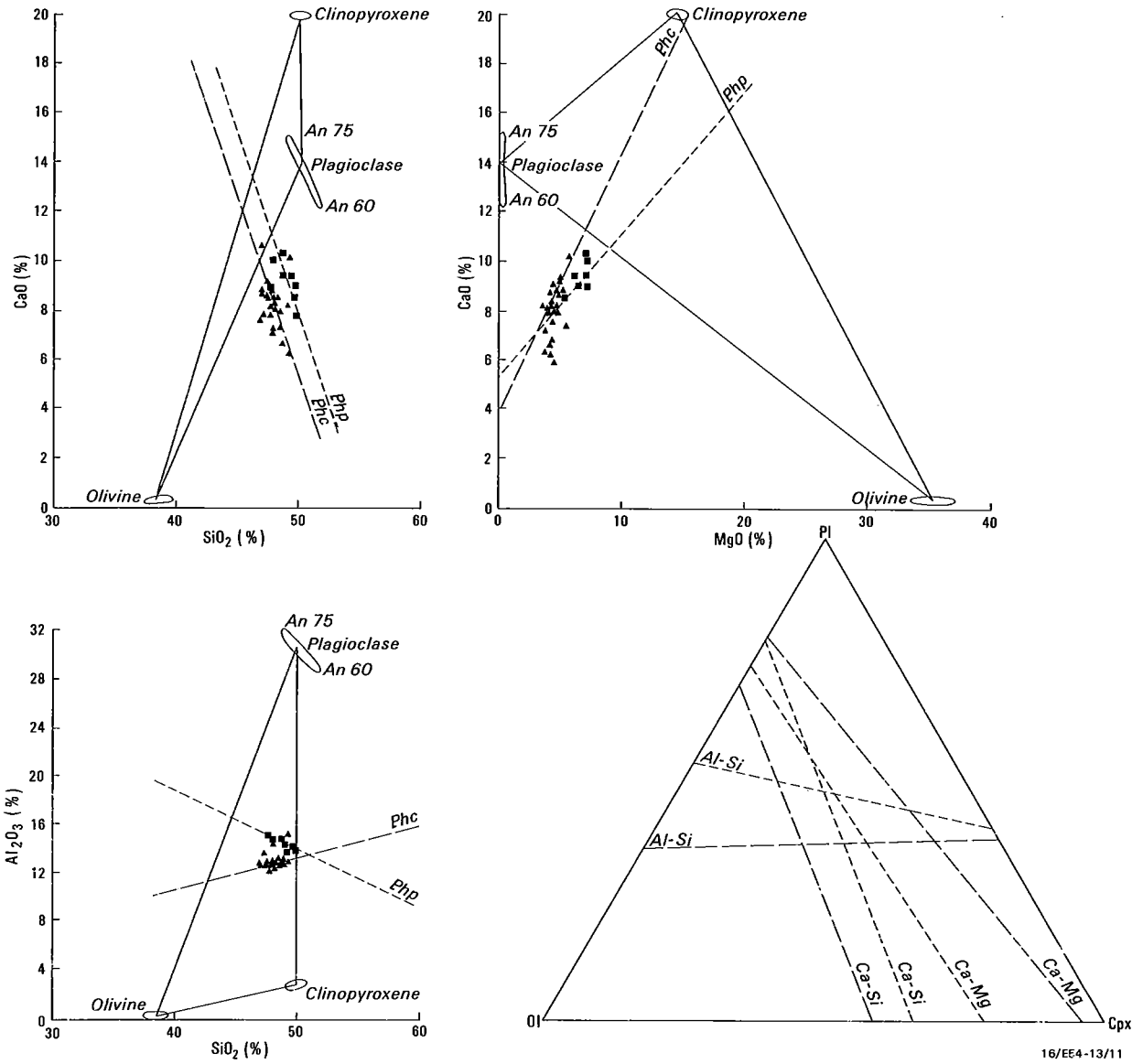

Figure 6. Plots of CaO: SiO_2, CaO: MgO, and Al_2O_3 : SiO_2 variation trends for the Pickwick Metabasalt and Cromwell Metabasalt Members shown in relation to the assumed compositions of plagioclase, clinopyroxene, and olivine.

If these minerals crystallised and separated from the magma to cause the observed trends, then the composition of the average extracts must lie on the trend, within the triangle. These three trends for each member are transformed into an equilateral triangle to define the composition of the extract.

The relatively low MgO content of the predicted extract from the Pickwick Metabasalt Member (about 15 per cent) and the Cromwell Metabasalt Member (probably about 9 per cent) places maximum limits on the MgO contents of the 'primitive' magmas from which these extracts could be derived. These levels of MgO are considerably less than values of about 20 per cent postulated for primary tholeiitic magmas (Green & others, 1979; Elthon, 1979; Cox, 1980). Fractionation of less than 20 per cent of olivine early in the crystallisation history of the magma could reduce MgO to these levels, but the absence of less fractionated specimens prevents testing of this model (Wilson, 1982).

A plot of 19 incompatible-element contents in 5 specimens of the Eastern Creek Volcanics, normalised to the primitive mantle composition (Tarney & others, 1980), is presented in Figure 7. The extreme depletion of Sr could be due to concentration in plagioclase (D^{Sr} = 1.83, Hanson, 1977) that has been fractionated from the magma. The Sr depletion is greater for specimens of the Cromwell Metabasalt Member than the Pickwick Metabasalt Member. The depletion could result from alteration.

The depletion of Eu is probably due to plagioclase fractionation and it is unlikely that the Eu content has been affected by metamorphism. The depletion of Ti suggests fractionation of an opaque phase such as titaniferous magnetite or ilmenite, but extraction of this phase cannot have been as rapid as other phases, because the absolute amount of Ti increases in the lower part of the Cromwell Metabasalt Member and in the Pickwick Metabasalt Member. High but uniform concentrations of the incompatible elements (Ce, Nb, Y, and Zr) in the upper part of the Cromwell Metabasalt Member (Fig. 4, Table 1) indicate a large but constant amount of fractional crystallisation, approaching double the amount involved in forming the remainder of the volcanics.

The behaviour of Cu during the fractional crystallisation is of particular interest in this study. Copper behaved as an incompatible element during the fractionation of the Pickwick Metabasalt Member and the basal part of the Cromwell Metabasalt Member (Fig. 4). The tendency for both Cu and S to increase in later differentiates is consistent with the existence of an immiscible sulphide phase. The sulphides

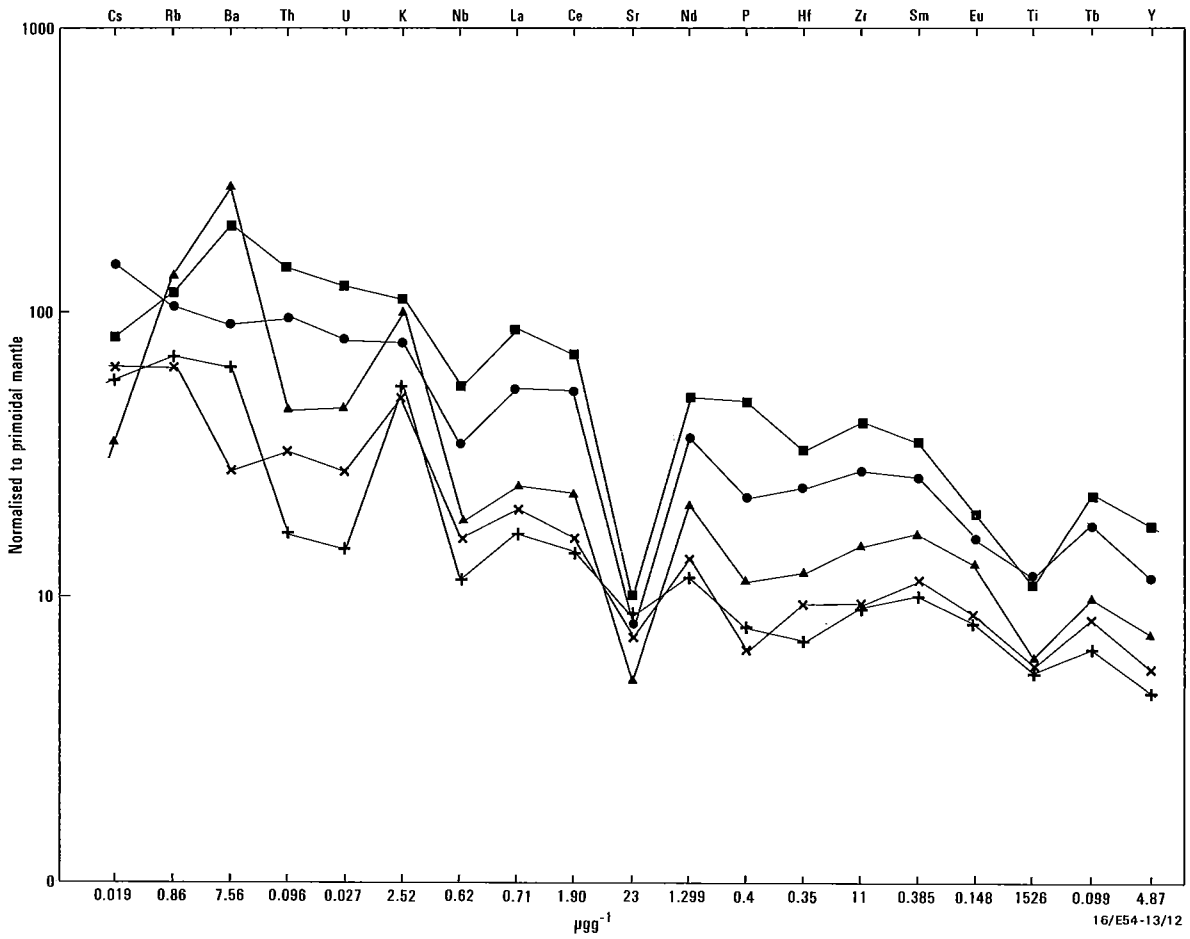

Figure 7. Plot of incompatible element concentrations normalised to the assumed primoidal mantle of Tarney & others (1980).

Table 1. Analyses of Cromwell Metabasalt Member and Pickwick Metabasalt Member

	Cromwell Metabasalt Member								*Pickwick Metabasalt Member*							
	Unaltered specimens, Gunpowder section				*Anomalous specimens Gunpowder section*	*Type section Glikson & Derrick, 1978*	*Crystallena Block Smith & Walker, 1971*	*Basement greenstone MIM Smith & Walker, 1971*	*Unaltered specimens, Gunpowder section*				*Mammoth mine area Scott & Taylor, 1982*	*Epidote alteration Scott & Taylor, 1982*	*Albite alteration Scott & Taylor, 1982*	*Glikson & Derrick, 1978*
	Max.	*Min.*	*Mean (n=22)*	*Std Dev*	*Mean (11)*	*Mean (15)*	*Mean (2)*	*Mean (3)*	*Max.*	*Min.*	*Mean (n=7)*	*Std Dev*	*Mean (8)*	*Mean (1)*	*Mean (1)*	*Mean (4)*
SiO_2	49.22	46.91	47.93	0.62	47.48	48.23	46.17	52.76	49.73	47.58	48.81	0.80	53.5	46.3	42.7	50.5
TiO_2	3.30	2.21	3.00	0.30	3.03	2.24	2.10	1.53	1.59	1.22	1.40	0.11	1.71	2.15	2.24	1.50
Al_2O_3	14.45	12.21	12.87	0.48	13.05	13.41	14.61	13.45	15.24	13.70	14.46	0.52	16.3	15.0	14.6	13.8
Fe_2O_3	5.91	2.62	4.55	0.99	6.46	5.76	2.99	3.37	4.02	2.63	3.30	0.45	0.97*	3.82*	3.55*	4.02
FeO	12.04	9.89	10.96	0.71	9.56	8.41	7.58	8.52	9.33	7.37	8.35	0.84	2.46*	9.66*	9.00*	8.29
MnO	0.31	0.20	0.25	0.03	0.26	0.20	0.04	0.09	0.22	0.14	0.18	0.03	0.15	0.16	0.20	0.20
MgO	5.47	3.65	4.46	4.41	4.29	5.79	16.58	11.52	7.22	5.33	6.72	0.72	4.02	2.02	4.35	6.35
CaO	9.08	6.27	8.04	0.72	6.73	7.69	0.39	0.30	10.31	8.54	9.39	0.62	3.99	17.2	8.49	8.00
Na_2O	2.56	1.52	1.91	0.29	2.65	2.99	0.00	0.90	2.93	1.76	2.13	0.38	0.08	<0.01	1.94	2.78
K_2O	2.52	0.83	1.97	0.36	1.65	0.98	0.21	0.29	2.17	0.99	1.52	0.36	9.40	0.19	0.74	1.89
P_2O_5	0.53	0.22	0.44	0.07	0.55	0.40	0.28	0.22	0.17	0.12	0.15	0.02	0.22	0.38	0.32	0.18
H_2O+	3.16	1.99	2.43	0.33	2.78	3.14			3.02	2.41	2.64	0.22	2.41	2.34	4.28	1.59
SO_3	0.38	0.04	0.13	0.09	0.14	<0.01			0.05	0.01	0.02	0.02	<0.02	<0.02	0.04	<0.01
CO_2	0.15	≤0.05	0.06	0.05	0.74	0.92			0.10	<0.05	0.05	0.04	5.98	0.20	6.67	0.11
Ba	660	260	410	99	505	202	16	23	480	110	264	131	600	58	210	384
Ce	120	40	89	20	100				70	27	47	17				
Co	55	40	47	4	46		23	26	60	45	51	5	12	25	25	
Cr	100	40	59	16	62	100			250	35	22	83	18	40	40	78
Cu	340	25	229	67	180	116	10	25	360	40	151	130	8 (5-15)	100	100	164
La	70	10	29	15	36		50	50*	40	12	21	12				
Nb	22	10	17	3	19				9	4	6	2				
Ni	60	35	45	9	36	78	83	55	140	50	94	34	21	20	25	83
Pb	34	6	13	7	16	40	<50	<50	9	2	5	3	<30			30
Rb	150	24	81	28	62	19			70	28	54	15	290	<2	9	48
Sc						38	51	41					66	15	15	38
Sr	220	100	141	29	166	197	5	7	270	130	176	46	11	1270	74	183
Th	16	<4	10	4	8				12	2	5	4				
U	8	1	4	2	3				6	<1	cl					
V	420	220	340	52	290	286	211	217	330	220	271	43	300	150	100	294
Y	60	32	51	7	55	50	64	60	28	20	23	3	20	32	33	35
Zn	190	85	153	30	162	115	28	70	130	65	103	23	160	40	100	75
Zr	320	150	276	40	298	270	331	414	150	90	108	20	140	170	190	151

* Estimated

are seen as intergranular blebs and have been reported in vesicles. As a result of extensive fractional crystallisation, the unaltered Eastern Creek Volcanics (Fig. 8) contain 2 to 4 times more Cu than the worldwide basalt average of 87 ppm (Turekian & Wedepohl, 1961).

In the proposed model the primary magma resulted from partial melting of the upper mantle. The melt separated from mantle residues and rose to large magma reservoirs, possibly near the base of the crust (Cox, 1980). Crystallisation began in these reservoirs, and olivine, in particular, settled out. Further crystallisation and separation of olivine, plagioclase, and pyroxene occurred during the rise of magma batches through the crust. The earliest lavas also show evidence of contamination with felsic material, probably from older crust surrounding either the magma chamber or the fractures through which the magma rose. Chilling of mafic magma adjacent to this crustal material appears to have prevented contamination of subsequent magma batches.

The uniformity of most of the Cromwell Metabasalt Member indicates that the composition in the magma chamber did not vary significantly during these eruptions and that the fractionation from each successive batch of rising magma was very similar. The few feldspar-phyric lava flows in this member may represent magma batches that rose more quickly than the others, not allowing separation of the plagioclase crystals, which are only slightly more dense than the magma (Krishnamurthy & Cox, 1977).

During a period of quiescence the Lena Quartzite Member was deposited and the magma chamber was evidently refilled with unfractionated magma. This magma was subsequently extruded rapidly, some explosively as tuff. The tuff and associated magma in the Pickwick Metabasalt Member generally retain more primitive compositions. Progressive depletion of MgO, Cr, and Ni is related to relatively higher rates of extraction of ferromagnesian minerals from these more primitive magmas, and produced trends similar to those at the beginning of the Cromwell Metabasalt Member.

Relation to copper mineralisation

It has been shown that unaltered Eastern Creek Volcanics are rich in Cu and that some types of alteration, notably K_2O, MgO and CO_2 enrichment, have been associated with removal of almost all Cu from the basalt. If suitably large amounts of Cu can be liberated in this manner, transported in a hydrothermal fluid, and subsequently precipitated, a mechanism then exists for the formation of large copper orebodies such as at Mount Isa.

The Native Bee–Jasper area, 10 km south of Mount Isa, illustrates the greenstone alteration described previously. Unpublished work by one of us (Perkin, 1968) described intense chlorite (magnesian) and albitic alteration in greenstone of the Eastern Creek Volcanics, and talc-chlorite-phlogopite- carbonate alteration in overlying dolomitic sediments of the Mount Isa Group (Native Bee Siltstone).

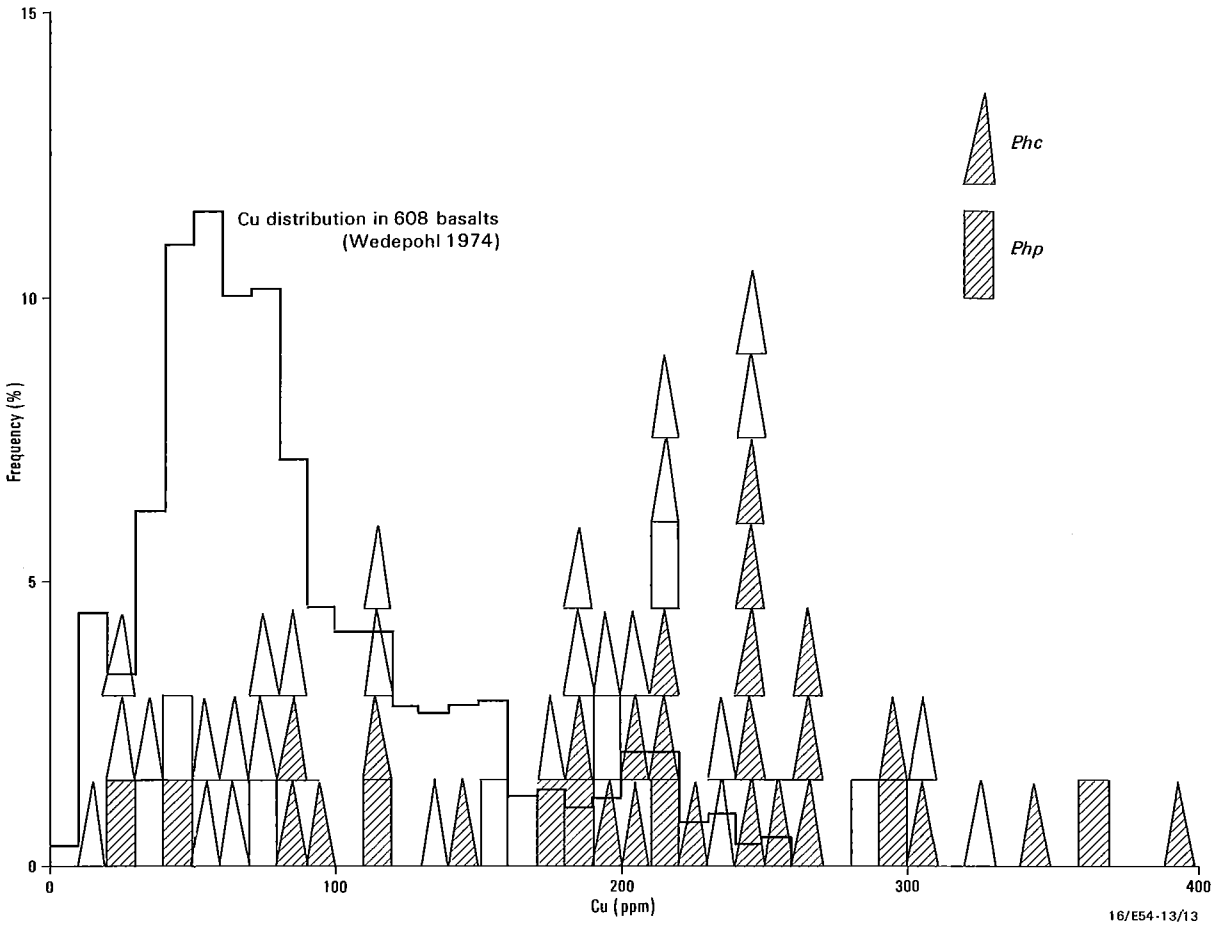

Figure 8. Distribution of copper in the Mammoth Mines section of the Eastern Creek Volcanics compared to the worldwide distribution of Wedepohl (1974).
Hollow symbols indicate altered specimens.

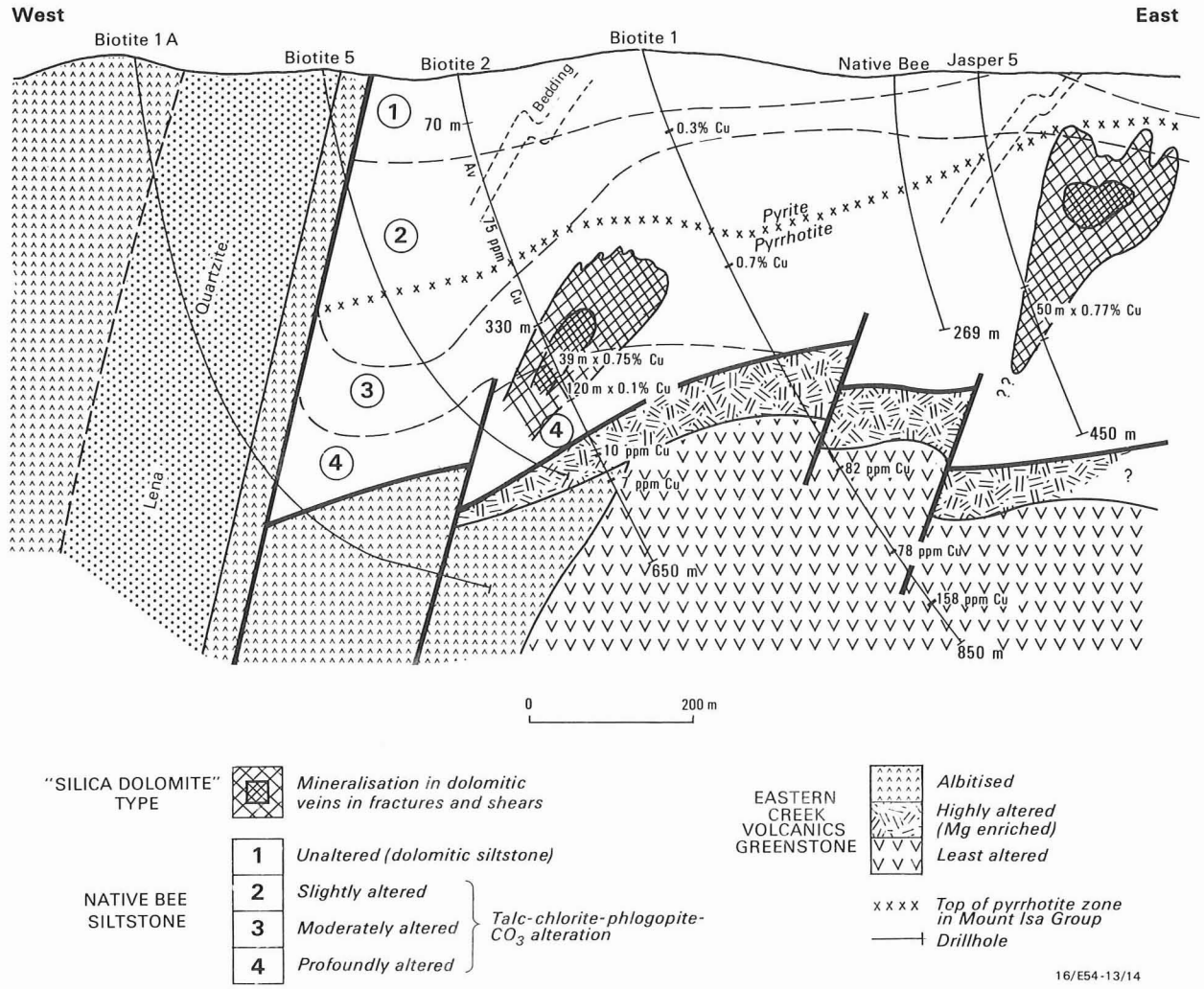

Figure 9. Diagrammatic cross-section and drill hole data near the southern boundary of the Crystallena Block.
A complex, shallow-dipping fault zone separates Native Bee Siltstone (Mount Isa Group) from Eastern Creek Volcanics. The fault transects bedding in Mount Isa Group. Both units display alteration assemblages in zones sub-parallel to the fault, and low-grade silica dolomite Cu mineralisation is structurally controlled.

Drilling in this area has established that the contact between greenstone and Native Bee Siltstone is a steep west-dipping fault to the west and a flat-lying to shallow south-dipping basement fault to the east (Fig. 9). Moreover, it is evident that a gross alteration zoning is present roughly parallel to the latter fault zone, the degree of magnesia and hydrous alteration decreasing away from the fault zone (Fig. 9). Pyrite in sediments is also apparently replaced by pyrrhotite above and near the fault zone. Typically, the greenstone shows extreme depletion of copper, from about 150 ppm Cu to 10 ppm or less associated with intense alteration in a transgressive zone of substantial thickness immediately below the flat-lying basement fault.

Subeconomic copper mineralisation (up to 1 Mt of 1% Cu) occurs in altered Native Bee Siltstone, in irregular dolomitic and quartz-filled shears and veins inclined to bedding (Lord, 1973). This silica-dolomite style of mineralisation, the fault juxtaposition of Mount Isa Group rocks and greenstone, and copper depletion of the latter are all directly analogous (except for tonnage and grade) with mineralisation at the Mount Isa mine itself.

The fact that alteration and mineralisation are transgressive and post-date the one or more deformations that produced near-vertical bedding in the Mount Isa Group clearly shows the copper mineralisation to be younger than Mount Isa Group deposition, and hence younger than the syngenetic or diagenetic lead-zinc mineralisation also present at the Mount Isa mine. The alteration zoning apparent in the Native Bee–Jasper area south of Mount Isa also shows that ingress of mineralising fluids was largely along fault zones (especially shallow thrust faults); fluid over-pressure in such areas may have induced hydraulic fracturing in much of the overlying sediments, which, coupled with chemical and metasomatic alteration, led to the deposition of copper mineralisation.

Whether all the copper in the Native Bee–Jasper area and at the Mount Isa mine was derived by leaching only from greenstone remains problematical. Gulson & others (1983) have shown from lead isotope measurements that only the smaller Cu orebodies at the Mount Isa mine have calculated Th/U ratios similar to those of the Eastern Creek Volcanics.

The larger orebodies have lower ratios and are inferred to have been derived from a different source, for example acid porphyries in deep basement areas. However, this conclusion does not follow if Th and U were not leached in the same proportions or if contamination occurred by lead leached from other rocks, such as the Mount Isa Group shales.

Conclusions

The Eastern Creek Volcanics are subalkaline continental tholeiites that have undergone various alteration effects mainly during greenschist facies metamorphism. The lowermost basalt member displays moderate fractionation trends, consistent with extraction of olivine, plagioclase, and clinopyroxene during crystallisation in large mantle-derived magma reservoirs near the base of the crust. The youngest basalt member contains the most primitive, least fractionated magma types.

At least 5 alteration enrichment types — Ca, Na, CO_2, K, and Mg — can be recognised. The copper content of less-altered basalts (200 ppm) is at least twice the world average for basalts, but copper is significantly depleted in basalts enriched in K_2O, MgO, CO_2, H_2O^+, and Fe_2O_3.

Such widespread alteration probably liberated vast quantities of copper from the greenstones, and transported it along faults and permeable beds, while reactive carbonate and sulphide lithologies may have been a major factor in its redeposition. These largely epigenetic, post-depositional processes attain their most notable development within and adjacent to the Mount Isa copper orebodies, but also appear to have operated in the Native Bee—Jasper area to the south.

Acknowledgement

The figures were drafted by M. Steele.

References

Bennett, E.M., 1965 — Lead-zinc-silver and copper ore deposits of Mount Isa. *In* McAndrews, J., (Editor), Geology of Australian ore deposits (2nd edition), *8th Commonwealth Mining and Metallurgical Congress*, 1, 233–246.

Beswick, A.E. & Soucie, G., 1978 — A correction procedure for metasomatism in an Archaean greenstone belt. *Precambrian Research*, 6,235–248.

Bryan, W.B., Finger, L.W., & Chayes, F., 1969 — Estimating proportions in petrographic mixing equations by least-squares approximation. *Science*, 163, 926–927.

Carter, E.K., Brooks, J.H., & Walker, K.R., 1961 — The Precambrian mineral belt of north-western Queensland. *Bureau of Mineral Resources, Australia, Bulletin* 51.

Chayes, F., 1964 — A petrographic distinction between Cainozoic volcanics in and around the open oceans. *Journal of Geophysical Research*, 69, 1573–1588.

Cordwell, K.S., Wilson, G.K., & Lord, J.H., 1963 — Geology of the area south of Mount Isa and its application to the structural control of the Mount Isa orebodies. *Australasian Institute of Mining and Metallurgy, Proceedings*, 206, 29–62.

Cox, K.G., 1980 — A model for flood basalt volcanism. *Journal of Petrology*, 21, 629–650.

Cox, K.G., Bell, J.D., & Pankhurst, R.J., 1979 — The interpretation of igneous rocks. *Allen & Unwin, London.*

Derrick, G.M., 1982 - A Proterozoic rift zone at Mount Isa, Queensland, and implications for mineralisation. *BMR Journal of Australian Geology & Geophysics*, 7, 81–82.

Derrick, G.M., Wilson, I.H., & Hill, R.M., 1976a — Revision of stratigraphic nomenclature in the Precambrian of Northwestern Queensland. II: Haslingden Group. *Queensland Government Mining Journal*, 77, 300–306.

Derrick, G.M., Wilson, I.H, & Hill, R.M., 1976b — Revision of stratigraphic nomenclature in the Precambrian of Northwestern Queensland. III: Mount Isa Group. *Queensland Government Mining Journal*, 77, 402–405.

Elthon, D., 1979 — High magnesia liquids as the parental magma for ocean floor basalt. *Nature*, 278, 514—518.

Finlow-Bates, T., & Large, D.E., 1978 — Water depth as major control on the formation of submarine exhalative ore deposits. *Geologisches Jahrbuch*, D30, 27–39.

Finlow-Bates, T., & Stumpel, E.F., 1979 — The copper and lead-zinc-silver orebodies of Mt Isa mine, Queensland: products of one hydrothermal system. *Annales de la Societe Geologique de Belgique*, T102, 497–517.

Fisher, N.H., 1960 — Review of the evidence and genesis of Mount Isa orebodies. *21st International Geological Congress, Norden*, 16, 99–111.

Glikson, A.Y., & Derrick, G.M., 1978 — Geology and geochemistry of Middle Proterozoic basic volcanic belts, Mount Isa/Cloncurry, northwestern Queensland. *Bureau of Mineral Resources, Australia, Record* 1978/48.

Glikson, A.Y., Derrick, G.M., Wilson, I.H., & Hill, R.M., 1976 — Tectonic evolution and crustal setting of the Middle Proterozoic Leichhardt River fault trough, Mt Isa area, northwestern Queensland. *BMR Journal of Australian Geology & Geophysics*, 1, 115–129.

Green, D.H., Hibberson, W.O., & Jaques, A.L., 1979 — Petrogenesis of midocean ridge basalts. *In* McElhinny, M.W., (Editor), The Earth: its origin, structure and evolution. *Academic Press, London*, 265–299.

Gulson, B.L., Perkins, W.G., & Mizon, K.J., 1983 — Lead isotope studies bearing on the genesis of copper ore bodies at Mount Isa, Queensland. *Economic Geology*, 78, 1466–1504.

Hanson, G.N., 1977 — Geochemical evolution of the suboceanic mantle. *Journal of the Geological Society, London*, 134, 235–253.

Krishnamurthy, P., & Cox, K.G., 1977 — Picrite basalts and related lavas from the Deccan Traps of Western India. *Contributions to Mineralogy and Petrology*, 62, 53–75.

Krishnamurthy, P., & Cox, K.G., 1980 — A potassium-rich alkalic suite from the Deccan Traps, Rajpipla, India. *Contributions to Mineralogy and Petrology*, 73, 179–189.

Lindstrom, M.M., & Haskins, L.A., 1981 — Compositional inhomogeneities in a single Icelandic tholeiitic flow. *Geochemica et Cosmochimica Acta*, 45, 15–31.

Lord, J.R., 1973 — Surface and subsurface geochemistry of the Native Bee-Jasper-Biotite copper prospects, northwest Queensland. *Journal of Geochemical Exploration*, 2, 349–365.

Mathias, B.V., & Clark, G.J., 1975 — Mount Isa copper and silver-lead-zinc orebodies - Isa and Hilton mines. *In* Knight, C.L., (Editor), Economic geology of Australia and Papua New Guinea, Volume 1 — Metals. *Australasian Institute of Mining and Metallurgy, Monograph* 5, 351–372.

Page, R.W., 1980 — Mount Isa Inlier. *In* Geological branch annual summary of activities, 1980. *Bureau of Mineral Resources, Australia, Report* 230, 127–128.

Page, R.W., 1981 — Depositional ages of the stratiform base metal deposits at Mount Isa and McArthur River, Australia, based on U-Pb zircon dating of concordant tuff horizons. *Economic Geology*, 76, 648–658.

Page, R.W., Bower, M.J., Zapasnik, T.K., Guy, D.B., & Hyett, N.C., 1982 — Mount Isa Project (Geochronological Laboratory). *In* Geological branch annual summary of activities. *Bureau of Mineral Resources, Australia, Report* 239, 138–141.

Pearce, J.A., 1976 — Statistical analysis of major element patterns in basalts. *Journal of Petrology*, 17, 15–43.

Pearce, J.A., & Cann, J.R., 1973 — Tectonic setting of basic volcanic rocks determined using trace element analysis. *Earth and Planetary Science Letters*, 19, 290–300.

Perkin, D.J., 1968 — An assessment of exploration in the Biotite, Jasper and Native Bee areas. *Mount Isa Mines Ltd, Technical Report*, GEO-105 (unpublished).

Perkins, W.G., 1981 — Mount Isa copper orebodies — evidence against a sedimentary origin (abstract). *BMR Journal of Australian Geology & Geophysics*, 6, 331.

Perkins, W.G., 1984 — Mount Isa silica dolomite and copper orebodies: the result of a syntectonic hydrothermal alteration system. *Economic Geology*, 79, 601–637.

Plimer, I.R., 1978 — Proximal and distal stratabound ore deposits. *Mineralium Deposita*, 13, 345–353.

Rittmann, A., 1957 — On the serial character of igneous rocks. *Egyptian Journal of Geology*, 1, 23–48.

Robertson, C.W., 1982 — The role of pre-existing sulphides and sulphates in primary copper orebody formation at Mount Isa. *BMR Journal of Australian Geology & Geophysics*, 7, 119–124.

Robinson, W.B., 1968 — Geology of the Eastern Creek Volcanics in the Mount Isa district (with discussion). *Australasian Institute of Mining and Metallurgy, Proceedings*, 226, 89–96.

Scott, K.M., & Taylor, G.F., 1982 — Eastern Creek Volcanics as the source of copper at the Mammoth mine, northwest Queensland. *BMR Journal of Australian Geology & Geophysics*, 7, 93–98.

Smith, S.E., & Walker, K.R., 1970 — Mount Isa Geochemical Project - analysis of core samples. *Bureau of Mineral Resources, Australia, Record* 1970/47.

Smith, S.E., & Walker, K.R., 1971 - Primary element dispersions associated with mineralisation at Mount Isa, Queensland. *Bureau of Mineral Resources, Australia, Bulletin* 131.

Solomon, P.J., 1965 — Investigations into sulphide mineralisation at Mount Isa, Queensland. *Economic Geology*, 60, 737–765.

Stanton, R.L., 1972 — Ore petrology. *McGraw-Hill, New York, Sydney.*

Swager, C.P., 1983 — Microstructural development of the silica-dolomite and copper mineralization at Mt Isa, NW Queensland, with special emphasis on the timing and mechanism of mineralization. *Ph.D. Thesis, James Cook University of North Queensland.*

Tarney, J., Wood, D.A., Saunders, A.D., Cann, J.R., & Varet, J., 1980 — Nature of mantle heterogeneity in the North Atlantic: evidence from deep sea drilling. *Philosophical Transactions of the Royal Society of London, Series A*, 297, 179–202.

Taylor, S.R., 1979 — Geochemical constraints on planetary compositions. *Inter-disciplinary Symposia, Abstracts and Timetable, International Union of Geodesy and Geophysics, XVII General Assembly, Canberra, Australia, 3-15 December, 1979.* p. 212.

Turekian, K.K., & Wedepohl, K.H., 1961 — Distribution of the elements in some units of the Earth's crust. *Geological Society of America, Bulletin*, 72, 175–191.

Wedepohl, K.H., 1974 — Handbook of geochemistry, II-3, 29-B-1 to 29-0-1. *Springer-Verlag, Berlin.*

Williams, N., 1980 — Precambrian mineralisation in the McArthur—Cloncurry region with special reference to stratiform lead-zinc deposits. *In* R.A. Henderson, R.A., & Stephenson, P.J., (Editors), Geology & geophysics of northeastern Australia. *Geological Society of Australia, Queensland* Division, 89–107.

Wilson, I.H., 1982 — Petrology and geochemistry of selected Proterozoic volcanics from the Mount Isa Inlier. *Ph.D. Thesis, University of Queensland.*

Winchester, J.A., & Floyd, P.A., 1977 — Geochemical discrimination of different magma series and their differentiation products using immobile elements. *Chemical Geology*, 20, 325–343.

BMR Journal of Australian Geology & Geophysics, 9, 329-338

Relationship of the Maloney Creek Inlier to other elements of the western Lawn Hill Platform Cover, northern Australia

I.P. Sweet[1]

The Maloney Creek Inlier is recognised as an element of the Proterozoic Lawn Hill Platform Cover. The Musselbrook Formation in the inlier is dominated by high-energy fluvial facies, probably braided stream or alluvial fan deposits. The overlying Lawn Hill Formation is finer grained over all, but nevertheless contains a significant coarse clastic component of similar composition to the underlying Musselbrook Formation. The Lawn Hill Formation can be divided into 5 lithofacies, which are interpreted in terms of alluvial fan deposition, either subaerial or subaqueous. Correlation of the Maloney Creek Inlier sequence with that in the Carrara Range region and other isolated outcrops of the western Lawn Hill Platform Cover has allowed an interpretation of the tectonic development of the cover. An initial tensional tectonic regime led to extrusion of bimodal volcanics and the development of a faulted margin on at least the northern side of the basin. During periods of faulting, coarse clastics were shed into the basin; carbonate environments predominated during quiet periods. The final phase of development of the platform cover was the development and filling of the Ploughed Mountain Trough, which was a deep-water basin in the east, but was dominated by shallow-water fan deltas or subaerial fans in the west.

Introduction

The Lawn Hill Platform Cover is a thick, slightly to moderately deformed, volcanic and sedimentary rock sequence, laid down west and northwest of the Mount Isa Orogen during the Middle Proterozoic, between 1680 Ma and about 1600 Ma. On the basis of work in the eastern part of the platform, Hutton & Sweet (1982) traced the evolution of the platform cover from an early episode of fluvial sedimentation and extrusion of potash-rich lavas (Bigie Formation, Fiery Creek Volcanics, and correlatives), through mixed fluvial and marine sedimentation (Surprise Creek Formation), to a protracted period of mainly marine deposition (McNamara Group).

In the west of the Lawn Hill Platform, the Maloney Creek Inlier (Fig. 1), which has not previously been recognised as a component of the Lawn Hill Platform Cover, contains a stratigraphic sequence significantly different from that in the Lawn Hill area to the east (Hutton & Sweet, 1982), and is seen as critical in any synthesis of the development of the Lawn Hill Platform as a whole In this paper, the sedimentary and tectonic development of the western Lawn Hill Platform is examined using data from the Maloney Creek Inlier with that from the Carrara Range region (Sweet, 1984), Seigal—Hedleys Creek region (Sweet & others, 1981), and the Benmara and Bauhinia Dome areas (unpublished data collected by J.W. Smith and H.G. Roberts, and summarised by Smith & Roberts, 1963, and Roberts & others, 1963).

Maloney Creek Inlier

The Maloney Creek Inlier, which occupies an area of about 150 km² north of the Carrara Range (Fig. 1), provides the key to the interpretation of the western Lawn Hill Platform. It was first mapped by Smith & Roberts (1963), who recognised only one unit, the Maloney Creek Formation, which they interpreted as a basal conglomeratic facies of the South Nicholson Group. Remapping in 1982 showed that the inlier comprises two formations of the McNamara Group, and is overlain unconformably by the basal formation of the South Nicholson Group, the Constance Sandstone (Fig. 2). The older unit, the Musselbrook Formation, is at least 900 m thick in the east of the inlier. Its base is faulted in some areas and not exposed in others. It is overlain by the Lawn Hill Formation, which has a maximum thickness of about 700 m in the north of the inlier. Thus, a minimum of about 1600 m of McNamara Group is preserved in the eastern part of the inlier, if it is assumed that the Lawn Hill Formation is of uniform thickness.

[1] Division of Continental Geology, BMR

Musselbrook Formation

The Musselbrook Formation has been subdivided into a lower sandstone-rich member and an upper conglomerate member (Fig. 2). The lower member (Pmb_s) is characterised by interbedded fine to medium, pink sandstone, gritty sandstone, and fine pebble (clasts < 1 cm) conglomerate. Plane bedding,

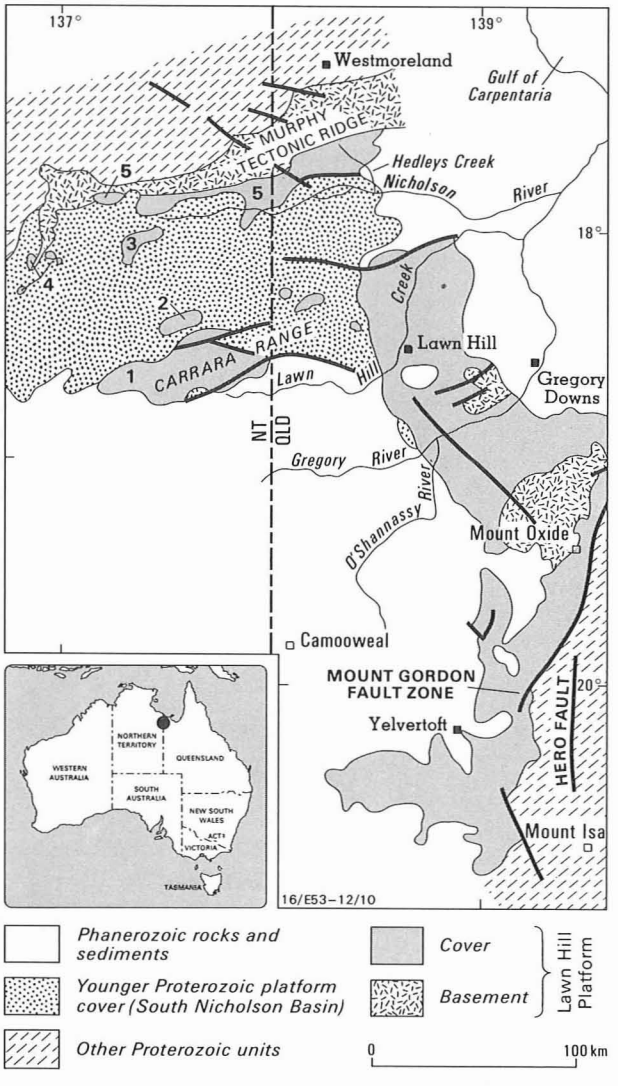

Figure 1. Geological outline of the Lawn Hill Platform.
Western outcrops are: (1) Carrara Range region; (2) Maloney Creek Inlier; (3) Bauhinia Dome; (4) four isolated outcrops of Benmara beds; (5) Seigal—Hedleys Creek region.

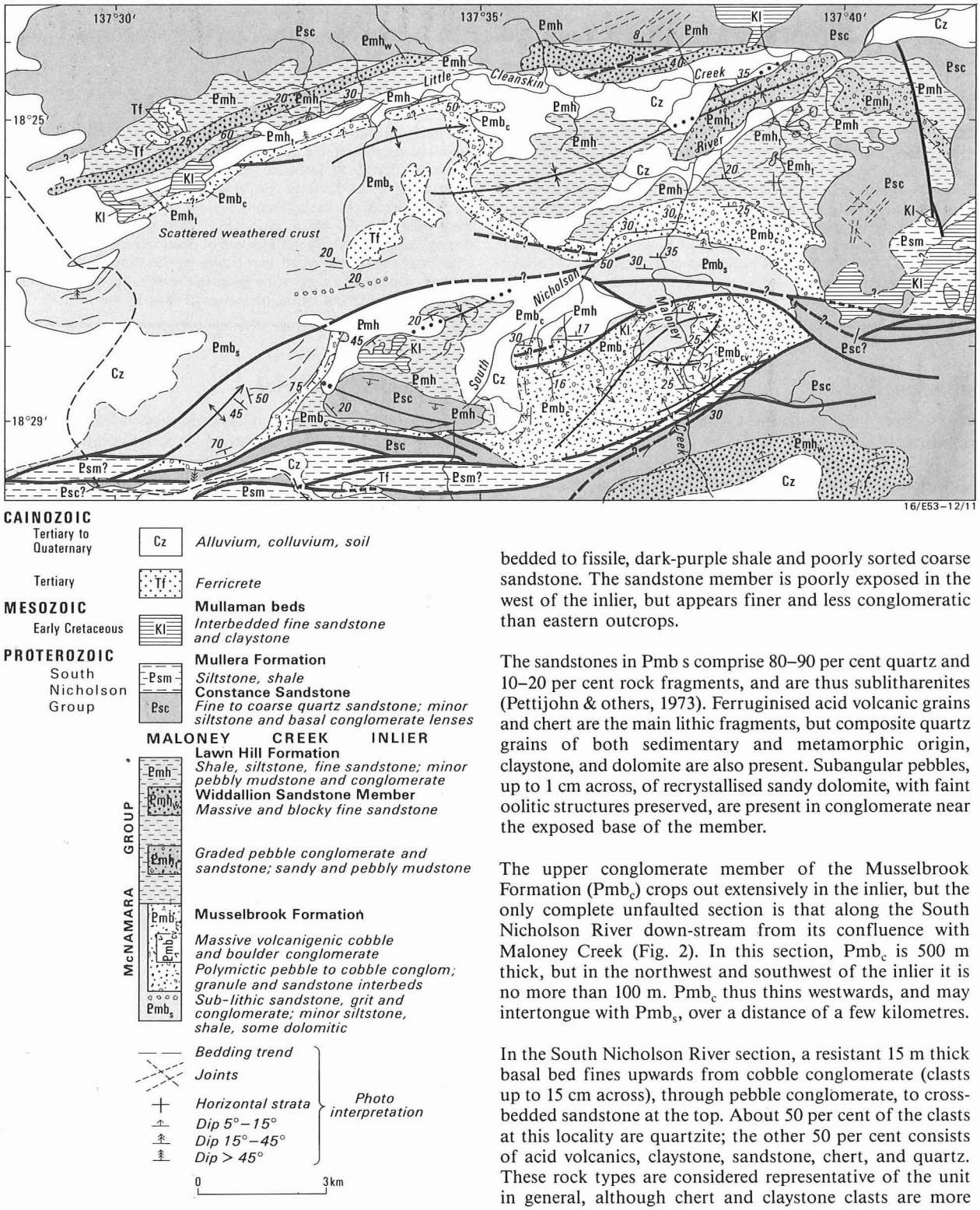

Figure 2. Geology of the Maloney Creek Inlier.
Area east of 137° 30′ lies in the Cleanskin 1:100 000 Sheet area; that to the west is in Benmara 1:100 000 Sheet area.

trough cross- bedding on a medium scale, and mudflakes are ubiquitous, and current ripples ar common; wave ripples were seen at only one place. The oldest beds exposed consist of interbedded, mudflake-rich, gritty and pebbly sandstone and mudstone arranged in fining-up cycles, 20 cm to 1 m thick (Fig. 3). Pink to brown, fine to medium sandstone, which dominates the member in the north, is overlain by thin-bedded to fissile, dark-purple shale and poorly sorted coarse sandstone. The sandstone member is poorly exposed in the west of the inlier, but appears finer and less conglomeratic than eastern outcrops.

The sandstones in Pmb s comprise 80–90 per cent quartz and 10–20 per cent rock fragments, and are thus sublitharenites (Pettijohn & others, 1973). Ferruginised acid volcanic grains and chert are the main lithic fragments, but composite quartz grains of both sedimentary and metamorphic origin, claystone, and dolomite are also present. Subangular pebbles, up to 1 cm across, of recrystallised sandy dolomite, with faint oolitic structures preserved, are present in conglomerate near the exposed base of the member.

The upper conglomerate member of the Musselbrook Formation (Pmb_c) crops out extensively in the inlier, but the only complete unfaulted section is that along the South Nicholson River down-stream from its confluence with Maloney Creek (Fig. 2). In this section, Pmb_c is 500 m thick, but in the northwest and southwest of the inlier it is no more than 100 m. Pmb_c thus thins westwards, and may intertongue with Pmb_s, over a distance of a few kilometres.

In the South Nicholson River section, a resistant 15 m thick basal bed fines upwards from cobble conglomerate (clasts up to 15 cm across), through pebble conglomerate, to cross-bedded sandstone at the top. About 50 per cent of the clasts at this locality are quartzite; the other 50 per cent consists of acid volcanics, claystone, sandstone, chert, and quartz. These rock types are considered representative of the unit in general, although chert and claystone clasts are more abundant in some other outcrops. The clasts vary from subangular to well rounded, chert and claystone generally being the most angular. Most of the conglomerates have a sand and granule matrix, which forms up to 50 per cent of the bulk of the rock. The beds are generally massive to plane-bedded, and cross-beds and erosionally based beds are rare. A second resistant zone, some 50 m above the basal conglomerate, consists of 20 m of conglomerate and sandstone, which alternate on a 0.5–3 m scale. Conglomerates at the top of Pmb_c, 4 km southwest of the outcrops discussed above, contain clasts up to boulder size. They overlie clast-supported pebble and cobble conglomerates (Fig. 4).

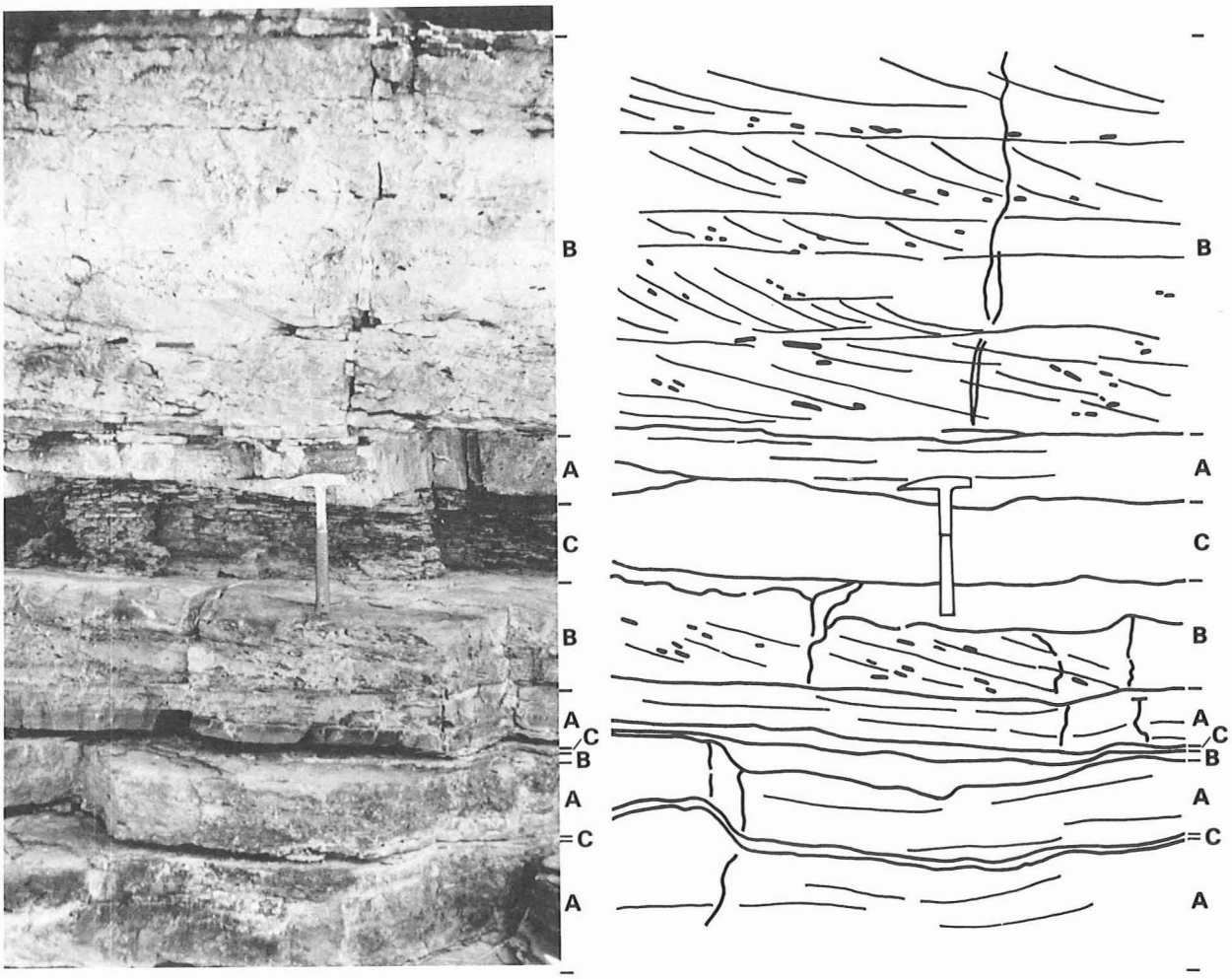

Figure 3. Fining-upwards cycles in the sandstone member of the Musselbrook Formation in Maloney Creek, 3 km south of its confluence with the South Nicholson River.

Plane-bedded (A) and cross-bedded (B) gritty and pebbly sandstone alternates with dark-grey fine siltstone or shale (C); mudflakes are common in the cross-bedded sandstones. The superposition of types A-B-C indicates decreasing energy of the transporting medium, which is consistent with deposition on bars in a small meandering stream.

Volcanic breccia (Pmb_{cv}). This breccia, which Smith & Roberts (1963) tentatively assigned to their Carrara Range Formation (now Carrara Range Group, unconformable beneath the McNamara Group — Sweet, 1982), is clearly a lens within the upper member of the Musselbrook Formation. It comprises poorly sorted subangular to subrounded clasts, up to 1 m across, set in a sparse, medium to coarse, lithic sandstone matrix. Up to 90 per cent of the clasts are vesicular or porphyritic, highly altered, reddish-brown acid volcanics, identical in appearance to the Top Rocky Rhyolite (Sweet, 1984) in the Carrara Range region. The remainder are clasts of white, fine-grained altered volcanics containing amygdales of a bright green mineral, possibly celadonite. Most of the breccia is massive, but vague bedding and a sandy interval visible near the eastern margin of the lens attest to its sedimentary origin. The breccia thins out or grades into normal (sandier and better bedded) Pmb_c on its northern margin.

Interpretation of depositional environments of the Musselbrook Formation

The presence of current ripples, trough cross-beds, and plane bedding, fining-up cycles, and ubiquitous mud flakes in the sandstone member of the Musselbrook Formation suggests deposition in a fluvial, possibly meandering-stream environment, whereas the overlying conglomerate member reflects a much higher-energy environment. Gravelly braided rivers or alluvial fans are most likely, but these two environments can be difficult to distinguish (Collinson, 1978) and no firm conclusion can be reached on the evidence available.

Lawn Hill Formation

The Lawn Hill Formation consists mainly of shale and siltstone. It contains two mappable sandstone members and several interbeds of sandstone and conglomerate (Fig. 2). The lower sandstone member, Pmh_l, has not been named, but the upper one is assigned to the Widdallion Sandstone Member, which is widely recognised in the Lawn Hill Platform (Hutton & others, 1981; Sweet, 1984).

Five main lithofacies are recognised in the Lawn Hill Formation: facies 1, *fine-grained clastics*, consists of grey and brown laminated shale and laminated to thin-bedded siltstone with very fine sandstone interbeds. It makes up most of the formation. Wave and current ripples, mudflakes, and mudcracks (distinguished from subaqueous synaeresis cracks by the criteria of Plummer & Gostin, 1981) were observed in thin interbeds of sandstone below Pmh_l. Facies 2, *cross-bedded sandstone and conglomerate*, is present only below the lower sandstone member, Pmh_l. Fifty metres stratigraphically above the base of the formation, in the northeast,

Figure 4. Pebble and cobble conglomerate in the upper Musselbrook Formation.
The conglomerate has a very high proportion of medium pebbles and coarser clasts set in a matrix of fine pebbles and granules. Most other conglomerate beds in Pmb c contain a higher proportion of sand matrix. Hammer head is 175 mm long.

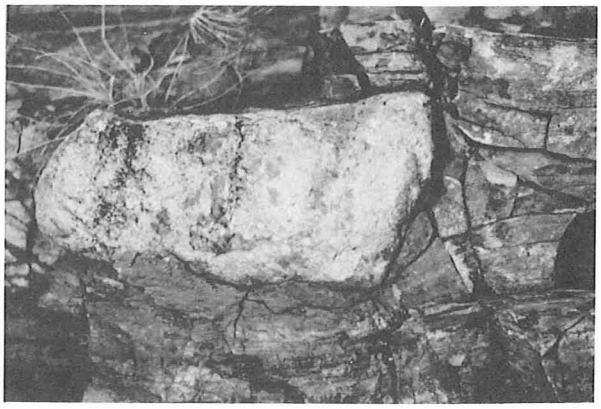

Figure 5. Isolated quartzite boulder from the lower Lawn Hill Formation.
30 cm long, in finely laminated siltstone and shale; 3 km east-northeast of the confluence of the South Nicholson River and Maloney Creek.

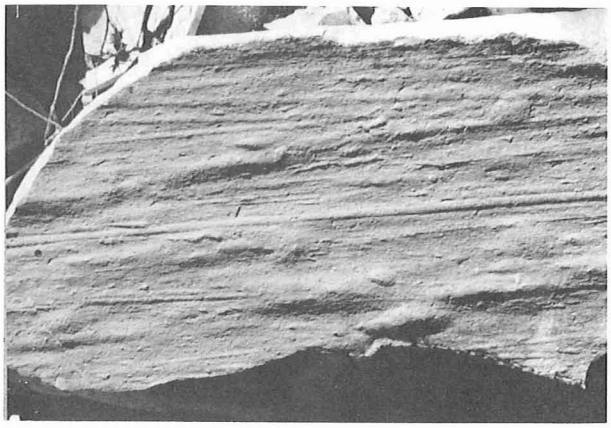

Figure 6. Groove moulds and rare flute moulds on the base of a fallen block of sandstone near outcrops of Pmb_t.
1.8 km north of the confluence of the South Nicholson River and Maloney Creek.

1 m of well-sorted pebble conglomerate (quartzite, chert, and claystone clasts) grades up into 2 m of pebbly to coarse sandstone, which is trough cross-bedded on a 0.5 m scale. Laminated siltstone and shale below this conglomeratic bed contain a single boulder of grey quartzite (Fig. 5), similar to a dropstone.

Unnamed member (Pmh_t). This 50 m sequence consists of facies 3 and 4 interbedded with facies 1. Facies 3 consists of *graded coarse to fine clastics,* in beds 2–50 cm thick. The beds are erosively based, and grade up from fine pebble conglomerate, through sandstone, to laminated shale; large mudflakes occur in the basal parts of beds. One bed, deposited in a channel cut 1 m into the underlying shale, has sole markings that indicate scour by currents to or from 080°. Well-sorted medium sandstone, with flute casts and other sole-markings, crops out at the base of the member (Fig. 6), and is also assigned to facies 3. Facies 4 is exemplified by a 1.5 m *pebbly mudstone* containing an unsorted assemblage of quartzite and other clasts up to 30 cm across, finer pebbles, grit, and sand in a structureless mudstone matrix. Similar thin (10–50 cm) pebbly mudstone beds were observed at several other places, both within and below Pmh_t.

The Widdallion Sandstone Member (Pmh_w), near the top of the Lawn Hill Formation, consists of *massive and blocky, friable fine-grained sandstone* (facies 5). It is mineralogically distinct from the sandstones lower in the sequence, in that it contains no chert, chalcedony, or other identifiable sedimentary rock fragments, but does contain feldspar, which is rare or absent in the older sandstones. Sedimentary structures include linguoid and other current-ripple marks, trough cross-beds, mudflakes, and primary current lineation.

Interpretation of the lithofacies in the Lawn Hill Formation

The rocks of the Lawn Hill Formation represent an abrupt transition to a much lower-energy depositional regime (facies 1) punctuated by episodes of higher-energy deposition (facies 2, 3, and 4). The hydrodynamic implications of the individual lithofacies are: facies 1 — low-energy suspended-sediment deposits and traction-current deposits. The wave-ripple marks indicate that a standing body of water, either a lake or the sea, existed at times. The ripple marks and mud cracks indicate that the water was shallow — no deeper than wave base. Facies 2 — traction-current deposits. The outcrop described is a simple fining-upwards cycle, representing deposition from an aqueous flow of rapidly decreasing energy. Facies 3 — deposited in the upper flow regime from currents that scoured the cohesive muddy substrate before deposition began. The grading indicates waning currents, and is consistent with turbidity-current deposition, resulting in Bouma A–E sequences. The deposits also bear a superficial similarity to graded beds developed on alluvial fans as a result

of single flood events (e.g. Allen, 1981; Hubert & Hyde, 1982). Facies 4 — the massive nature and the matrix support of clasts point to an origin as a 'cohesive debris flow' (Lowe, 1979). Such flows are 'effective transporting agents in both subaerial and subaqueous environments' (Lowe, 1982, p. 293). Facies 5 — traction-current deposits, which could be either fluvial or shallow marine. Further study would be needed for a confident environmental interpretation to be made of this facies, but a report by Sweet & Hutton (1980, p. 50) of possible glauconite in the Widdallion Sandstone Member makes a marine environment more likely.

Depositional environments of the Lawn Hill Formation

The facies interpretations presented above are consistent with deposition either in a non-marine environment, such as an alluvial fan–mudflat/playa lake system, or in a lacustrine or marine environment as a fan delta. Wescott & Ethridge (1980) pointed out that the nature and distribution of facies in fan deltas may be very similar to that in subaerial fans. In either situation the Lawn Hill Formation is interpreted as an indication of a more subdued or distant source, leading to an encroachment of fine-grained facies over the coarse alluvial facies of the Musselbrook Formation. The products of higher-energy events — flood deposits on alluvial fans or the products of gravity flows (turbidites and debris flows) in subaqueous fans — can be very similar (e.g. Heward 1978). The occurrence of a boulder similar to a dropstone does not resolve the question of environment, as isolated megaclasts, similar in appearance to glacial dropstones, have been recorded from both alluvial fan and subaqueous sediments (Conybeare & Crook, 1968, p. 21). A more detailed analysis of sedimentary facies would be required to resolve this question.

Palaeocurrent study. Measurable palaeocurrent indicators are rare, owing to the prevalence of massive or plane beds. Results from a very small sample (Fig. 7) suggest that sediment transport was from the west and southwest.

Clast provenance. The composition of the sandstones and conglomerates in the lower part of the Lawn Hill Formation is similar to those in the Musselbrook Formation, suggesting that both formations were derived from the same source. Quartzite and acid volcanic clasts dominate the coarser fractions, and quartz, chert/chalcedony, and claystone dominate the finer fractions. The acid volcanic clasts, including those in the lens Pmb^{cv} are indentical to the Top Rocky Rhyolite, suggesting that the rhyolite or one of its correlatives was being eroded from the source area. Some of the chert fragments contain vague outlines of oolites. This and the presence of sandy dolomite pebbles in conglomerate indicate that partly silicified carbonate sediments were also present in the terrain being eroded.

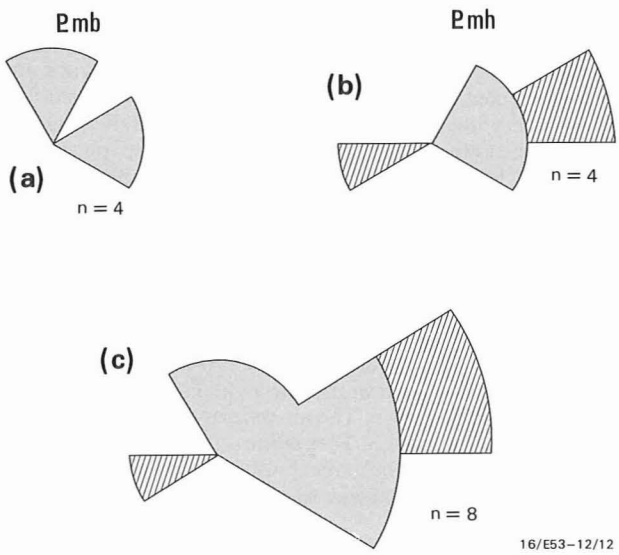

Figure 7. Palaeocurrent roses for the McNamara Group in the Maloney Creek Inlier.
(a) foreset-bedding readings from the upper Musselbrook Formation; (b) foresets and one sole marking (orientationknown, but not direction) from the Lawn Hill Formation; (c) both sets of readings combined, 30° class interval used.

Reassessment of the geology of the Bauhinia Dome

The Bauhinia Dome (Fig. 1) contains about 1100 m of 'cobble to very coarse boulder conglomerate, dolomitic feldspathic sandstone, siltstone, dolomite, and arkosic conglomerate' (Smith & Roberts, 1963, p. 8) assigned to the Fickling beds (now Fickling Group — Sweet, 1981). A replotting of Smith & Roberts's unpublished field observations (Fig. 8) outlines four units (Table 1). The conglomeratic beds of unit 3, in the southwest, appear to grade laterally into unit 2, the poorly sorted, micaceous, gritty to pebbly 'greywacke' (this equates with dolomitic feldspathic sandstone in Smith & Roberts, 1963) that characterises much of the dome. Significant lithological features include the presence of clasts of granite, quartzite, and chert in the conglomerates, mica and feldspar-rich sandstones, and a green mineral, probably glauconite or a clay. With the exception of unit 1, which is probably lower Fickling Group, the rocks in the dome are tentatively assigned to the Doomadgee Formation (Sweet, 1981; Sweet & others 1981), which also contains conglomerates and green clay-rich beds (Sweet & Slater, 1975). Their similarity to the Musselbrook Formation in the Maloney Creek Inlier is also striking. The pink micaceous 'greywackes' are probably equivalent to the lower Musselbrook Formation, and the coarse boulder conglomerates may be equivalent to the upper conglomeratic member of the Musselbrook Formation.

Reassessment of the geology of the Benmara beds

Of four isolated outcrops that constitute the Benmara beds (Smith & Roberts, 1963) (Fig. 1), three contain intermediate

Table 1. Lithology of four informal stratigraphic units recognised in the Fickling Group, Bauhinia Dome.

Unit	*Description*	*Remarks*
4	60—80 m of laminated, crystalline dolomite overlain by cross-bedded, medium, silicified quartz sandstone.	Sandstone interpreted as Constance Sandstone by Smith & Roberts (1963), but could be within Fickling Group.
3	Conglomerate containing cobbles and boulders up to 1.8 m across of silicified quartz sandstone, granite, quartz, dolomite, basalt, and feldspar porphyry in a lithic and feldspathic sandy matrix.	Appears to lens eastwards into unit 2
2	Light-brown to pink micaceous feldspathic, quartz-rich, and rarely calcareous, greywacke; contains green clay (?glauconite) in places; interbeds of grit and fine pebble conglomerate; scattered pebbles in places	Sedimentary structures include ripple marks, cross-beds and clay pellets. Term 'greywacke' abandoned by Smith & Roberts (1963) in favour of dolomitic feldspathic sandstone and arkosic conglomerate
1	Grey crystalline dolomite or limestone, possibly stromatolitic; flaggy siltstone, dolomitic shale, dolomitic breccia	Relationship with unit 2 uncertain; possibly equivalent to Fickling Group below Doomadgee Formation

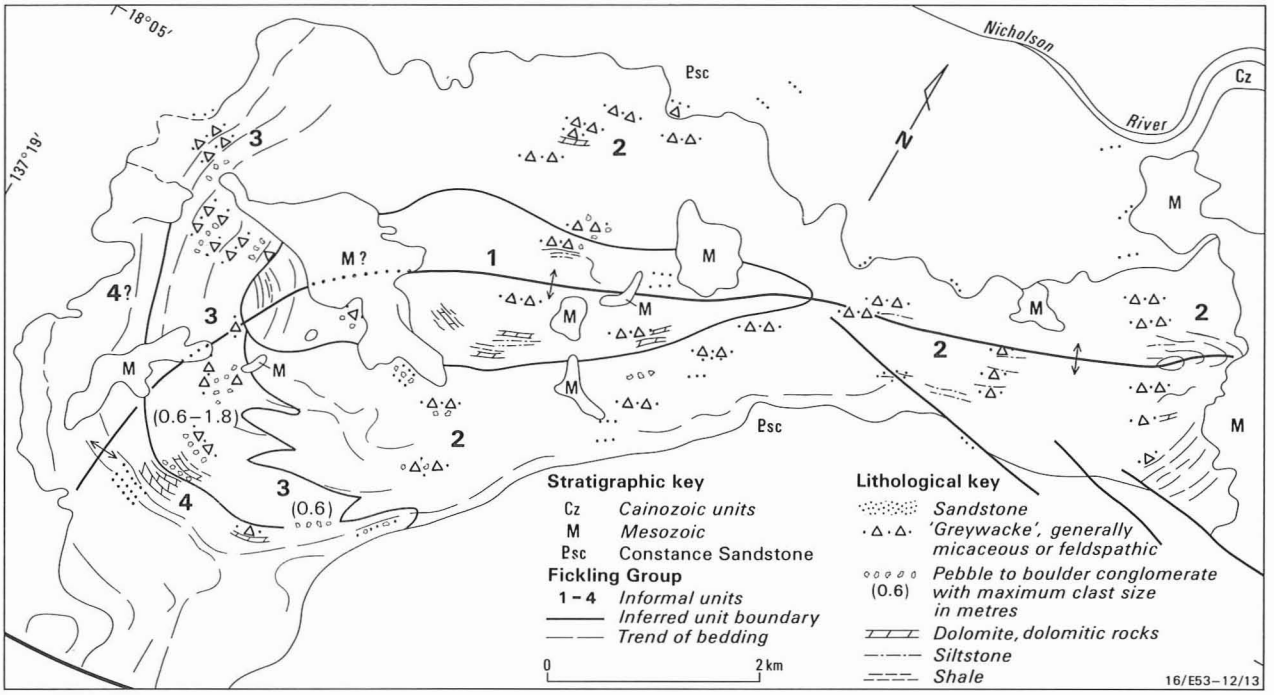

Figure 8. Geology of the Bauhinia Dome.
Based on field notebook data of J.W. Smith and H.G. Roberts.

to acid volcanics and interbedded sediments. The best outccrop, 18 km west-southwest of Old Benmara homestead, contains 1000 m of ripple-marked quartz sandstone overlain by 55 m of porphyritic, amygdaloidal trachyte (Roberts, unpublished MS). The trachyte is composed of orthoclase groundmass (65%), iron oxides (25%), orthoclase phenocrysts (5%), and micas and other minerals (5%). Such feldspar—iron oxide assemblages characterise the lavas of the Fiery Creek Volcanics and the Carrara Range Group (Hutton & Sweet, 1982; Sweet, 1984), and the trachyte-bearing Benmara beds are therefore correlated with those units.

The fourth outcrop of Benmara beds, 10 km west-southwest of Old Benmara homestead, consists of 520 m of silty and feldspathic sandstone, and siltstone containing abundant pebbles and cobbles of quartz and red quartzite; the base of the sequence is unexposed (Roberts, unpublished MS). The association of coarse clasts with siltstone is one that has only been seen in debris-flow beds in the Lawn Hill Formation in the Maloney Creek Inlier, and I therefore tentatively correlate this outcrop of Benmara beds with the upper Fickling Group and McNamara Group in the Bauhinia Dome and Maloney Creek Inlier, respectively (Fig. 9).

Comparison and correlation of sequences in the western Lawn Hill Platform cover.

Correlations within the western Lawn Hill Platform and with the sequences in the eastern part of the platform are shown in Figure 9. Two major differences from Hutton & Sweet's correlations (fig. 3, 1982) are noted: (1) the Kamarga Volcanics are older than the Fiery Creek Volcanics. They unconformably overlie the Yeldham Granite (D. Jones, written communication), which has been dated at 1821 Ma (R.W. Page, personal communication), and are most likely equivalents of the Eastern Creek Volcanics; and (2) the Carrara Range Group is correlated with the Fiery Creek and Peters Creek Volcanics and the Bigie Formation, and is thus considerably younger than the Eastern Creek Volcanics. These revisions have implications for the age of the McArthur Basin sequence, the oldest part of which has also been correlated with the Peters Creek Volcanics and Wire Creek Sandstone (Plumb & Sweet, 1974).

The main differences between the four sequences in the western Lawn Hill Platform Cover are described below.

Maloney Creek Inlier. The McNamara Group in the Maloney Creek Inlier is significantly different from that in the Carrara Range region, despite the small distance between them. For example, outcrops of Musselbrook Formation in the two areas are separated by as little as 14 km, and those of Lawn Hill Formation by less than 10 km. Conglomerates containing chert and claystone clasts in the Carrara Range region are present only at the top of the Musselbrook Formation, where they consist of several 1–2m thick fining-upwards cycles (pebble conglomerate, through plane-bedded sandstone to current-rippled sandstone). This thin conglomeratic interval is equated with Pmb_c in the Maloney Creek Inlier, where most of the lower Musselbrook Formation is apparently not exposed. The exposed 1500 m sequence in the inlier is thus equated with the upper 2000 m of the McNamara Group in the Carrara Range region.

The Lawn Hill Formation in the inlier is thinner, but better exposed than in the Carrara Range region, and contains many coarse-grained interbeds. The Plain Creek Formation is not recognised in the inlier, although its equivalents probably are present in the lower part of the Lawn Hill Formation or upper Musselbrook Formation. The unconformity identified at the base of the Doomadgee Formation in the Seigal–Hedleys Creek region has not been recognised in either the Maloney Creek Inlier or the Carrara Range region.

Bauhinia Dome. The sequence is poorly sorted, micaceous, and feldspathic, much coarser than the Doomadgee Formation in the Seigal and Hedleys Creek 1:100 000 Sheet areas (Sweet & others, 1981), but rather similar to the Musselbrook Formation in the Maloney Creek Inlier. It provides the link between the relatively complete sequences

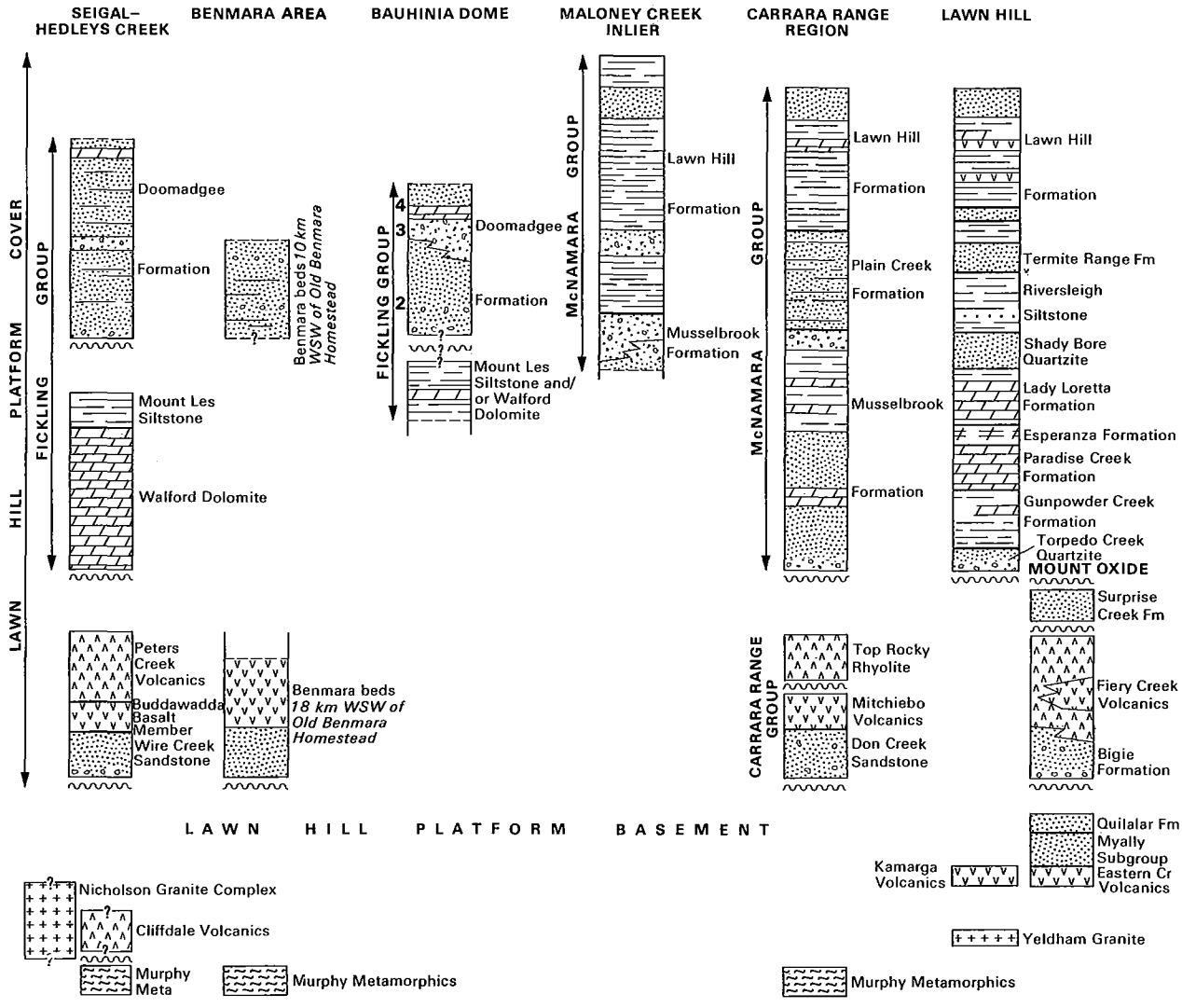

Figure 9. Correlations between sequences in the western Lawn Hill Platform Cover and other parts of the platform.
Numbers against Bauhinia Dome column relate to units identified in Figure 8 and Table 2.

in the Hedleys Creek and Carrara Range regions. Smith & Roberts' unpublished data provide no indication of an unconformity at the base of the Doomadgee Formation (base of unit 2) in the Bauhinia Dome, but bedding trends near the fold axis (Fig. 8) suggest the possibility that one exists.

Benmara beds. These are tentatively correlated with the Carrara Range and McNamara Groups in the Carrara Range region, and with the Peters Creek Volcanics and Fickling Group in the Seigal and Hedleys Creek 1:100 000 Sheet areas (Fig. 9).

Discussion

The early development of the western Lawn Hill Platform Cover was marked by the deposition of a quartz-rich fluvial sand blanket (Don Creek Sandstone, Wire Creek Sandstone, and basal sandstone in the Benmara beds; Fig. 10A). The source of this sediment is not known, but at least some was supplied as a result of uplift east of the Murphy Tectonic Ridge (Sweet & others, 1981, p. 25). Some may have come from the Lawn Hill region, as the Fiery Creek Volcanics and its associated sediments are absent there. This sedimentation was followed by widespread acid and mafic volcanism of the Fiery Creek type (Fig. 10B) (Hutton & Sweet, 1982), which is correlated with the 1678 ± 1 Ma Carters Bore Rhyolite in the Mount Isa Inlier (Page, 1978). The bimodal volcanism has been interpreted in the southern part of the Mount Isa Inlier as indicating a tensional tectonic regime (Bultitude & Wyborn, 1982).

The sandstones and volcanics were partly eroded during minor uplift prior to initiation of the main depositional episode on the Lawn Hill Platform — the deposition of the McNamara and Fickling Groups and the younger part of the Benmara beds. The Surprise Creek Formation, which is widespread in the southeastern Lawn Hill Platform Cover, does not extend north or west of the Mount Oxide area, suggesting that either post-Fiery Creek Volcanics erosion was more prolonged in the northwest or that Surprise Creek Formation equivalents are present in the basal Musselbrook Formation.

Fluvial clastic sedimentation dominated the McNamara Group in the west (Fig. 10C), in contrast to carbonate deposition in the east. However, dolomite and chert (mostly silicified oolitic and stromatolitic dolomite) interbedded with the clastics in the lower part of the sequence in the west indicate that several incursions by the sea or lakes took place

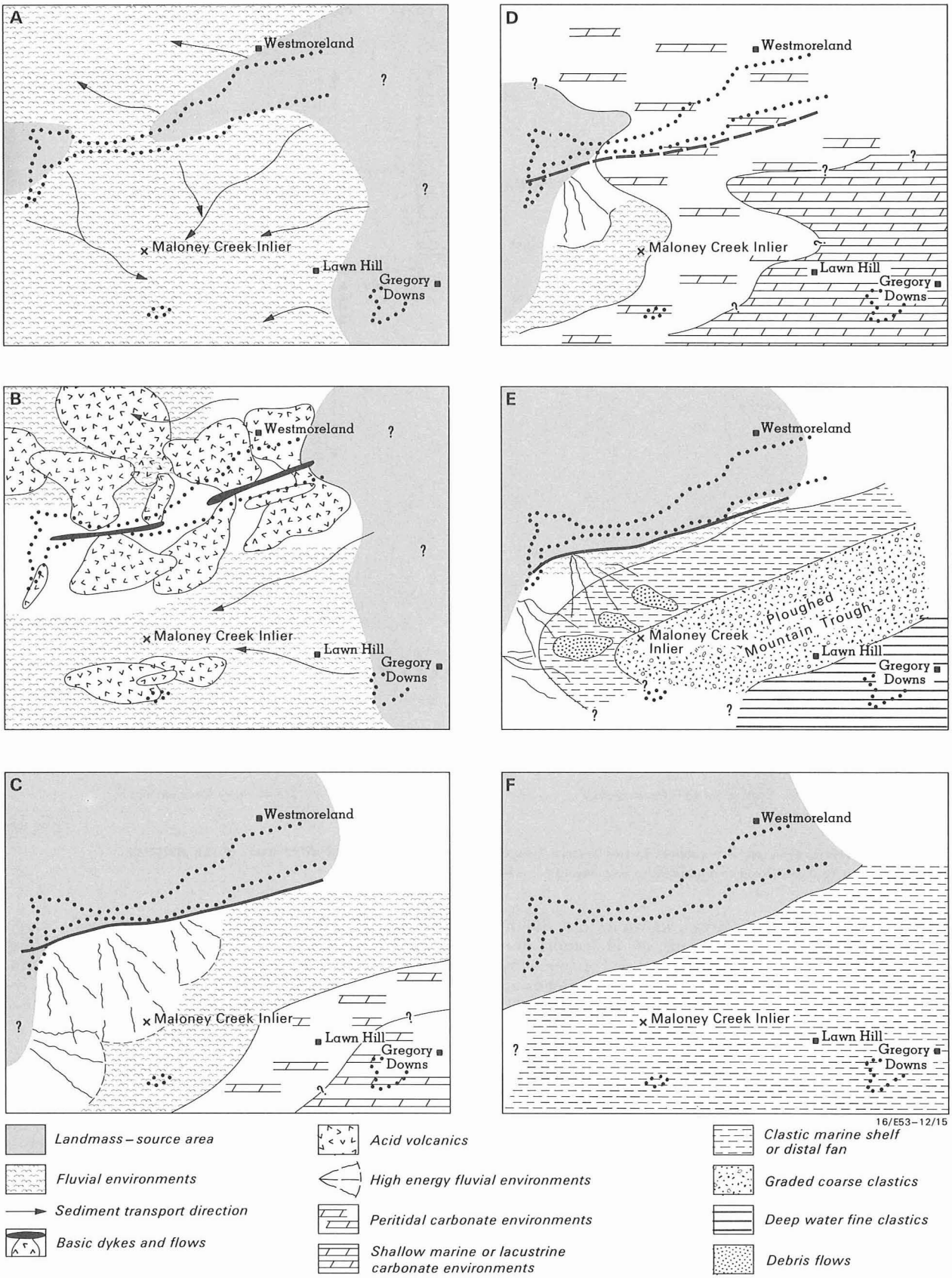

Figure 10. Evolution of the Lawn Hill Platform.

Dotted outlines delineate main areas of basement. Boundaries of major sedimentary environments are approximate or inferred.
(A) — Initial deposition of fluvial sands. (B) — Tensional regime leading to widespread eruption of basic lava, partly from fissures in the Murphy Inlier, followed by more localised acid volcanism. (C) — Faulting at margin of Murphy Tectonic Ridge, resulting in the shedding of coarse clastics southwards; carbonate sabkhas, and lake or marine margin environments farther south and east. (D) — Transgressive phase with little faulting leading to widespread carbonate deposition: an expansion of the carbonate environments shown in C. Distribution of environments reverted to those shown in C after renewed faulting; silicified carbonates eroded from uplifted areas. (E) — Major basinal subsidence with continued faulting at northern margin; narrow shelf or piedmont zone in west, and deep-water trough in the east. (F) — Termination phase: broad clastic shelf or fluvial plain; gradual filling of basin. Sedimentation terminated by uplift and mild deformation.

(Fig. 10D). The widespread silicification of these carbonates may be the result of influxes of silica-rich groundwater during regressive episodes.

The platform sequence coarsens both westwards along the southern margin of the Murphy Inlier and north-northwestwards towards the Bauhinia Dome from the Carrara Range region. The presence of lenses containing quartzite and granite boulders up to 1.8 m across (Table 2) in the Bauhinia Dome indicates a nearby source, and confirms the view of Roberts & others (1963) that in this area at least, the Murphy Tectonic Ridge still existed as a topographic feature. The present Murphy Inlier is 10–15 km wide in this area, and bounded on the south by the Fish River Fault Zone (Sweet & others, 1981), which was almost certainly the site of the syndepositional fault from which very coarse clastics were shed (Fig. 10C). The presence of clasts of quartzite and basic volcanics indicates that cover rocks, as well as granitic and acid volcanic basement, were being eroded. The sediment could have come from Tawallah Group in the Wearyan Shelf, north of the Murphy Inlier, or from the equivalent Wire Creek Sandstone/Peters Creek Volcanics on the Murphy Tectonic Ridge. The presence of angular chert clasts in the sequence is believed to indicate more local erosion of silicified carbonates, perhaps during regressive episodes. The volume of sediments south of the Murphy Inlier is large enough to suggest that the source area was considerably bigger than the 10–15 km wide Murphy Inlier. The Wearyan Shelf may have also contributed silicified carbonates from such units as the Karns Dolomite, if it is a McArthur Group equivalent (for a discusssion of this possibility see Jackson & others, in press). The presence of a disconformity at the base of the Doomadgee Formation also suggests that uplift of the Murphy Tectonic Ridge led to erosion of some of the lower Fickling Group. This break does not occur farther basinwards, but is reflected in the coarser clastic units (Fig. 9). Mainly on evidence from the Maloney Creek Inlier, the depositional environments are believed to have been predominantly fluvial, probably with alluvial fans or high-energy braided stream channels extending from a fault scarp, alternating with low-energy, carbonate-depositing environments. The source for the coarse, massive volcaniclastic conglomerate lens within the Musselbrook Formation in the Maloney Creek Inlier is likely to have been much closer than the Murphy Tectonic Ridge, and was perhaps only a few kilometres away. The most likely source would have been a small fault block exposing Top Rocky Rhyolite and Mitchiebo Volcanics.

The abrupt change from coarse to fine sediments in the Maloney Creek Inlier and Carrara Range region at the base of the Lawn Hill Formation marks the beginning of a distinctly different depositional environment. A deep-water basin, for which the name Ploughed Mountain Trough is herein proposed, was recognised in the Lawn Hill region (Sweet & Hutton, 1980; Hutton & Sweet, 1982). The locus of sedimentation lay in the centre and south of the Lawn Hill region, where up to 5500 m of black shale, turbiditic sandstone, siltstone, and tuff was deposited.

A much thinner equivalent sequence, including the Lawn Hill Formation, was recognised in the Carrara Range region (Sweet, 1984), although turbidites and black shales were not recognised in the poor outcrops. The discovery of graded clastics and debris-flow deposits in the Maloney Creek Inlier supports the view that the inlier lies within, but probably near the margin of, the Ploughed Mountain Trough. The uncertainty regarding the depositional environments of the McNamara Group in the inlier means that the area can only be seen as a subaerial or subaqueous part of a major fan system, whose more distal deposits in the Lawn Hill region are undoubtedly deep water (Hutton & Sweet, 1982). It is not possible to assess, on the present evidence, whether the water was a large lake or sea.

The descriptions of the Bauhinia Dome (Table 2) provide no evidence of graded clastics in the upper part of the sequence there. On the contrary, the laminated carbonates in unit 4 suggest very low-energy depositional environments and the possibility that the northern fault margin was relatively inactive by this time. The palaeocurrent data suggest that sediment transport was roughly along the axis of the Ploughed Mountain Trough, implying that a source lay to the west. The trough is therefore interpreted as an elongate depression extending east-northeasterly through the western Lawn Hill Platform, roughly parallel to the Murphy Inlier (Fig. 10E).

The final phase of sedimentation on the platform was fluvial or shallow marine (Fig. 10F). The latter is preferred, because of the uniform thickness and extent of the Widdallion Sandstone Member and the possible occurrence of glauconite. Until then, a mainly volcanic and sedimentary source terrain was being eroded. The appearance of feldspar in the Widdallion Sandstone Member and in the Doomadgee Formation in Hedleys Creek (Sweet & others, 1981) may indicate widespread erosion of granite, suggesting the unroofing of the Nicholson Granite Complex in the Murphy Inlier.

Only the northern and southeastern margins of the Lawn Hill Platform and Ploughed Mountain Trough can be adequately delineated. The platform cover is concealed to the east by Mesozoic and Cainozoic sediments, and to the west and south by the South Nicholson and Georgina Basins, respectively. Geophysical evidence, pointing to the existence of the 'Aljawarra Craton' (Tucker & others, 1979), appears to be of little help, as the eastern margin of the craton lies within the platform. This suggests that the geophysical data may reflect changes in the basement, but not the cover. At the western margin of the Lawn Hill Platform and Ploughed Mountain Trough, northerly and north-northeasterly fold trends in the South Nicholson Group and Benmara beds and the occurrence of metamorphic basement outcrops may indicate a basement high and, therefore, a western margin to the platform cover. The sparse palaeocurrent data (Fig. 7) also support a western source for some McNamara Group sediments, and suggest transport along the axis of the trough. Such axial transport of sediment is common in turbidite basins (Rupke, 1978). Thus the structural trends and palaeocurrent data suggest that the western margin of the Lawn Hill Platform Cover is little farther west than the outcrops of Benmara beds.

Conclusions

A tensional tectonic regime was important during the development of the Lawn Hill Platform Cover, as shown by the widespread potash-rich volcanism and the development of a faulted northern contact with the Murphy Tectonic Ridge. The relief of the source areas was probably greatest in the northwest, as indicated by the higher clastic to carbonate ratio, and coarser grainsize of the clastics. Minor marine transgressions or deposition at lake margins during tectonically less active periods resulted in carbonate deposition on the western Lawn Hill Platform and, briefly, on the Murphy Tectonic Ridge; the carbonates were silicified and later stripped off during renewed faulting.

Rapid subsidence brought about an abrupt change to marine sedimentation in the east at least, and the development of an east-northeast-trending trough, the Ploughed Mountain Trough, Alluvial fans or gravel-bed streams, the dominant transporting agents during Musselbrook Formation time, continued to feed coarse sediment into the marginal areas of the fault-bounded depression. Black shales, common in the Lawn Hill region to the east, are absent in the west, suggesting more oxygenated environments. The Widdallion Sandstone Member, near the top of the Lawn Hill Platform Cover, reflects termination of the Ploughed Mountain Trough either by filling or by tectonic uplift.

Acknowledgements

H.G. Roberts and J.W. Smith made geological observations in the Bauhinia Dome and Benmara areas in 1959, during mapping of the Mount Drummond and Calvert Hills 1:250 000 Sheet areas. Access to their original data is gratefully acknowledged. L.J. Hutton assisted with field work in the Carrara Range region in 1977. I thank I.H. Crick, L.J. Hutton, K.A. Plumb, and K.A.W. Crook for valuable comments, which led to substantial improvements to a draft of this paper. The figures were drafted by Brian Pashley.

References

Allen, P.A., 1981 — Sediments and processes on a small stream-flow dominated, Devonian alluvial fan, Shetland Islands. *Sedimentary Geology*, 29, 31–66.

Bultitude, R.J., & Wyborn, L.A.I., 1982 — Distribution and geochemistry of volcanic rocks in the Duchess — Urandangi region, Queensland. *BMR Journal of Australian Geology & Geophysics*, 7, 99–112.

Collinson, J.D., 1978 — Alluvial sediments. *In* Reading, H.G. (editor), Sedimentary environments and facies. *Blackwell, Oxford*, 15–60.

Conybeare, C.B., & Crook, K.A.W., 1968 — Manual of sedimentary structures. *Bureau of Mineral Resources, Australia, Bulletin* 102.

Heward, A.P., 1978 — Alluvial fan sequence and megasequence models: with examples from Westphalian D—Stephanian B coalfields, Northern Spain. *In* Miall, A.D., (editor), Fluvial sedimentology. *Canadian Society of Petroleum Geologists, Memoir* 5, 669–702.

Hubert, J.F., & Hyde, M.G., 1982 — Sheet flow deposits of graded beds and mudstones on an alluvial sandflat-playa system: Upper Triassic Blomidon redbeds, St Marys Bay, Nova Scotia. *Sedimentology*, 29, 457–474.

Hutton, L.J., Cavaney, R.J., & Sweet, I.P., 1981 — New and revised stratigraphic units, Lawn Hill Platform, northwest Queensland. *Queensland Government Mining Journal*, 82, 423–434.

Hutton, L.J., & Sweet, I.P., 1982 — Geological evolution, tectonic style and economic potential of the Lawn Hill Platform Cover — northwest Queensland. *BMR Journal of Australian Geology & Geophysics*, 7, 125–134.

Jackson, M.J., Muir, M.D., & Plumb, K.A., in press — Geology of the southern McArthur Basin, Northern Territory. *Bureau of Mineral Resources, Australia, Bulletin* 220.

Lowe, D.R., 1979 — Sediment gravity flows: their classification and some problems of application to natural flows and deposits. *In* Doyle, L.J., & Pilkey, O.H., Jr., (editors), Geology of continental slopes. *Society of Economic Paleontologists and Mineralogists, Special Publication* 27, 75–82.

Lowe, D.R., 1982 — Sediment gravity flows: II. Depositional models with special reference to the deposits of high-density turbidity currents. *Journal of Sedimentary Petrology*, 52, 279–297.

Page, R.W., 1978 — Response of U-Pb zircon and Rb-Sr total-rock and mineral systems to low-grade regional metamorphism in Proterozoic igneous rocks, Mount Isa, Australia. *Journal of the Geological Society of Australia*, 25, 141–164.

Pettijohn, F.J., Potter, P.E., & Siever, R., 1973 — Sand and sandstone. *Springer-Verlag, New York*.

Plummer, P.S., & Gostin, V.A., 1981 — Shrinkage cracks: desiccation or synaeresis? *Journal of Sedimentary Petrology*, 51, 1147–1156.

Roberts, H.G., Rhodes, J.M., & Yates, K.R., 1963 — Calvert Hills, N.T. — 1:250 000 Geological Series. *Bureau of Mineral Resources, Australia, Explanatory Notes*, SE/53–8.

Rupke, N.A., 1978 — Deep clastic seas. *In* Reading, H.G. (editor), Sedimentary environments and facies. *Blackwell, Oxford*. 372—415.

Smith, J.W., & Roberts, H.G., 1963 — Mount Drummond, Northern Territory — 1:250 000 Geological Series. *Bureau of Mineral Resources, Australia, Explanatory Notes*, SE/53–12.

Sweet, I.P., 1981 — Definitions of new stratigraphic units in the Seigal and Hedleys Creek 1:100 000 Sheet areas, Northern Territory and Queensland. *Bureau of Mineral Resources, Australia, Report* 225.

Sweet, I.P., 1982 — Definitions of new stratigraphic units in the Carrara Range Region, Northern Territory. *Bureau of Mineral Resources, Australia, Report* 242.

Sweet, I.P., 1984 — Carrara Range Region, Northern Territory. *Bureau of Mineral Resources, Australia 1:100 000 Geological Map Commentary*

Sweet, I.P., & Hutton, L.J., 1980 — The geology of the Lawn Hill/Riversleigh Region, Queensland. *Bureau of Mineral Resources, Australia, Record*, 1980/43.

Sweet, I.P., & Hutton, L.J., 1982 — Lawn Hill Region, Queensland. *Bureau of Mineral Resources, Australia, 1:100 000 Geological Map Commentary.*

Sweet, I.P., & Slater, P.J., 1975 — Precambrian geology of the Westmoreland region, northern Australia. Part I: Regional setting and cover rocks. *Bureau of Mineral Resources, Australia, Record*, 1975/88.

Sweet, I.P., Mock, C.M., & Mitchell, J.E., 1981 — Seigal, Northern Territory, and Hedleys Creek, Queensland. *Bureau of Mineral Resources Australia. 1:100 000 Geological Map Commentary.*

Tucker, D.H., Wyatt, B.W., Druce, E.C., Mathur, S.P., & Harrison, P.L., 1979 — The upper crustal geology of the Georgina Basin region. *BMR Journal of Australian Geology & Geophysics*, 4, 209–226.

Wescott, W.A., & Ethridge, F.G., 1980 — Fan-delta sedimentology and tectonic setting — Yallahs Fan Delta, southeast Jamaica. *American Association of Petroleum Geologists, Bulletin*, 64, 374–99.

BMR Journal of Australian Geology & Geophysics, 9, 339-351

Geochemistry and tectonic significance of Proterozoic mafic rocks from the Georgetown Inlier, north Queensland

I.W. Withnall[1]

Mafic igneous rocks were emplaced during deposition of the Robertson River Subgroup, part of the early or Middle Proterozoic Etheridge Group in the Georgetown Inlier. They comprise the Dead Horse Metabasalt and the Cobbold Metadolerite, which forms a multitude of sills both above and below the Dead Horse Metabasalt. They are metamorphosed to lower greenschist to granulite facies, and are probably equivalant to amphibolite and mafic granulite in the Einasleigh Metamorphics. The rocks are geochemically similar to modern mid-ocean ridge basalts (MORB). However, sedimentological evidence indicates that the Etheridge Group was deposited in shallow water on a shelf or in an epicontinental sea. The mafic rocks may, therefore, be similar to the low-K flood basalts of Greenland and Baffin Island, although the low K could be partly due to depletion during metamorphism. Except for the much lower K, they are similar to the relatively incompatible-element depleted Karoo basalts and dolerites. They are also similar geochemically to some Proterozoic mafic rock suites from the Mount Isa and Pine Creek areas in northern Australia. The mafic rocks from the Etheridge Group may be the expression of convective mantle upwelling, which could have produced extension of the Proterozoic crust and the formation of a shallow epicontinental sea in which the Etheridge Group was deposited. No evidence of any associated rifting occurs in the Georgetown Inlier.

Introduction

The Georgetown Inlier, about 25 000 km², is the largest area of Precambrian rocks in northeastern Queensland (Fig. 1). It consists largely of metamorphosed Early or Middle Proterozoic sedimentary and mafic igneous rocks intruded by Proterozoic to Late Palaeozoic granitoids. Late Palaeozoic felsic volcanic rocks overlie the inlier, which is surrounded by Mesozoic and Cainozoic fluviatile sedimentary rocks of the Eromanga and Carpentaria Basins and Pliocene to Holocene basalt.

Reconnaissance mapping in the late 1950s (White, 1965) by the Bureau of Mineral Resources (BMR) and Geological Survey of Queensland (GSQ) outlined the main features of the Georgetown Inlier. In the 1970s the BMR and GSQ began a more detailed study of the inlier, involving geological mapping at 1:100 000 scale as well as geochronological, geophysical, and geochemical studies. The data in this paper were collected as a part of this study. Staff and students of the James Cook University and University of Queensland have also made detailed studies of various aspects of the structure and metamorphic petrology of the area, in particular McNaughton (1980) and McNaughton & Wilson (1983), who studied some of the mafic rocks. Withnall & others (1980a) reviewed the geology of the Georgetown Inlier, from work done up to the middle of 1978. A more up-to-date synthesis of the geology of the central part of the inlier, where the BMR/GSQ work was initially confined, is in preparation.

Most of the Early Proterozoic rocks of the central Georgetown Inlier have been assigned to the Etheridge Group (Figs. 2, 3) (Withnall & Mackenzie, 1980; Withnall, 1983, 1984), which has been multiply deformed and metamorphosed to grades ranging from lower greenschist to granulite facies. The low-grade metasedimentary rocks are predominantly fine sandstone, siltstone, and mudstone. They were deposited in a mainly shallow-water environment on a shelf or in an epicontinental sea, and facies are continuous from north to south across the inlier. The rocks grade into schist, quartzite, and gneiss, the grade of metamorphism and intensity of deformation increasing to the east, where the lowermost units of the sequence are exposed. The basement to the Etheridge Group has not been recognised and probably does not crop out.

[1] Geological Survey of Queensland
GPO Box 194, Brisbane, Queensland 4001

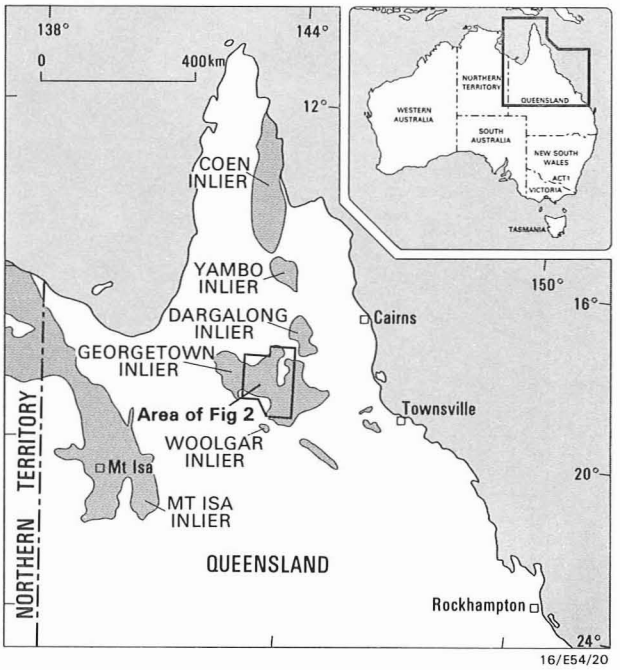

Figure 1. Location map, showing the distribution of Precambrian rocks (shaded) in northern Queensland.

Sm/Nd studies in the Georgetown Inlier (Black & McCulloch, 1984) suggested that the Etheridge Group is older than 2000 Ma, and possibly 2400–2500 Ma. However, the first deformation and accompanying metamorphic event have been dated at 1570 Ma (Black & others, 1979), indicating a long period of quiescence after deposition, if the Sm/Nd age is accepted as the age of the Etheridge Group. Alternative interpretations of the Sm/Nd age are discussed later in this paper.

Metamorphosed mafic rocks are common in the lower part of the Etheridge Group. Their distribution is shown in Figure 2. They are assigned to two units, the extrusive Dead Horse Metabasalt and the intrusive Cobbold Metadolerite. Amphibolite and mafic granulite in the Einasleigh Metamorphics, are probably mainly equivalent to the Cobbold Metadolerite, but some extrusive rocks have also been recognised.

Geology of the mafic rocks

Field relationships and petrographic features of the mafic rocks in the Etheridge Group are described briefly below.

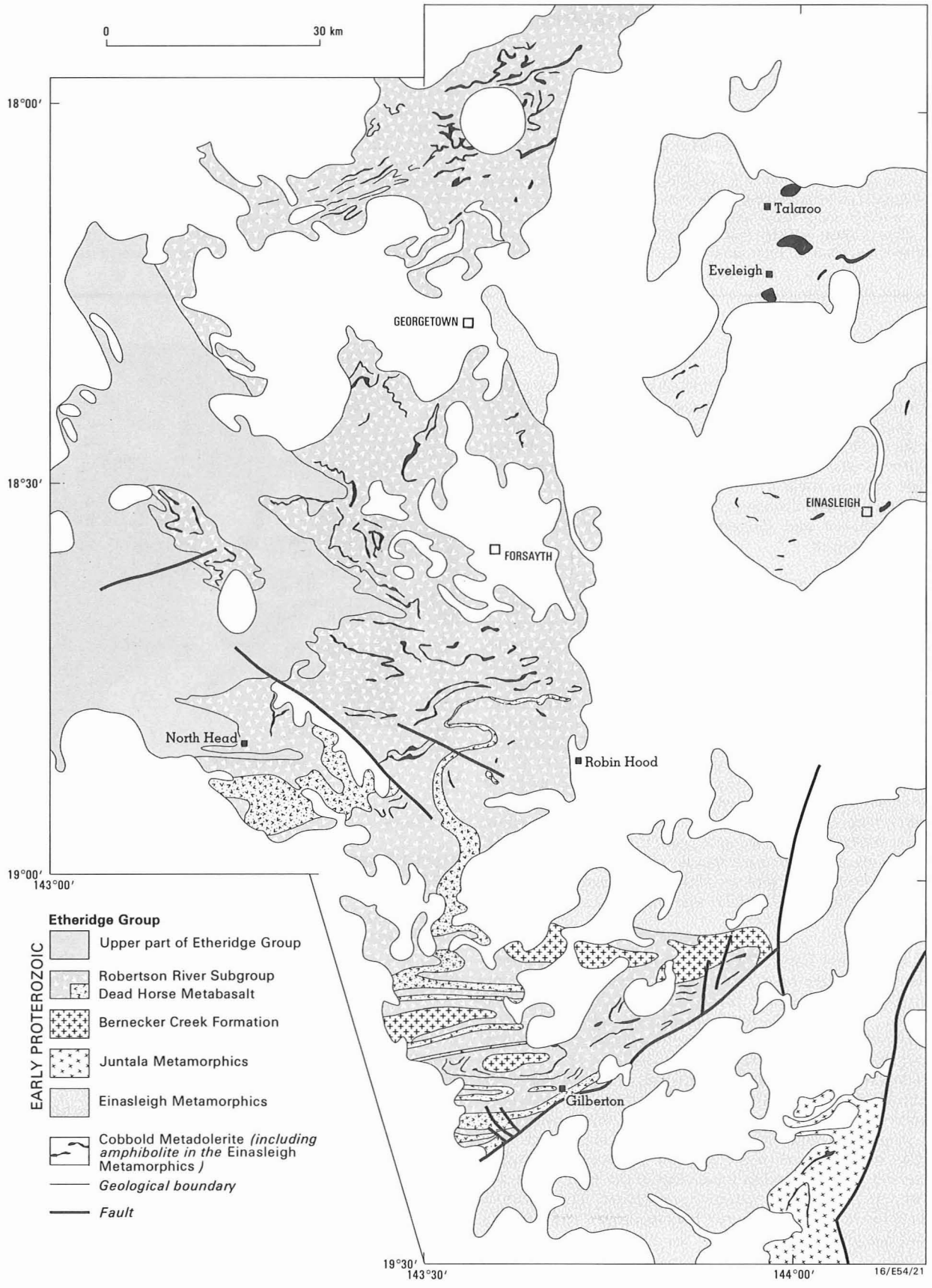

Figure 2. Generalised geology of the central Georgetown Inlier, showing the distribution of mafic rocks.

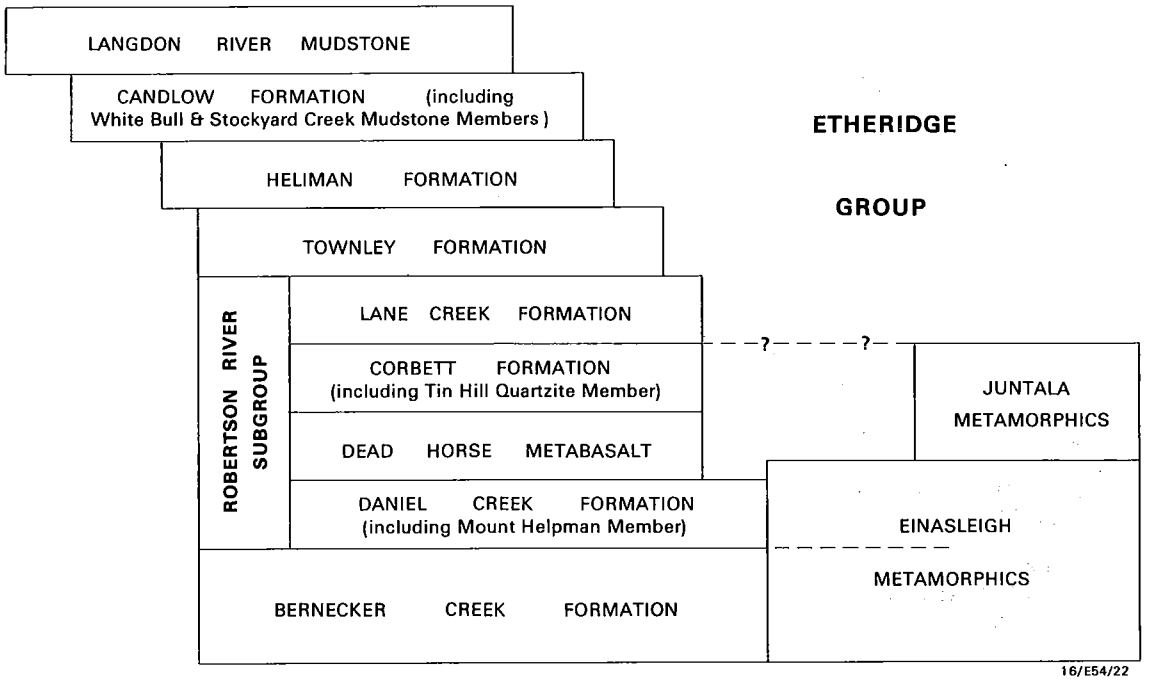

Figure 3. Stratigraphic relationships within the Etheridge Group.

More detailed descriptions are given by Bain & others (1976), Oversby & others (1978), Withnall & others (1980b), Withnall & Mackenzie (1981), Withnall (1984), and McNaughton (1979, 1980).

Dead Horse Metabasalt

Field relationships. The Dead Horse Metabasalt (Withnall & Mackenzie, 1980; Withnall, 1983) consists of up to 1000 m of metamorphosed mafic lava, and minor mudstone and siltstone interbeds, conformable between the Daniel Creek Formation and Corbett Formation in the Robertson River Subgroup (Fig. 3). It crops out mainly in the Gilberton and North Head areas, and pinches out north of the Robin Hood area (Fig. 2). Pillow lavas, amygdales, and hyaloclastic breccias are common near the top of the unit, and also occur locally near the base. Flows in the middle of the unit are structureless and difficult to distinguish from intrusive rocks, except that they are generally finer grained. Locally, some coarser rocks may be intrusive, but others could be the interiors of thick flows. Some of the metabasalt is foliated, and pillows and amygdales are flattened parallel to the foliation.

In the higher grade part of the Robertson River Subgroup, the Dead Horse Metabasalt consists mainly of fine-grained, well-folidated amphibolite, and minor interbedded mica schist and quartzite. Amygdales, possible metamorphosed hyaloclastic breccia, and vague outlines of pillows have been recognised in a few places.

Petrography. The metabasalts are generally dark-green, fine to very fine-grained, and aphyric. They mostly consist of randomly oriented albite laths less than 1 mm long, in a matrix of pale green, acicular actinolite or hornblende (depending on the metamorphic grade), epidote/clinozoisite, chlorite, and minor calcite, sphene, and opaque oxides. Amygdales are filled with quartz, minor epidote, and/or calcite. In the foliated metabasalts, igneous textures have been obliterated. Such rocks are commonly chlorite schists, containing quartz, chlorite, and calcite. The amphibolites are mineralogically similar to those derived from metadolerite and metagabbro (see below), but are finer-grained.

Cobbold Metadolerite

Field Relationships. The Cobbold Metadolerite forms a multitude of separate intrusions, mainly sills, in the lower part of the Etheridge Group. The sills are from a few metres to over 500 m thick, and some can be traced along strike for more than 10 km. Complex interference fold structures in the Lane Creek Formation in the Western Creek area are outlined by sills, which, before folding, could have extended for more than 50 km. Some of the sills in the Lane Creek Formation have alternating leucocratic and melanocratic layers, particularly in the north of the area. Dykes are not common, the main example being the one that is host to copper mineralisation at Ortona (Withnall, 1981). Some apparently discordant bodies with irregular outlines may be stocks.

The Cobbold Metadolerite may have been intruded in at least two pulses. One possibly accompanied the extrusion of the Dead Horse Metabasalt, and a younger pulse occurred during the deposition of the Lane Creek Formation, the uppermost unit of the Robertson River Subgroup. No mafic rocks occur in the Etheridge Group above the Lane Creek Formation.

Petrography. In the lower greenschist facies, the metadolerite and metagabbro consist of albite, epidote, actinolite, chlorite, sphene, opaque oxides, and rare relict clinopyroxene. In the upper greenschist facies, albite is replaced by oligoclase, and actinolite by blue-green hornblende. In the amphibolite facies, the mafic rocks contain plagioclase (andesine or labradorite) and hornblende, but no epidote or chlorite. Sphene and ilmenite are also present. Plagioclase generally forms a granoblastic mosaic, but relict laths are preserved in some rocks well into the amphibolite facies. Blastophitic hornblende is the most commonly preserved igneous texture, and is even present locally in the upper amphibolite facies. Generally, however, hornblende forms aggregates of randomly oriented prisms. It changes progressively from bluish-green to brown with increasing metamorphic grade. Metamorphic clinopyroxene occurs in the upper amphibolite facies.

In the amphibolites, the igneous texture and appearance have been destroyed. Generally, the rocks have a fabric, usually

a hornblende lineation, although a foliation may also be present. The rocks contain similar mineral assemblages to the massive metadolerite. Garnet porphyroblasts occur locally. In the upper amphibolite facies, the mafic rocks have a granuloblastic polygonal texture.

Mafic rocks in the Einasleigh Metamorphics

Mafic rocks are also common in the Einasleigh Metamorphics, which are thought to be equivalent to the Bernecker Creek and Daniel Creek Formations. Although some of the mafic rocks are definitely of intrusive origin, and can be equated with the Cobbold Metadolerite, the origin of many is equivocal, and they are, therefore, treated separately. Some rocks are almost certainly of extrusive origin. The grade of metamorphism in the Einasleigh Metamorphics is upper amphibolite to granulite facies. Mafic granulites occur sporadically in a 50 km belt extending northeast from Einasleigh (McNaughton, 1979, 1980; Withnall, 1984). Oversby & others (1978) recorded several occurrences outside this belt, in the Talaroo area.

Field Relationships. The mafic rocks commonly occur as tabular bodies, which range from less than a metre to more than 100 m wide, and are concordant with the layering of the enclosing gneiss. The rocks are foliated and, commonly, strongly lineated. Larger, more irregular bodies of amphibolite, several kilometres across, have also been mapped. However, large sills that can be traced along strike for many kilometres, like those in the Robertson River Subgroup, are not apparent in the Einasleigh Metamorphics, probably because the complex folding, coupled with poorer outcrop, makes such bodies difficult to trace. Alternatively, some other factor, perhaps greater thickness of sediment cover, may have favoured the emplacement of stocks and smaller, less extensive sills in the Einasleigh Metamorphics. Probable pillow structures in amphibolite in the Einasleigh Metamorphics, near the abandoned Eveleigh silver-lead mine, were described by Oversby & others (1978).

Petrography. Amphibolite in the Einasleigh Metamorphics is similar to the amphibolite described from the Cobbold Metadolerite, but the texture is generally granuloblastic polygonal. Some igneous textures are also preserved in these amphibolites: the most common is a coarse blastophitic texture, but relict laths of plagioclase are preserved in places. The mafic granulite has the typical mineral assemblage of plagioclase (labradorite or bytownite) + brown hornblende + orthopyroxene + clinopyroxene + quartz, and has a granuloblastic texture. Both types of pyroxene form poikiloblastic grains up to 2 cm long.

Geochemistry

The objectives of the geochemical study were to determine any significant differences between the various groups of mafic rocks, attempt a petrochemical classification of them, and, by comparison with modern volcanic rocks, attempt to assess their origin and tectonic setting.

Details of analytical techniques and some petrographic information are presented in the Appendix. The 54 analysed samples are divided into six categories (Table 1 and Appendix).

The Cobbold Metadolerite samples are divided into two categories to distinguish those that definitely postdate the Dead Horse Metabasalt. Those that intruded the Dead Horse Metabasalt or units stratigraphically below it could be comagmatic with either the Dead Horse Metabasalt or the younger metadolerites, or could represent a separate intrusive pulse.

Geochemical effects of alteration and metamorphism

An obvious difference between the metamorphosed mafic rocks and unaltered basalts (Table 2) is the higher water content. The average H_2O^+ content of the greenschist facies rocks in this study is about 3.2 per cent (ranging up to 5.8 per cent in the metabasalts). Dehydration with increasing metamorphic grade has resulted in an average of only 1.7 per cent H_2O^+ in amphibolite facies mafic rocks, and 1.4 per cent in the granulites.

The Dead Horse Metabasalt is probably largely, if not totally, submarine, and the intrusions of the Cobbold Metadolerite were all emplaced during the deposition of the Robertson River Subgroup, which would have contained some connate water. Therefore, at least some of the increased H_2O^+ content could be due to seawater hydration. Seawater hydration should alter the oxygen isotope ratios of the rocks, but McNaughton (1980) and McNaughton & Wilson (1983) found that amphibolite and mafic granulite from the Einasleigh Metamorphics had identical $\delta^{18}O$ to unaltered mid-oceanic ridge basalts (MORB), suggesting that seawater did not have pervasive access to them. The other most likely origin for the water is dehydration of hydrous minerals in the metasedimentary rocks during metamorphism.

Fe_2O_3/FeO ratios range from less than 0.1 to 0.6, with a mode between 0.15 and 0.20. Oxidation was probably partly associated with seawater hydration and/or mobilisation of fluids during metamorphism. The oxygen fugacity of the metamorphic fluid phase was probably highly variable, because of the presence of abundant organic carbon in parts of the sequence, particularly in the Lane Creek Formation. This may account for the less oxidised state of iron in metadolerites from above the Dead Horse Metabasalt (average $Fe_2O_3/FeO = 0.15$), compared with those in the lower part of the sequence (average $Fe_2O_3/FeO = 0.26$). Increasing metamorphic grade can also affect the oxidation state (Engel & Engel, 1962); McNaughton (1980) showed that iron in the mafic granulites from the Einasleigh area is more reduced than in the amphibolites.

To compensate for the oxidation and possible reduction, analyses used in the calculation of 'Mg' numbers and norms have been corrected by adjusting the Fe_2O_3/FeO ratio to 0.15, as suggested by Green & others (1974) and Brooks (1976).

Initial hydration of the mafic rocks and subsequent dehydration at higher metamorphic grades may result in redistribution of the more mobile elements, such as alkali and alkalinerth elements. Reactions with seawater can produce both increases and decreases in these elements (Thompson, 1973; Humphris & Thompson, 1978a, 1978b; Menzies & Seyfried, 1979). Most studies of the low-grade metamorphism of mafic rocks indicate that K is depleted (e.g. Smith, 1968; Vallance, 1974; Jolly & Smith, 1972; Jolly, 1980). Clough & Field (1980) showed that in the transition from amphibolite to granulite facies in metabasites from Norway, K, Rb, Sr, Ba, and even Zr were depleted, and Na was enriched.

Therefore, it is possible that the low levels of K_2O in the mafic rocks of this study (Table 1, Fig. 6) are partly the result of depletion during metamorphism, (particularly when plagioclase broke down to albite and epidote) or even before metamorphism began. McNaughton (1980) and McNaughton & Wilson (1983) found similar or even lower levels of K_2O in amphibolite and granulite facies mafic rocks from the Einasleigh Metamorphics. They argued, however, that the metamorphism was isochemical with respect to alkalies, mainly on the basis of K/Rb ratios, which should increase

Table 1. Average chemical analyses and CIPW norms for the main categories of Early Proterozoic mafic rocks from the Georgetown Inlier.

	All mafic rocks excluding xenoliths (this study)		*Dead Horse Metabasalt (DHM)*				*Cobbold Metadolerite*				*Einasleigh Metamorphics*		*mafic xenoliths*	
			metabasalt		*amphibolite*		*in & below DHM*		*above DHM*		*amphibolite & granulite*		*GSQ/R5294*	*GSQ/R5299*
Symbol on figures			*star*		*solid circle*		*open square*		*open circle*		*asterisk*		*cross*	*cross*
No. of analyses	*52*		*11*		*5*		*12*		*15*		*9*		*1*	*1*
	$\bar{X}$	S	$\bar{X}$	S	$\bar{X}$	S	$\bar{X}$	S	$\bar{X}$	S	$\bar{X}$	S		
SiO_2	48.66	1.48	48.42	2.01	49.62	1.55	48.23	1.41	48.68	1.24	48.95	1.13	47.97	38.29
TiO_2	1.25	0.46	1.53	0.25	1.69	0.47	1.24	0.52	0.93	0.41	1.20	0.23	2.15	2.19
Al_2O_3	14.14	1.59	12.83	0.96	14.03	0.85	14.81	1.39	14.70	2.02	13.97	1.11	15.01	19.94
Fe_2O_3	2.29	1.20	3.52	1.38	2.31	0.68	2.62	1.10	1.46	0.40	1.70	0.61	1.36	1.71
FeO	10.52	2.01	10.99	1.86	12.11	1.41	9.94	1.80	9.77	2.04	11.10	1.84	17.10	17.20
FeO_t	12.57	2.26	14.14	1.57	14.19	1.71	12.30	2.14	11.07	2.26	12.63	1.84	18.32	18.74
MnO	0.21	0.04	0.22	0.04	0.22	0.05	0.21	0.03	0.20	0.04	0.22	0.03	0.28	0.24
MgO	6.96	1.41	6.36	1.17	5.64	0.90	6.77	1.48	7.62	1.28	7.59	1.36	5.95	7.80
CaO	10.77	1.95	9.82	2.64	9.46	0.72	10.22	1.53	11.85	1.69	11.61	1.17	5.40	6.99
Na_2O	1.94	0.83	1.71	0.96	2.16	0.80	2.22	0.79	2.11	0.77	1.46	0.68	2.95	2.10
K_2O	0.28	0.27	0.12	0.05	0.30	0.20	0.45	0.42	0.24	0.17	0.33	0.26	0.07	0.09
P_2O_5	0.12	0.04	0.14	0.02	0.16	0.04	0.11	0.04	0.09	0.04	0.12	0.03	0.17	0.16
H_2O+	2.26	1.00	3.31	1.32	1.90	0.22	2.62	0.92	1.75	0.34	1.56	0.22	1.31	1.81
CO_2	0.26(16)	0.29	0.40(5)	0.23	0.01(1)	—	0.15(8)	0.15	0.03(2)	—	—	—	—	—
Ba	96	88	94	117	91	69	117	99	95	78	74	63	30	130
Li	12(12)	4	11(5)	4	—	—	12(7)	4	—	—	—	—	—	—
Rb	10*	14	5*	4	13	10	20	23	9	8	6	3	4	6
Sr	158	77	118	80	132	58	163	26	168	79	199	110	160	440
Pb	6*	8	8	15	4	3	7	6	4*	2	7	5	6	10
Th	4	—	4	—	4	—	4	—	4	—	—	—	—	—
U	1	—	1	—	1	—	1	—	1	—	—	—	—	—
Zr	71	28	93	16	101	27	68	29	49	22	65	14	119	105
Nb	3.5*	1.5	4.5	1.5	5	1	3.5	1	2.5*	1	3	1.5	5	4
Y	23	7	26	6	30	8	22	7	18	6	24	4	40	32
Ce	5*(14)	2	5*(5)	2	—	—	5.5*(7)	2.5	2*(2)	—	—	—	—	—
V	418	163	485	84	641	82	438	213	320	126	351	98	634	530
Cr	196	207	123	50	95	51	149	177	282	310	263	150	61	215
Co	54	8	52	7	57	7	49	8	57	11	55	4	68	69
Ni	90	43	66	16	67	17	95	59	104	44	102	39	48	91
Cu	140	79	133	63	125	56	128	58	165	120	130	45	213	14
Zn	99	26	113	26	113	22	98	27	86	24	95	17	145	169
Mo	6(12)	1	6(5)	1	—	—	6(7)	1	—	—	—	—	—	—
As	2(1)	1	2(5)	1	—	—	1(6)	2	—	—	—	—	—	—
S	621	601	560	519	740*	850	408*	375	600	392	860	902	200	100
K/Rb	232		199		192		186		208		457		145	125
K/Ba	24		11		27		32		20		37		19	6
Ti/Zr	106		99		100		109		114		111		119	125
Y/Nb	6.6		5.8		6		6.3		7.2		88		8	
Zr/Nb	20		21		20		19		20		22		24	26
Zr/Y	3.1		3.6		3.4		3.1		2.7		2.7		3.0	3.3
'Mg'(wt %)	38.6		33.8		31.1		38.5		42.6		40.1		26.9	32.1
'Mg'(atomic)	52.9		47.7		44.6		52.7		57.0		54.9		39.7	45.8
Fe_2O_3/FeO	0.22		0.32		0.19		0.26		0.15		0.15		0.08	0.10
CIPW Norm (volatile free)														
Q	0.57		3.82		3.13		—		—		1.23		—	—
Or	1.65		0.71		1.77		2.66		1.42		1.95		0.41	0.53
Ab	16.41		14.47		18.28		18.78		17.85		12.35		24.96	16.34
An	29.05		26.98		27.70		29.12		29.93		30.59		25.68	33.63
Ne	—		—		—		—		—		—		—	0.77
Di	19.51		17.33		15.19		17.25		23.22		21.62		—	—
Hy	24.64		26.01		25.07		20.69		15.86		25.31		35.29	—
Ol	—		—		—		3.04		5.14		—		4.67	34.12
Il	2.37		2.91		3.21		2.36		1.77		2.28		4.08	4.16
Mt	2.38		2.71		2.71		2.35		2.03		2.42		1.97	2.48
Ap	0.28		0.33		0.38		0.26		0.21		0.28		0.40	0.38
C	—		—		—		—		—		—		0.67	4.06
Plag An	63.89		65.09		60.25		60.79		62.64		71.23		50.71	67.30

1. Where fewer samples were analysed for a particular element, the number of analyses is shown in parentheses
2. Values marked with an asterisk are where some samples contained concentrations below the detection limit. A value equal to the detection limit was assigned during calculation of the average
3. 'Mg' ratios and CIPW norms were calculated using an Fe_2O_3/FeO ratio of 0.15

as K is depleted, because of the greater mobility of Rb. Although K/Rb and K show no such negative correlation here (Fig. 4) (or in McNaughton & Wilson's study), any systematic variation in K/Rb ratio may be masked by poor precision of Rb determinations at levels close to the detection limit.

To account for the supposed isochemical behaviour, McNaughton (1980) suggested that the onset of metamorphism may have been relatively rapid, so that many rocks escaped greenschist facies alteration and recrystallised in the amphibolite facies. Plagioclase in such rocks would not have broken down, and K and Rb may have been retained. In several of the amphibolite facies metadolerites in this study, although the plagioclase is present entirely as relict igneous laths, the rocks contain similar levels of K_2O to metadolerites in the greenschist facies, in which plagioclase is completely altered. Depletion of alkalies, if it occurred, was therefore not necessarily dependent on alteration of plagioclase. The greenschist facies metabasalts have lower K_2O than the metadolerites and amphibolite (Table 1, Fig. 6), suggesting that the metabasalts, at least, have been depleted in K_2O (assuming that the metabasalts and metadolerites are related).

Therefore, with the available data, it is not possible to determine whether or not the contents of K and Rb have been significantly modified during metamorphism, and any conclusion made regarding these elements should be treated with caution. Similarly, mobilisation of Na and the alkaline-earth elements is suggested by the considerable scatter and lack of systematic variation with fractionation in Figures 6 and 7.

To test the extent of mobilisation of some other major elements, the analyses have been plotted on log molecular proportion ratio (LMPR) diagrams, after Beswick & Soucie (1978), who demonstrated that a wide range of unaltered volcanic rocks of diverse tectonic environments fell in narrow fields (Fig. 5), whereas altered greenstones were scattered widely. Alkali migration would result in point dislocation along at 45°-slope line, mainly within the fields of modern volcanic rocks. The generally good fit between the metamorphosed mafic rocks in the Georgetown area and the modern fields suggests that the elements tested have not been mobilised markedly more than those in the samples used to define the fields. Certainly, they are much less altered than the greenstones studied by Beswick & Soucie.

Table 2. Average analyses of various unaltered tholeiitic suites

	1	2	3	4	5	6	7
SiO_2	49.34	50.1	52.7	51.8	47.34	47.5	48.88
TiO_2	1.49	2.17	1.16	1.13	2.05	0.97	2.57
Al_2O_3	17.04	14.0	15.4	14.8	14.99	13.8	13.68
Fe_2O_3	1.99		1.38	3.92	4.31	3.3	
FeO	6.82		9.35	7.26	7.8	6.7	
FeO_t	8.61	13.5	10.59	10.79	11.68	9.7	13.43
MnO	0.17	0.18	0.22	0.17	0.2	0.17	0.20
MgO	7.19	6.46	6.6	7.1	7.47	11.8	6.57
CaO	11.72	9.82	9.96	10.57	11.47	11.7	11.29
Na_2O	2.73	2.54	2.22	2.40	2.27	1.53	2.35
K_2O	0.16	0.80	0.87	0.74	0.26	0.10	0.26
P_2O_5	0.16		0.16	0.13	0.22	0.10	0.28
H_2O+	0.69				1.27	2.20	
Ba	14	352	200	256	77	56	68
Rb	2	36	17	30	2	2	2.5
Sr	130	428	168	34	224	161	287
Zr	95	224	88	110	101	66	151
Y	43		22	23	29	21	31
V	292		225	317			338
Cr	297		293		223	890	148
Co	32		38	34			47
Ni	97	124	70	73	115	315	79
Cu	77					133	191
Zn					96	57	
K/Rb	664	184	424	204	1080	415	863
K/Ba	95	19	36	24	28	15	32
Ti/Zr	94	58	79	62	122	88	102
Zr/Y	2.2	—	4.0	4.8	3.5	3.1	4.9
'Mg' (atomic)	62.9	49.2	55.8	57.2	56.5	71.2	49.8

1. Average oceanic tholeiite (Engel & others, 1965), except Rb which is averaged from the data of Kay & others (1970)
2. Average continental tholeiite (Condie & others, 1969)
3. Average of 44 Karoo dolerites:16 analyses for trace elements (Cox & Hornung, 1967)
4. Average of 19 Basutoland basalts (Cox & Hornung, 1967)
5. Average of 14 high-magnesia basalts from eastern Iceland (Wood, 1978)
6. Average of 21 olivine-poor basalts, Baffin Island (Clarke, 1970)
7. Average of plateau basalts, Blosseville Coast, east Greenland (Brooks & others, 1976)

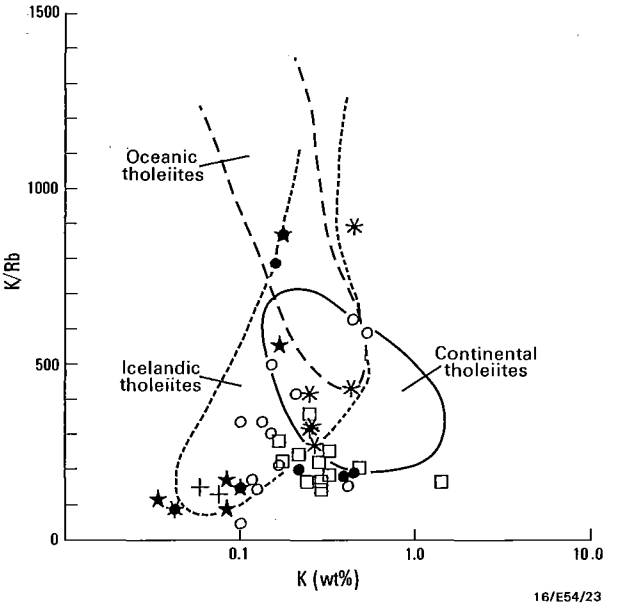

Figure 4. K/Rb v. K for the mafic rocks.
Fields of continental and oceanic tholeiites after Condie & others (1969) and Icelandic tholeiites after Sigvaldson (1974).
For explanation of symbols see Table 1.

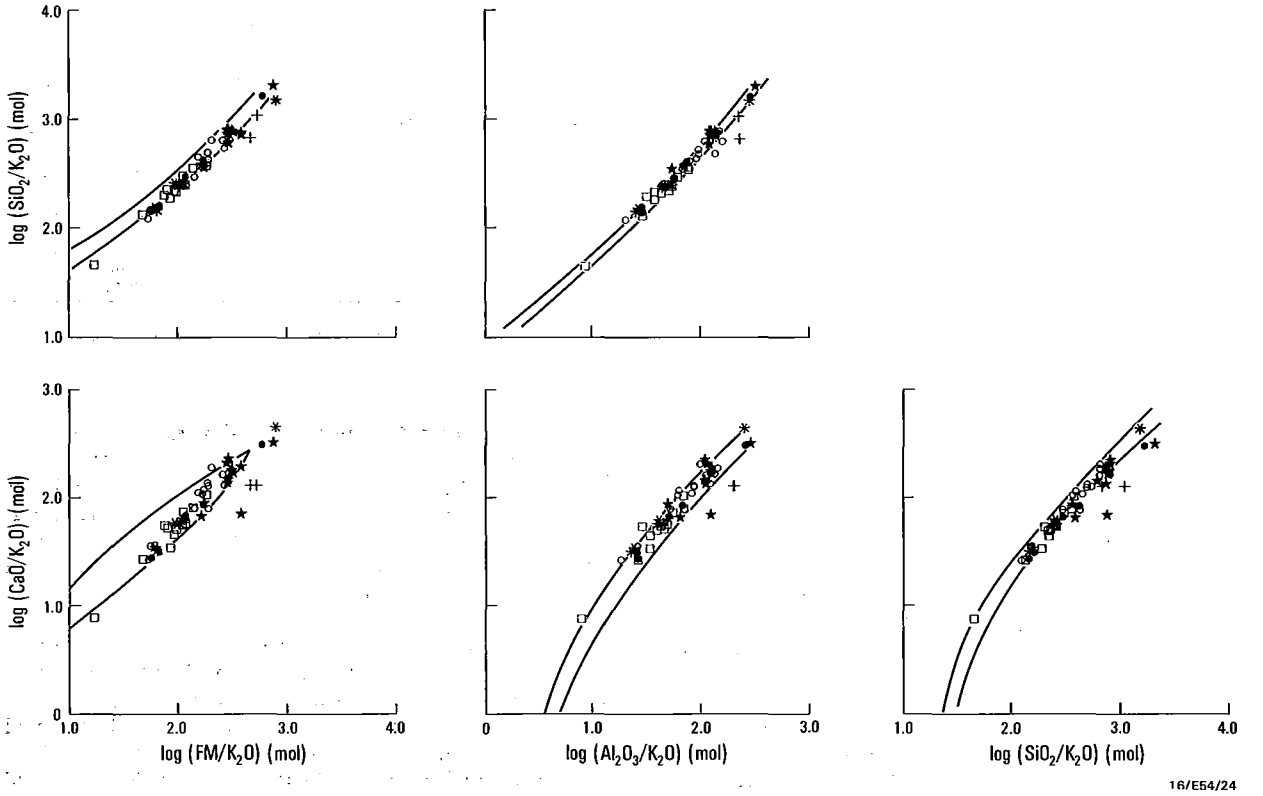

Figure 5. LMPR (log molecular proportion ratio) plots of the mafic rocks.
The delineated fields are those of least altered modern volcanic rocks after Beswick & Soucie (1978). For explanation of symbols see Table 1.

Because the FeO and MgO (as FM in the LMPR plots) appear not to have been mobilised markedly, the 'Mg' number (defined here as 100 Mg/(Mg + Fe^{2+}) atomic) should be a reliable fractionation index.

Correlation coefficients between Ti, Fe, Mn, P, Zr, Y, Nb, V, and Zn, and between Mg, Ni, and Cr are positive and mostly above 0.7 (Withnall, 1984). Such correlations are to be expected in sequences of mafic rocks showing various degrees of differentiation, and, together with the correlation of some of these elements with 'Mg' number (Figs. 6, 7), provide evidence of the preservation of magmatic features for all but the alkali and alkalinerth elements. This is in agreement with the observation of various authors (e.g. Pearce & Cann, 1973; Floyd & Winchester, 1975) that these elements, in particular Ti, Zr, Y, Nb, P, Cr, and Ni, are relatively immobile during most alteration processes, and are therefore potentially useful for discriminating between basaltic magma types in metamorphosed terrains.

Comparison between the different classes of mafic rocks in the Etheridge Group

The variation diagrams (Figs. 6, 7) indicate that the Cobbold Metadolerite that intruded the Corbett Formation and Lane Creek Formation is less fractionated than the Dead Horse Metabasalt (including its amphibolite equivalents). The higher degree of fractionation in the metabasalts is consistent with their being quartz normative on average, whereas the younger metadolerites are olivine normative (Table 1). Samples from Cobbold Metadolerite sills emplaced in or beneath the Dead Horse Metabasalt fall into two groups. Three samples are relatively fractionated, but the others are similar to the metadolerites from the upper part of the sequence. The mafic rocks from the Einasleigh Metamorphics overlap the fields of both the metabasalts and metadolerites.

The correlations between 'Mg' number and various incompatible elements (TiO_2, P_2O_5, Zr, Y, and Nb) (Figs. 6, 7) are consistent with the mafic rocks being derived from chemically similar parent magmas. However, the behaviour of the compatible elements Ni and Cr (Fig. 7) indicates that some rocks have had different fractionation histories. Although most samples show the expected depletion in Ni and Cr with decreasing 'Mg', owing to olivine and clinopyroxene fractionation, several metadolerite samples have anomalously low Cr values in spite of high 'Mg' numbers. Three of these are from layered sills in the Lane Creek Formation, and also have Ni values slightly below the main trend.

Because Zr and Nb have similar distribution coefficients for most mineral phases (Pearce & Norry, 1979), the Zr/Nb ratio will remain constant during fractionation. Therefore, if the rocks are comagmatic or derived from the same source, there should be little variation in the Zr/Nb ratio: the mean values in Table 1 are relatively constant, suggesting that the rocks are related. Ti and Y have higher distribution coefficients for clinopyroxene than Zr and Nb (Pearce & Norry, 1979) so that Ti/Zr, Y/Nb, and Zr/Y ratios should show slight systematic variation during clinopyroxene fractionation: the mean values in Table 1 show the expected variations. The less

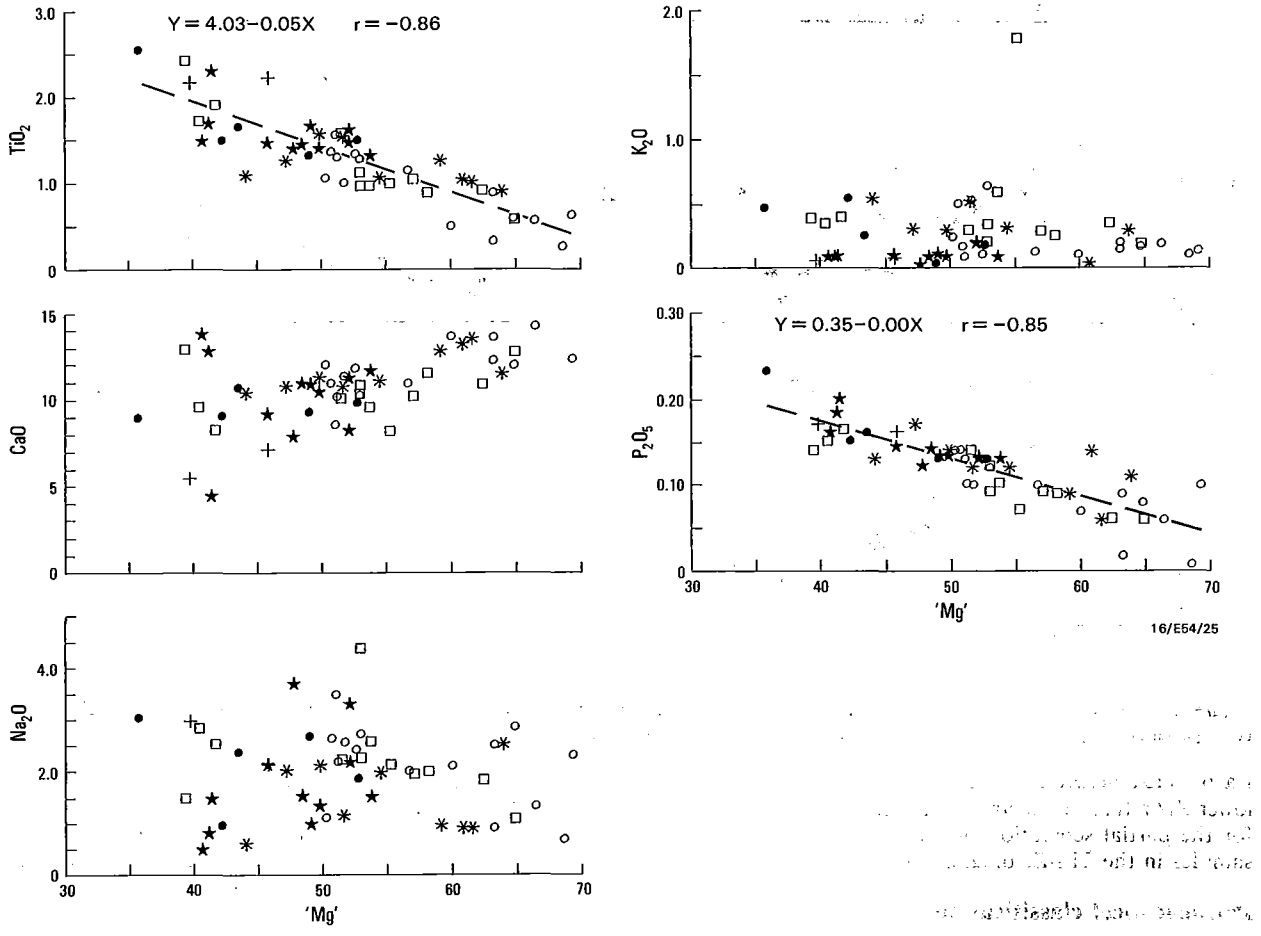

Figure 6. Major elements (in weight per cent and recalculated on a volatile-free basis) v. 'Mg' ratio (100 Mg/(Mg + Fe^{2+}) atomic) for the mafic rocks.

For explanation of symbols see Table 1. Dashed line corresponds to the printed regression equation.

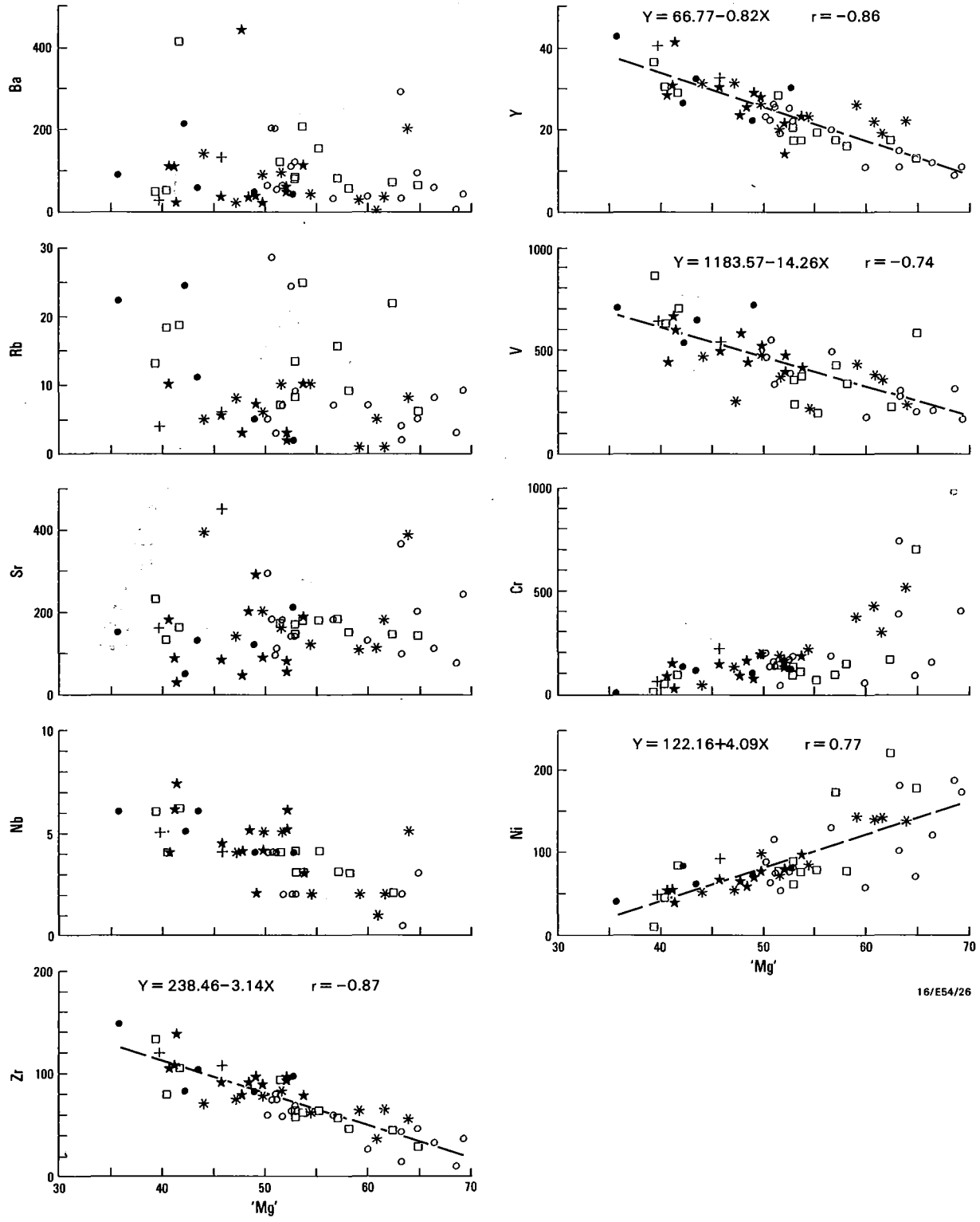

Figure 7. Trace elements (in ppm and recalculated on a volatile-free basis) v. 'Mg' ratio (100 Mg/(Mg + Fe^{2+}) atomic) for the mafic rocks. For explanation of symbols see Table 1. Dashed line corresponds to the printed regression equation.

fractionated metadolerites, have higher Ti/Zr and Y/Nb, and lower Zr/Y than the metabasalts. These variations account for the partial separation of metadolerite and metabasalt samples in the Ti-Y-Zr diagram (Fig. 9).

Petrochemical classification

The mafic rocks of this study (with two exceptions) contain less than 52.5 per cent SiO_2 on a volatile-free basis, and are therefore of basaltic composition. The Dead Horse Metabasalt is quartz normative on average, whereas the Cobbold Metadolerite is olivine normative. The rocks are hypersthene normative, indicating tholeiitic or subalkaline rather than alkaline affinities. The iron enrichment, characteristic of tholeiites is demonstrated by the FMA plot (Fig. 8).

Schemes of classification involving chemical parameters rather than mineralogy have been established for young

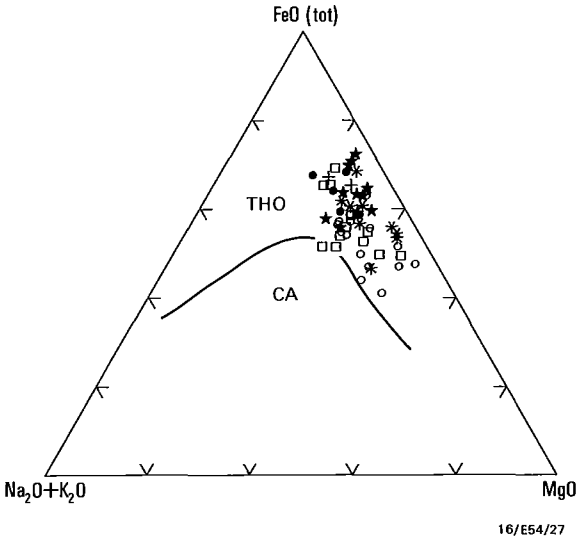

Figure 8. FeO total—MgO—alkalies for the mafic rocks.
Tholeiitic (THO) and calc-alkali (CA) fields after Irvine & Baragar (1971). For explanation of symbols see Table 1.

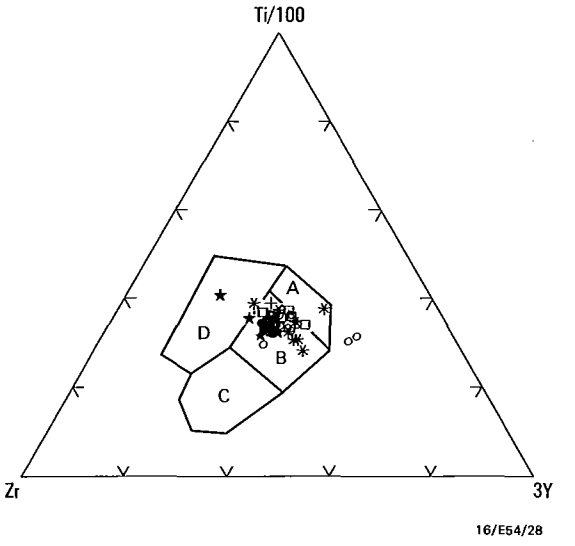

Figure 9. Ti/100—Zr—3Y plot for the mafic rocks.
Fields are low-K tholeiites (A & B), ocean-floor basalts (B), calc-alkali basalts (B & C), and within-plate basalts (D), after Pearce & Cann (1973). For explanation of symbols see Table 1.

(mostly post-Mesozoic) volcanic suites. These schemes are suited to metamorphosed suites, provided it can be established that metamorphism has been isochemical. As discussed above, although alkali and alkaline-earth elements may have been mobilised to some extent in the Proterozoic mafic rocks of the Georgetown region, most other major and various trace elements appear to be relatively unaffected.

In spite of this, the geochemistry on its own provides no unequivocal tectonic classification. Stratigraphic and sedimentological evidence (see later) indicates that the Etheridge Group was deposited in an epicontinental sea or shelf environment. Neither an ocean basin or island-arc environment is therefore likely. Nevertheless, comparisons between the average of the mafic rocks in this study and average compositions of Cainozoic tholeiitic basalts from oceanic and continental environments (Table 2, columns 1 and 2) suggest that the suite is more like ocean-floor tholeiites (N-MORB) than continental tholeiites. Data for the more immobile trace elements, when plotted on the various discrimination diagrams devised by Pearce & Cann (1973) and Pearce (1980), (e.g. figs. 9, 10, and others in Withnall, 1984), also highlight this similarity.

However, as Holm (1982) showed, most undisputed continental tholeiites of Mesozoic and Cainozoic age plot in either the ocean-floor or calc-alkali basalt fields of the Ti-Y-Zr diagram, and so these types cannot be distinguished using this diagram. Floyd & Winchester (1975) had earlier suggested that the ocean-floor field of the diagram included some non-oceanic tholeiites formed in a rifting environment. Even when the data used by Holm (1982) are plotted on the modified TiO_2-Zr diagram of Pearce (1980), more than half still fall outside the 'within-plate basalt' field, indicating that this diagram also is of limited use for recognising continental tholeiites (Fig. 10).

The K/Rb ratios (Fig. 4) are generally much lower than in N-MORB and more like those in continental tholeiites or E-MORB (ocean island tholeiites, such as in Iceland, associated with presumed mantle plumes). The Etheridge Group rocks show other geochemical similarities to the basalts from Iceland (Table 2, column 5). McNaughton & Wilson (1983) also pointed out the similarities between the mafic granulites of the Einasleigh Metamorphics and 'plume' MORB, using K/Rb ratios as well as the plots of Pearce & Cann (1975). As they also pointed out, even if K and Rb have been depleted to some extent, the low K/Rb ratios may be significant: because Rb might be expected to be more mobile than K during metamorphic depletion, the original K/Rb ratios may have been even lower.

In view of the probable continental setting inferred from non-geochemical evidence, the Etheridge Group mafic rocks can be compared with the Tertiary flood basalts of Greenland and Baffin Island (Brooks & others, 1976, Clarke, 1970). Average analyses of the more fractionated basalts of these suites are shown in Table 2. These basalts, which are similar geochemically to abyssal tholeiites (MORB), except for the higher Ba, are the best known examples of low-K tholeiites erupted in a continental environment. However, the TiO_2, P_2O_5, Zr, and Y contents of these basalts are higher than those of rocks with corresponding 'Mg' ratios from the

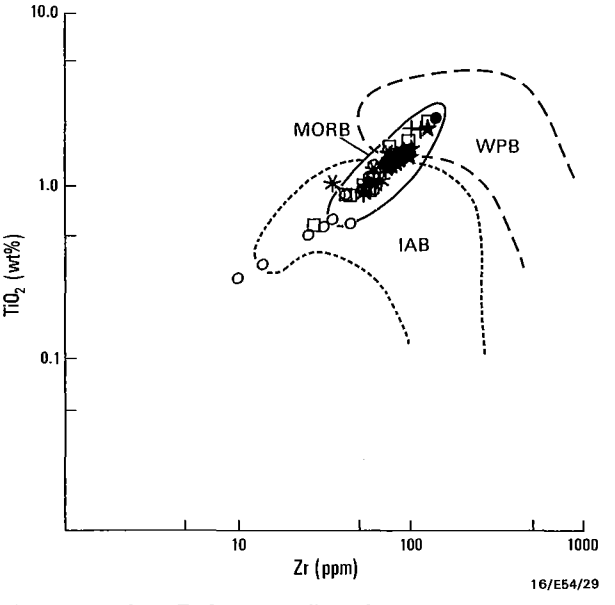

Figure 10. TiO_2 v. Zr for the mafic rocks.
Fields are within-plate basalts (WPB), mid-ocean ridge basalts (MORB), and island-arc basalts (IAB) after Pearce (1980). For explanation of symbols see Table 1.

Etheridge Group (compare Table 2, columns 6 and 7, and Figs. 6 and 7). The TiO 2 and Zr values of the Etheridge Group rocks are comparable to those in the relatively incompatible-element depleted Karoo basalts and dolerites (Table 2, columns 3 and 4), although K is higher in the Karoo rocks.

Tectonic significance and age of the mafic rocks

The Etheridge Group consists largely of shallow-water, fine-grained, quartzose to quartzofeldspathic sandstone, siltstone, and mudstone (Withnall, 1984). Although showing local evidence of rapid deposition, the various formations within the group are relatively uniform in thickness and the members within them are continuous over the more than 100 km of exposed strike length. Subsidence, although apparently rapid at times, was therefore relatively uniform over the entire exposed area. Deposition of the Etheridge Group is, accordingly, interpreted as having taken place on continental crust in a quiet stable shelf or epicontinental sea environment (Draper & others, 1981; Withnall, 1984).

The major occurrences of tholeiitic mafic rocks in continental settings, such as the Karoo, Ferrar, Deccan, and Greenland provinces, are associated with Phanerozoic plate separation. Others, such as the Columbia and Snake River plateau basalts, have been regarded as continental analogues of rocks in back-arc basins, (McDougall, 1976). In all cases an extensional environment appears to be important (Hughes, 1982).

Rifting might be expected in such an extensional tectonic environment. For example, it is a feature in the Mid-Proterozoic succession of the Mount Isa region, where it is associated with the extrusion of large quantities of tholeiitic basalts (Glikson & others, 1976; Derrick, 1982), some of which, as noted below, show similarities to those in the Etheridge Group. However, no evidence of rifting, such as coarse clastic sedimentary rocks, or penecontemporaneous faults associated with rapid thickness changes along strike, have been found in the Etheridge Group.

The absence of any evidence of rifting may be consistent with the Early Proterozoic Sm-Nd age (2400–2500 Ma), which is at least 600 Ma older than the rocks of the Mount Isa region. Various authors, including Kröner (1977, 1979) and Wynne-Edwards (1976), have postulated that tectonic processes in the Early Proterozoic involved ductile crust rather than rigid-plate motion, and spreading rather than subduction. The crust was thicker than in the Archaean, and had cooled sufficiently so that hypersolidus diapirism was no longer active. However, it was still hot enough to be capable of subsolidus ductile flow. Ductile crust could extend and thin over upwelling convecting mantle material. The surface of the crust would subside and platformal sedimentary rocks would accumulate in the depression.

The mafic rocks in the Etheridge Group could be the expression of such a process. It may be significant that the eruption of the Dead Horse Metabasalt was accompanied by a change from the shallow-water facies of the Bernecker Creek and Daniel Creek Formations to the monotonous sequence of mudstone and minor chemical sediments of the Corbett Formation, which is interpreted as a deep-water facies. This rapid subsidence may have been related to accelerated thinning. After the deposition of the Lane Creek Formation and the cessation of magmatism, shallow water conditions returned.

However, the Sm-Nd data of Black & McCulloch (1984) may be subject to alternative interpretations, and not indicate the depositional age of the Etheridge Group. All Early Proterozoic terrains in northern Australia underwent an orogenic and magmatic event between 1820 and 1920 Ma (Page & others, 1984; Etheridge & others, 1984). This is not recorded in the Georgetown Inlier, suggesting that the rocks there are younger. The Sm-Nd isochron of Black & McCulloch was derived from samples of Cobbold Metadolerite, mafic granulite from the Einasleigh Metamorphics, and granophyre from within a dyke of Cobbold Metadolerite. A more precise isochron was obtained by including two metasedimentary gneisses from the Einasleigh Metamorphics. However, these gneisses might be expected to reflect the isotopic composition of their provenance, and the granophyre may be contaminated or not chemically related to the metadolerite at all: it could have been derived by melting of the metasedimentary wall-rocks by the dolerite or by remelting of lower crustal mafic rocks. The metadolerite and granulite samples are too close to mantle isotopic compositions to provide reliable Sm-Nd ages on their own. Therefore, the Early Proterozoic age could simply reflect the isotopic composition of the metasedimentary rocks and their provenance and/or a widespread mantle-melting event and underplating of the crust, which Etheridge & others (1984) suggested occurred at about 2000–2200 Ma.

Etheridge & others (1984) further suggested that the 1820–1920 Ma event separated two tectonostratigraphic cycles. Each cycle commenced with crustal extension and rifting, accompanied by extensive bimodal volcanism and coarse fluviatile sedimentation ('rift phase'). This was followed by a transgressive, finer-grained, clastic sequence (commonly carbonaceous and with abundant carbonates), which represents widespread, post-extensional subsidence ('sag phase'). The pre-1920 Ma cycle contains fewer igneous rocks, but mafic compositions are dominant, whereas the later cycle has felsic rocks throughout and mafic rocks concentrated in the 'rift phase'. The lack of felsic rocks in the Etheridge Group is consistent with it belonging to the older cycle in spite of the absence of the 1820–1920 Ma orogeny. In either case the Etheridge Group would correspond mainly to the 'sag phase', the 'rift phase' occurring either at depth or beneath younger cover rocks beyond the Georgetown Inlier. The mafic rocks may reflect the final stages of the extensional part of the cycle.

Comparisons with the geochemistry of mafic rocks in some other northern Australian Precambrian terranes

Because of the uncertainty in the age of the Etheridge Group, it is relevant to compare the mafic rock geochemistry with that from both tectonostratigraphic cycles in other terranes in northern Australia. Such comparisons could provide clues to the age of the Etheridge Group. Average analyses and 'Mg' ratios of mafic rocks from such terranes are given in Table 3; they are best compared with rocks from the Etheridge Group by pairing them with equivalent 'Mg' ratios in the variation diagrams (Figs. 6, 7).

The mafic rocks from the Mount Isa Inlier are the best studied geochemically, and were erupted during the second tectonostratigraphic cycle. The mafic rocks from the Etheridge Group show most similarities to those from the Soldiers Cap Group and Pickwick Metabasalt Member, although Zr is slightly lower in the Etheridge Group rocks and Ce is much lower than in the Pickwick Metabasalt Member (Ce is not available for the Soldiers Cap Group). The Cromwell Metabasalt Member is much more enriched in all of the incompatible elements. The Magna Lynn Metabasalt has higher P_2O_5, Nb, Zr, Y, and Ce, and the

Table 3. Average analyses of various Precambrian tholeiitic suites, in particular those from the Mount Isa Inlier, Queensland

	1	2	3	4	5	6	7
SiO_2	48.69	48.25	49.54	50.63	48.95	48.00	48.88
TiO_2	1.62	2.77	1.43	1.60	1.79	1.03	1.57
Al_2O_3	14.04	13.28	14.09	14.45	14.21	14.55	15.42
Fe_2O_3	4.41	5.22	3.68	4.69		2.70	1.67
FeO	9.68	9.66	8.35	7.94		10.46	10.29
FeO_t	13.64	14.35	11.66	12.16	10.68	12.89	11.79
MnO	0.23	0.23	0.19	0.27	0.26	0.28	0.17
MgO	5.40	4.75	6.47	5.33	5.29	7.80	6.93
CaO	10.21	7.50	8.61	8.66	11.04	11.43	10.08
Na_2O	2.57	2.44	2.46	1.89	2.23	1.83	2.25
K_2O	0.82	1.63	1.71	1.67	0.35	0.44	0.71
P_2O_5	0.16	0.45	0.15	0.22	0.34	0.07	0.16
H_2O+	0.71			0.17	1.42	0.28	1.45
CO_2	0.33		0.53				
Ba	247	443	314	791	78	142	220
Rb	28	64	55	35	9	10	20
Sr	186	160	187	152	246	110	280
Pb	8	23	14	12	12		3
Zr	137	290	119	147	188		93
Nb		18	6		14		6
Y	33	51	27	34	40	21	
Ce		97	47		47	25	38
V	372			237	296	435	283
Cr	85			114	215	241	
Co	47			45	40	59	
Ni	56			71	75	94	
Cu	61			56	87	72	
Zn	29			75	90		
K/Rb	243	211	258	396	323	365	295
K/Ba	28	31	45	18	37	26	27
Ti/Zr	71	57	72	65	57	—	101
Y/Nb		2.8	4.5		2.9	—	3.4
Zr/Nb		16	20		13	—	16
Zr/Y	4.2	5.7	4.4	4.3	4.7	—	4.4
'Mg' (atomic)	45	40	53	47	50	35	54

1. Average of 25 metabasites from the Soldiers Cap Group, Mount Isa Inlier (Glikson & Derrick, 1978)
2. Average of 60 samples from the Cromwell Metabasalt Member of the Eastern Creek Volcanics, Mount Isa Inlier (Bultitude & Wyborn, 1982)
3. Average of 15 samples from the Pickwick Metabasalt Member of the Eastern Creek Volcanics, Mount Isa Inlier (Bultitude & Wyborn, 1982)
4. Average of 6 samples from the Marraba Volcanics, Mount Isa Inlier (Glikson & Derrick, 1978)
5. Average of 3 samples from the Magna Lynn Metabasalt, Mount Isa Inlier (Wilson, 1978)
6. Average of 13 Early Proterozoic mafic granulites from the Arunta Complex (Shaw & others, 1979, table A1)
7. Average of 12 samples of Oenpelli Dolerite, Pine Creek Province (Stuart- Smith & Ferguson, 1978)

Marraba Volcanics have higher P_2O_5 and Zr (Nb and Ce are not available). An obvious feature of the Mount Isa rocks is their much higher K_2O, although the difference is least in the rocks from the Soldiers Cap Group.

The Oenpelli Dolerite in the Pine Creek Province of the Northern Territory was also emplaced during the second cycle, at about 1720 Ma (Stuart-Smith & Ferguson, 1978). Except for having higher Ce, it is very similar to the mafic rocks from the Etheridge Group.

Analyses of mafic rocks emplaced during the first cycle are available from the Arunta Complex (Shaw & others, 1979). They show much greater depletion in TiO_2 and P_2O_5 than the Georgetown rocks, but Ce is higher. No analyses are available for Y and Nb, and only one of the samples was analysed for Zr. No other analyses of first-cycle mafic rocks from northern Australia are presently available for comparison.

Conclusions

Proterozoic extrusive and intrusive mafic rocks in the Georgetown Inlier represent a tholeiitic suite emplaced in at least two pulses during the deposition of the lower half of the Etheridge Group. The Etheridge Group is mainly a shallow-water sedimentary sequence, interpreted as having been deposited on a shelf or in an epicontinental sea. This conflicts with the interpretation from some geochemical discrimination diagrams that the mafic rocks are oceanic or low-K (arc) tholeiites. The mafic rocks of the Etheridge Group can be compared most closely with the K-poor Tertiary continental tholeiites of Greenland and Baffin Island, and the relatively incompatible-element-depleted Karoo basalts and dolerites.

The mafic rocks may be the expression of convective mantle upwelling, which produced extension of the sialic crust and the formation of a shallow epicontinental sea, in which the Etheridge Group was deposited. Whether there was an early rifting phase is not known. It is also uncertain whether the Etheridge Group was formed during the first or second of the major Proterozoic tectonostratigraphic cycles now recognised in northern Australia, or whether it is even older. Except for having lower Ce, the mafic rocks from the Etheridge Group are similar geochemically to some second-cycle mafic rocks from the Mount Isa and Pine Creek areas.

Analyses of more first-cycle mafic rocks and further analyses of samples from some suites already studied, to provide a uniform range of elements, are needed to allow better comparisons between rocks of the two cycles and to determine whether the Etheridge Group rocks show greater similarities to rocks from one or other cycle. However, in view of the chemical variation in rocks from one cycle in the Mount Isa area, geochemistry is unlikely to provide conclusive evidence on the age of the Etheridge Group, and further isotopic studies will probably be necessary.

Acknowledgements

The Bureau of Mineral Resources provided most of the analytical results, either from its own laboratories or under contract from the Australian Mineral Development Laboratories. The Queensland Government Analyst also provided some of the results, and Dr N.J. McNaughton and Mr R.D. Holmes allowed me to use several analyses from their Ph.D. theses. Data processing was carried out at the BMR using programs written by Dr M. Owen. Fruitful discussions have been held with Drs B.S. Oversby, D.E. Mackenzie (BMR), and N.J. McNaughton (formerly University of Queensland), and Mr J.H.C. Bain (BMR). The paper benefitted from constructive criticism made by Drs Mackenzie and A.L. Jaques (BMR) and an anonymous reviewer. The paper is published with the permission of the Chief Government Geologist, Department of Mines, Queensland. The figures were drafted by I. Hartig.

References

Bain, J.H.C., Withnall, I.W., & Oversby, B.S., 1976 — Geology of the Forsayth 1:100 000 Sheet area (7660) north Queensland — Georgetown project progress report. *Bureau of Mineral Resources, Australia, Record* 1976/4.

Beswick, A.E., & Soucie, G., 1978 — A correction procedure for metasomatism in an Archaean greenstone belt. *Precambrian Research*, 6, 235–248.

Black, L.P., & McCulloch, M.T., 1984 — Sm-Nd ages of the Arunta, Tennant Creek and Georgetown Inliers of northern Australia. *Australian Journal of Earth Sciences*, 31, 49–60.

Black, L.P., Bell, T.H., Rubenach, M.J., & Withnall, I.W., 1979 — Geochronology of discrete structural-metamorphic events in a multiply deformed Precambrian terrain. *Tectonophysics*, 54, 103–137.

Bultitude, R.J., & Wyborn, L.A.I., 1982 — Distribution and geochemistry of volcanic rocks in the Duchess-Urandangi region, Queensland. *BMR Journal of Australian Geology & Geophysics*, 7, 99–112.

Brooks, C.K., 1976 — The Fe_2O_3/FeO ratio of basalt analyses: an appeal for a standardised procedure. *Bulletin of Geological Society of Denmark*, 25, 117–120.

Brooks, C.K., Nielsen, T.F.D., & Petersen, T.S., 1976 — The Blosseville Coast basalts of east Greenland: their occurrence, composition and temporal variations. *Contributions to Mineralogy and Petrology*, 58, 279–292.

Clarke, D.B., 1970 — Tertiary basalts of Baffin Bay: possible primary magma from the mantle. *Contributions to Mineralogy and Petrology*, 25, 203–224.

Clough, P.W.L., & Field, D., 1980 — Chemical variation in metabasites from a Proterozoic amphibolite—granulite transition zone, South Norway. *Contributions to Mineralogy and Petrology*, 73, 277–286.

Condie, K.C., Barsky, C.K., & Mueller, P.A., 1969 — Geochemistry of Precambrian diabase dykes from Wyoming. *Geochimica et Cosmochimica Acta*, 33, 1371–1388.

Cox, K.G., & Hornung, G., 1967 — The petrology of the Karoo basalts of Basutoland. *American Mineralogist*, 51, 1414–1432.

Derrick, G.M., 1982 — A Proterozoic rift zone at Mount Isa, Queensland, and implications for mineralisation. *BMR Journal of Australian Geology & Geophysics*, 7, 81–92.

Draper, J.J., Mackenzie, D.E., & Withnall, I.W., 1981 — Proterozoic shelf sedimentation in the Georgetown Inlier, northeastern Queensland. *In* Sediments through the ages. Fifth Australian Geological Convention, Perth, August 1981, *Geological Society of Australia, Abstracts*, 3, 42–43.

Engel, A.E.J., & Engel, C.G., 1962 — Progressive metamorphism of amphibolite, northwest Adirondack Mountains, New York. *In* Engel, A.E.J., James, H.L., & Leonard, B.F., (editors), Petrologic studies: a volume in honour of A.F. Buddington. *Geological Society of America*, 37–82.

Engel, A.E.J., Engel, C.G., & Havens, R.G., 1965 — Chemical characteristics of oceanic basalts and upper mantle. *Bulletin of the Geological Society of America*, 76, 719–734.

Etheridge, M.A., Wyborn, L.A.I., Rutland, R.W.R., Page, R.W., Blake, D.H., & Drummond, B.J., 1984 — Workshop on Early to Middle Proterozoic of northern Australia, 5-6 November, 1984. The BMR model - a discussion paper. *Bureau of Mineral Resources, Australia, Record* 1984/31.

Floyd, P.A., & Winchester, J.A., 1975 — Magma type and tectonic setting discrimination using immobile elements. *Earth and Planetary Science Letters*, 27, 211–218.

Glikson, A.Y., & Derrick, G.M., 1978 — Geology and geochemistry of Middle Proterozoic basic volcanic belts, Mount Isa/Cloncurry, northwestern Queensland. *Bureau of Mineral Resources, Australia, Record* 1978/48.

Glikson, A.Y., Derrick, G.M., Wilson, I.H., & Hill, R.M., 1976 — Tectonic evolution and crustal setting of the Middle Proterozoic Leichhardt River fault trough, Mt Isa region, northwestern Queensland. *BMR Journal of Australian Geology & Geophysics*, 1, 115–129.

Green, D.H., Edgar, A.D., Beasley, P., Kiss, E., & Ware, N.G., 1974 - Upper mantle source for some hawaiites, mugearites, and benmoreites. *Contributions to Mineralogy and Petrology*, 48, 33–43.

Hart, S.R., 1969 — K, Rb, Cs contents and K/Rb, K/Cs ratios of fresh and altered submarine basalts. *Earth and Planetary Science Letters*, 6, 295–303.

Holm, P.E., 1982 — Non-recognition of continental tholeiites using the Ti-Y-Zr diagram. *Contributions to Mineralogy and Petrology*, 79, 308–310.

Hughes, C.J., 1982 — Igneous petrology. *Elsevier, Amsterdam.*

Humphris, S.E., & Thompson, G., 1978a — Hydrothermal alteration of oceanic basalts by seawater. *Geochimica et Cosmochimica Acta*, 42, 107–125.

Humphris, S.E., & Thompson, G., 1978b — Trace element mobility during hydrothermal alteration of oceanic basalts. *Geochimica et Cosmochimica Acta*, 42, 127–136.

Irvine, T.N., & Baragar, W.R.A., 1971 — A guide to the chemical classification of the common volcanic rocks. *Canadian Journal of Earth Sciences*, 8, 523–548.

Jolly, W.T., 1980 — Development and degradation of Archaean lavas, Abitibi area, Canada, in light of major element geochemistry. *Journal of Petrology*, 21, 323–363.

Jolly, W.T., & Smith, R.E. , 1972 — Degradation and metamorphic differentiation of the Keweenawan tholeiitic lavas of northern Michigan, USA. *Journal of Petrology*, 13, 272–309.

Kay, R.W., Hubbard, N.J., & Gast, P.W., 1970 — Chemical characteristics and origin of oceanic ridge volcanic rocks *Journal of Geophysical Research*, 75, 1585–1613.

Kröner, A., 1977 — Precambrian mobile belts of southern and eastern Africa — ancient sutures or sites of ensialic mobility? *Tectonophysics*, 40, 101–135.

Kröner, A., 1979 — Precambrian crustal evolution in the light of plate tectonics and the undation theory. *Geologie en Mijnbouw*, 58, 231–240.

McDougall, I., 1976 — Geochemistry and origin of the Columbia River Group, Oregon and Washington. *Bulletin of the Geological Society of America*, 87, 777–792.

McNaughton, N.J., 1979 — The extent and age of a granulite facies metamorphism in the Einasleigh Metamorphics east of the Newcastle Range, north Queensland. *Queensland Government Mining Journal*, 80, 126–131.

McNaughton, N.J., 1980 — An isotopic, geochemical, and structural study of the Proterozoic Einasleigh Metamorphics, northern Queensland. *Ph.D. Thesis, University of Queensland.*

McNaughton, N.J., & Wilson, A.F., 1983 — The geochemical and oxygen isotope affinities of Proterozoic mafic granulites from the Einasleigh Metamorphics, northern Queensland. *Precambrian Research*, 21, 21–37.

Menzies, M., & Seyfried, W.E., 1979 — Basalt—seawater interaction; trace element and strontium isotopic variations in experimentally altered glassy basalt. *Earth & Planetary Science Letters*, 44, 463–472.

Oversby, B.S., Withnall, I.W., Baker, E.M., & Bain, J.H.C., 1978 — Georgetown project progress report — Geology of the Georgetown 1:100 000 Sheet area (7661), north Queensland; part A. *Bureau of Mineral Resources, Australia, Record* 1978/44.

Page, R.W., McCulloch, M.T., & Black, L.P. 1984 — Isotopic record of major Precambrian events in Australia. *Proceedings of the 27th International Geological Congress*, 5.

Pearce, J.A., 1980 — Geochemical evidence for the genesis and eruptive setting of lavas from Tethyan ophiolites. *Proceedings of the International Ophiolite Symposium, Cyprus 1979*, 261–272.

Pearce, J.A., & Cann, J.R., 1973 — Tectonic setting of basic volcanic rocks determined using trace element analysis. *Earth and Planetary Science Letters*, 19, 290–300.

Pearce, J.A., & Norry, M.J., 1979 — Petrogenetic implications of Ti, Zr, Y and Nb variations in volcanic rocks. *Contributions to Mineralogy and Petrology*, 69, 33–47.

Shaw, R.D., Langworthy, A.P., Offe, L.A., Stewart, A.J., Allen, A.R., & Senior, B.R., 1979 — Geological report on 1:100 000-scale mapping of the southeastern Arunta Block, Northern Territory. *Bureau of Mineral Resources, Australia, Record* 1979/47; *BMR Microform* MF133.

Sigvaldason, G.E., 1974 — Basalts from the centre of the assumed Icelandic mantle plume. *Journal of Petrology*, 15, 497–524.

Smith, R.E., 1968 — Redistribution of major elements in the alteration of some basic lavas during burial metamorphism. *Journal of Petrology*, 9, 191–219.

Stuart-Smith, P.G. & Ferguson, J., 1978 — The Oenpelli Dolerite - a Precambrian continental tholeiitic suite from the Northern Territory, Australia. *BMR Journal of Australian Geology & Geophysics*, 3, 125–133.

Vallance, T.G., 1974 — Spilitic degradation of a tholeiitic basalt. *Journal of Petrology*, 15, 79–96.

White, D.A., 1959 — New stratigraphic units in north Queensland geology. *Queensland Government Mining Journal*, 60, 442–447.

White, D.A., 1965 — The geology of the Georgetown/Clarke River area, Queensland. *Bureau of Mineral Resources, Australia, Bulletin* 71.

Wilson, I.H., 1978 — Volcanism on a Proterozoic continental margin in northwestern Queensland. *Precambrian Research*, 7, 205–235.

Withnall, I.W., 1981 — Mines and mineral deposits of the Gilberton 1:100 000 Sheet area. *Geological Survey of Queensland, Publication* 370.

Withnall, I.W., 1983 — The Robertson River Subgroup and Cobbold Metadolerite — revised units in the Georgetown Inlier, north Queensland. *Queensland Government Mining Journal*, 84, 182–190.

Withnall, I.W., 1984 — Stratigraphy, structure and metamorphism of the Proterozoic Etheridge and Langlovale Groups, central Georgetown Inlier, north Queensland. *Geological Survey of Queensland, Record* 1984/59 (unpublished).

Withnall, I.W., & Mackenzie, D.E., 1980 — New and revised stratigraphic units in the Proterozoic Georgetown Inlier, north Queensland. *Queensland Government Mining Journal*, 81, 28–43.

Withnall, I.W., & Mackenzie, D.E., 1981 — Precambrian stratigraphy, metamorphism, and structure of the North Head—Forest Home area, north Queensland. *Bureau of Mineral Resources, Australia, Record* 1981/63.

Withnall, I.W., Bain, J.H.C., & Rubenach, M.J., 1980a — The Precambrian geology of northeast Queensland. *In* Henderson, R.A., & Stephenson, P.J., (editors), The geology and geophysics of northeastern Australia. *Geological Society of Australia Inc., Queensland Division, Brisbane*, 109–127.

Withnall, I.W., Oversby, B.S., Baker, E.M., & Bain, J.H.C., 1980b - Geology of the Gilberton 1:100 000 Sheet area (7659), north Queensland: data record. *Bureau of Mineral Resources, Australia, Record* 1980/2.

Wood, D.A., 1978 — Major and trace element variations in the Tertiary lavas of eastern Iceland and their significance with respect to the Iceland geochemical anomaly. *Journal of Petrology*, 393–436.

Wynne-Edwards, H.R., 1972 - Proterozoic ensialic orogenesis; the millipede model of ductile plate tectonics. *American Journal of Science*, 276, 927–953.

Appendix

Forty-nine samples of mafic rocks were analysed for major elements at either the Australian Mineral Development Laboratories (AMDEL) or the Queensland Government Analyst (QGA), using a combination of X-ray fluorescence (XRF), atomic absorption (AAS), and classical techniques. Most trace elements were determined F at BMR and AMDEL. Cu, Pb, Zn, Cr, Ni, and Co were determined at BMR by either XRF or AAS after HF digestion. These elements, as well as V, were also determined by emission spectroscopy by the QGA, but, where available, the BMR results are used. Three additional analyses of major rocks from the Einasleigh Metamorphics by McNaughton (1980) and two by Holmes (personal communication) from the Cobbold Metadolerite are also included in the study.

The data were stored on disc and processed by the author on a Hewlett-Packard 9825 microcomputer and plotter at BMR, using programs written by M. Owen. The analyses have been tabulated by Withnall (1984).

In the various plots of chemical data and in the averages presented in Table 1, the samples have been divided into the following categories:

1. Dead Horse Metabasalt (greenschist facies metabasalt). These eleven samples are from the greenschist facies and are all considered to be extrusive. They are predominantly unfoliated, the exception being a chlorite schist containing about 20 per cent calcite (75300348).
2. Dead Horse Metabasalt (amphibolite facies equivalents). These five samples of foliated amphibolite were collected from areas interpreted as high-grade equivalents of the Dead Horse Metabasalt. Most are fine grained and probably represent metamorphosed lavas, although one sample (GSQ/R5310), which is coarser grained, may have been intrusive.
3. Cobbold Metadolerite. The metadolerite samples were divided into two categories according to the stratigraphic level at which they were intruded.
   (a) Twelve samples of Cobbald Metadolerite from within or stratigraphically below the Dead Horse Metabasalt were analysed. Eight of these were metamorphosed to greenschist facies, and the remaining ones to amphibolite facies. All of the samples are unfoliated. Most retain at least some igneous textures.
   (b) Fifteen samples of Cobbold Metadolerite from above the metabasalt were analysed. Thirteen samples are from sills intruding the Lane Creek Formation, and two are from the Corbett Formation. Only one sample in this category (from the Corbett Formation) was metamorphosed to greenschist facies. The remainder were metamorphosed to amphibolite facies, and all are unfoliated. Most retain some igneous textures, but several samples are completely recrystallised and have a granuloblastic texture.
4. Einasleigh Metamorphics. Nine samples are included in this study. Three samples are of mafic granulite and the remainder are of amphibolite, but they are considered as a single category in this study. Most of the amphibolite samples are well foliated, but two have blastophitic textures.
5. Xenoliths. Two samples of mafic xenoliths ccontaining unusual mineralogy were analysed. The xenoliths (GSQ/R5294 and 5299), which were in normal metadolerite, contain abundant cummingtonite and gedrite, respectively.

BMR Journal of Australian Geology & Geophysics, 9, 353-359

Cretaceous coccoliths in the middle Eocene of the western and southern margins of Australia: evidence of a significant reworking episode

Samir Shafik[1]

A reworking episode is indicated by occurrences of upper Cretaceous coccoliths among middle Eocene assemblages in four basins (Carnarvon, Perth, Eucla, and Otway Basins) along the Australian western and southern margins. The episode falls within the coccolith biostratigraphic interval from the lowest occurrence of *Cyclicargolithus reticulatus* to the highest occurrence of *Daktylethra punctulata*, which correlates with the foraminiferal zonal interval P.12–P.13. At the time of the episode (about 45–44 Ma) the sea advanced along the southern margin from the west, causing a transgression in the Eucla Basin and an ingression in the Otway Basin. Coincident with this sea-level rise, and probably the cause of it, was a major acceleration in the spreading rate south of Australia. In the absence of known in-situ occurrences of upper Cretaceous coccoliths on the southern margin or offshore to the south, the Naturaliste Plateau is thought to have been the most likely provenance for the reworked taxa in the Eocene of the Eucla and Otway Basins — short-lived strong currents stripped off coccolith-rich upper Cretaceous sediments on the plateau and transported them eastward. In the Perth Basin a local source, the upper Cretaceous coccolith-rich Gingin Chalk/Lancelin Beds, is suggested for the reworked taxa, whereas in the Carnarvon Basin a distant source is more likely.

Introduction

My studies of the biostratigraphy of the early Tertiary calcareous nannofossils of the Australian region (Shafik, 1973, 1978a, 1983) indentified occurrences of upper Cretaceous coccolith taxa among Eocene assemblages in four basins situated along the western and southern margins of Australia, from northwest to southeast, the Carnarvon, Perth, Eucla, and Otway Basins (Fig. 1). The occurrences in the Eucla and Otway Basins are anomalous, because in-situ upper Cretaceous coccoliths are not known there or in the offshore areas to the south.

Coccoliths are prone to reworking because of their very small size and their usual great abundance. Detection of reworking in an assemblage can be difficult if the stratigraphic gap between the indigenous and reworked taxa is short. However, in the present case this gap is not only great (late Cretaceous–Eocene) but also, because of the mass extinction of Cretaceous coccoliths at the Cretaceous/Tertiary boundary and appearance of new forms during the early Tertiary, differentiation of the reworked taxa is a simple matter.

This paper explores the significance of the reworked upper Cretaceous coccoliths in the middle Eocene of the Australian western and southern margins and attempts to locate their provenance, particularly for those in the Eucla and Otway Basins.

Carnarvon Basin

The lower Tertiary sequence of the Carnarvon Basin is best exposed along the flanks of the Giralia Anticline and nearby structures, where Paleocene greensand and calcarenites (containing coccoliths) underlie the Eocene Jubilee and Giralia Calcarenites. The facies of the Eocene calcarenites is unsuitable for coccoliths, but their subsurface equivalents further north include facies with abundant coccoliths. Four WAPET wells from these northern areas (Fig. 2A), Ningaloo-1, Rough Range South-1, Long Island-1, and Pasco-1, contain reworked upper Cretaceous coccolith taxa in association with middle Eocene assemblages.

The indigenous coccoliths are generally well preserved in most of the Eocene of the sections studied. However, within the relevant interval (middle Eocene levels with the reworked taxa), they are distinctly poorly preserved. It appears that the reworked taxa occur at more than one level within the middle Eocene biostratigraphic interval bracketed by the lowest occurrence of *Cyclicargolithus reticulatus* and the highest occurrence of *Daktylethra punctulata*, an interval within which a regional unconformity is suspected.

Perth Basin

Shafik (1978a) recorded a middle Eocene coccolith assemblage from the Rottnest Island Bore (Fig. 2B) in the Perth Basin. Before then, the known marine lower Tertiary of the Perth Basin was limited to the late Paleocene and earliest Eocene calcareous microfossils of the Kings Park Formation.

The Rottnest Island Bore assemblage (Shafik, 1978a) also contains reworked upper Cretaceous coccolith taxa of Campanian to early Maastrichtian age. These taxa include the cosmopolitan forms *Arkhangelskiella cymbiformis*, *Ahmuellerella octoradiata*, *Biscutum blackii*, *Broinsonia parca*, *Cretarhabdus crenulatus*, *Cribrosphaerella ehrenbergii*, *Cribrocorona gallica*, *Eiffellithus eximius*, *E. turriseiffeli*, *Gartnerago obliquum*, *Lithraphidites carniolensis*, *Micula staurophora*, *Prediscosphaera cretacea*, *P. spinosa*, *Vekshinella imbricata*, *Watznaueria barnesae*, and *Zygodiscus diplogrammus*, in addition to the nearshore forms *Kamptnerius magnificus*, *Lucianorhabdus cayeuxii*, *Calculites obscurus*, and *C. ovalis*. It is worth noting that nearshore species are usually the least resistant to destruction.

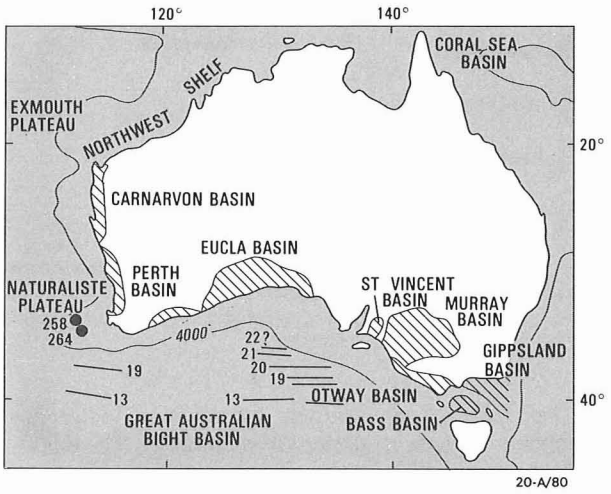

Figure 1. Sketch map of Australia and surroundings, showing the sedimentary basins of the Australian western and southern margins, and the Naturaliste Plateau.

Note that anomalies 19 to 22 south of Australia are remodelled as 20 to 34 by Cande & others (1981).

[1] Division of Marine Geosciences & Petroleum Geology, BMR

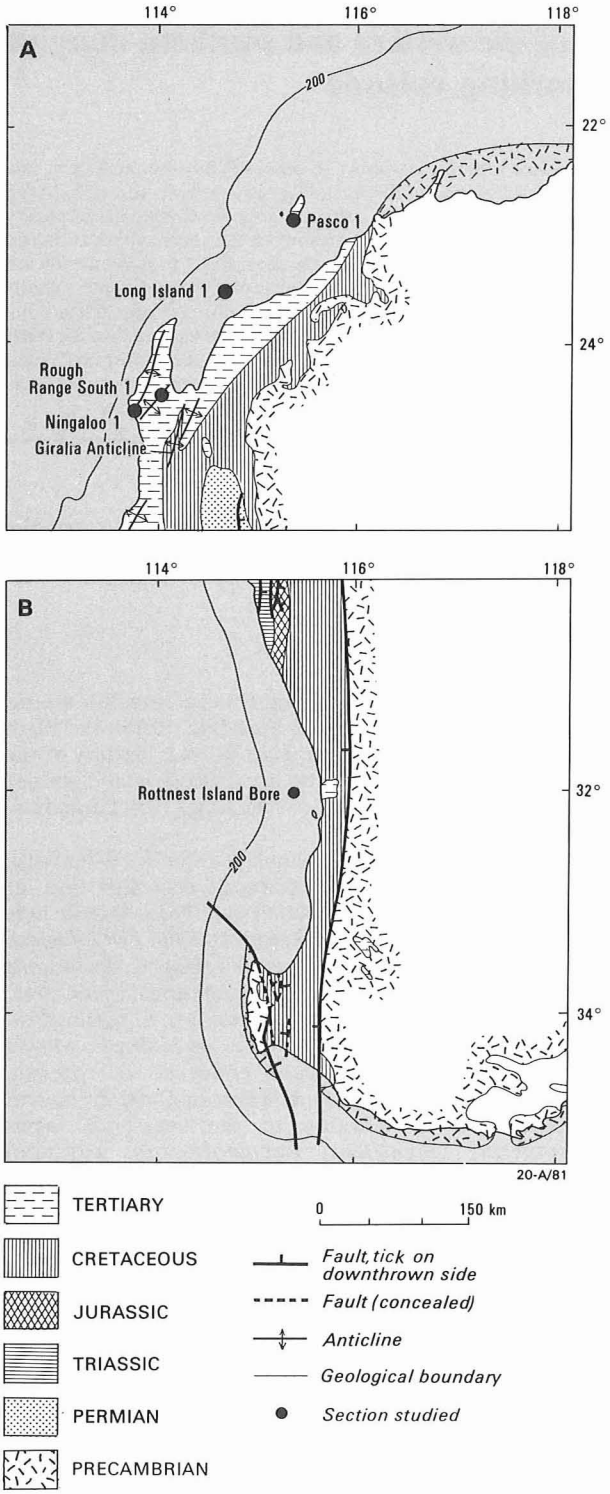

Figure 2. Location of material studied from the Australian western margin: (A) Carnarvon Basin, and (B) Perth Basin.
Note that the widely occurring Cretaceous sediments in both basins include upper Cretaceous units rich in coccoliths.

The key taxa of the Rottnest Island Bore indigenous assemblage include *Chiasmolithus grandis*, *C. solitus*, *Cyclicargolithus reticulatus*, *Cyclococcolithus formosus*, *Discoaster barbadiensis*, *D. tani nodifer*, *D. saipanensis*, *Helicosphaera compacta*, *H. reticulata*, *Reticulofenestra scrippsae*, *R. umbilica*, *Daktylethra punctulata*, and *Pemma papillatum* (Shafik, 1978a). The evidence, discussed by Shafik (1978a), seems to suggest that this middle Eocene assemblage represents a short-lived transgression or a major ingression in the basin.

Eucla Basin

The lower Tertiary sequence of the Eucla Basin is composed of the Hampton Sandstone (or its probable correlative, the Pidinga Formation) and the overlying Wilson Bluff Limestone. It rests disconformably on the Cretaceous Madura Formation or on Permian and Proterozoic rocks. The contact is not exposed and the lowest part of the Tertiary sequence is known only from bore holes. Material studied, representing the Hampton Sandstone and the basal Wilson Bluff Limestone, came from four sections (Fig.3): Guinewarra and Albala Karoo Bores (in South Australia) and Eyre-1 and Gambanga-1 wells (in Western Australia). In all these sections, reworked upper Cretaceous taxa were encountered consistently at the base of the marine Tertiary sequence, immediately above the disconformity with the older rocks. The indigenous assemblages, containing the reworked taxa are middle Eocene and similar in the four sections. Their main elements include *Chiasmolithus grandis*, *Cyclicargolithus reticulatus*, *Helicosphaera compacta*, *H. reticulata*, *Reticulofenestra umbilica*, *R. scrippsae*, and *Neococcolithes dubius. Chiasmolithus solitus* is either very rare or absent, and a form similar to *Reticulofenestra scissura* is present. The reworked taxa include *Arkhangelskiella cymbiformis*, *Eiffellithus eximius*, *E. turriseiffeli*, *Gartnerago obliquum*, *Lithastrinus floralis, Micula staurophora, Prediscosphaera cretacea*, and *Watznaueria barnesae*. Although these reworked taxa are rare, they are undoubtedly more abundant and more diversified than those reworked in the middle Eocene of the Otway Basin to the east (see below). The reverse is true when compared with the reworked taxa in the middle Eocene of the Perth Basin to the west.

Otway Basin

The lower Tertiary sequence in the western portion of the Otway Basin (Gambier Embayment) comprises a clastic section of sand grit, silt, clay, and a little marl (Knight Formation, Kongorong Sand, and Lacepede Formation, in ascending order), and an overlying carbonate unit (Gambier Limestone). Coccoliths are absent from the lower part of the clastic section (Knight Formation) and their record higher in the section (lower part of the combined Kongorong Sand/Lacepede Formation) is noticeably discontinuous before becoming continuous. The counterpart clastic section in the eastern part of the basin at Browns Creek is composed of sand, clay, and marl (Johanna River Sand and Browns Creek Clays), and its lower part (Johanna Sand) is devoid of coccoliths.

In a study of the coccolith biostratigraphy of the Eocene of several Otway Basin sections (Fig. 4), I concluded (Shafik, 1983) that middle Eocene marine ingressions, represented by isolated assemblages, occurred in the Gambier Embayment, but did not reach the eastern parts of the basin. Reworked upper Cretaceous taxa were encountered in a single section in the Gambier Embayment (Beachport-1) among an assemblage containing the key species *Chiasmolithus expansus*, *C. grandis*, *C. solitus*, *Cyclicargolithus reticulatus*, and *Daktylethra punctulata*. A coeval assemblage, described as representing the first middle Eocene marine ingression in the Gambier Embayment, was also identified (Shafik, 1983) in Kingston Construction Camp Bore (Fig. 4).

The reworked upper Cretaceous taxa in the Beachport-1 middle Eocene amount only to a few specimens of a very

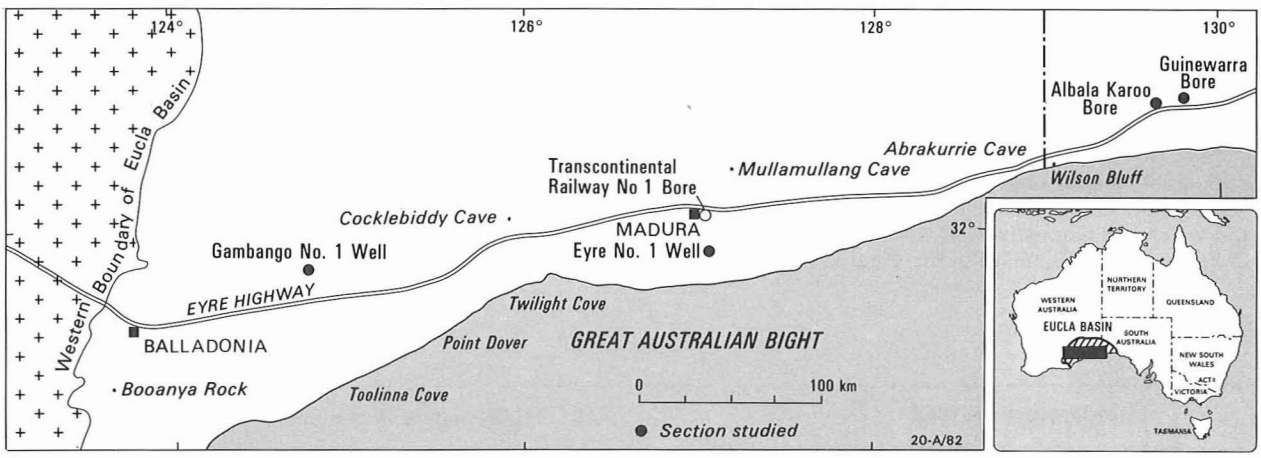

Figure 3. Location of material studied from the Eucla Basin.

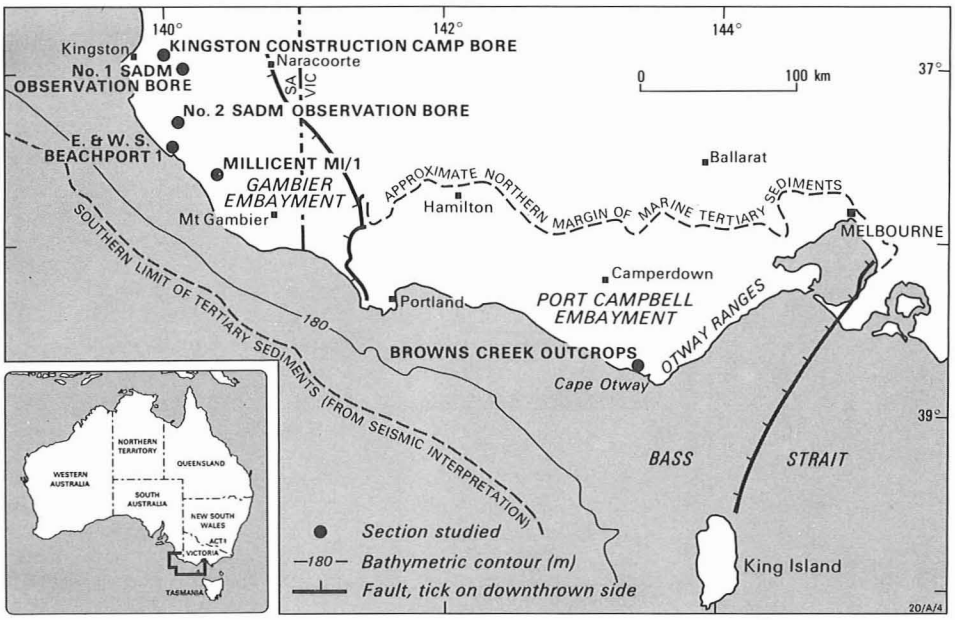

Figure 4. Location of material studied from the Otway Basin.

few species. They include *Watznaueria barnesae* and *Prediscosphaera cretacea*, species highly resistant to destruction, and usually among the more common taxa in indigenous Cretaceous assemblages.

Discussion

The Otway Basin assemblage (Beachport-1) and the Rottnest Island Bore assemblage from the Perth Basin share the same indigenous key species, *Chiasmolithus grandis*, *C. solitus*, *Cyclicargolithus reticulatus*, and *Daktylethra punctulata*. The presence of *Chiasmolithus solitus* in association with *Cyclicargolithus reticulatus* suggests a correlation within the low-latitude foraminiferal zone P.12, at about the 45–44 Ma (Shafik, 1978a, 1983). Except for *Chiasmolithus solitus*, which is either very rare or absent from the relevant assemblages in the Carnarvon and Eucla Basins sections, other key taxa, including *Cyclicargolithus reticulatus* and *Daktylethra punctulata*, are the same as those in the Beachport-1 and Rottnest Island Bore assemblages. A correlation with a level near the foraminiferal zonal boundary P.12/P.13 is suggested. This is consistent with the occurrence only of forms similar to *Reticulofenestra scissura*, and not the typical form, in the Eucla Basin assemblages; typical *R. scissura* in association with *Daktylethra punctulata* indicates a younger correlation within the foraminiferal zone P.13.

In the four basins studied, the coccolith assemblages containing the reworked upper Cretaceous taxa are contemporaneous, being assignable to the middle Eocene biostratigraphic interval from the lowest occurrence of *Cyclicargolithus reticulatus* to the highest occurrence of *Daktylethra punctulata*. The implication is that the occurrences of the reworked upper Cretaceous taxa in the middle Eocene of the four basins are coeval and can, therefore, be considered as a single reworking episode. That the reworked taxa are restricted to the basal part of the Tertiary sections studied from the Eucla Basin and to a single horizon in the Beachport-1 in the western Otway Basin suggests that the agents responsible for the reworking episode along the southern margin were short-lived.

At the time of the reworking episode and immediately after, i.e. during the interval post-dating the lowest occurrence of *Cyclicargolithus reticulatus*, but before the extinction of *Daktylethra punctulata* (foraminiferal zonal interval P.12–P.13) the depositional scenarios in the four basins (Shafik, 1984) were different in detail, though apparently

related: a normal pre-existing shelf setting in the Carnarvon Basin, which apparently was interrupted briefly sometime before the end of the interval; a short-lived transgression (or a pronounced ingression) in the Perth Basin, which started and ended in the mid middle Eocene; initial stages of a transgression in the Eucla Basin, which persisted into the late Eocene; and marine ingressions in the Gambier Embayment of the Otway Basin, which did not reach the east of the basin and which, subsequently, were followed by a transgression at the end of the middle Eocene (Shafik, 1983).

Western margin

The reworked upper Cretaceous coccolith taxa in the middle Eocene of the Perth Basin (Rottnest Island Bore) are unlikely to have been transported far, because they include species prone to destruction (particularly those indicative of nearshore deposition). Coccolith-rich upper Cretaceous sediments in the Perth Basin (Gingin Chalk and Lancelin Beds) also contain these relatively fragile taxa (including those indicative of nearshore deposition) (Shafik, 1978b, and

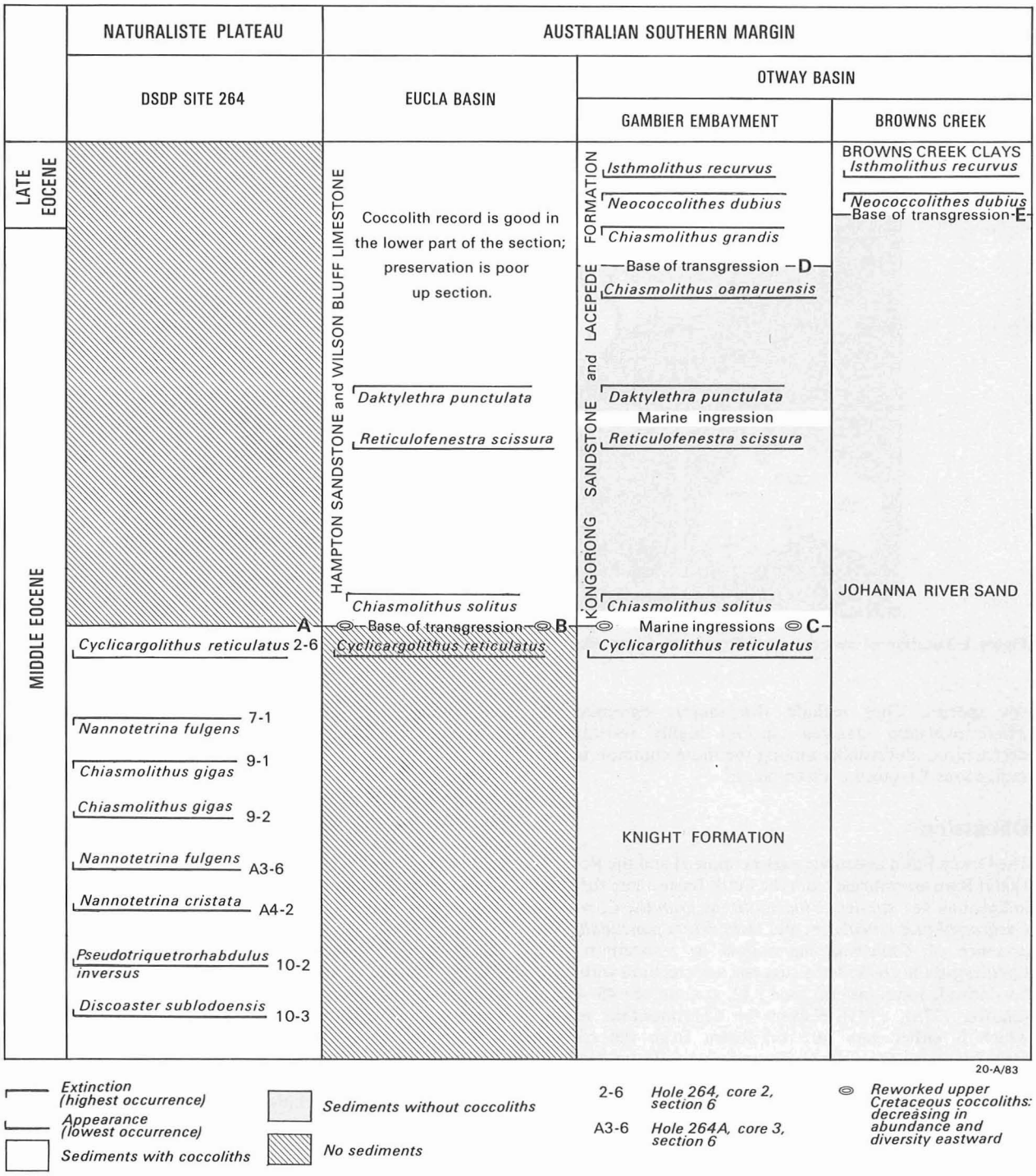

Figure 5. Eocene events at DSDP site 264 (Naturaliste Plateau) and along the Australian southern margin (Eucla and Otway Basins). A, B, & C are virtually isochronous. *Chiasmolithus grandis* occurs with *C. oamaruensis* at D. E is younger than the extinction of *Chiasmolithus grandis*.

unpublished data). Shafik (1978a) suggested the Lancelin Beds as the source of the reworked upper Cretaceous taxa in the middle Eocene of Rottnest Island Bore, because of agreement between the age of the Lancelin Beds (Campanian) and the Campanian or younger age of the reworked taxa. The age of the Gingin Chalk was thought then to be Santonian (Shafik, 1978b, and references therein). However, new data (Shafik, unpublished) indicate that the Gingin Chalk is as young as the latest Maastrichtian, so this unit, too, is a possible source for the reworked taxa in the Rottnest Island Bore.

In the Carnarvon Basin and adjacent offshore areas, upper Cretaceous sediments with abundant coccoliths are widely distributed. The reworked upper Cretaceous coccoliths in the middle Eocene occur at more than one level, mostly without nearshore taxa, suggesting contributions from distant provenances or some oceanic source.

Southern margin

According to Cande & others (1981), a major acceleration in the seafloor spreading rate occurred south of Australia at 45 Ma, i.e. at about or slightly before the time of the reworking episode in the Eucla and Otway Basins. This acceleration in the spreading rate is consistent with the rise in sea level that resulted in the middle Eocene transgression in the Eucla Basin and the coeval ingressions in the Otway Basin. Along the southern margin, the base of the marine lower Tertiary sediments — as detected by the lowest occurrence of coccoliths — is progressively younger eastward (Shafik, 1973), suggesting that the sea advanced from the west. Accordingly, it is not unreasonable to suggest that the middle Eocene ingressions in the Otway Basin, and its subsequent transgression (Shafik, 1983; Fig. 5) were the distal expression of the coeval transgression in the Eucla Basin. That these ingressions were confined to the Gambier Embayment in the western Otway Basin is consistent with the above argument. The argument is strengthened further by the coeval reworking episode: the reworked taxa are restricted to the very base of the Eucla Basin transgression and the coeval first middle Eocene ingression in the Otway Basin.

In-situ upper Cretaceous coccoliths are not known along the Australian southern margin or in the offshore areas to the south. Although the break up of Australia and Antartica may have occurred during the mid late Cretaceous (Cande & others, 1981), it is unlikely that during the late Cretaceous the proto-Southern Ocean was deep enough, with good connections to the open sea, to give water conditions favourable to coccoliths. In the Eucla and Great Australian Bight Basins, open marine conditions did not exist during the late Cretaceous (Deighton & others, 1976). Further to the east, in the Otway Basin, the same is also true, and even the accepted 'marine' upper Cretaceous unit (the Belfast Mudstone) 'would have been deposited in intertidal salt marshes to very shallow marine, delta front environments' (Deighton & others, 1976, p. 26).

On the other hand, upper Cretaceous sediments rich in coccoliths occur widely on the Naturaliste Plateau, off southwestern Australia, and they were eroded from time to time, including the Eocene — at the time of the reworking episode in the Eucla and Otway Basins. A widespread disconformity separating upper Cretaceous and younger sediments of the plateau has been reported by several investigators. Burkle & others (1967) recorded upper Cretaceous directly below Pleistocene (Core RC8-56) in the northeastern slope of the plateau. Davies, Lyendyk & others (1974) recorded a Santonian/Miocene unconformity at DSDP site 258 (northern part of the plateau). The sedimentary sequence at DSDP site 264 (southern edge of the plateau) contains two relevant unconformities: Campanian/Paleocene, and mid middle Eocene/upper Miocene (Shafik, unpublished data); these unconformities were reported by Hayes, Frakes & others (1975) as Cenomanian/Paleocene and upper Eocene/upper Miocene, respectively.

With the available biostratigraphic resolution, the top of the middle Eocene section at DSDP site 264 (which is

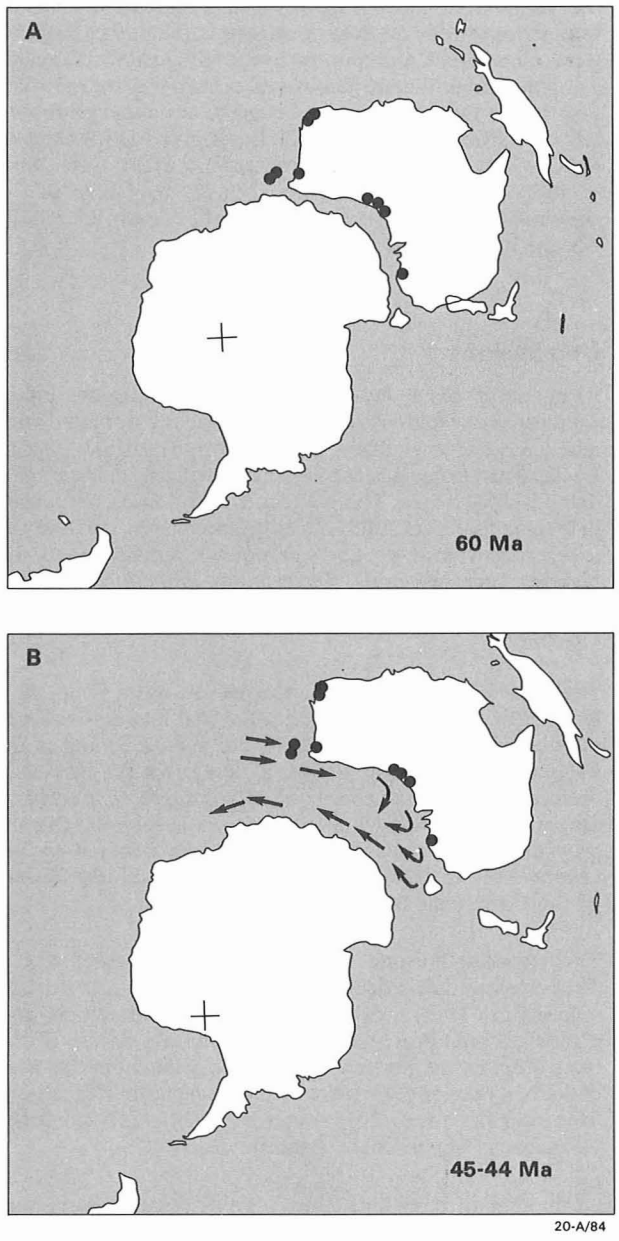

Figure 6. Reconstruction of the relative positions of Australia and Antarctica during the late Cretaceous (A) and mid Eocene (B). During the late Cretaceous and Paleocene, the proto-Southern Ocean was narrow and shallow, and generally unsuitable for coccoliths, but by the mid Eocene it was deep and wide enough for coccolith assemblages to flourish in the Eucla Basin; at about 45 to 44 Ma, strong currents, marking the advent of a transgression in the Eucla Basin, were apparently developed, but only for a short time. These currents would have circulated clockwise in the proto-Southern Ocean as the eastern end of this 'ocean' was not sufficiently deep to permit flow past the South Tasman Rise. The easterly flowing currents would have been responsible for erosion of upper Cretaceous sediments on the Naturaliste Plateau, of southwestern Australia, and eastward transportation of the claysized coccoliths derived from them.

immediately above the lowest occurrence of *Cyclicargolithus reticulatus*) can be equated with the time of the reworking episode in the Eucla and Otway Basins (Fig. 5). The records in the northern parts of the plateau too (Core RC8-56, and DSDP site 258) fit the scenario of erosion of upper Cretaceous sediments during the middle Eocene.

The Naturaliste Plateau is probably the best candidate for a source of the reworked upper Cretaceous coccolith taxa in the middle Eocene of the Eucla and Otway Basins. I envisage that the onset of the Eucla Basin transgression was marked by strong currents coming from the west and passing over the Naturaliste Plateau (Fig. 6). Upper Cretaceous sediments were stripped off and their constituents (mainly coccoliths) were transported and progressively redeposited eastward, along the currents' path. This would explain why the reworked taxa in the Eucla Basin samples are much more abundant and diversified than those in the Beachport-1 assemblage in the Otway Basin. Evidently, these strong currents were short-lived, being active only during the very beginning of the transgresssion in the Eucla Basin and the coeval first middle Eocene ingression in the Otway Basin.

Conclusions

As a result of a short-lived reworking episode, upper Cretaceous coccoliths were displaced and incorporated with middle Eocene assemblages in four basins (Carnarvon, Perth, Eucla, and Otway Basins) along the western and southern margins of Australia. The indigenous assemblages are coeval, belonging to the coccolith biostratigraphic interval from the lowest occurrence of *Cyclicargolithus reticulatus* to the highest occurrence of *Daktylethra punctulata*, which correlates with the low-latitude foraminiferal zonal interval P.12–P.13.

The reworking episode in the Carnarvon Basin is one in a long history of marine sedimentation that laid down widely distributed Paleocene and Eocene sediments. Evidence for the reworking episode occurs at levels where there is a noticeable drop in the quality of coccolith preservation, and also where a regional unconformity is suspected. Distant provenances or some oceanic source contributed to the reworked upper Cretaceous coccoliths in the middle Eocene of the Carnarvon Basin.

The reworking episode in the Perth Basin coincided with a short-lived middle Eocene transgression (or a pronounced ingression). The reworked taxa are more abundant and diversified than those recorded in the middle Eocene of the three other basins studied, and also are different in that they contain several species indicative of nearshore deposition. This indicates a nearshore source, probably the local upper Cretaceous Gingin Chalk/Lancelin Beds.

At the time of reworking, the sea advanced eastward along the Australian southern margin, causing a transgression in the Eucla Basin and an ingression in the western Otway Basin. The Naturaliste Plateau is thought of as the probable provenance area for the reworked upper Cretaceous coccoliths in the middle Eocene of these basins, in the absence of known in-situ upper Cretaceous coccoliths along the southern margin or offshore to the south. The reworking episode on the southern margin apparently was caused by short-lived strong currents stripping coccolith-rich upper Cretaceous sediments from the plateau and transporting them eastward. The coccoliths were progressively redeposited along the currents' path, only a few reaching the western Otway Basin.

Acknowledgements

I thank Drs. N.F. Exon and D.J Belford of BMR, who read the manuscript. Their comments were most valuable. The figures were drafted by T. Kimber.

References

Burckle, L.H., Saito, T., & Ewing, M., 1967 — A Cretaceous (Turonian) core from the Naturaliste Plateau, southeast Indian Ocean. *Deep-Sea Research*, 14, 421–426.

Cande, S.C., Mutter, J., & Weissel, J.F., 1981 — A revised model for the break- up of Australia and Antarctica. *Eos*, 62, 384.

Davies, T.A., Luyendyk, B.P., & others, 1974 — Initial Reports of the Deep Sea Drilling Project, 26, *Washington (U.S. Government Printing Office)*.

Deighton, I., Falvey, D.A., & Taylor, D.J., 1976 — Depositional environments and geotectonic framework: southern Australian continental margin. *APEA Journal* 16, 25–36.

Hayes, D.E., Frakes, L.A., & others, 1975 — Initial Reports of the Deep Sea Drilling Project, 28, *Washington (U.S. Government Printing Office)*.

Shafik, S., 1973 — Eocene—Oligocene nannoplankton biostratigraphy in the western and southern margins of Australia. *Abstracts, 45th Congress, Australian and New Zealand Association for Advancement of Science*, Section 3, 101–103.

Shafik, S., 1978a — Paleocene and Eocene nannofossils from the Kings Park Formation, Perth Basin, Western Australia. *Bureau of Mineral Resources, Australia, Bulletin*, 192, 165–172.

Shafik, S., 1978b — A new nannofossil zone based on the Santonian Gingin Chalk, Perth Basin, Western Australia. *BMR Journal of Australian Geology & Geophysics*, 3, 211–226.

Shafik, S., 1983 — Calcareous nannofossil biostratigraphy: an assessment of foraminiferal and sedimentation events in the Eocene of the Otway Basin, southeastern Australia. *BMR Journal of Australian Geology & Geophysics*, 8, 1–17.

Shafik, S., 1984 — Displaced Cretaceous nannofossils and middle Eocene marine sedimentation along the Australian western and southern margins. *Geological Society of Australia, Seventh Australian Geological Convention, Sydney, 1984, Abstracts*, 12, 477.

Appendix. List of coccoliths referred to in this paper

Eocene taxa

Chiasmolithus expansus (Bramlette & Sullivan) Hay, Mohler & Wade, 1966, Eclogae Geologicae Helvetiae, 59, p. 388.

Chiasmolithus gigas (Bramlette & Sullivan) Perch-Nielsen, 1971, Det Kongelige Danske Videnskabernes Selskab, Biologiske Skrifter, 18, p. 17.

Chiasmolithus grandis (Bramlette & Riedel) Hay, Mohler & Wade, 1966, Eclogae Geologicae Helvetiae, 59, p. 388.

Chiasmolithus oamaruensis (Deflandre) Hay, Mohler & Wade, 1966, Eclogae Geologicae Helvetiae, 59, 388.

Chiasmolithus solitus (Bramlette & Sullivan) Perch-Nielsen, 1971, Det Kongelige Danske Videnskabernes Selskab, Biologiske Skrifter, 18, p. 21.

Cyclicargolithus reticulatus (Gartner & Smith) Bukry, 1971, Transactions of the San Diego Society of Natural History, 16, p. 313.

Cyclococcolithus formosus Kamptner, 1963, Annalen des Naturhistorishen Museums in Wien, 66, p. 163.

Daktylethra punctulata Gartner *in* Gartner & Bukry, 1969, Journal of Paleontology, 43, p. 1219.

Discoaster barbadiensis Tan Sin Hok, 1927, Jaarbock van het Mijnwezen in Nederlandsch-Oost-Indie, 1926, p.119.

Discoaster saipanensis Bramlette & Riedel, 1954, Journal of Paleontology, 28, p. 398.

Discoaster sublodoensis Bramlette & Sullivan, 1961, Micro-paleontology, 7, p. 162.

Discoaster tani nodifer Bramlette & Riedel, 1954, Journal of Paleontology, 28, p. 397.

Helicosphaera compacta Bramlette & Wilcoxon, 1967, Tulane Studies in Geology, 5, p. 105.

Helicosphaera reticulata Bramlette & Wilcoxon, 1967, Tulane Studies in Geology, 5, p. 106.
Isthmolithus recurvus Deflandre *in* Deflandre & Fert, 1954, Annales de Paleontologie, 40, p. 119.
Nannotetrina cristata (Martini) Perch-Nielsen, 1971, Det Kongelige Danske Videnskabernes Selskab, Biologiske Skrifter, 18, p. 66.
Nannotetrina fulgens (Stradner) Achuthan & Stradner, 1969, Proceedings of the First International Conference on Planktonic Microfossils, Geneva 1967, I, p. 7.
Neococcolithus dubius (Deflandre) Black, 1967, Proceedings of the Geological Society, London, 1640, p. 143.
Pemma papillatum Martini, 1959, Erdol und Kohle, 12, p. 139.
Reticulofenestra scissura Hay, Mohler & Wade, 1966, Eclogae Geologicae Helvetiae, 59, p. 387.
Reticulofenestra scrippsae (Bukry & Percival) Shafik, 1981, BMR Journal of Australian Geology & Geophysics, 6, p. 113.
Reticulofenestra umbilica (Levin) Martini & Ritzkowski, 1968, Nachrichten Akademie der Wissenschaften in Gottingen, II, math. Phys. Kl., 13, p. 345.
Pseudotriquetrorhabdulus inversus (Bukry & Bramlette), Wise & Constans, 1976, Transactions of the Gulf Coast Association of Geological Societies, 26, p. 154.

Cretaceous taxa

Ahmuellerella octoradiata (Gorka) Reinhardt; 1966, Freiberger Forschungshefte, C196 Palaont., p. 24.
Arkhangelskiella cymbiformis Vekshina, 1959, Trudy Sibirskogo Nauchno-Issledovatel'skogo Instituta Geologii Geofiziki i Mineral'nogo Syr'ya (SNIIGGIMS), 2, p. 63.
Biscutum blackii Gartner, 1968, University of Kansas Paleontological Contributions, 48, p. 18.
Broinsonia parca (Stradner) Bukry, 1969, University of Kansas Paleontological Contributions, 51, p. 23.
Calculites obscurus (Deflandre) Prins & Sissingh *in* Sissingh, 1977, Geologie en Mijnbouw, 56, p. 60.
Calculites ovalis (Stradner) Prins & Sissingh *in* Sissingh, 1977, Geologie en Mijnbouw, 56, p. 60.
Cretarhabdus crenulatus Bramlette & Martini, 1964, Micropaleontology, 10, p. 300.
Cribrocorona gallica (Stradner) Perch-Nielsen, 1973, Meddelelser fra Dansk Geologisk Forening (Bulletin of the Geological Society of Denmark), 22, p. 312.
Cribrosphaerella ehrenbergii (Arkhangelsky) Deflandre *in* Piveteau, 1952, Traite de Paléontologie, Paris, 1, p. 111.
Eiffellithus eximius (Stover) Perch-Nielsen, 1968, Det Kongelige Danske Videnskabernes Selskab, Biologiske Skrifter, 16, p. 30.
Eiffellithus turriseiffeli (Deflandre) Reinhardt, 1965, Monatsbericht der Deutschen Akademie der Wissenschaften zu Berlin, 7, p. 36.
Gartnerago obliquum (Stradner) Reinhardt, 1970, Frieberger Forschungsheft, 2, p. 66.
Kamptnerius magnificus Deflandre, 1959, Revue de Micropaléontologie, 2, p. 13
Lithraphidites carniolensis Deflandre, 1963, Compte Rendu de l' Academie des Sciences (Paris), 256, p. 3486.
Lithastrinus floralis Stradner, 1962, Verhandlungen der Geologischen Bundesanstalt (Wien), p. 370.
Lucianorhabdus cayeuxii Deflandre, 1959, Revue de Micropaléontologie, 2, p. 142.
Micula staurophora (Gardet) Stradner, 1963, Proceedings of the Sixth World PetroleumCongress (Frankfurt am Main, 1963) sec.1, paper 4.
Prediscosphaera cretacea (Arkhangelsky) Gartner, 1968, University of Kansas Paleontological Contributions, 48, p. 19.
Prediscosphaera spinosa (Bramlette & Martini) Gartner, 1968, University of Kansas Paleontological Contributions, 48, p. 20.
Vekshinella imbricata Gartner, 1968, University of Kansas Paleontological Contributions, 48, p. 30.
Watznaueria barnesae (Black) Perch-Nielsen, 1968, Det Kongelige Danske Videnskabernes Selskab, Biologiske Skrifter, 6, p. 68.
Zygodiscus diplogrammus (Deflandre) Gartner, 1968, University of Kansas Paleontological Contributions, 48, p. 32.

BMR Journal of Australian Geology & Geophysics, 9, 361-364

Late Triassic conodonts from Sahul Shoals No. 1, Ashmore Block, northwestern Australia

P.J. Jones[1] & Robert S. Nicoll[1]

The conodont *Epigondolella primitia* Mosher, 1970 has been recovered from core 4 (1883.2–1889.6 m) in Sahul Shoals No. 1 well on the Ashmore Block, offshore northwestern Australia. It has been dated as latest Karnian to earliest Norian (Late Triassic). The Late Triassic sequence in the well is correlated with the Triassic of Austria and British Columbia, Canada.

Introduction

The recovery of a small conodont fauna of Late Triassic age from Sahul Shoals No. 1 petroleum exploration well drilled on the Ashmore Block off the northwestern Australian coast is important because it is the first record of conodonts of this age in Australia.

McTavish's (1973) description of an Early Triassic fauna from the offshore Perth and Carnarvon Basins is the only previously published description of Triassic conodonts from Australia. This is partly because Triassic rocks are mostly restricted to the offshore margins, and the wells that have penetrated marine sequences have not been specifically examined for conodonts. A study of material from both old and new offshore wells would probably yield many more conodont faunas of Triassic age, which could be very useful in the establishment of a detailed biostratigraphic zonation for the Triassic sequence in these areas.

Localities in Timor (Nogami, 1968), Papua New Guinea (Skwarko & others, 1976) and New Zealand (Jenkins & Jenkins, 1971) represent the only Late Triassic conodont faunas to have been described in areas immediately adjacent to Australia.

Geologic setting

Sahul Shoals No. 1 well is situated at the western end of the offshore Bonaparte Basin (11°25′36″S, 124°32′50″E), 375 km northwest of Cape Londonderry, Western Australia, and 137 km south of Timor, Indonesia (Fig. 1). Structurally, it is on the eastern end of the Ashmore Block (Laws & Kraus, 1974), near the point where this structure and the Vulcan Sub-basin are truncated by the southern margin of the Timor Trough (Kraus & Parker, 1979, fig. 3). The well, sited in 28 m of water, was drilled in late 1969–early 1970 by Burmah Oil Company of Australia Limited (BOCAL) to a total depth of 3802 m.

The well completion report (BOCAL, 1970) includes palaeontological studies on Foraminiferida by D.R. Wall, M. Apthorpe, and A.R. Lloyd; Ostracoda by P.J. Jones; Mollusca by S.K. Skwarko; Polyzoa and Brachiopoda by K.S.W. Campbell; and microflora by B.E. Balme.

Stratigraphy

The well passed through 1756 m of Quaternary, Tertiary, and Cretaceous carbonates and minor shale that unconformably overlie Triassic rocks. The Triassic sequence (Fig. 2) is 1955 m thick and can be separated into an upper marine unit of mixed shale and calcareous lithology; a middle unit, partly non-marine, of sandstone and shale; and a lower marine unit of siltstone and shale. The hole bottomed in 53 m of recrystallised Permian limestone.

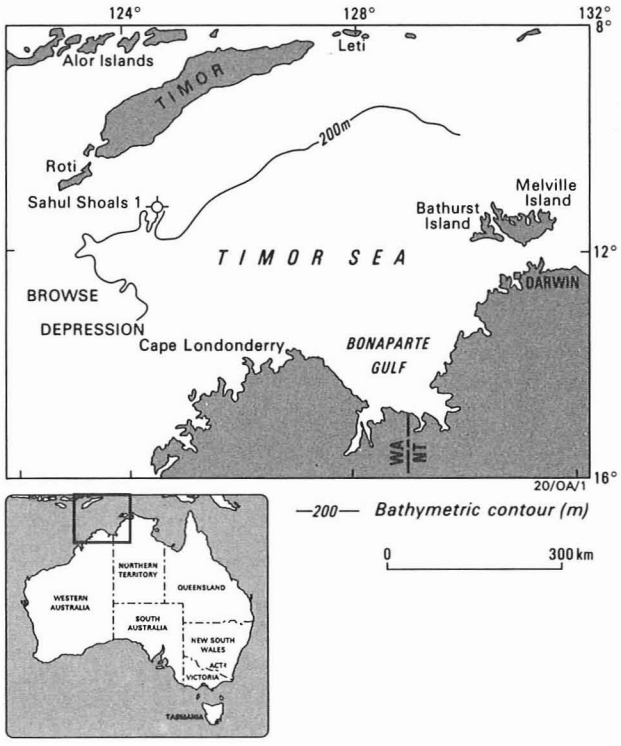

Figure 1. Location of BOCAL Sahul Shoals No. 1 well, Ashmore Platform, northwestern Australia.

Stratigraphic control of the Triassic succession (1793.66–3748.86 m) is based on evidence from palynology by B.E. Balme, Ostracoda by P.J. Jones, and Mollusca by S.K. Skwarko (in BOCAL, 1970). Balme assigned the strata between 3529.4 and 3748.86 m to the Lower Triassic, which is consistent with the early Middle Triassic age determined by Skwarko (in BOCAL, 1970) for molluscans slightly higher in the succession. Balme referred the sequence between 1811 and 2564 m to the Upper Triassic, but was unable to establish a boundary between the Middle and Upper Triassic on a palynological basis. He recognised that the Upper Triassic spore–pollen assemblages resembled those from the Mungaroo Beds of the Carnarvon Basin. The ostracods between 1828.9 and 1888.4 m are marine and indicate a general Late Triassic age (Jones in BOCAL, 1970).

Material

Four samples from Sahul Shoals No. 1, core 4 (1883.2–1889.6 m) were examined for microfossils. Ostracods were recovered from all samples, but conodonts were found only in the intervals 1884.45–1885.67 m and 1888.35–1889.56 m. They were obtained from a shaly limestone as a by-product of the ostracod processing; the samples have not been treated with acid.

[1] Division of Continental Geology, BMR.

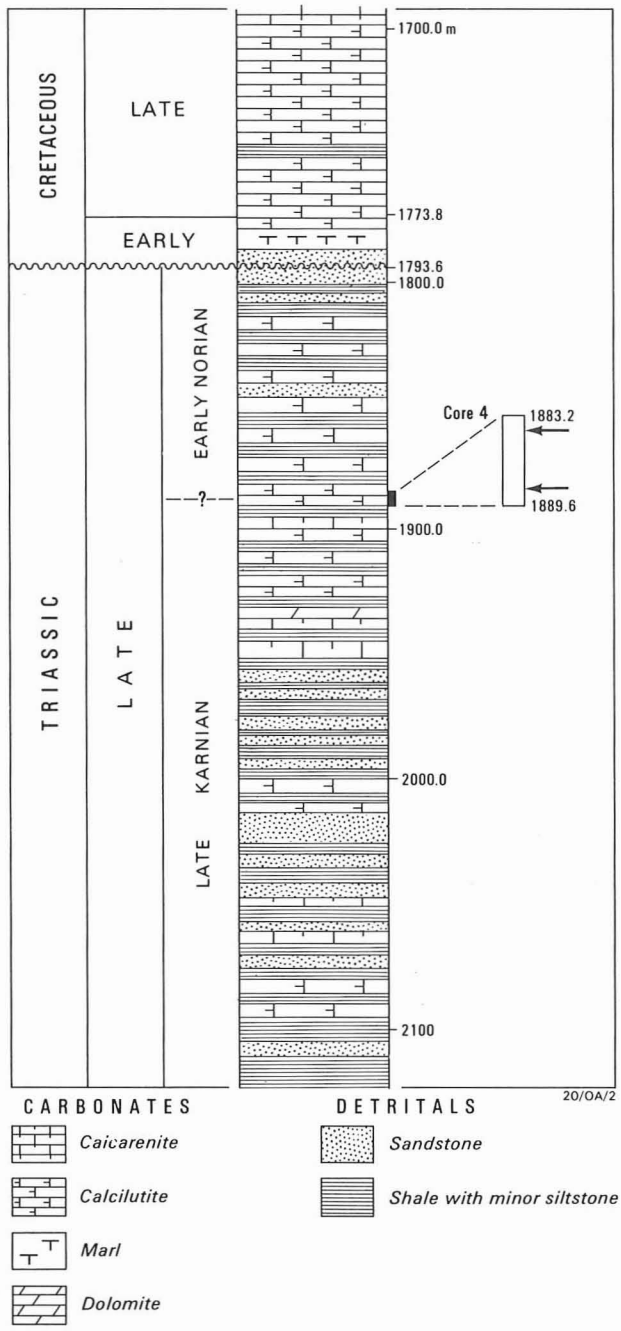

Figure 2. Portion of the graphic log of Sahul Shoals No. 1 well (adapted from BOCAL, 1970), showing the location of conodonts (arrowed) in core 4; 1883.2 m (6177 ft) to 1889.6 m (6198 ft).

Conodont fauna

The conodont fauna recovered as part of this study is restricted to a single species, *Epigondolella primitia* Mosher, 1970. The material has a conodont colour alteration index (CAI) value of 1, indicating that the sediments containing the conodont fauna have not been exposed to temperatures greater than about 80°C. (Epstein & others, 1977).

Systematic palaeontology

Genus ***Epigondolella*** Mosher, 1968

Type species *Polygnathus abneptis* Huckriede, 1958

Epigondolella primitia Mosher, 1970

Figure 3

Synonymy

1970 *Epigondolella primitia* n. sp.; Mosher, p. 740, Pl. 110, figs 7–13, 16, 17.

1980 *Epigondolella primitia* Mosher; Krystyn, p. 76, P. 13, figs 1–7.

1982 *Epigondolella primitia* Mosher; Koike, p. 18, Pl. 1, fig. 29–36.

Material studied. Six specimens; all deposited in the Commonwealth Palaeontological Collection (CPC) at the Bureau of Mineral Resources, Canberra under the CPC numbers 25712 to 25717. (Specimens 25716 and 25717 are not figured.)

Remarks. The specimens are all broken: two have complete platforms (Fig. 3C, D), one has the anterior part of the platform preserved (Fig. 3B), and a fourth is a blade with only the anteriormost part of the platform attached (Fig. 3A). Two additional specimens are partial blades that closely resemble the specimen illustrated. No ramiform elements were recovered.

The specimens are unquestionably assigned to *Epigondolella primitia* on the basis of the presence of nodes on the anterior part of the platform and reduced node development on the posterior part of the element. The aboral surface has a well-developed keel that bifurcates posteriorly to the pit. The oral surface ornamentation distinguishes our material from *E. abneptis* and the well developed bifurcated keel distinguishes the specimens from *Gondolella nodosa.*

Age

Epigondolella primitia has a very restricted stratigraphic range. In the Salzkammergut area of Austria (Krystyn, 1980) it is found in the uppermost part of the Upper Karnian (Tuvalian) and extends into the lowermost part of the Lower Noriann (Lacian), over a maximum thickness of less than 10 m. In terms of Krystyn's conodont zonation it extends from the Upper *Gondolella nodosa* Assemblage Zone to the top of the *Epigondolella primitia* Assemblage Zone. This corresponds to the upper part of the *Anatropites* Bereich through to the lower part of the *Guembelites jandianus* Zone of the ammonoid zonation (Krystyn, 1980).

In British Columbia, Canada, Orchard (1983) reported *E. primitia* from the uppermost part of the Upper Karnian and extending into the lowermost part of the Lower Norian in what he refers to as the *E. primitia* conodont zone. This corresponds to the upper part of the *Klamathites macrolobatus* and most of the *Mojsisovicsites kerri* zones of Tozer's (1967) ammonoid zonation.

The recovery of additional diagnostic conodont elements is required to determine if the fauna described in this study belongs in the Late Karnian or the Early Norian (viz., *Gondolella polygnathiformis* or *G. navicula,* respectively).

Discussion

The recorded distribution of Triassic conodont faunas in Australia and adjacent areas is very limited (McTavish, 1975). McTavish (1973) reported an Early Triassic conodont fauna from the subsurface of the offshore Perth and Carnarvon Basins. Unidentified conodonts have been recovered from the Blina Shale (Lower Triassic) in wells from the onshore portion of the Canning Basin (Nicoll, 1984). Berry & others (1984) reported on a limited Lower Triassic fauna from the northern side of eastern Timor.

Upper Triassic conodont localities are more common in the Indonesian Archipelago. Nogami (1968) described a series

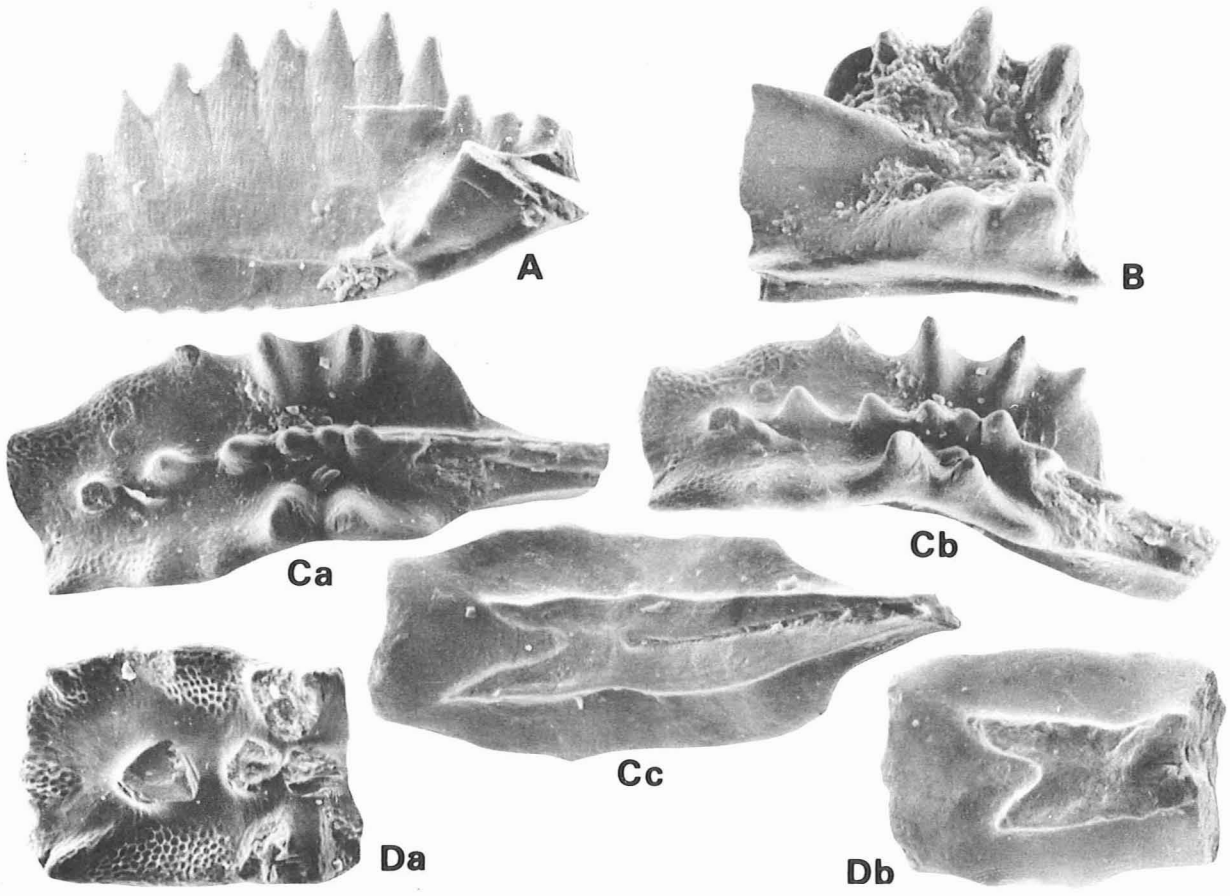

Figure 3. ***Epigondolella primitia,*** **Pa elements.**

All figs. × 150. A–C from Sahul Shoals No. 1, core 4, interval 1888.35–1889.45 m; D from core 4, interval 1884.45–1885.67. A, lateral view (CPC25712). B, lateral view (CPC25713). Ca, oral view; Cb, lateral view; Cc, aboral view (CPC25714). Da, oral view; Db, aboral view (CPC25715).

of conodont faunas from spot samples obtained from Timor, and one of his illustrated specimens (Nogami, 1968, Pl. 8, fig. 8) has since been assigned to *Epigondolella primitia* by Mosher (1973).

Metcalfe & others (1979) described a Late Karnian conodont fauna from Sumatra that includes *E. primitia.* Other Upper Triassic conodont faunas have been reported from peninsular Malaysia (Koike, 1973), western Thailand (Kemper & others, 1976), and Papua New Guinea (Skwarko & others, 1976).

The initial biostratigraphy proposed for Sahul Shoals No. 1 well (BOCAL, 1970) has been refined by later studies. Skwarko & Kummel (1974) studied the ammonite and pelecypod fauna present in core 9 (3268.2–3274.7 m) and suggested that the association of the ammonite *Nicomedites*? with halobiid pelecypods probably indicated an early Middle Triassic (early Anisian) age.

Application of Dolby & Balme's (1976) Triassic spore–pollen zonation of the Carnarvon Basin to Balme's spore–pollen distribution (in BOCAL, 1970) indicates that in the Upper Triassic succession in Sahul Shoals No. 1 the interval between at least 1859 m and 2564 m falls within the *Samaropollenites speciosus* Zone of the Onslow Microflora. Dolby & Balme regarded this zone as Late Karnian in age. Recent studies of the dinoflagellate floras (Helby & others, in press) in Sahul Shoals No. 1 indicate a Late Karnian or possibly basal Norian age for the interval 1808.8–2102.7 m.

The discovery of the conodont species *Epigondolella primitia* Mosher 1970 in Sahul Shoals No. 1, core 4 (1883.2–1889.6 m) adds more precision to the dinoflagellate and spore–pollen data, in that this species indicates that the Karnian–Norian boundary is within a few metres of this depth, and suggests a basal Norian age for at least the upper 75 m of the Triassic sequence in this well.

Finally, this find has certain palaeogeographical implications. On the basis of Triassic conodont distributions, McTavish (1975) argued for the presence of Malaya adjacent to northwestern Australia and Timor as part of the Gondwanaland margin. Audley-Charles (1983) later recognised a Late Triassic magmatic arc that united eastern Australia, the Kubor range of New Guinea, Borneo, Sumatra, the Thai-Malay Peninsula, Burma, and southern Tibet into an active continental margin during the Late Permian to Late Triassic. The discovery of *Epigondolella primitia* in an autochthonous Upper Triassic sequence on the northwestern continental margin of Australia now provides a palaeogeographical link with the Late Triassic (latest Karnian–earliest Norian) conodont faunas of Timor, western Malaya, Thailand, and Sumatra.

Acknowledgements

We thank Frank Hadzel (BMR) for preparation of the material and Arthur T. Wilson (BMR) for the photography and assistance with plate preparation. The manuscript was critically reviewed by D.J. Belford and E. M. Truswell (BMR).

References

Audley-Charles, M.G., 1983 — Reconstruction of eastern Gondwanaland. *Nature,* 306, 48–50.

Berry, R., Burrett, C., & Banks, M., 1984 — New Triassic faunas from East Timor and their tectonic significance. *Geologica et Palaeontologica,* 18, 127–138.

BOCAL, 1970 — Sahul Shoals No. 1, Well Completion Report. *Bureau of Mineral Resources, Australia, Petroleum Search Subsidy Acts File* 69/2042 (unpublished).

Dolby, J.H. & Balme, B.E. 1976 — Triassic palynology of the Carnarvon Basin, Western Australia. *Review of Palaeobotany & Palynology* 22, 105–169.

Epstein, A.G., Epstein, J.B. & Harris, L.D., 1977 — Conodont colour alteration—an index to organic metamorphism. *United States Geological Survey, Professional Paper* 995, 1–27.

Helby, R., Morgan, R. & Partridge, A., in press — A palynological zonation of the Australian Mesozoic. *Memoirs of the Association of Australasian Palaeontologists.*

Jenkins, T.B.H. & Jenkins, D.G., 1971 — Conodonts of the Haast and Torlesse Groups of New Zealand. Part 1—Biostratigraphic significance of the Triassic conodonts from the Mount Mason and Okulu Limestones. *New Zealand Journal of Geology & Geophysics,* 14, 782–794.

Kemper, E., Maronde, H.-D. & Stoppel, D., 1976 — Triassic and Jurassic Limestone in the region northwest and west of Si Sawat (Kanchanaburi Province, western Thailand). *Geologisches Jahrbuch,* B, 21, 93–127.

Koike, T., 1973 — Triassic conodonts from Kedah and Pahang, Malaysia. *Geology & Palaeontology of Southeast Asia,* 12, 91–113.

Kraus, G.P. & Parker, K.A., 1979 — Geochemical evaluation of petroleum source rock in Bonaparte Gulf-Timor Sea region, northwestern Australia. *American Association of Petroleum Geologists Bulletin* 63(11), 2021–2041.

Krystyn, L., 1980 — Stratigraphy of the Hallstatt region. *Abhandlungen der geologischen Bundesanstalt,* 35, 69–98.

Laws, R.A. & Kraus, G.P., 1974 — The regional geology of the Bonaparte Gulf-Timor Sea area. *The APEA Journal,* 14, 77–84.

McTavish, R.A., 1973 — Triassic conodont faunas from Western Australia. *Neues Jahrbuch fur Geologie und Palaontologie Abhandlungen,* 143, 275–303.

McTavish, R.A., 1975 — Triassic conodonts and Gondwana stratigraphy. *In* Campbell, K.S.W., (editor), Gondwana geology: papers from the 3rd Gondwana Symposium. *Australian National University Press, Canberra.* 481–490.

Metcalfe, I., Koike, T., Rafek, M.B. & Haile, N.S., 1979 — Triassic conodonts from Sumatra. *Palaeontology,* 22, 737–746.

Mosher, L.C., 1970 — New conodont species as Triassic guide fossils. *Journal of Palaeontology,* 44, 737–742.

Mosher, L.C., 1973 — Triassic conodonts from British Columbia and the northern Arctic Islands. *Geological Survey of Canada, Bulletin,* 222, 140–193.

Nicoll, R.S., 1984 — Conodont studies in the Canning Basin—a review and update. *In* Purcell, P.G., (editor), The Canning Basin, W.A. *Proceedings of Geological Society of Australia/Petroleum Exploration Society of Australia Symposium, Perth, 1984,* 439–443.

Nogami, Y., 1968 — Trias-conodonten von Timor, Malaysien und Japan (Palaeontological study of Portuguese Timor, 5). *Memoirs of the Faculty of Science, Kyoto University, Series of Geology & Mineralogy,* 34, 115–136.

Orchard, M.J., 1983 — *Epigondolella* populations and their phylogeny and zonation in the Upper Triassic. *Fossils and Strata,* 15, 177–192.

Skwarko, S.K. & Kummel, B., 1974 — Marine Triassic Mollusca of Australia and Papua New Guinea. *Bureau of Mineral Resources, Australia, Bulletin,* 150, 111–127.

Skwarko, S.K., Nicoll, R.S. & Campbell, K.S.W., 1976 — The Late Triassic molluscs, conodonts, and brachiopods of the Kuta Formation, Papua New Guinea. *BMR Journal of Australian Geology & Geophysics,* 1, 219–230.

Tozer, E.T., 1967 — A standard for Triassic time. *Geological Survey of Canada, Bulletin,* 156.

CORRECTION

G.C. Young — Further petalichthyid remains (placoderm fishes, Early Devonian) from the Taemas—Wee Jasper region, New South Wales Volume 9, number 2, 121—131

The contents of pages 127 and 128 were inadvertently transposed. The sequence for correct reading of the paper is .... pp. 126, 128, 127, 129 ....

VOLUME 9

1984

CONTENTS

VOLUME 9 NUMBER 1 MARCH 1984

VOLUME 9 NUMBER 2 JUNE 1984

VOLUME 9 NUMBER 3 SEPTEMBER 1984

VOLUME 9 NUMBER 4 DECEMBER 1984

CONTENTS

R83/614(4) Cat. No. 84 2140 5